

PHUONG DOAN

Novel Treatment Strategies for Glioblastoma

Therapeutic Potential of Phenolic Derivatives and Orphan G-protein Coupled Receptor Ligand

PHUONG DOAN

Novel Treatment Strategies for Glioblastoma
Therapeutic Potential of Phenolic Derivatives and
Orphan G-protein Coupled Receptor Ligand

ACADEMIC DISSERTATION

To be presented, with the permission of
the Faculty of Medicine and Health Technology
of Tampere University,
for public discussion at Tampere University
on 18 March 2022, at 12 o'clock.

ACADEMIC DISSERTATION

Tampere University, Faculty of Medicine and Health Technology
Finland

<i>Responsible supervisor</i>	Adjunct Professor Meenakshisundaram Kandhavelu Tampere University Finland	
<i>Supervisor</i>	Professor Olli Yli-Harja Tampere University Finland	
<i>Pre-examiners</i>	Associate Professor Gabriella Marucci University of Camerino Italy	Associate Professor Achiraman Shanmugan Bharathidasan University India
<i>Opponent</i>	Associate Professor Stefania Maria Ceruti University of Milan Italy	
<i>Custos</i>	Professor Olli Yli-Harja Tampere University Finland	

The originality of this thesis has been checked using the Turnitin OriginalityCheck service.

Copyright ©2022 author

Cover design: Roihu Inc.

ISBN 978-952-03-2307-3 (print)

ISBN 978-952-03-2308-0 (pdf)

ISSN 2489-9860 (print)

ISSN 2490-0028 (pdf)

<http://urn.fi/URN:ISBN:978-952-03-2308-0>

PunaMusta Oy – Yliopistopaino
Joensuu 2022

ACKNOWLEDGEMENTS

The dissertation was implemented and completed in the Faculty of Health and Medicine Technology, Tampere University, Finland, 2017–2021. This study was funded by Tampere University graduate school (formerly Tampere University of Technology) and the Academy of Finland.

First of all, I would like to thank my supervisor, Adjunct Professor **Meenakshisundaram Kandhavelu**, who has always supported me on the study during the past few years. My deepest gratitude is expressed to him for giving me a great opportunity to participate in his laboratory and work on the glioblastoma study. His expertise and academic experience are irreplaceable. I extend my gratitude to Professor **Olli Yli-Harja**, my co-supervisor, and Professor **Frank Emmert-Streib**, my instructor, for sharing their profound knowledge of computational biology, which helped me finalize this dissertation.

I am also highly indebted to my wonderful colleagues in the Molecular Signaling Lab, especially to my soul-lab-mate **Phung Ha Tien Nguyen** and my co-authors; together, they brought me through a huge academic world gate with their enthusiasm. It is my privilege to have such a productive collaborator, to whom I am indeed grateful. Without them, the study would not be finished. I would like to thank **Akshaya Murugesan**, **Khanh Ma**, and **Hieu Trinh** for proofreading my dissertation. This dissertation could not have been finished without the abundant help and consistent support that I received cheerfully from all.

I thank **Khanh Ma**, **Dong Giang**, **Minh Minh**, and **Hong Ngoc** for their steady support, help, share, care, and love, even though some of them are far away from me here in Finland. I must also thank **Ca Phe Khia** for bringing laughter and joy during my PhD.

Finally, I would like to thank my family sincerely. My parents have truly supported my career and my future by giving me lots of encouragement to reach my goal in life. For this, I will be grateful to you throughout my entire life. Also, to my siblings, thank you so much for your mighty love, patience, confidence, and faith in me, which enabled me to travel this ambitious path.

ABSTRACT

Glioblastoma (GBM) is a prevalent brain tumor with a high mortality rate worldwide. Although many efforts have been made to explore potential therapeutic strategies, the treatment for GBM remains obscure. Phenolic compounds have received considerable attention in cancer biology owing to their therapeutic applications. Indeed, phenolic compounds with alkylaminophenol core have been approved by the U.S. Food and Drug Administration to treat several diseases. The present study aims at exploring the anti-tumor activity of three different alkylaminophenols, namely 2-((3,4-dihydroquinolin-1(2H)-yl)(p-tolyl)methyl)phenol (**THTMP**), 2-((1,2,3,4-tetrahydroquinolin-1-yl)(4-methoxyphenyl)methyl)phenol (**THMPP**), and N-(2-hydroxy-5-nitrophenyl(4'-methylphenyl)methyl)indoline (**HNPMI**) against GBM cell growth and proliferation. Our results reveal that THTMP has potent inhibitory activity against GBM cells and could target GBM cancer stem cells (GSCs) via arresting the cell cycle at the G1/S phase and inducing reactive oxygen species-mediated apoptosis. Furthermore, THTMP could target GSCs by modulating epidermal growth factor receptor (EGFR) and GSC signaling pathways. In addition, the G-protein coupled receptor 17 (GPR17) targeted signaling pathway has also grasped attention in the treatment of GBM. Our preliminary study has revealed that GPR17 interaction with its ligand, 2-[[5-(3-morpholin-4-ylsulfonylphenyl)-4-[4-(trifluoromethoxy) phenyl]-1,2,4-triazol-3-yl] sulfanyl]-N-(4-propan-2ylphenyl)acetamide (namely, **T0510.3657** or **T0**), could potentially regulate the intracellular signaling communication of GBM. We have identified that T0 downregulates the concentration of adenosine 3',5'-cyclic monophosphate (cAMP) through activating GPR17 signaling. Here, we have characterized the effect of T0 and the underlying molecular mechanism in inducing GBM cell death.

Towards combinatorial drug development, the lead phenolic compound and the GPR17 ligand were used to investigate the anti-cancer effect against GBM. The results show that THTMP has a higher synergistic effect when combined with T0 than the temozolomide (TMZ) in inducing GBM cell death. Furthermore, this study reveals that combining THTMP with T0 would increase the inhibitory effect against mesenchymal GBM cells compared to a single THTMP/T0/TMZ treatment. In addition, the combination THTMP+T0 could decrease the migration, invasion, and

colony formation ability of glioblastoma cells. The combination also has the ability to arrest the cell cycle at the S phase as well as to induce ROS-, caspase- and mitogen-activated protein kinase (MAPK)-mediated apoptosis. The activation of intrinsic apoptosis is found to be regulated by XIAP, p53, cIAP-1, cIAP-2, HSP27, cytochrome c, cleaved caspases-3, and Bcl-2. The combinatorial drug treatment shows the promising anti-tumor property in the GBM xenograft model since it can reduce tumor volume. Our findings imply the coordinated administration of THTMP and T0 as a potential therapy that can be used for GBM treatment.

CONTENTS

1	Introduction.....	1
2	Review of the literature.....	5
2.1	Glioblastoma and current treatment options	5
2.1.1	Glioblastoma (GBM)	5
2.1.2	Current treatment options for GBM.....	6
2.1.2.1	Surgery.....	6
2.1.2.2	Radiation therapy	7
2.1.2.3	Chemotherapy.....	8
2.2	Phenolic compounds.....	9
2.2.1	Natural phenolic compounds	9
2.2.2	Synthesized phenols	10
2.2.3	Alkylaminophenols	11
2.3	G protein-coupled receptor (GPCR) and its orphan G protein-coupled receptor 17 (GPR17)	12
2.3.1	G protein-coupled receptor	12
2.3.2	GPR17	14
2.4	Cell cycle and programmed cell death.....	16
2.4.1	Cell cycle	16
2.4.2	Apoptosis in programmed cell death	18
2.4.2.1	Intrinsic pathway	20
2.4.2.2	Extrinsic pathway.....	20
2.5	Cancer stem cells (CSCs) and CSC signaling pathways.....	22

2.5.1	Cancer stem cells	22
2.5.2	Cancer stem cell signaling pathways.....	23
2.6	Important signaling pathways associated with PCD	27
2.6.1	P53 pathway.....	27
2.6.2	Mitogen-activated protein kinase (MAPK).....	28
2.6.3	Epidermal growth factor receptor pathway	30
3	Aims of the study	33
4	Materials and methods.....	34
4.1	Materials	34
4.2	Cell lines and cell culture.....	36
4.2.1	GBM primary cell lines and MEF cells	36
4.2.2	GSC and NSCC cells.....	37
4.2.3	Patient-derived GBM (PdG) cell lines.....	37
4.3	Preparation of samples	38
4.4	Cell growth inhibitory assay	38
4.5	Cytotoxicity assay using kinetic studies	39
4.6	Synergy screening assay.....	39
4.7	Scratch/wound healing assay.....	39
4.8	Transwell migration and invasion assay.....	40
4.9	Clonogenic assay	41
4.10	RNA sequencing assay.....	42
4.11	Cell cycle assay	42
4.12	Apoptosis assay	43
4.13	Protein-protein docking and protein-ligand docking.....	44
4.14	Expression of GPR17 analyzed by RT-PCR and immunoblotting.....	44
4.15	cAMP-Glo™ Assay.....	46

4.16	Calcium assay	46
4.17	Measuring mitochondrial membrane potential (MMP)	47
4.18	Caspase 3/7 assay	47
4.19	Reactive oxygen species assay	48
4.20	Apoptotic proteome profiling assay	49
4.21	Animal study	49
4.22	Statistical analysis	50
5	Results	52
5.1	Characterization of alkylaminophenols on GBM cells	52
5.1.1	Cytotoxicity of alkylaminophenols on GBM cells and non-tumor cells.....	52
5.1.2	Whole-genome profiling of GBM cells treated with THTMP	53
5.1.3	THTMP induces G1/S cell cycle arrest on GBM cells	54
5.1.4	THTMP induces ROS- and caspase 3/7-mediated apoptosis	55
5.2	Alkylaminophenol targets glioblastoma cancer stem cell	57
5.2.1	Cytotoxicity of THTMP on GSC and NSCC	57
5.2.2	Whole-genome profiling of GSC and NSCC population treated with THMTP	58
5.2.3	THTMP induces cell cycle arrest in GSC and NSCC	59
5.2.4	THTMP induces ROS- and caspase 3/7-mediated apoptosis in GSC and NSCC.....	60
5.2.5	THTMP inhibits EGFR and cancer stem cell signaling pathways.....	62
5.3	Characterization of GPR17 agonist on GBM	64
5.3.1	GPR17, a potential biomarker for low-grade glioma and glioblastoma	64

5.3.2	T0 can be recognized as a potential GPR17 agonist	65
5.3.3	Cytotoxicity of T0 on GBM cells	66
5.3.4	T0 induces apoptosis and cell cycle arrest on GBM	67
5.3.5	T0 modulated various GBM signaling pathways	68
5.3.6	T0 can cross the blood-brain barrier (BBB) and its inhibitory effect on xenograft mice model	69
5.4	Combinatorial treatment of alkylaminophenol and GPR17 agonist on PdG cells	70
5.4.1	Cytotoxicity of THTMP and T0 single treatment on PdG cells	70
5.4.2	Synergistic effect of THTMP and T0 on PdG cells	71
5.4.3	Effect of combinatorial treatment on migration, invasion, and colony formation properties of PdG cells	72
5.4.4	Combinatorial treatment induces PdG cell cycle arrest at S phase	73
5.4.5	Combinatorial treatment induces intrinsic ROS- mediated and mitochondrial apoptosis	73
5.4.6	In vivo study of combinatorial treatment on xenograft model	75
6	Discussion	76
6.1	The anti-tumor activity of alkylaminophenols, especially THTMP, on glioblastoma cell growth and proliferation	76
6.2	Role of THTMP in GSC and NSCC growth and proliferation by modulating selective signaling pathways:	77
6.3	T0 as GPR17 agonist and its anti-tumor activity on GBM cells	80
6.4	The synergistic effect of THTMP and T0 and the use of combinatorial treatment as novel therapeutic agent for glioblastoma	82
7	Summary and conclusions	85
8	References	87

List of Figures

Figure 1. Phenols can be produced via replacement of functional groups	10
Figure 2. Preparation of alkylaminophenols via Petasis borono–Mannich reaction.....	11
Figure 3. The diversity of G family and their downstream signaling processes. Abbreviations: GDP: Guanosine diphosphate, IP3: Inositol 1,4,5- triphosphate, PIP2: phosphatidylinositol bisphosphate, PLC- β : phospholipase-C β	14
Figure 4. Illustration of cell cycle of mammalian cell.	17
Figure 5. Apoptotic cell death morphological change: blebbing of plasma membrane occurs forming apoptotic bodies containing different cell fragmentations. These fragmentations are enclosed with intact plasma membrane (Rode, 2008).....	19
Figure 6. Schematic representation of apoptosis pathways: extrinsic and intrinsic (Elmore, 2007)	21
Figure 7. Schematic overview of MAPKs and their family signaling pathways. There are three types of kinases that form different signal transduction cascade and result in different outputs.	30
Figure 8. Representative images of scratch assay. The scratch is created on a confluent monolayer of cells. A thin tip is used to scratched on the cell layer to achieve straight gap. The first image is taken. After that, cells migrate to close the gap (Hulkower and Herber, 2011).....	40

List of Tables

Table 1. Alkylaminophenols and their IC ₅₀ values on osteosarcoma cells.....	12
Table 2. Significant of Wnt, Notch and Hedgehog signaling pathway genes in cancer.....	23
Table 3. Synthetic alkylaminophenols, GPR17 agonist and temozolomide structure.	35
Table 4. Detail of signaling proteins β AR, Gal, and GPR17 used in protein-protein docking	44

ABBREVIATIONS

BBB	Blood-brain barrier
CAD	Caspase-activated DNase
CNS	Central nervous system
CSC	Cancer stem cell
CDK	Cyclin dependent kinase
CysLT	Cysteinyl leukotriene receptor
DAG	Diacylglycerol
DEGs	Differentially expressed genes
DIG	Digalloylresveratrol
EGFR	Epidermal growth factor receptor
EGF	Epithelial growth factor
FDA	U.S. Food and Drug Administration
IP3	Inositol 1,4,5- triphosphate
GBM	Glioblastoma
GDP	Guanosine diphosphate
GSC	Glioma stem cell
GM	Glioblastoma multiforme
GTP	Guanosine triphosphate
GPCR	G-protein couple receptor
GPR17	G-protein receptor 17
H ₂ DCF	2',7'-dichlorodihydrofluorescein

H ₂ DCFDA	2',7'-dichlorodihydrofluorescein diacetate
Hh	Hedgehog signaling pathway
iMRI	Intraoperative magnetic resonance imaging
MAPK	Mitogen-activated protein kinase
MEFs	Mouse embryonic fibroblasts
MEK	MAP kinase-ERK kinase
MGMT	O ⁶ -methylguanine-DNA methyltransferase
MMP	Mitochondrial membrane potential
MPT	Mitochondrial permeability transition
MTP	Mitochondrial transmembrane potential
NF-κB	Nuclear factor kappa B
NSCC	Non-stem cancer cell
P2Y	Purinergic receptor
PBS	Phosphate-buffered saline
PCD	Programmed cell death
PdG	Patient-derived GBM
PI	Propidium iodide
PLC-β	Phospholipase-Cβ
PIP2	Phosphatidylinositol biphosphate
ROS	Reactive oxygen species
RVs	Resistant variants
RTKs	Receptor tyrosine kinases
TKIs	Tyrosine kinase inhibitors
TMZ	Temozolomide
TNF	Tumor necrosis factor

ORIGINAL PUBLICATIONS

- Publication I P. Doan, A. Musa, N. R. Candeias, F. Emmert-Streib, O. Yli-Harja and M. Kandhavelu. "Alkylaminophenol Induces G1/S Phase Cell Cycle Arrest in Glioblastoma Cells Through p53 and Cyclin-Dependent Kinase Signaling Pathway." *Frontiers in pharmacology* 10 (2019): 330
- Publication II P. Doan, A. Musa, A. Murugesan, V. Sipilä, N. R. Candeias, F. Emmert-Streib, P. Ruusuvoori, K. Granberg, O. Yli-Harja and M. Kandhavelu. "Glioblastoma Multiforme Stem Cell Cycle Arrest by Alkylaminophenol through the Modulation of EGFR and CSC Signaling Pathways." *Cells* 9.3 (2020): 681
- Publication III P. Doan, P. Nguyen, A. Murugesan, K. Subramania, S. K. Mani, V. Kalimuth, B. G. Abraham, B. W. Stringer, K. Balamuthu, O. Yli-Harja and M. Kandhavelu. "Targeting orphan G Protein-Coupled Receptor 17 with T0 ligand impairs glioblastoma growth." *Cancers* 13.15 (2021): 3773
- Publication IV P. Doan, P. Nguyen, A. Murugesan, N. R. Candeias, O. Yli-Harja and M. Kandhavelu. "Alkylaminophenol and GPR17 agonist for glioblastoma therapy: a combinational approach for enhanced cell death activity." *Cells* 10.8 (2021): 1975

AUTHOR CONTRIBUTIONS

- Publication I P. Doan conceived of methods to evaluate the effects of phenolic compounds on GBM, performed biological and biochemical experiments, and conducted experimental statistical analysis. P. Doan wrote the manuscript. A. Musa carried out RNA-seq analysis. N. Candeias synthesized compounds. F. Emmert-Streib contributed to the project's development. O. Yli-Harja and M. Kandhavelu managed and conceived the project. All authors provided critical feedback and helped shape the research.
- Publication II P. Doan conceived of methods to evaluate the effect of phenolic compounds on glioblastoma cancer stem cells, performed biological and biochemical experiments, and conducted experimental statistical analysis. P. Doan and A. Musa wrote the manuscript. A. Musa and V. Sipilä executed computational analysis. A. Murugesan, F. Emmert-Streib, P. Ruusuvoori, K. Granberg, O. Yli-Harja and M. Kandhavelu contributed to the project's development.
- Publication III P. Doan and P. Nguyen conceived of methods to evaluate the properties of T0 as a GPR17 agonist, performed biological and biochemical experiments studying the effect of T0 on GBM cells, and performed experimental data analysis. P. Doan performed RNA-seq experiments and experiments on patient-derived GBM cells. P. Doan and P. Nguyen wrote the manuscript. A. Murugesan and V. Kalimuthu executed the animal study. K. Subramanian, S. K. Mani and B. Stringer performed computational analysis. B. G. Abraham executed protein expression. O. Yli-Harja and M. Kandhavelu managed and conceived the project.
- Publication IV P. Doan conceived the methods to evaluate the effect of the combination of GPR17 agonist and phenolic compound, performed biological and biochemical experiments, and conducted experimental statistical analysis. P. Doan wrote the manuscript. P. Nguyen joined in cytotoxicity assay. A. Murugesan executed the animal study. N. Candeias synthesized compounds. O. Yli-Harja and M. Kandhavelu managed and conceived the project.

1 INTRODUCTION

More than 8 million patients were reported to be killed by cancer in 2014, according to the World Health Organization (WHO), and new cases kept climbing. New cases are estimated to escalate approximately 70% within the next two decades (Stewart and Wild, 2014). According to WHO classification, glioblastoma or glioblastoma multiform (GBM), which is a grade IV tumor, is a prevalent, aggressive brain cancer (Hanif *et al.*, 2017). The current treatment for GBM is the combination of surgical resection with radiation therapy and chemotherapy using temozolomide (TMZ; Temodar®) (Davis, 2016). However, these treatments still bring poor outcomes due to complex pathogenesis such as gene mutation and cellular pathway alteration. The utilization of TMZ remains limited due to the overexpression of O⁶-methylguanine-DNA methyltransferase (MGMT) or the absence of a DNA repair pathway in glioblastoma cells (Hegi *et al.*, 2005). The development of resistance when using existing anti-cancer drugs also produces severe medicinal complications (Li *et al.*, 1999; Rojo *et al.*, 2015). Therefore, identifying novel potent drugs with fewer adverse effects on normal cells with a broad spectrum is necessary to combat the severity of GBM disease progression.

An extensive understanding of the molecular strategy behind the GBM cell response to the anti-tumor compounds and the mechanism of action contributing to chemotherapy resistance may help find and improve the efficacy of glioma chemotherapy. Until now, a broad range of anti-tumor compounds has been studied for treating GBM, such as erlotinib (Van Den Bent *et al.*, 2009), bevacizumab (Friedman *et al.*, 2009), carmustine (Reithmeier *et al.*, 2010), and kaempferol (Sharma *et al.*, 2007). These compounds have been reported as apoptosis inducers in GBM cells, thus leading to cell cycle arrest. Over the past few decades, abundant attempts have been made to study the mode of induction of DNA damage by chemotherapy. A previous study showed that the DNA damage checkpoint increases the DNA repair property, thus contributing to glioma chemotherapy resistance (Erasimus *et al.*, 2016). Although GBM cells have a complex genetic heterogeneity, typical molecular transduction pathways are found to be modulated, including Bcl-2 family members, cyclin-dependent kinases, phosphatidylinositol-3-kinase/Akt,

caspases, nuclear factor kappa B (NF- κ B), and mitogen-activated protein kinase (MAPK). Modulating these signaling pathways results in the alteration of cellular biological processes and functions by deregulation of genes and proteins. For instance, sorafenib helps inhibit GBM growth by regulating the activators of transcription factor 3 (STAT3; Tyr705) and phosphorylated signal transducers (Yang *et al.*, 2010). Therefore, it is noteworthy to have an insight study on the mechanism of how anti-tumor compounds play a role in GBM cells. Besides the understanding of glioblastoma's response, the presence of cancer stem cells having the ability to initiate tumor progression in patients is another obstacle that needs to be addressed.

Phenolic compounds are promising structural units that have been identified as possessing valuable features, e.g., being anti-tumor, anti-bacterial, anti-viral, and anti-inflammatory, in developing therapeutic compounds (Selassie *et al.*, 1999; Cai *et al.*, 2004; Nandi, Vracko and Bagchi, 2007). For example, eugenol dimers demonstrate anti-cancer activities on primary melanoma cell lines (Pisano *et al.*, 2007). Digalloylresveratrol (DIG) inhibits HT-29 cell growth, a human colorectal adenocarcinoma cell line, by disturbing the cell division and prohibiting the progression of the S phase from entering G2/M (Bernhaus *et al.*, 2009). The FDA has approved several compounds derived from phenols such as paclitaxel (Miller *et al.*, 2007), vincristine (Von Pawel *et al.*, 1999), or omacetaxine (Alvandi *et al.*, 2014). The FDA also accepts phenols containing alkylaminophenol moieties like hycamtin and amodiaquine as anti-cancer agents (Creemers *et al.*, 1996; Salentin *et al.*, 2017). Although the anti-tumor property of phenolic derivatives has been demonstrated against different human cancers, their cytotoxicity and signaling pathway response on brain cancer are still mysterious.

Currently, advancement in the analysis of cellular signaling pathways or signal transduction pathways has paved the way for exploring possible cancer therapies. Understanding the interaction between cell-cell, cell-matrix, and the receptor-ligand binding mechanism could explain the behavior of cancer cells and drug utilization in cancer therapy. Targeting the receptor tyrosine kinases (RTKs) is one of the novel GBM therapies based on the signaling pathway (Ren, Yang and Rainov, 2008). Many ligands targeting RTKs, such as erlotinib (Prados *et al.*, 2009), gefitinib (ZD1839/Iressa) (Stea *et al.*, 2003), vatalanib (PTK787), sorafenib and tivozanib (Gerstner *et al.*, 2011), have been tested to improve the treatment of GBM. However, most of these molecules have failed in clinical trials to show anti-tumor responses.

On the other hand, G protein-coupled receptors (GPCRs) are important targets for current drugs and drug discovery. Several preclinical studies have shown the efficacy of GBM treatment on GPCR-based therapies. For instance, vismodegib has been clinically approved in basal cell carcinoma treatment (Axelson *et al.*, 2013). Antagonist receptor CXCR4 has also been tested in the clinical phase to treat GBM (Lv *et al.*, 2015). However, the diversity of the GPCR family, along with the complexity in the GPCR signaling pathway, challenges its usage for discovering anti-cancer drugs. In fact, approximately 140 or even more GPCR and their target ligands are still unidentified (Levoye *et al.*, 2006). Hence, the deorphanization of GPCRs is recognized as a promising approach for developing cancer treatments that identify the specific ligand for GPCRs. Among the vast majority of GPCRs, GPR17 is identified as a possible candidate, which shows as a promising target to treat brain injury (Lecca *et al.*, 2008). In addition, a novel ligand T0, a GPR17 agonist, has been described to acquire a strong binding activity compared to the known GPR17 agonist, MDL 29,951. T0 induces GPR17 signaling pathway and leads to the inhibition of a secondary messenger, cAMP (Saravanan *et al.*, 2018). Due to the high expression of GPR17 in glioblastoma, it implies the crucial role of GPR17 receptor in GBM. Thus, this suggests that T0 can be used to develop a novel therapy for GBM treatment.

Recently, combination therapy, a strategy of combining two or more therapeutic agents, has grasped more attention in cancer therapy. Combination therapy improves the probability and the magnitude response of tumor cells to the drugs (Mokhtari *et al.*, 2017). Several cancer therapies are based on combining drugs, which could modulate different targets. Combinatorial therapy is mostly based on the synergistic effects of the potential therapeutic agents in cell lines or animal models. It is noted that the administration of combinatorial treatment could increase cytotoxicity remarkably since several pathways are targeted. Also, applying combination treatment reduces the dosage-dependent side effects of each single therapeutics agent (Albain *et al.*, 2008; Mokhtari *et al.*, 2013). In GBM treatment, several combinatorial trials have been tested so far and resulted in improving the anti-cancer efficacy; for example, the combination of bevacizumab and TMZ in GBM xenograft models (Mathieu *et al.*, 2008), bromodomain inhibitor and TMZ (Lam *et al.*, 2018), or anti-PD-1 and TMZ (Park *et al.*, 2019). Thus, it is noteworthy to develop the strategy of combining drugs to produce a synergistic effect in treating GBM.

In this work, we have evaluated the anti-tumor characteristic of novel alkylaminophenols, previously reported as an apoptosis inducer with a potential

anti-cancer property on osteosarcoma (Doan *et al.*, 2016, 2017; Karjalainen *et al.*, 2017). In parallel, we aim to find the potential GPR17 agonist that could activate the GPR17 signaling pathway and induce GBM cell death. We have also investigated the potential anti-tumor property of the combination therapy utilizing alkylaminophenol and GRP17 agonist-T0 simultaneously. The in-depth mechanism of action and targeted signaling pathways of the combinatorial compounds have also been studied to explore the promising drug for treating GBM.

2 REVIEW OF THE LITERATURE

Cancer is an aggressive disease and causes high mortality worldwide. Brain cancer is known to have some of the most aggressive tumors among many cancers. Understanding current treatments as well as the pros and cons of each treatment helps to identify efficient therapy. In the past, people knew how to use several natural substances from plants to prevent or cure some types of cancer. In the early 20th century, using compounds as chemotherapy started to develop and grasped scientists' attention. The fundamental objective of chemotherapy is to inhibit cancerous cell growth thus leading cells to be subjected to programmed cell death mechanisms. Thus, research on those drug-like compounds and their in-depth mechanisms to target cancer cells is necessary to improve current treatments. This chapter presents the overview of glioblastoma and its current treatment options, as well as phenolic compounds and the GPR17 agonist as new drug-like compounds that can inhibit glioblastoma cell growth. Moreover, a short description of programmed cell death mechanisms and crucial signaling pathways that might be targeted upon phenolic compounds and GPR17 agonists will be presented to clarify how drug-like compounds work on glioblastoma.

2.1 Glioblastoma and current treatment options

2.1.1 Glioblastoma (GBM)

Glioblastoma is reported to be the most aggressive brain cancer. Glioblastoma is classified into a group of tumors called astrocytomas, astrocytes being groups of cells with a star-like shape, which support and nourish nerve cells or neurons. Astrocytoma growth and replication happen quite fast inside the brain; however, astrocytoma of a tumor barely expands to other parts of the body. GBM is also identified as astrocytoma at grade IV. Grades of tumors are defined from I to IV based on the different levels of their morphology in comparison to normal cells. The morphological difference helps to evaluate the growth rate and the spreading rate

of the tumor cells. The grade IV astrocytoma is recognized as the most aggressive and fastest-growing tumor type; thus, it can quickly spread throughout the brain. GBM is often found in the frontal and temporal lobes of the brain. They also grow in the stem of the brain or cerebellum and the spinal cord (Hanif *et al.*, 2017).

Glioblastoma is categorized into primary and secondary GBM. The primary GBM (or *de novo*) is more aggressive and more common, occurring in 60% of lesions, while the secondary GBM is less common and slower growing, occurring in 40%. This secondary GBM usually develops from a lower-grade astrocytoma, and it affects about 10% of GBM patients under the age of 45 (Ostrom *et al.*, 2014; Theeler and Gilbert, 2015).

It is reported that the average survival time of GBM patients getting treatments of surgery, radiotherapy, and chemotherapy is about 15–16 months. However, responses to treatment differ from patient to patient; thus, some patients may survive up to five years or more. Notably, children with higher-grade tumors tend to have a longer survival time than adults. About 25% of them can live for more than five years (Tamimi and Juweid, 2017).

2.1.2 Current treatment options for GBM

2.1.2.1 Surgery

In cancer treatment, surgical diagnosis is a crucial approach for performing histopathological confirmation. Surgery also improves prognosis when the pre-intervention functional activity of patients is maintained properly because the level of resection is one of the decisive factors contributing to survival (Lacroix *et al.*, 2001; Bloch *et al.*, 2012). Thus, surgery is considered a curative modality for GBM, especially in treating low-grade GBM (Eseonu *et al.*, 2017).

It is reported that gross total resection of low-grade GBM helps to increase survival rate by 160% while the survival rate of high-grade GBM increases to 200% compared to patients subjected to subtotal resection (McGirt *et al.*, 2009; Chaichana, Jusue-Torres, Navarro-Ramirez, *et al.*, 2014). Indeed, according to a study conducted on 41 000 diagnosed GBM cases, gross total resection increased 61% in likelihood of one-year survival compared to subtotal resection (Brown *et al.*, 2016). Although a complete resection of high-grade GBM is an impossible task given

the presence of microscopic infiltrative cells, an eradication of approximately 90% without interfering with a patient's functional pathway is a desired target of neurosurgeons. A subtotal resection of 70% has indicated significant enhancement in seizure control and survival rate. If complete eradication is unachievable, supramarginal resection is another option. The supramarginal resection is a resection of the tumor mass with the help of imaging technology to enhance tumor mass display (Chaichana, Jusue-Torres, Navarro-Ramirez, *et al.*, 2014).

With the development of neurosurgical oncology, it is possible to obtain a maximal cytoreduction while maintaining the functional pathway of patients (Ronkainen and Tervonen, 2006). Radiographic analysis, including intraoperative magnetic resonance imaging (iMRI), is crucial for determining suitable surgical intervention for GBM patients. iMRI helps to define the exact tumor location, edema, and eloquent area involved. Moreover, using iMRI can determine the prognosis of patients having butterfly GBM, a tumor involving both hemispheres. Chichana et al. reported that patients having butterfly GBM show a lower survival rate of approximately 7 months compared to 11.6 months in patients without butterfly GBM (Chaichana, Jusue-Torres, Lemos, *et al.*, 2014). Thereby, iMRI has become a crucial tool that can obtain real-time images of a particular patient's brain during the surgical operation. Thus, this enables the evaluation to define whether the resection was achieved completely before closing the surgical operation. Although iMRI possesses abundant benefits, its drawbacks must also be considered; it is time-consuming and high cost (Ronkainen and Tervonen, 2006).

2.1.2.2 Radiation therapy

Radiation therapy has been widely used to treat many cancers, including GBM. In the last few decades, it was reported that radiation therapy could improve survival time from approximately 3.5 months to 9.0 months with the combination of surgery and supportive care (Shapiro *et al.*, 1989). Shapiro et al. reported that "the standard dose for GBM is 60 Gy at 1.8–2 Gy per fraction." In addition, Davis's study indicates a failure in prolonging GBM patients' survival of using radiotherapy with higher than 60 Gy. Therefore, to achieve the benefits of radiation therapy, several factors such as dose, target delineation, fractionation, and combination of agents have been studied constantly to improve the efficacy (Davis, 2016).

It is noted that GBM is one of the cancers on which it is difficult to perform radiation therapy since GBM can infiltrate throughout the brain, despite rare

metastasis to other parts beyond the central nervous system (CNS). Moreover, malignant cells are able to migrate significantly; however, the majority of tumor recurrence happens within the original tumor site. Additionally, Halperin et al. (Halperin *et al.*, 1989) reported that while performing whole-brain radiation therapy would prolong the patient's survival, it would also increase the incidence of treatment-induced brain injury in comparison with regional radiation therapy (Halperin *et al.*, 1989). Hence, applying radiation therapy is more likely to reduce tumor burden and decrease disease development.

2.1.2.3 Chemotherapy

Many compounds have been extensively utilized in the treatment of cancer. In GBM treatment, chemotherapy has been studied and evaluated for patients with primary GBM and patients with recurrent disease. Combination of radiation therapy and semustine or carmustine did not yield any enhancement of survival. Indeed, a study performed on 3 000 patients receiving radiotherapy with the support of those compounds demonstrated only a 6% increase in survival rate compared with those receiving single-treatment radiation therapy (Fine *et al.*, 1993). After that, the introduction of using temozolomide has become a promising reagent as chemotherapy for GBM, especially for recurrent disease. TMZ shows excellent oral bioavailability, no cumulative myelotoxicity, and no significant drug-drug interaction. Thus, TMZ has been used in combination with other chemotherapies. It was examined that using TMZ alone with 150–200 mg/mg² or TMZ with 75 mg/mg² combined with 60 Gy in 30 fractions improved the survival rate by about 2.5 months. Moreover, the long-term survivorship was also increased from 10.4 to 26.5% (Stupp *et al.*, 2005).

Along the same lines, previous research had found an interaction of the MGMT (methylguanine-DNA methyltransferase) protein expression and the efficacy of using TMZ as chemotherapy for GBM treatment. There is a significant enhancement in two-year survival rate as well as median survival when using TMZ for patients having methylated MGMT. Indeed, patients with a methylated MGMT promotor revealed an increase of median survival to 21.7 months when they were treated with both TMZ and radiation therapy. In comparison, patients who got radiation therapy alone had a median survival of 15.3 months. However, in the same treatments as previously, the median survival of patients without a methylated MGMT promotor did not change significantly (Hegi *et al.*, 2005, 2008). This implies

that MGMT methylation has a crucial function as a prognostic factor in GBM treatment with TMZ. Although using TMZ shows increasing median survival, its effectiveness in a subset of patients having methylation MGMT has shown a big gap for GBM treatment. Thus, finding a novel drug-like compound achieving a better effect has grabbed the attention of many scientists.

2.2 Phenolic compounds

In the early 20th century, chemotherapy started being used in cancer treatment. Chemotherapy is one of the methods of destroying cancer cells using chemical compounds. This method works based on the growth-inhibitory effect and division of cancer cells. Many compound derivatives, including phenols from natural and synthetic pathways, have proven anti-cancer ability. This section describes both natural and synthetic phenol derivatives having anti-cancer activity.

2.2.1 Natural phenolic compounds

Phenolic compounds, or phenols, are defined as chemical compounds containing single or multiple (-OH) groups bonded with one or more than one aromatic ring. In the past, phenols were identified in many plant species and many microorganisms. Phenols also have been synthesized industrially for the past several decades (Kuehne and Hesse, 1993; Dai and Mumper, 2010; Vijendra Kumar *et al.*, 2014).

Phenolic compounds in plant species are acknowledged as one of the most abundant types of secondary metabolites, given more than 8000 phenols. The discovery also includes simple and complex structures such as phenolic acid and tannins, respectively (Michałowicz and Duda, 2007). In the plant kingdom, phenolic compounds play different roles; for example, phenols can defend against ultraviolet radiation or act as immune barriers fighting pathogens, parasites, and predators. Moreover, phenols can be involved in plants' growth and reproduction process or function as plant pigments (Manach *et al.*, 2004). Furthermore, phenols have been studied and used widely in many fields, including chemistry, biology, agriculture, and medicine. Specificity, phenolic compounds have been applied as drug-like compounds because of their antibacterial and anti-tumor properties (Duvoix *et al.*, 2005; Shankar, Ganapathy and Srivastava, 2007; Casaburi *et al.*, 2013).

The properties of phenolic compounds have been intensively examined against several diseases, including cancers (Cole *et al.*, 2005; Wang *et al.*, 2012; Carocho and CFR Ferreira, 2013; Su *et al.*, 2019; Duan *et al.*, 2020). One example of candidates with an anti-cancer effect is kaempferol, which is extracted from berries. Kaempferol demonstrated inhibitive activity against human prostate, colon, and breast cancers (Seeram *et al.*, 2006; Yoshida *et al.*, 2008; Zhang *et al.*, 2008; Han *et al.*, 2018). Flavonoid is a representative group of phenols having strong anti-cancer properties. Citrus flavonoid was reported to slow down the growth of leukemia cells (Manthey, Grohmann and Guthrie, 2001). Furthermore, phenols also contribute to the modulation of various enzyme and cell receptor activity; therefore, other activities of phenolic compounds are recommended to be explored further to gain more knowledge about their roles in controlling disease development (Kampa *et al.*, 2004; Labrecque *et al.*, 2005; Wang *et al.*, 2012; Soares *et al.*, 2013).

2.2.2 Synthesized phenols

Despite the fact that natural phenols have been proven to be potentially effective compounds for inhibiting cancer, chemically synthesized phenols have also been studied to produce new anti-cancer compounds (Gomes *et al.*, 2003; Torres de Pinedo, Peñalver and Morales, 2007). For instance, several phenolic compounds having a structure similar to gallic and caffeic acids have been proven as potential candidates that can affect the growth of human cervix adenocarcinoma cells (HeLa) (Fiuza *et al.*, 2004). The IC_{50} of these caffeic and gallic acids varies from 8 to 12 μM on HeLa cells after 48-hour treatment. In this study, the authors also claim that a slight variation of phenol structure affects its biological activity (Fiuza *et al.*, 2004). Thereby, the investigation of other phenolic derivatives would give more chances to find alternative cancer chemopreventive agents.

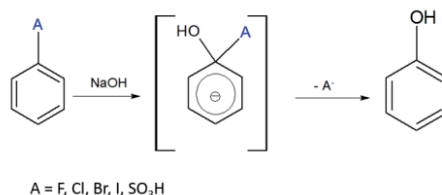


Figure 1. Phenols can be produced via replacement of functional groups

Until now, many efforts have been directed at the synthesis of phenol derivatives. At the very first stage, phenols can be produced via "displacement of functional groups" (Figure 1). Alkaline fusion is the most popular approach to producing phenols industrially. The process involves treating aryl sulfonic acids with potassium hydroxide at high temperatures (>270 °C) to deliver phenols. Moreover, phenols can be synthesized from nitrogen derivatives via hydrolysis of arylamines in acidic conditions and high temperatures or synthesized by Bucherer reaction in which the "amino group of naphthylamines is replaced by hydroxyl group by treatment with aqueous bisulfite" (Rappoport, 2003).

Oxidation is another common method of synthesizing phenols. One of the most important reactions in this method is the hydroxylation with peroxides or hydrogen peroxides. However, in the reaction with hydrogen peroxide, control of hydroxylation is necessary to avoid further oxidation. For example, substitution at the *meta* position of a nitrobenzene derivative with electro-withdrawing groups (e.g., A=CF₃, C₆H₅, SO₂Me, NO₂, CN, and halogens) results in the formation of the corresponding *p*-nitrophenols (Rappoport, 2003). Nowadays, several methods can be used to produce phenolic compounds, such as displacement of functional groups, oxidation, condensation, cycloaddition, and rearrangement.

2.2.3 Alkylaminophenols

Alkylaminophenols belong to the group of synthesized phenols produced via the Petasis borono–Mannich reaction (Roman, 2015; Biersack *et al.*, 2018). Previously, alkylaminophenols were described as quinone methides precursors, and they have a function to react with biomacromolecules (Thompson *et al.*, 1993; Weinert *et al.*, 2006). Recently, several FDA-approved drugs containing alkylaminophenol moieties, such as topotecan as a chemotherapeutic agent and amodiaquine as malaria treatment (Olliaro *et al.*, 1996; Pommier, 2006).

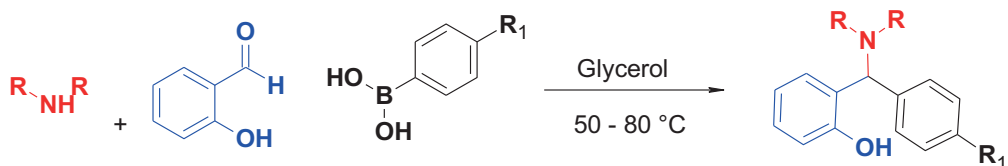
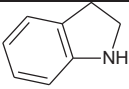
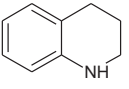
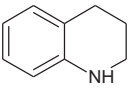


Figure 2. Preparation of alkylaminophenols via Petasis borono–Mannich reaction

Table 1. Alkylaminophenols and their IC₅₀ values on osteosarcoma cells

Compound	R ¹	Amine	IC ₅₀ value
HNPMI	Me		74.0 ± 5.7 (Doan <i>et al.</i> , 2016)
THMPP	OMe		50.5 ± 3.8 (Karjalainen <i>et al.</i> , 2017)
THTMP	Me		36.6 ± 2.5 (Doan <i>et al.</i> , 2017)

Recently, other novel alkylaminophenols were synthesized successfully using the Mannich reaction (Figure 2). Interestingly, these alkylaminophenols including 2-((3,4-dihydroquinolin-1(2H)-yl)(p-tolyl)methyl)phenol (THTMP), 2-((1,2,3,4-tetrahydroquinolin-1-yl)(4-methoxyphenyl)methyl)phenol (THMPP), and N-(2-hydroxy-5-nitrophenyl)(4'-methylphenyl)methylindoline (HNPMI) have proven their ability to induce apoptosis of osteosarcoma cells (Table 1). Although alkylaminophenols have revealed their promising anti-tumor activity on different cancers, a study in their underlying mechanism against brain cancer is still limited.

2.3 G protein-coupled receptor (GPCR) and G protein-coupled receptor 17 (GPR17)

2.3.1 G protein-coupled receptor

G protein-coupled receptors (GPCRs) are defined as a large family of cell surface receptors that respond to different external signals, including light energy, peptides, lipids, sugars, and proteins (Ji, Grossmann and Ji, 1998). When these molecules bind to a GPCR, G protein is activated, triggering the production of various second messengers.

GPCR is composed of α , β and γ subunits. Without the binding of ligands, GPCR is in the inactive state in which α subunit binds to the nucleotide guanosine

diphosphate (GDP) and forms a complex with β and γ subunits. When a ligand binds to GPCR, GPCR is active, leading to the exchange of GDP to nucleotide guanosine triphosphate (GTP) at the α subunit. Then, the complex of α subunit and GTP is disassociated with β and γ subunits as shown in Figure 3 (Hamm, 1998). When GPCR is activated, various cellular responses occur through the activation of secondary messengers such as Ca^{2+} , cAMP, diacylglycerol (DAG), and inositol 1,4,5-trisphosphate (IP3) (González-Espinosa and Guzmán-Mejía, 2013).

As shown in Figure 3, G protein is categorized into 4 families, including Gas, Gai/o, $\text{G}\alpha_{12/13}$ and $\text{G}\alpha_q/11$. Gas leads to cAMP increase via activation of adenylyl cyclase, while Gai/o functions in inhibiting adenylyl cyclase activity, thus decreasing cAMP level (Taussig, Iñiguez-Lluhi and Gilman, 1993). Besides, $\text{G}\alpha_q$ stimulates phospholipase-C β , converting phosphatidylinositol biphosphate (PIP2) to diacylglycerol (DAG) and inositol 1,4,5- triphosphate (IP3), thus resulting in either accumulation of calcium or elevation of the calcium level in the cytosol (Kamoto *et al.*, 2015). $\text{G}\alpha_{12/13}$ functions in controlling the activity of GTP-binding protein involved in Ras and Rho families; however, its downstream signaling has not been fully discovered (Kozasa *et al.*, 1998). Regarding the β and γ complex, the complex is associated with PI3 kinase, Rho and K^+ , and Ca^{2+} channels (Dorsam and Gutkind, 2007).

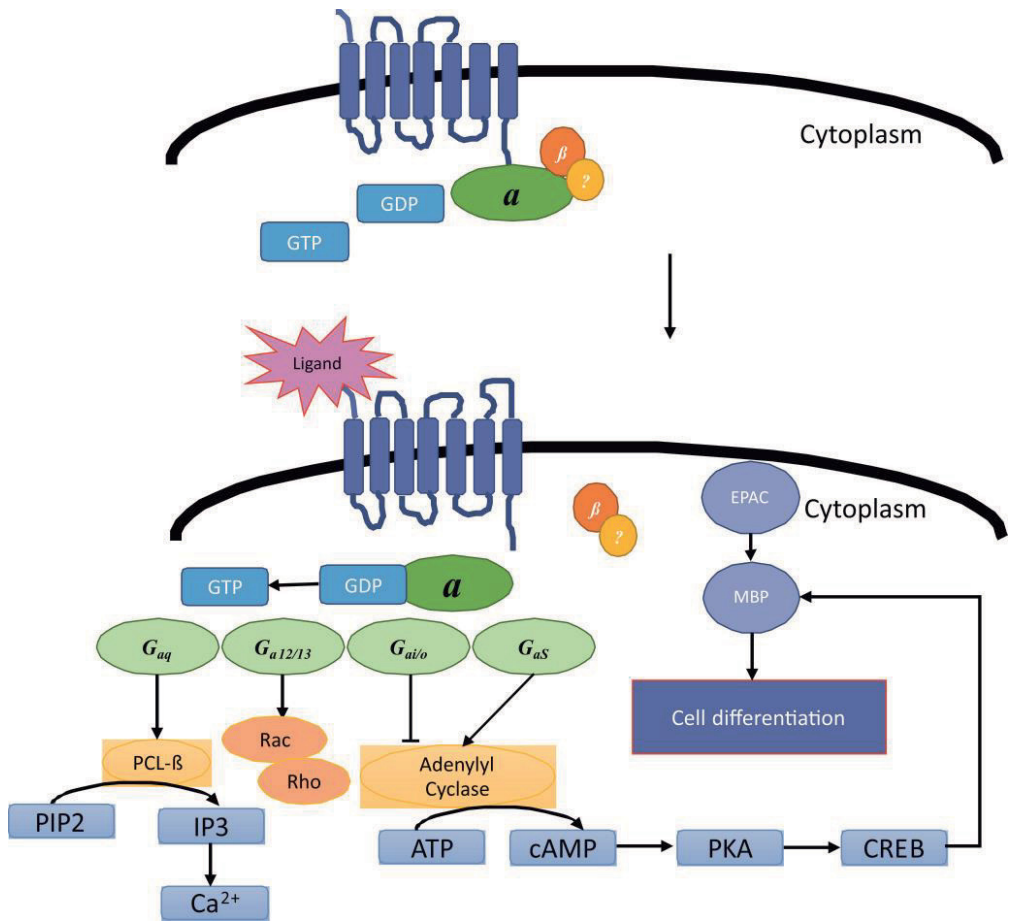


Figure 3. The diversity of G protein family and their downstream signaling processes.
 Abbreviations: GDP: guanosine diphosphate, IP3: inositol 1,4,5- triphosphate, PIP2: phosphatidylinositol bisphosphate, PLC-β: phospholipase-Cβ.

2.3.2 GPR17

GPR17, a member of the GPCR family, is known as a receptor at a phylogenetic location between the receptor families: purinergic (P2Y) and cysteinyl leukotriene (CysLT) (Ciana, Fumagalli and Trincavelli, 2006). GPR17 has a similar structure to GPCR, which contains seven transmembrane proteins joined by intracellular and extracellular loops having N-terminal and C-terminal segments, respectively. GPR17 has been discovered to be greatly present in CNS and in other tissues/organs that undergo ischemic damage, e.g., heart, brain, lung, kidney, and liver (Ciana, Fumagalli and Trincavelli, 2006).

Orphan GPR17 has been recognized as a possible target for developing brain injury therapy (Franke *et al.*, 2013). Many studies have indicated an important role of GPR17 in oligodendrocyte differentiation and maturation (Ceruti *et al.*, 2011). Moreover, GPR17 has been noted to be highly expressed in traumatic brain injury, thus indicating the ability involved in the neurorepair process when coupling with brain cell markers (Franke *et al.*, 2013). Indeed, GPR17 is found to be upregulated in neurons and highly expressed in microglia and astrocytes when the brain is injured. However, the intracellular signaling mechanisms of the GPR17 receptor are still being explored for extensive understanding. For example, ligand binding to GPR17 is still controversial; some state that they belong to the P2Y ligand group, while others believe they are CysLT ligand groups. Therefore, finding the GPR17 ligand formula is still in progress in order to develop a novel drug for CNS.

Several agonists and antagonists which can activate and deactivate GPR17 have been developed recently, like stromal cell-derived factor 1 (SDF-1) (Parravicini *et al.*, 2016) or oxysterols (Sensi *et al.*, 2014). Notably, agonist 2-carboxy-4,6-dichloro-1H-indole-3-propionic acid (MDL 29,951) has recently been recognized as a promising GPR17 agonist in primary oligodendrocyte (Köse *et al.*, 2014). Köse *et al.* indicate that MDL 29,951 activates GPR17 via G α i and G α q signaling pathways, subsequently decreasing cAMP and intracellular calcium levels. Another research group also reports that GPR17 is coupled to G α i and Gq proteins in GPR17- transfected 1321N1 cells (Buccioni *et al.*, 2011). Further downstream signaling pathways are affected by modulating cAMP and calcium signaling pathways, such as an exchange protein EPAC and protein kinase A (PKA) (Figure 3). Hence, the oligodendrocyte maturation is inhibited upon the binding of MDL 29,951, GPR17 agonist (Katharina Simon *et al.*, 2016).

The development of computational biology allows us to understand the binding of ligands with a receptor. Therefore, ligands with higher binding affinity have been analyzed to minimize the workload and time-consuming screening. Using a virtual screening and docking study, the novel ligands, GPR17 agonists, have been further developed to be a promising treatment for GBM. The need to discover novel molecules capable of reproducibly activating GPR17 is a crucial mission in seeking GBM therapy.

2.4 Cell cycle and programmed cell death

Although cell death is an indispensable event in normal cell cycles, it is important in cell pathology because cell death mechanisms interfere with homeostasis. An abnormal amount of cell death leads to various severe diseases, which have not been treated completely yet (Raff, 1992). For example, the following diseases are caused by dysfunction of cell death mechanisms: autoimmune syndromes, Alzheimer's and Parkinson's diseases, AIDS, and cancer (Fischer and Schulze-Osthoff, 2005). Therefore, many efforts have been made to research and discover effective therapeutic treatments to address these tremendous problems.

During the past few decades, physiological cell death has been extensively observed and studied in multicellular organisms (Zörnig *et al.*, 2001). However, physiological cell death still has not been well defined, especially for single-cell organisms, despite the rising evidence of several forms of physiological cell death found in unicellular organisms like bacteria (Yarmolinsky, 1995). Prior to studying cell death mechanisms, it is better to have an overview of the cell cycle to know how a cell grows and divides. Moreover, understanding details of cancerous cell cycle regulation aids in more in-depth knowledge of programmed cell death; thus, it is one step closer to exploring an effective cancer treatment.

2.4.1 Cell cycle

The cell cycle is an essential mechanism to maintain cell life, and it varies among species even though they share the same characteristics at a certain level. The cell cycle process helps to control the replicating DNA and proliferating, arresting at a distinct phase or continually differentiating. The regulation of the cell cycle depends on several external and internal stimuli. The cell cycle consists of gap 1 (G1), synthesis (S), gap 2 (G2), and mitosis (M) phases (Cooper and Hausman, 2007) (Figure 4).

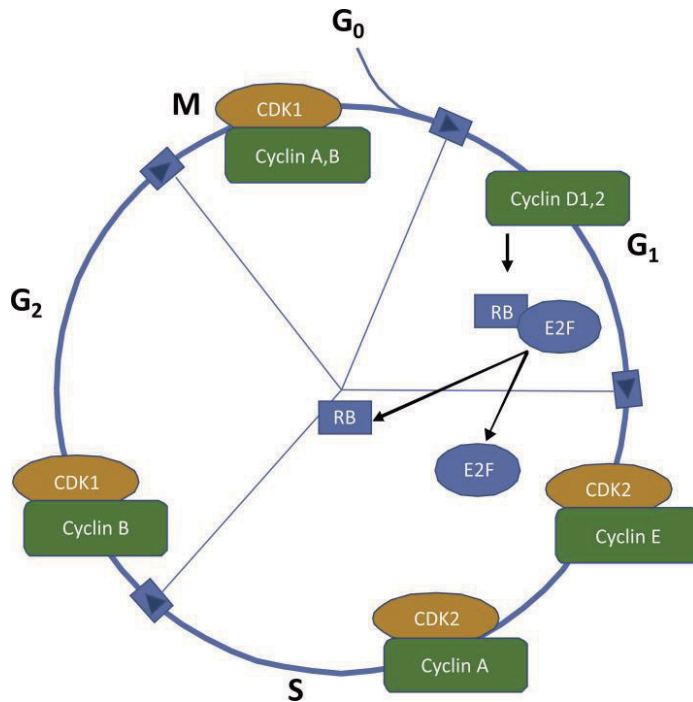


Figure 4. Illustration of cell cycle of mammalian cell.

The cell cycle takes place in an appropriate order in an individual cell. To enter another phase, cells require cell cycle checkpoints called G₁ checkpoint, G₂ checkpoint, and M checkpoint for the transitions of G₁-S, S-G₂, and G₂-M, respectively (Barnum and O’Connell, 2014). Signal transduction pathways of checkpoints that assist in regulating the order of progression and integrate the cell cycle with DNA repair are complicated. Indeed, checkpoints function to interrupt the cell cycle and arrest it when damaged genomes or any inappropriate events are detected. Subsequently, the cells undergo programmed cell death (apoptosis), which is discussed in detail in section 2.4.2. To perform the role, the checkpoint control must detect the damage and transduce the signals. Cyclin-dependent kinase (CDK) proteins and their correlated protein play crucial functions in cell growth and proliferation during the cell cycle and checkpoints. It is reported that CDK1 and CDK2 function in monitoring S and G₂ transitions that can either activate the DNA damage checkpoint or initiate DNA repair process (Weinert, 1997). CDKs are categorized into cell cycle CDK targeting cell cycle progress and transcriptional CDK for mRNA synthesis progress (Malumbres and Barbacid, 2009). The cell cycle CDK includes CDK1, CDK2, and CDK4/6, which play essential roles in cell cycle machinery. CDK4/6 associates with cyclin D1,2, while CDK2 associates with cyclin E to regulate G₁/S

transition (Harbour *et al.*, 1999). CDK1, together with cyclin B and cyclin A, help regulate S checkpoint (Gopinathan, Ratnacaram and Kaldis, 2011).

In addition to CDKs and their cyclin family, the p53 signaling pathway also plays a vital role in cell cycle regulation. Indeed, p53 is predominantly active in G1 phase (Levine, 1997). When the DNA of a cell is damaged, p53 triggers the formation of p21, leading to cell cycle arrest at G1. Furthermore, p53 is able to inhibit CDK2 and cyclin D complex, resulting in a delay in G1/S transition (Schneider, Montenarh and Wagner, 1998). Notably, the gene which encodes for p53 protein is commonly mutated in cancerous cells. Consequently, mutated p53 does not have the function to arrest G1 phase under DNA damage response; thus, the damaged DNA is passed to the daughter cells and contributes to cancer development (Vermeulen, Berneman and Van Bockstaele, 2003).

Given the crucial roles of p53 and CDK-cyclin complex, these factors need to be investigated to observe and monitor the cell cycle. Although much effort has been given to studying cell cycle protein regulators, their whole process is still not fully discovered due to multiple crosstalk signaling pathways. Despite these challenges, CDK-cyclin complex and p53 are still potential targets contributing to novel therapeutic development in cancer treatment.

2.4.2 Apoptosis in programmed cell death

Programmed cell death (PCD) is recognized as programmed apoptosis, necrosis, and autophagy in which the cell is nominated to be dead in any pathologic pattern by an intracellular factor. In this section, apoptosis is the focus since it is the most critical pathway of cell death. PCD keeps the balance normal between survival and cell death (Zörnig *et al.*, 2001). To explain the relation of the PCD signaling pathway and the development of anti-cancer therapeutic treatment, in this section, a brief introduction of apoptosis, which is associated with the regulation of cells in cancer, is presented. Deep knowledge of PCD increases the chances of finding potent chemotherapeutic agents.

Apoptosis is known as a process that depends on energy and is controlled by genes in which the organisms remove damaged cells or unnecessary cells (Schulze-Osthoff *et al.*, 1998; Kam and Ferch, 2000). In 1972, apoptosis was first reported by Kerr *et al.*, and it is considered the most dominant type of cell suicide among three types of PCD (Kerr, Wyllie and Currie, 1972). Apoptotic cell death occurs typically

within development and aging. This mechanism occurs when the cell needs to defend in some immune reactions or when damaged cells appear due to noxious agents or diseases (Norbury and Hickson, 2001). The morphological changes of apoptotic cells may be revealed by microscopy. "Cell shrinkage and chromatin condensation" are the most specific characteristics to recognize apoptotic cells. Cell shrinkage results in a smaller size of cell; moreover, "the cytoplasm is condensed, and the organelles are more tightly packed." After that, blebbing of plasma membranes occurs, forming apoptotic bodies containing different cell fragmentations such as cytoplasm and organelles. These organelles are enclosed with intact plasma membrane; thus, the integrity of such organelles is not damaged (Figure 5). In the end, these apoptotic fractions are phagocytosed by macrophages or neoplastic cells and parenchymal cells. It is also found that apoptosis does not lead to inflammatory reactions for the following reasons. Firstly, the organelle integrity is maintained so that cellular contents are located inside the plasma membrane and cannot leak into the surrounding environment. Secondly, macrophages quickly digest these apoptotic bodies so that further development, like necrosis of apoptotic bodies, is prevented. Lastly, there are no anti-inflammatory cytokines produced by the engulfing cells (Kurosaka *et al.*, 2003; Pfeiffer and Singh, 2018; Carneiro and El-Deiry, 2020).

Apoptosis mechanisms involve two essential pathways: extrinsic and intrinsic pathways (Figure 6). It is also indicated that the two mentioned pathways somehow associate together and could affect each other (Igney and Krammer, 2002). Both intrinsic and extrinsic pathways meet at the execution pathway. Generally, the execution is commenced by the caspase-3 activation resulting in morphological changes, e.g., DNA fragmentation, apoptotic bodies formation. These apoptotic bodies are then further digested by phagocytic cells (Lowe and Lin, 2000; Elmore, 2007; Carneiro and El-Deiry, 2020).

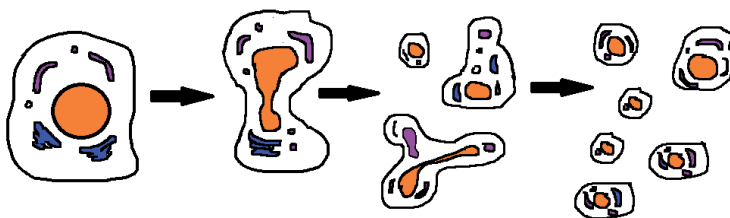


Figure 5. Apoptotic cell death morphological change: blebbing of plasma membrane occurs, forming apoptotic bodies containing different cell fragmentations. These cell fragmentations are enclosed with intact plasma membrane (Rode, 2008).

2.4.2.1 Intrinsic pathway

The intrinsic pathway, or mitochondrial pathway, is initiated by non-receptor mediated stimuli. These stimuli produce intracellular signals, and they affect different targets in the cells. The stimuli initiating the intrinsic pathway might be classified into negative and positive types. Negative signals are those without growth factors, cytokines, and hormones. This type of signal results in the collapse of death programs suppression, thus triggering apoptosis. Alternative stimuli are classified as positive types, including toxins, hyperthermia, hypoxia, free radicals, radiation, and viral infections. Negative and positive stimuli affect the mitochondrial membrane, thus opening the pore of mitochondrial permeability transition (MPT).

Consequently, mitochondrial transmembrane potential (MTP) is lost, cytochrome *c* is released, and caspase-activated DNase (CAD) is released to the cytosol (Saelens *et al.*, 2004). Then, cytochrome *c* activates the mitochondrial pathway independent-caspase via the binding of cytochrome *c* and activates procaspase-9 and Apaf-1, resulting in apoptosome formation (Chinnaiyan, 1999; Hill *et al.*, 2004). The function of procaspase-9 is to activate caspase-9. In addition, when CAD is secreted from mitochondria, it is cleaved by caspase-3, then translocated into the nucleus. Caspase-3 has a function in forming DNA fragmentation and chromatin condensation (Enari *et al.*, 1998). In the intrinsic pathway, the Bcl-2 protein family functions as control and regulation factors of the apoptotic mitochondrial activity (Cory and Adams, 2002). In detail, the Bcl-2 proteins manage the permeability of mitochondrial membranes, and they function as anti-apoptotic or pro-apoptotic factors. Up to now, total 25 genes have been discovered in the Bcl-2 family. The pro-apoptotic proteins of the Bcl-2 family are Bcl-10, Bak, Bax, Bid, Blk, Bim, Bad, and Bik, and the others, such as Bcl-2, Bcl-XL, Bcl-X, Bcl-w, Bcl-XS, and BAG, are also listed as pro-apoptotic proteins. These proteins have tremendously important roles since they can decide whether the cell forces to apoptosis. The scientists had supposed that the fundamental mechanism of the Bcl-2 family functions in controlling cytochrome release. Studies have been conducted, but the actual fact has not been totally proven yet (Elmore, 2007).

2.4.2.2 Extrinsic pathway

Extrinsic signaling is activated by the action of transmembrane receptor activity, which involves the death receptors (tumor necrosis factor (TNF) receptor gene). Therefore, it is also called the death receptor pathway. The TNF receptor functions

to transmit the death signal to the intracellular signaling pathway (Locksley, Killeen and Lenardo, 2001). To date, lots of death receptors and corresponding ligands have been explored, including TNF- α /TNFR1, FasL/FasR, DR3/Apo2L, DR4/Apo2L, and DR5/Apo2L (Chicheportiche *et al.*, 1997; Ashkenazi and Dixit, 1998). Among these pair ligands and receptors, TNF- α /TNFR1 and FasL/FasR are known as the most used for characterizing the extrinsic pathway of apoptosis. Generally, they are groups of receptors that bind to homologous trimeric ligands. The binding of the mentioned two pairs leads to the binding of TRADD protein with FADD and RIP (Hsu, Xiong and Goeddel, 1995; Wajant, 2002), in which FADD correlates to procaspase-8 throughout dimerization of the death domain. After that, a signaling complex, which induces death, is established, thus leading to procaspase-8 activation. The execution pathway (caspase 3) is initiated when caspase-8 is activated (Kischkel *et al.*, 1995). Besides these factors, several other proteins can also trigger extrinsic pathways (Figure 6).

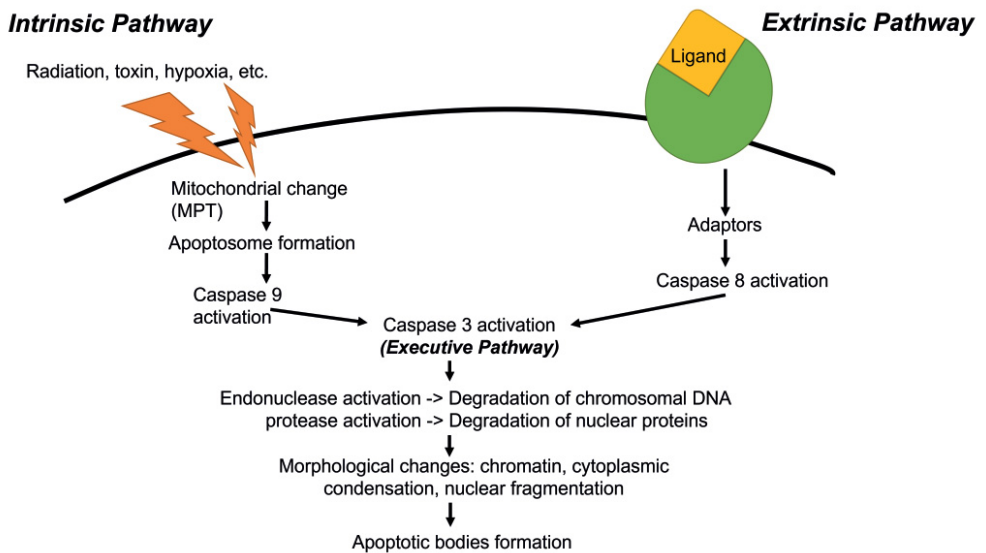


Figure 6. Schematic representation of apoptosis pathways: extrinsic and intrinsic (Elmore, 2007)

2.5 Cancer stem cells (CSCs) and CSC signaling pathways

Although a vast effort has been made in developing cancer treatments, the current treatment strategy has been limited in survival benefits. One reason for this limitation is that current treatment regimens mainly target tumor bulk instead of CSCs (Ayob and Ramasamy, 2018; Najafi, Farhood and Mortezaee, 2019). Conventional cancer therapies combining surgery, radiotherapy and chemotherapy seem to target neoplastic cells, leaving CSCs behind, since these cells are highly resistant to drugs (Jones, Matsui and Smith, 2004; Gottschling *et al.*, 2012). Thereby, eradicating CSCs has been admitted as a promising strategy to develop a more effective cancer treatment. Here, a short introduction of CSCs and their related signaling pathway is provided to better understand CSCs characteristics and, hence, encourage more in-depth studies for novel cancer therapies.

2.5.1 Cancer stem cells

Cancer stem cells (CSCs) are described as a subpopulation of cancerous cells that can be found within tumors. "CSCs possess self-renewal and differentiation ability that can develop and differentiate to all cell types." In cancer treatment, CSCs have been reported to be linked with the increase of resistance to chemo and radiotherapy (Dean, Fojo and Bates, 2005). Moreover, CSCs were found to arise from various sources, including differentiated cells, progenitor cells, and normal adipose-derived stromal cells (Visvader and Lindeman, 2008). To identify and recognize CSCs, cell surface markers have been used commonly in research. Indeed, CSCs have been isolated from a fast-growing tumor mass by identifying the presence of CD24, CD44, and CD133. In addition to cell surface markers, cellular activities including those of aldehyde dehydrogenase (ALDH) and ABCG2 have also been used as biomarkers for identifying CSCs.

CSCs have been recognized as the root of origin and recurrence of cancer; thus, eradicating CSCs is considered a promising means of improving current cancer therapy. In research on eradicating CSCs, various promising approaches were proposed and developed, such as targeting molecular signaling pathways, molecular targeted therapy, and CSC-targeted immunotherapy (Takahashi-Yanaga and Kahn, 2010; Badrinath and Yoo, 2019). Regardless, using any methods, understanding cellular and signaling pathways associated with CSCs is recommended for achieving better outcomes in cancer therapeutic options.

2.5.2 Cancer stem cell signaling pathways

CSCs can manage to avoid cancer treatments due to the dysregulation of signaling pathway networks (Dragu *et al.*, 2015). Recently, various strategies have been conceived aiming to destroy CSCs by focusing on CSC signaling pathways. Many signaling pathways have been reported to be associated with the regulation of CSC characteristics, e.g., Wnt/ β -catenin, Notch, and Hedgehog signaling pathways. Aberrant activation of these pathways could maintain and promote the recurrence of CSCs after the surgical removal of the tumor (Chen, Huang and Chen, 2013). The significant Wnt, Notch, and Hedgehog signaling pathway genes in different cancers are summarized in Table 2.

Table 2. Significant Wnt, Notch and Hedgehog signaling pathway genes in cancer

	Affected genes	Function	Reference
Wnt signaling	APC	Reduced regulatory activity	(Sansom <i>et al.</i> , 2004)
	Axin I and Axin II	Reduced regulatory activity	(Mao <i>et al.</i> , 2001)
	CREBP	Inactive acetyltransferase	(Li <i>et al.</i> , 2007)
	CTNNB1	Enhanced protein stability	(van Schie and van Amerongen, 2020)
	GSK3b	Inactive kinase	(Wu and Pan, 2010)
	LRP5	Loss of repression by DKK1	(He <i>et al.</i> , 2004)
	TCF/L2	Loss of repression	(Cadigan and Waterman, 2012)
Notch signaling	DLL1	Govern cell fate	(Sørensen, Adams and Gossler, 2009)
	DLL3	Suppress cell growth	(Heuss <i>et al.</i> , 2008)

	DLL4	Activate NF-kb signaling	(Williams <i>et al.</i> , 2006)
	JAG1	Promote cell survival	(Katoh and Katoh, 2006)
	JAG2	Promote cell survival	(Casey <i>et al.</i> , 2006)
	Notch1	Proliferation and invasion	(Nicolas <i>et al.</i> , 2003)
	Notch2	Induce tumor	(Lewis <i>et al.</i> , 2011)
	Notch3	Promote proliferation	(Cui <i>et al.</i> , 2013)
	Notch4	Promote proliferation	(Rad <i>et al.</i> , 2016)
	Hes1	Cellular proliferation and differentiation	(Kobayashi and Kageyama, 2010)
Hedgehog	Gli1	Proliferation and metastasis	(Infante <i>et al.</i> , 2015)
	Gli2	Proliferation and metastasis	(Javelaud <i>et al.</i> , 2011)
	Shh	Embryonic development	(Memi, Zecevic and Radonjić, 2018)
	Ptch1	Proliferation and metastasis	(You <i>et al.</i> , 2010)
	SMO	Mediates signal transduction and affects EGFR	(Della Corte <i>et al.</i> , 2015)
	YAP1	Promote proliferation and transformation	(Fernandez-L <i>et al.</i> , 2009)

Wnt/ β -catenin belongs to secreted signaling proteins, which can bind to a receptor located on the cells' surface. Wnt signaling is considered highly complex signaling, which contributes to pluripotency maintenance for embryonic development. This signaling also functions in regulating homeostasis in somatic stem cells (Kim *et al.*, 2017). Evidence show that Wnt signaling has been increased in CSCs compared to non-CSCs in multiple cancers, including colon, breast, liver, and lung cancers, given the high elevation expression of Wnt downstream molecules. Indeed, the expression of frizzled receptors (FZD4/5) was found to be highly expressed (Skoda *et al.*, 2016). Wnt signaling is also defined as Wnt/ β -catenin signaling since β -catenin is an important mediator of Wnt signaling that helps to preserve cell-cell adhesion. Moreover, the accretion of β -catenin results in activation of various Wnt target genes, including c-Myc, c-Jun, cyclin D1, and fibronectin, thus regulating metastasis progression and epithelial-mesenchymal transition of epithelial cancer cells (Zhao *et al.*, 2007). Many studies have identified several drug-like compounds that can disrupt aberrant Wnt/ β -catenin by the destruction of degradation complexes, such as APC, suggesting they are potent agents against cancer. Many efforts have been made seeking compounds that specifically modulate Wnt/ β -Catenin signaling. These compounds also help eliminate CSCs, known as drug-resistant cell populations accounting for tumor relapse and metastasis. For example, Wnt signaling is inhibited by nonsteroidal anti-inflammatory drugs (NSAIDs) by regulating COX2 or by advocating degradation of TCF protein (Takahashi-Yanaga and Kahn, 2010). Besides NSAIDs, natural compounds also have the ability to compete with β -Catenin/TCF interaction, subsequently leading the relocation of β -Catenin to the membrane with the help of E-cadherin. Recently, monoclonal antibodies and small interfering RNAs have been subjected to preclinical trials to be proven as Wnt/ β -Catenin signaling inhibitors (Hu and Fu, 2012; Baron and Gori, 2018; Chen and Duan, 2018). Therefore, the target Wnt/ β -Catenin signaling pathway is a promising approach in pharmacology.

Notch signaling contributes to various critical cellular processes, including cell proliferation, differentiation, and stem cell maintenance (Song and Miele, 2005; Hu and Fu, 2012). Inhibiting the signaling pathways of two groups of Notch inhibitors can help to target the Notch signaling. The first approach is primarily focused on developing effective compounds that could counteract Notch receptor cleavages like γ -secretase inhibitors. Another approach to the development of these compounds is to hamper Notch ligand-receptor interaction using monoclonal antibodies. Notch signaling involves Delta-like 1, Delta-like 3, Delta-like 4, Jagged 1 and Jagged 2 ligands and Notch 1, Notch 2, Notch 3, and Notch 4 receptors. The

expression of these proteins has been studied in different cancers. For example, in lung cancer, Notch 3 was found to be overexpressed, leading to a poor overall survival rate. Notch signaling is also recognized as both oncogenic and suppressed signaling. For instance, Notch 1 signaling has been determined to have a dual role in colon cancer. Notch 1 can escalate the tumor progression; however, on the other hand, it can prevent β -Catenin signaling, which is known as essential signaling in colon carcinogenesis (Kim *et al.*, 2012). Thus, it is reported that using a specific inhibitor to downregulate Notch signaling could lead to cell growth inhibition or apoptosis induction (Osanyingbemi-Obidi *et al.*, 2011; Hassan *et al.*, 2013). Many efforts have been made to find an effective Notch signaling inhibitor. BMS-906024, a γ -secretase inhibitor involved in Notch activation, was tested in clinical trials, and the result showed that more than 50% of bone marrow blasts were reduced in patients who have relapsed T cell acute lymphoblastic leukemia (Gavai *et al.*, 2015). Recently, tarextumab (OMP-59R5), an antibody, has been reported to inhibit Notch 3 as well as Notch 2. Tarextumab also shows significant inhibition of xenograft tumor growth in combination with other chemotherapeutic agents via downregulated Notch signaling-associated genes (Notch 3, HeyL, and Rgs5) of breast, ovarian, and pancreatic cancers (Yen *et al.*, 2015). According to these findings, the Notch signaling pathway has grasped more attention to be developed further in cancer therapy as it could kill differentiated cells and CSCs.

In addition to Wnt and Notch signaling, Hedgehog (Hh) is another signaling pathway contributing to stem cell maintenance, proliferation, differentiation, and recurrence. Hh signaling is identified to be aberrantly activated in several cancers such as glioblastoma, chronic myeloid leukemia, pancreatic cancer, and breast cancer (Merchant and Matsui, 2010; Cohen, 2012). There are three ligands involved in Hh signaling: Desert (DHH), Sonic (SHH), and Indian (IHH). Depend on the cell type, the expression level of these ligands varies. For example, SHH is mainly found within the embryogenesis period; IHH is mainly expressed in hematopoietic, cartilage, and bone cells; and DHH is found primarily on testes and peripheral nervous systems. The activation of Hh happened when Patched receptors were bound by Hh ligands, resulting in the activation of transcriptional effectors of the GLI family. In attempting to inhibit the Hh signaling, several preclinical studies have reported the promising results of utilizing Smoothed inhibitors. This approach drives a decrease in drug/compound resistance, reoccurrence, and metastasis of cancer cells. Indeed, using vismodegib, a Smoothed inhibitor, resulted in promising anti-tumor activity in treating basal cell carcinoma as well as medulloblastoma patients. Similar results were also reported when applying other

Smoothed inhibitors such as BMS-833923, sonidegib, saridegib, TAK-441, LEQ 506, and LY2940680 (Justilien and Fields, 2015). As mentioned before, the GLI family has a function in regulating Hh signaling. A study reported a negative correlation of the expression of GLI1, GLI2 expression with the overall survival rate of leukemia patients. According to their study, the authors indicated that inhibiting GLI1/2 leads to apoptosis induction and proliferation inhibition and colony formation reduction (Wellbrock *et al.*, 2015). Hh signaling commonly interacts with Notch, mTOR, and Ras/Raf/ERK. Hence, several studies suggested that combinatorial therapy targeting multiple signaling pathways would enhance anti-tumor efficacy in animal models (Brechbiel, Miller-Moslin and Adjei, 2014).

2.6 Important signaling pathways associated with PCD

PCD, specifically apoptosis, comprises intrinsic and extrinsic signaling pathways. However, various cellular signaling pathways are also associated with programmed cell death. For example, p53 signaling is an important pathway directing to apoptosis since p53 has a pivotal role in regulating DNA damage. Besides, other pathways such as MAPK and EGFR are also signaling pathways that could be proposed as a promising target for treating GBM. This section provides a general introduction to these three signaling pathways: p53, MAPK and EGFR.

2.6.1 P53 pathway

Many efforts have been made to study the p53 pathway, which fulfills a crucial role in DNA damage in order to improve conventional cancer treatment. P53 can induce cell death, DNA repair, and cell cycle arrest depending on the level of cellular compromise (Vousden and Lane, 2007). The p53 target genes also play pivotal roles in senescence, angiogenesis, and autophagy. Extensive research on p53 indicated that p53 signaling is complicated with different connectivity, thus having a vital function in the regulation and development of metabolism and stem cell biology (Vousden and Prives, 2009; Bieging, Mello and Attardi, 2014).

Cancer cells with or without p53 function indicate the pro-apoptotic action of p53. Indeed, the expression of p53 in p53-deficient murine myeloid leukemia resulted in apoptosis induction. Also, multiple cancerous cells, such as thymocytes, intestinal stem cells, and mouse embryonic fibroblast cells, originated from p53-deficient mice were resistant to radiotherapy and chemotherapy (Clarke *et al.*,

1993; Lowe, Ruley, *et al.*, 1993; Lowe, Schmitt, *et al.*, 1993). P53 induces apoptosis by transcriptional activation of the intrinsic regulator (mitochondria-mediated apoptosis signaling) and extrinsic regulator (death receptor-dependent). P53 also can induce apoptosis via directly impacting mitochondrial membrane, which is associated with Bcl-2 family proteins. Regarding transcriptional target, p53 binds to the CD95 gene in response to DNA damage stimuli, thus inducing CD95 expression in various cancer cells. Likewise, chemotherapy-induced p53 induction results in high expression of DR5 and DR4. By directly impacting the mitochondrial membrane target, mitochondrial outer membrane permeabilization (MOMP) functions in a vital role. Anti- and pro-apoptotic Bcl-2 family proteins help to control the MOMP. When anti-apoptotic members are embedded into the outer mitochondrial membrane containing death agonists (Bad and Bax), MOMP is induced. This leads to the accumulation of cytochrome *c* in the cytosol, subsequently activating the caspase cascade (Youle and Strasser, 2008). Moreover, p53 signaling is associated with various mitochondrial genes, including Bax, PUMA, NOXA, Apaf-1, and caspase 9 (Haupt *et al.*, 2003).

Besides the role in apoptosis induction, p53 also regulates the cell cycle progression, since p53 can control G1/S, S, and G2/M cell cycle checkpoint (Giono and Manfredi, 2006). The central role of p53 in inhibiting the cell cycle is the capacity of p53 in upregulated expression of the CDK inhibitor p21 (CIP1/WAF1). P53 proficiently binds and thus inhibits cyclin A/CDK2 complexes and cyclin E/CDK2. Therefore, it arrests the cell cycle and allows the DNA repair process to be activated. The role of p21 in G1/S checkpoint has been revealed in p21-deficient mouse embryonal fibroblast cells and cancerous colon cells, indicating the deficiencies in the DNA damage process and leading to arrest the cell cycle at G1 (Brugarolas *et al.*, 1995). Besides, p53 regulates G2/M checkpoint by modulating several genes' expression, e.g., CDC25, p21, and GADD45, resulting in G2/M transition arrest (Giono and Manfredi, 2006). Given the crucial role of p53, it could be recognized as a potent approach to developing novel cancer treatment.

2.6.2 Mitogen-activated protein kinase (MAPK)

MAPK pathway is considered an omnipresent transduction pathway because it is associated with all aspects of life-controlling fundamental cellular processes, including development, differentiation, apoptosis, and migration. MAPK is also deregulated in many diseases (Dhillon *et al.*, 2007; Rezatabar *et al.*, 2019). The

MAPK pathway comprises MAPK, MAPKK, and MAPKKK kinase modules in which MAPK is activated when a mitogen-activated protein kinase (MAPKK) is phosphorylated, while MAPKK is activated upon phosphorylation by MAPKKK. MAPK responds to different input signals, including growth factors, cytokines, hormones, endogenous stress, and environmental surrounding signals. Thereby, MAPK is grouped into mitogen-activated MAPKs (ERK pathway) and stress-activated MAPKs (JNK and p38 pathways) (Figure 7). However, there is always a crosslink among these three families of pathways (Lee, Rauch and Kolch, 2020).

The MAPK signaling pathway comprises the cooperation of growth factors along with their corresponding receptors. One of the most critical growth factors is epithelial growth factor (EGF), which binds to epidermal growth factor receptor (EGFR). Growth factors firstly bind to transmembrane glycoproteins of the receptor tyrosine kinase (RTK), thus activating Ras protein, which consists of over 150 small G-proteins. Activated Ras results in membrane recruitment and then activates Raf protein. Raf is dependent on the activated Ras interaction because Raf is known as the downstream effector of Ras. Then, a series of phosphorylation happens in which Raf protein phosphorylates MEK (MAP kinase-ERK kinase) and MEK phosphorylates ERK1/2 (extracellular signal-regulated kinases), thus activating multiple transcription factors. These factors modulate gene expression that controls the proliferation and survival of the cells. Generally, the MAPK cascade is activated in a series of events: MAPKKK (represented by Ras/Raf), followed by MAPKK (MEK1/2/3/4/5/6/7), and MAPK as the final.

Among three main classes of MAPKs (p38, JNK, and ERK), ERK is the most extensively studied mammalian pathway. ERK1/2 is involved in various cellular processes. Notably, ERK1/2 varies depending on the location. For example, in the nucleus, ERK1/2 can activate CREB, c-Myc, and NF- κ B. Hence, the ERK1/2 pathway is recognized as a pivotal target for developing novel anti-tumor therapy.

The ERK1/2 pathway (Ras-Raf-MEK-ERK) is commonly modulated in approximately 40% of human cancers because of the high possibility of mutation of Braf and Ras. Thereby, MEK inhibitors were first developed as anti-cancer agents; however, their application and selectivity did not meet the requirements in clinical trials (Wu and Park, 2015; Mahapatra, Asati and Bharti, 2017). MEK has to be inhibited almost completely in order to achieve a significant effect, thus suggesting a combination with another inhibitor would bring potent efficacy. Indeed, combining Raf and MEK inhibitors as a dual treatment has recently been

recommended as conventional therapy for melanoma and other cancers (Flaherty *et al.*, 2012; Faghfuri *et al.*, 2018; Roskoski, 2018).

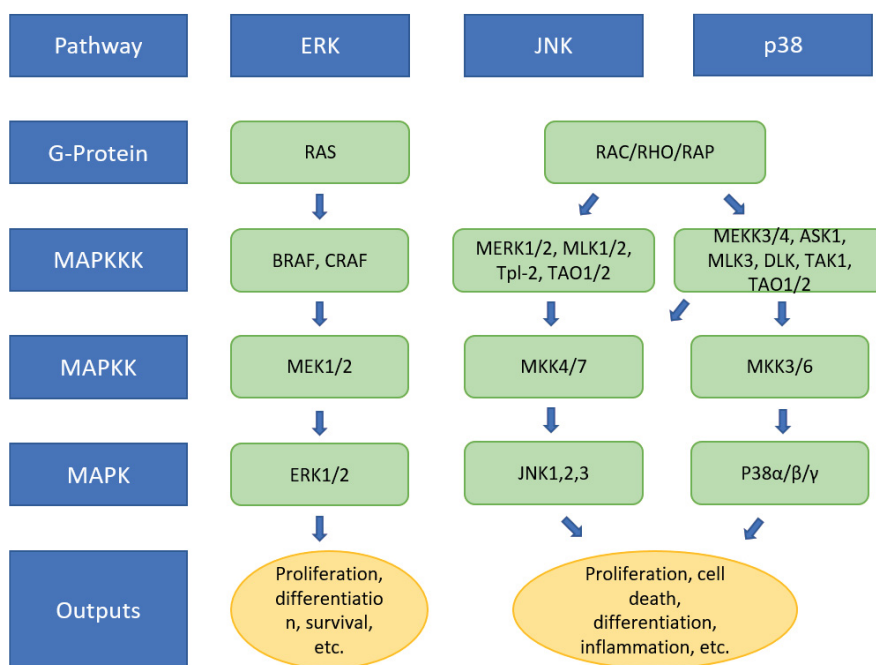


Figure 7. Schematic overview of MAPKs and their family signaling pathways. There are three types of kinases that form different signal transduction cascades and result in different outputs.

2.6.3 Epidermal growth factor receptor pathway

Epidermal growth factor receptor (EGFR), a member of the ErbB family, which belongs to receptor tyrosine kinases (RTK). With the binding of the growth factors, e.g., EGF proteins, EGFR is activated. It has been reported that EGFR is associated with pathogenesis and contributes to several carcinoma types. The EGFR and its corresponding ligands, such as EGF-like proteins, are overexpressed in many tumors leading to cell transformation induction that has been confirmed. Aberrant expression of EGF-like ligands or EGFR confers a more aggressive tumor that is associated with poor prognosis (Sigismund, Avanzato and Lanzetti, 2018).

EGFR signaling is altered in multiple cancers because of protein amplification, overexpression, mutations, or deletions. The most common mutations are found in glioblastoma and lung cancer, as well as colorectal cancer. These mutations often appear with increased EGFR ligand, thus contributing to altering signaling and developing tumors. For instance, an increment of EGFR density at the plasma membrane could lead to activating kinase (Chung *et al.*, 2010). In other circumstances, mutations such as EGFRvIV and EGFRvV mutants can prevent or destroy the recruitment site of E3 ligase leading to lysosomal degradation (Roskoski, 2014). Generally, EGFR signaling activation transduces a series of signaling pathways such as JNK, PI3K/AKT, Ras/MAPK, JAK/STAT, and PLC (phospholipase C)/PKC (protein kinase) signaling cascades, since these signaling pathways are interlinked. Among these signaling cascades, the Ras-Raf-MEK-ERK-MAPK pathway is the most crucial signaling cascade mediated in response to EGFR. These signaling cascades facilitate crucial activities in cellular responses like cell growth, cell development, differentiation, apoptosis, and migration mechanism. Thereby, EGFR recently grasped huge attention to serve as a target of several cancer therapies adopted in clinical trials.

Up to now, two approaches of EGFR-targeted therapy have been explored and studied. One approach is using “humanized monoclonal antibodies against the EGFR domain,” in which the antibodies are designed to mediate its downregulation or to block the receptor, thus escaping the binding of ligands (Martinelli *et al.*, 2009). Another approach is to design tyrosine kinase inhibitors (TKIs) that could mimic the ATP binding to the receptor's kinase pocket, thus avoiding signal transduction (Tanoue, 2009). Currently, the FDA has approved several EGFR monoclonal antibodies such as Vectibix and Erbitux for treating colorectal cancer, while erlotinib, lapatinib, and gefitinib were FDA-approved as TKIs for treating pancreatic cancer, breast, and non-small-cell lung cancer, respectively (Modjtahedi and Essapen, 2009). Notably, EGFR inhibitors are usually utilized alone or combined with other anti-cancer chemotherapies or high-dose radiotherapy. Therapy using EGFR inhibitors generally increases survival in EGFR-positive patients (Harandi *et al.*, 2009). TKIs especially have been reported to be effective against tumor cells with exon 19 deletions and EGFR L858R mutation (Shukuya *et al.*, 2011). Nevertheless, utilizing anti-EGFR therapy remains a certain challenge because of the resistance of EGFR-positive tumor cells to EGFR inhibitors. Given this challenge, huge attention has been put into finding biomarkers that predict response to anti-EGFR therapy. Many attempts have been made to enhance the response to current anti-EGFR therapy; however, the results still have not met the requirements. For example, high

expression of EGFR showed no correlation with EGFR inhibitors (Cunningham *et al.*, 2004; Chung *et al.*, 2005). Also, GBM with EGFRvIII mutation did not respond to currently approved EGFR inhibitors (Gan, Cvrljevic and Johns, 2013). In the case of EGFR pathway mutation, research has revealed that therapy that inhibits the activation of EGFR has promising efficacy in K-Ras mutations containing cancers (Sorich *et al.*, 2015). Therefore, nowadays, the FDA requires a diagnostic test for K-Ras before using panitumumab or cetuximab for colon cancer. Although there are several challenges associated with EGFR inhibitors, an in-depth understanding of EGFR cross-talking signaling pathways response to EGFR inhibitors would bring more benefits, thus improving the conventional cancer treatment.

3 AIMS OF THE STUDY

The present study aims to characterize alkylaminophenol and GPR17 agonist activity and their combinatorial action for treating glioblastoma. We also aim to explore the driving mechanism and interaction of molecular signaling pathways of glioblastoma cells upon the action of alkylaminophenol, GPR17 agonist, and combinatorial treatments.

We have focused our study on four specific aims, which are as follows:

1. To study the anti-tumor activity of alkylaminophenols, especially THTMP, on glioblastoma cells
2. To study the activity of THTMP on the growth and proliferation of glioblastoma stem cells and non-stem cancer cells as well as the modulation of corresponding signaling pathways
3. To study the potential ability of T0 as a GPR17 agonist and its anti-tumor activity on glioblastoma cells
4. To study the synergistic effect of THTMP and T0 in vitro and preclinical validation in xenograft mouse models to check its potential as a novel therapeutic strategy for GBM therapy

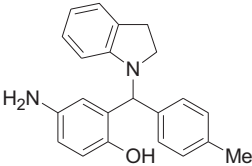
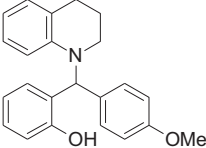
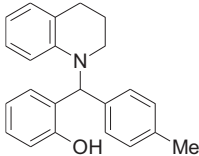
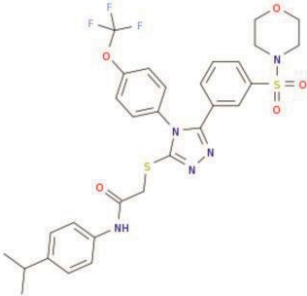
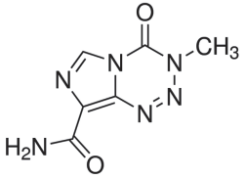
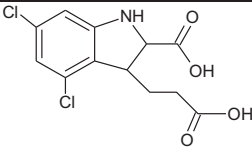
4 MATERIALS AND METHODS

The work aims to assess the potential anti-cancer activity of alkylaminophenol and GPR17 agonist in single treatment and in combination with TMZ and T0. Different methods in this work have been selected carefully to support the hypothesis and strengthen the conclusions. This chapter contains the entire experimental procedure used to acquire the preliminary data. These data have been analyzed and studied further using image and signal processing methods and statistical analysis.

4.1 Materials

Alkylaminophenols compounds, namely 2-((3,4-dihydroquinolin-1(2H)-yl)(p-tolyl)methyl)phenol (THTMP) (Neto, Andrade, A. S. Fernandes, *et al.*, 2016), 2-((1,2,3,4-tetrahydroquinolin-1-yl)(4-methoxyphenyl)methyl)phenol (THMPP) (Karjalainen *et al.*, 2017) and N-(2-hydroxy-5-nitrophenyl(4'-methylphenyl)methyl)indoline (HNPMI), were synthesized, characterized and provided by Docent Nuno Rafael Candeias. The three compounds were prepared using the Petasis borono–Mannich multicomponent reaction with the help of ethanol or glycerol solvents (Rosholm *et al.*, 2015; Neto, Andrade, A S Fernandes, *et al.*, 2016). GPR17 agonist (2-[[5-(3-morpholin-4-ylsulfonyl)phenyl]-4-[4-(trifluoromethoxy) phenyl]-1,2,4-triazol-3-yl] sulfanyl]-N-(4-propan-2ylphenyl)acetamide) (T0510.3657) was synthesized by AKos Consulting & Solutions Deutschland GmbH (reference no. AKOS001054878). The previous study built T0510.3657 chemical structure (C₃₀H₃₀F₃N₅O₅S₂) based on the docking model system (Saravanan *et al.*, 2018). Temozolomide and MDL 29,951 were acquired from Sigma-Aldrich, St. Louis, MO, USA. Table 3 shows the molecular structures of all compounds used in this work.

Table 3. Synthetic alkylaminophenols, GPR17 agonist and temozolomide structure.

Compound	Name	Chemical structure
HNPMI	N-(2-hydroxy-5-nitrophenyl(4'-methylphenyl)methyl)indoline	
THMPP	2-((1,2,3,4-tetrahydroquinolin-1-yl)(4-methoxyphenyl)methyl)phenol	
THTMP	2-((3,4-dihydroquinolin-1(2H)-yl)(p-tolyl)methyl)phenol	
T0510.3657	2-({5-[3-(morpholine-4-sulfonyl)phenyl]-4-(trifluoromethoxy)phenyl]-4H-1,2,4-triazol-3-yl)sulfanyl)-N-[4-(propan-2-yl)phenyl]acetamide	
Temozolomide (TMZ)	3,4-Dihydro-3-methyl-4-oxoimidazo[5,1-d]-1,2,3,5-tetrazine-8-carboxamide	
MDL 29,951	2-carboxy-4,6-dichloro-1H-indole-3-propanoic acid	

4.2 Cell lines and cell culture

In this work, multiple GBM cell types were used, including LN229 and Snb19 (SNB19); GBM cancer stem cells (GSC-LN229 and GSC-Snb19); non-stem cancer cells (NSCC-LN229 and NSCC-Snb19), which were isolated from primary GBM cells; and four patient-derived GBM (PdG) cells lines (MMK1, JK2, RN1, and PB1). In addition to these GBM cell lines, mouse embryonal fibroblast (MEF) and HEK293T cells were also used to examine the non-toxicity activity of the compounds on normal cells. Details of specific cell lines' culture medium and culture conditions are mentioned in the next section.

The initial densities of the cells used to perform experiments in this study are as follows: 5×10^5 cells/well for 6-well plate, 1×10^5 cells/well for 12-well plate, and 1×10^4 cells/well for 96-well plate.

4.2.1 GBM primary cell lines and MEF cells

Two GBM primary LN229 and Snb19 and MEF cells were obtained from Dr. Kirsi Granberg (Faculty of Medicine and Health Technology, Tampere University). The LN229 cell line was derived from a 60-year-old female with right frontal parieto-occipital glioblastoma while Snb19 (otherwise designated as SNB19) was collected from a 75-year-old male patient with the left parieto-occipital glioblastoma tumor. MEF cells were used as normal cells to examine the non-toxicity activity of the tested compounds.

A complete culture medium for LN229, Snb19, and MEF was prepared using DMEM medium with 0.025 mg/ml amphotericin B, 100 U/ml penicillin, 10% FBS, and 0.1 mg/ml streptomycin. A complete culture medium for HEK293T cells was prepared using DMEM medium with 2 mM sodium pyruvate, 0.025 mg/ml amphotericin B, 100 U/ml penicillin, 10% FBS, and 0.1 mg/ml streptomycin. Amphotericin B needs to be dissolved completely in 500 μ l dimethyl sulfoxide (DMSO) before adding to DMEM medium. DMEM and other culture supplements were obtained from Sigma-Aldrich, St. Louis, MO, USA. After adding all components, the solution was filtered using a Nalgene Rapid-Flow filter (Thermo Scientific, USA).

Primary GBM, MEF, and HEK293T cells were maintained in an incubator supplemented with 5% CO₂ at 37 °C and humidified. The caps were loosened to

allow proper oxygenation/aeration to the cells. They were adherent cells, and the splitting ratio followed was 1:3–1:6 at 70–80% confluency.

4.2.2 GSC and NSCC cells

In glioma, CD133 has been considered one of the important biomarkers for CSCs. Here, we used a CD133 MicroBead Kit (Miltenyi Biotec) to isolate CSCs. Here, the glioma stem cells (GSCs) are the cells with CD133 enrichment, and glioma non-stem cancer cells (NSCCs) are those with CD133 depletion. A GSC and NSCC isolation procedure was performed, followed the manufacturer's instructions. Briefly, the progenitor cells were collected using trypsinization, followed by adding 300 μL buffer to 1×10^8 total cells included in the kit. Then, the cells were mixed gently with 100 μL CD133 MicroBeads and 100 μL FcR blocking reagent and then incubated for 30 min at 4 °C. The same buffer was used to wash the cells to remove the excess of CD133 MicroBeads and FcR blocking reagent. The cells underwent magnetic separation using the columns and MACS separator as instructed by the manufacturer.

In this study, the progenitor GBM cells lines LN229 and Snb19 were used to isolate GSC and NSCC populations. StemPro hESC SFM medium, purchased from Life Technologies (USA), was used to maintain the GSC population, whereas the complete medium was used for progenitor GBM cells to maintain the NSCC population. The cells were maintained in an incubator supplemented with 5% CO₂ at 37 °C and humidified.

4.2.3 Patient-derived GBM (PdG) cell lines

PdG cell lines including PB1, RN1, JK2, and MMK1 were gifted from Brett Stringer, Ph.D. (QIMR Berghofer, Medical Research Institute, Australia). PdG cell lines were isolated from GBM patients, and the procedure was approved and previously reported elsewhere (Day *et al.*, 2013). A serum-free medium was used to culture these cells. PdG cell lines were cultured in a culture flask coated with 1% matrigel, as described previously (Pollard *et al.*, 2009). Specifically, the medium for PdG cells was maintained in RHB-A (AH Diagnostics, Finland) medium, which contained EGF Recombinant Human Protein (ThermoFisher Scientific, Carlsbad, CA, USA), FGF-Basic Recombinant Human Protein (ThermoFisher Scientific, Carlsbad, CA, USA), and

streptomycin and penicillin antibiotics (Sigma-Aldrich, USA). All the PdG cells were cultured in the same conditions as primary GBM cells.

4.3 Preparation of samples

DMSO was used to dissolve the tested compound to achieve 100 mM concentration. The required volume of DMSO was calculated using the following formula (1). Other concentrations of tested compounds were prepared by diluting 100 mM solution in MQ water.

$$C_M = \frac{m}{M \times V} \quad (1)$$

where C_M is molar concentration (M), m is compound's mass (g), M is molecular weight, and V is volume (L).

4.4 Cell growth inhibitory assay

Cell viability assay was conducted at the highest concentration of 100 μ M for the tested compounds. The cells were seeded in a 12-well plate and incubated overnight, as mentioned in section 4.2. The cells were washed with phosphate-buffered saline (PBS) (Sigma-Aldrich, St. Louis, MO, USA) to remove the old medium and the dead cells prior to the collecting step. The cells were exposed to 100 μ M of the compound when they reached 65–70% confluence. The cells were kept in the culture incubator. The cells were harvested after 24 hours of treatment using 500 μ l of Trypsin-EDTA (Sigma-Aldrich, St. Louis, MO, USA). After 5 min of trypsin incubation, 500 μ l of complete culture medium was added to each well to stop the trypsin reaction. The cells were then collected by centrifugation at 3000 rpm for 5 min. Trypan Blue solution with 1:1 ratio was used to determine the cell viability. Cell viability determination was done by Countess II FL Automated Cell Counter (ThermoFisher Scientific, Carlsbad, CA, USA). The DMSO vehicle sample and TMZ were used as the negative control (NC) and positive control (PC), respectively. The percentage of cell growth inhibition was determined using formula (2) (Periasamy *et al.*, 2015) for each sample:

$$\text{Inhibition (\%)} = \frac{\text{Mean No. of untreated cells} - \text{Mean No. of treated cells}}{\text{Mean No. of untreated cells}} \times 100 \quad (2)$$

4.5 Cytotoxicity assay using kinetic studies

Kinetic experiments were implemented using a series concentration of 1 μM , 10 μM , 25 μM , 50 μM , 75 μM , and 100 μM . The cells were seeded in a 12-well plate. When the cells reached approximately 65–70% confluence, dead cells were removed by PBS, and the cells were treated with specific concentrations of each compound. The cells were harvested after 24 hours, as mentioned in section 4.4. Each compound's half-maximal inhibitory concentration (IC_{50}) was evaluated using IC_{50} Tool Kit according to the dose-response curve. The lowest IC_{50} was selected for further study.

4.6 Synergy screening assay

The cells were seeded in 12-well plates to conduct the synergy screening assay. Then, the cells were exposed to a combination of three-point dose series of either TMZ (100 μM , 50 μM , 10 μM), T0 (70 μM , 40 μM , 10 μM) and/or THTMP (50 μM , 30 μM , 10 μM). Therefore, there were a total of nine combination concentrations of two compounds, including THTMP+T0, T0+TMZ, and THTMP+TMZ. After treatment, the cells were cultured for 48 hours prior to performing the cell viability assay as previously described in section 4.4. After performing combination treatment, the coefficient of drug interaction (CDI) of each combination was determined using COMPUSYN version 1.0.

4.7 Scratch/wound healing assay

Scratch assay is considered a straightforward approach to investigate cell movement/migration in vitro (Todaro, Lazar and Green, 1965). The assay was conducted by observation in which a gap or "scratch" is created on the monolayer of adherent cells. The cells then move toward the gap to close the scratch area until the gap is completely closed (Figure 8). This method was done using microscopy to capture the images during testing time, from which the percentage of migration was

calculated from the images. Although this method is time-consuming, it is often used to evaluate cell migration in vitro due to its simplicity and cost-effectiveness (Liang, Park and Guan, 2007).

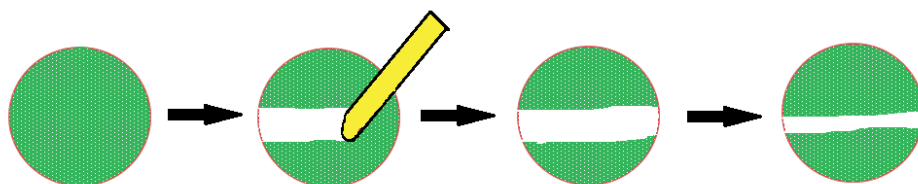


Figure 8. Representative images of scratch assay. The scratch is created on a confluent monolayer of cells. A thin tip is used to scratch on the cell layer to achieve a straight gap. The first image is taken. After that, cells migrate to close the gap (Hulkower and Herber, 2011)

In this assay, the cells were seeded in 12-well plates with initial number of 1×10^5 cells/well. When the cell growth reached the monolayer, a gap was created using a 10 μ l pipette tip after the PBS washing step. After creating the scratch, the second washing step using PBS was performed to remove debris and smoothen the edge of the scratch. Tested compounds were added to the well at the IC_{50} concentration in a 2% FBS medium. The scratch was captured every 2 hours within over 10 hours using confocal microscopy (Nikon, Eclipse TE200-U). The DMSO vehicle and TMZ were used as NC and PC, respectively. The assay was conducted in triplicates for all conditions. Invaded inhibition percentage was calculated using formula (3):

$$\text{Invaded inhibition (\%)} = \frac{\text{Area A} - \text{Area B}}{\text{Area A}} \times 100\% \quad (3)$$

where Area A is measured distance of the gap at 0 hour and Area B is measured distance of the gap at 2, 4, 6, 8, and 10 hours, respectively.

4.8 Transwell migration and invasion assay

The movement of individual cells or clusters of cells from one site to another is known as cell migration (Friedl and Bröcker, 2000). Invasive and metastatic activities are considered the crucial characteristics of tumor cells. Metastasis is basically defined as a complex process to spread tumor cells into other parts of the body

(Friedl and Wolf, 2003). Therefore, the ability of chemotherapy to significantly inhibit migration and metastasis is required.

Here, migration and invasion assays were carried out in 6-well plates (Transwell) (Corning Life Science, St. Louis, MO, USA) with a pore size of 8 μm . The cells were seeded in the upper compartment containing fresh medium with or without compounds with the density of 5×10^5 cells/well, while the lower compartment contained 1 ml of medium containing FGFb (10 ng/ml) and EGF (20 ng/ml). The wells were incubated in culture conditions for 18 hours. After the incubation, the membrane was fixed with ethanol and acetic acid at the ratio of 3:1 and then stained with 0.5% crystal violet. A cotton swab was used to remove immigrated cells. The wells were then dried in RT prior to capturing the images. Six random fields of the membrane were captured using 40x magnification. The total number of cells in each field was counted to determine the percentage of migrated cells.

For invasion assay, before adding the cells, 100 μl of matrigel (0.5 mg/ml) was used to coat the upper compartment for 2 hours. The procedure of invasion assay was conducted similarly to migration assay as mentioned above.

4.9 Clonogenic assay

Colony formation is a trait of cancer cells that defines tumor-initiating capabilities. This ability of cancer cells can be evaluated using the clonogenic assay (Franken *et al.*, 2006).

Clonogenic assay was conducted on PdG cells as previously described by Franken (Franken *et al.*, 2006). A 6-well plate coated with matrigel, as mentioned in section 4.2.3, was used. The cells were exposed to the compound for 48 hours at IC_{50} concentration. After the cells were harvested, they were plated again in the 6-well plate without matrigel coating and with the same density. The cells were maintained in a culture incubator for 14 days. After observing colonies, the old medium was removed prior to the fixation step. The cells were fixed using acetic acid (3:1) and ice-cold ethanol solution for 10 min. Then, the plates were washed with MQ water. The colonies were stained for 10 min using 0.5% crystal violet. The plates were washed under running tap water thrice to remove the crystal violet solution. Then, the well was capture randomly to obtain six images prior to performing manual counting. The counted colonies are larger than 30 μm .

4.10 RNA sequencing assay

RNA samples were isolated to conduct this assay. The cells were plated in a 6-well plate. After obtaining 60% confluency, the cells were exposed to the tested compounds at IC₅₀ concentration. After 24 hours, we isolated the total RNA using the GeneJET RNA purification kit (ThermoFisher Scientific, Carlsbad, CA, USA). The whole transcriptome sequence was performed by Illumina NextSeq 500 at the Biomedicum Functional Genomics Unit (FuGU, University of Helsinki, Finland).

For the RNA-seq data analysis pipeline, we used a quality control called FastQC version 0.11.2 to confirm the quality score above Q30. Then, the gene annotation (GTF file) and the human genome (FASTA file) were achieved from Ensembl STAR ver. 2.6, an up-to-date source tool among various RNA-seq tools utilized to generate indexes and map reads to the human genome (Dobin *et al.*, 2013). SAM tool version 1.2 (Li *et al.*, 2009) and HTSeq version 0.9.1 (Anders, Pyl and Huber, 2015) were selected for further assembly. Following this, DESeq2 ver.3.2.4 was used to obtain the differentially expressed genes (DEGs) (Love, Huber and Anders, 2014). We also performed statistical analysis following Benjamini-Hochberg's instructions (Y.Benjamini and Y.Hochberg, 1995). To select DEGs, P-values <0.05 were used to indicate a false discovery rate.

The PANTHER overrepresentation test version 13.1 was used to analyze the gene ontology (GO) pathway as illustrated previously (Ashburner *et al.*, 2000; Mi *et al.*, 2009; Emmert-Streib and Glazko, 2011). The default settings were used for the statistical analysis in both GO and pathway analysis. To select GO terms and pathways, the P-value <0.05 was used, and the fold change of 1.5 was used as a cutoff value.

4.11 Cell cycle assay

The cell cycle is a necessary set of events that happen in the growing process of each cell. The DNA content in each cell is represented for the characteristic changes throughout each cell cycle. Therefore, cell cycle techniques that stain cells in different cell cycle phases were used to separate a population of cells based on their DNA content. In this study, propidium iodide (PI) stain was used. The cell cycle protocol was modified from a Zhang *et al.* paper (Zhang *et al.*, 2018).

The cells were plated on a 6-well plate and cultured until they reached 60–70% confluency. After discarding the old medium, the cells were exposed to tested compounds at the IC₅₀ concentration. The cells were harvested by centrifugation after incubating for the desired period. Then, the pellets were suspended in 1 mL ice-cold PBS. The cells in PBS were centrifuged again at 3000 rpm for 5 min, and the pellets were mixed gently with 100 µl cold PBS. The suspended cells were added slowly to 900 µl of 70% cold ethanol. The solutions were stored for at least 30 min at 4 °C before the next centrifugation. Then, the pellets were collected and suspended in 500 µl cold PBS and washed by centrifugation. Meanwhile, the mixture of dye solution containing 20 µg/mL PI (P3566 ThermoFisher Scientific, Carlsbad, CA, USA), 0.1% Triton X -100 (Promega, Madison, WI, USA), and 0.2 µg/mL RNase (ThermoFisher Scientific, Carlsbad, CA, USA) was prepared in PBS. The cell pellets were collected after centrifugation, then they were suspended in 50 µl of the loading dye solution and kept in a culture incubator for 15 min before the images were captured. EVOS™ FL Cell Imaging System (Thermo Fisher Scientific, Carlsbad, CA, USA) was used to capture all the fluorescent images at 20× objective magnification. These images were used for the cell cycle phase analysis using CellProfiler ver. 3.9 and MATLAB ver. 2018.

4.12 Apoptosis assay

Apoptosis induction is an indication of the potential activity of a compound as an anti-cancer agent. We used the Dead Cell Apoptosis Kit with annexin V-FITC and PI (ThermoFisher Scientific, Carlsbad, CA, USA) to determine whether our compound could induce apoptosis. The apoptosis assay was conducted according to the manufacturer's instructions. In brief, 5×10^5 cells/well were cultured in a 6-well plate until the cells reached 60% confluency. The cells were exposed to IC₅₀ concentration of tested compounds for 24 hours. Then, the cells were collected by trypsinization and centrifugation. The 1X annexin-binding buffer included in the kit was used to resuspend the cell pellets. The volumes of 1 µL PI (100 µg/mL) and 5 µL FITC conjugated annexin V were mixed with a volume of 100 µL cell suspension for 15 min at RT. The images were obtained an EVOS™ FL Cell Imaging System.

4.13 Protein-protein docking and protein-ligand docking

To conduct a molecular interaction study, we used three signaling proteins, including β AR (Han *et al.*, 2001), Gal (Kimple *et al.*, 2002) and GPR17 (Saravanan *et al.*, 2018). The details of these three signaling proteins are presented in Table 4. We conducted ClusPro protein-protein docking to identify the binding efficiency of these three proteins (Comeau *et al.*, 2004). Also, we used HADDOCK protein-protein docking to support the ClusPro docking results (De Vries, Van Dijk and Bonvin, 2010).

Table 4. Detail of signaling proteins β AR, Gal, and GPR17 used in protein-protein docking

Protein	Protein Data Bank identifier	Resolution (Å)	Experiment
Beta arrestin (β AR)	1G4R	2.2	X ray
Guanine nucleotide binding protein [Alpha]11 (Gal)	1KJY	2.7	X ray
G-protein coupled receptors (GPR17)	NIL	NIL	Computational Model

After generating the protein-protein complex model, we performed protein-ligand docking simulations of GPR17 with MDL 29,951, a known GPR17 agonist, and the novel GPR17 agonist T0510-3657. The protein-ligand docking simulation was conducted using the Achilles blind docking server (<http://bio-hpc.ucam.edu/webBD/index.php/entry>). It was noted that about 200 binding poses were obtained according to the conformation and the binding energy in the protein's binding site.

4.14 Expression of GPR17 analyzed by RT-PCR and immunoblotting

We used the GeneJET RNA Purification Kit, which was obtained from ThermoFisher Scientific, Carlsbad, CA, USA, to isolate the RNA of the cells after treating them with the compounds as described in section 4.10. cDNA was isolated using Reverse Transcription using High-Capacity cDNA Reverse Transcription Kit (Applied

Biosystems™). The housekeeping gene, beta-actin, was utilized to monitor the parallel expression to normalize the cDNA quantity (Ciana, Fumagalli and Trincavelli, 2006).

PCR reaction mix was prepared as follows:

cDNA	–	1 μ L (generated from 1 μ g of total RNA)
10x Pfu Ultra II buffer	–	5 μ L (Agilent Technologies)
DNTP	–	1.25 μ L (10 mM)
Forward primer	–	2.5 μ L (10 μ M)
Reverse Primer	–	2.5 μ L (10 μ M)
Pfu Ultra II fusion Polymerase	–	1 μ L (Agilent Technologies)

The mix is finally made up to 50 μ L with Milli Q.

Gene-specific primers used are mentioned below: Human Beta-actin - 5' CTGGGACGACATGGAGAAAA 3' as the forward primer and 5' AAGGAAGGCTGGAAGAGTGC 3' as the reverse primer. The expected amplicon for human beta-actin was 564 bp. The primers for hGPR17 were taken from Ciana et al. (2006) in which 5' GACTCCAGCCAAAGCATGAA 3' and 5' GGGTCTGCTGAGTCCTAAACA 3' were used as forward and reverse primers, respectively. The expected product size of hGPR17 is 1087 bp.

The PCR was run with the following setups: initial denaturation (95 °C, 2 minutes), 30 cycles of denaturation (95 °C, 0.5 min), annealing (57 °C, 0.5 min) and extension (72 °C, 1 min) and final extension (72 °C, 10 min). The amplicon was checked in agarose gel with Gene Ruler 1kb (Catalog number: SM0311 from ThermoFisher Scientific, Carlsbad, CA, USA).

Western blot assay was carried out from the previous publication (Ciana, Fumagalli and Trincavelli, 2006). Briefly, cell lysis was performed in an ice-cold lysis buffer (pH 7.4, 1% IGEPAL, 1% Triton X-100, 1 mM EDTA, 150 mM NaCl, and 25 mM Tris). A protease inhibitor mixture was added to the cell lysis solution. Then, 10% SDS-polyacrylamide gel electrophoresis was used to separate the protein before transferring to 0.45 μ m nitrocellulose membrane. After the washing step, membranes were blocked in blocking buffer (2% BSA in 0.05% Tween-TBS) for 1 hour

at RT and incubated with antibodies specific for α Tubulin (1:1000) (Santa Cruz Biotechnology) and GPR17 (1:500). Membranes were washed with PBS containing 0.5%, 0.1%, and 0.01% Tween. Secondary antibody adding was conducted on the membranes using Goat anti-Rabbit IgG (H+L), HRP. The immunoreactive proteins were visualized using Odyssey CLx.

4.15 cAMP-Glo™ Assay

The cell lines were seeded in a white 96-well plate with initial number of 1×10^4 cells/well and cultured overnight before the PBS washing step. The cells were exposed to 10 μ M Forskolin (Sigma-Aldrich, St. Louis, MO, USA) for 15 min before adding the tested compounds for 2 hours. The cAMP-Glo™ Assay (Promega, USA) was performed as instructed by the manufacturer. An amount of 20 μ l of cAMP-Glo® lysis buffer was used to put to the wells. The plate was subjected to the shaking condition for 30 sec and then 30 min incubation time at RT. An amount of 40 μ l cAMP Detection Solution was loaded into the wells containing samples. Then, the plate was shaken shortly before incubation for 20 min. Kinase-Glo® Reagent (80 μ l) was finally loaded into the wells. The plate was again shaken shortly and followed by an incubation of 10 min prior to the luminescence measurement using a Spark plate reader (Spark®, Tecan).

4.16 Calcium assay

Cells with initial density of 1×10^4 cells/well were seeded in a 96-well plate until they reached 60% confluency. A calcium assay was performed using Fura-2 AM (Sigma-Aldrich, USA). The cells were first exposed to 5 μ M Fura-2 AM for 30 min. Then, PBS was used to wash the cells to remove the excess Fura-2 AM reagent prior to the recovery in a 50 μ L complete medium. Next 50 μ L of medium containing IC₅₀ concentration of the tested compounds was loaded to the cells. A microplate reader (Spark®, Tecan) with two dual excitation/emission wavelengths 340/510 nm and 380/310 nm were used to measure the fluorescent signal every 5 min over 2 hours. The calcium assay was carried out with three replicates in all the experimental conditions. The ratio of the fluorescent signal at two wavelengths 340nm/380nm was calculated using formula (4). The 340/380 ratio was used to determine the changes in $[Ca^{2+}]_i$ as described previously (Grynkiewicz, Poenie and Tsien, 1985).

$$\frac{340\text{nm}}{380\text{nm}} \text{ratio} = \frac{F_{\text{sample } 340} - F_{\text{blank } 340}}{F_{\text{sample } 380} - F_{\text{blank } 380}} \quad (4)$$

where $F_{\text{sample } 340}$ and $F_{\text{sample } 380}$ are the fluorescent intensities obtained from the treated well at 340 and 380 nm excitation, respectively. $F_{\text{blank } 340}$ and $F_{\text{blank } 380}$ are the fluorescent intensities obtained from the blank well 340 and 380 nm excitation, respectively. The emission of 510 nm was used in all cases.

4.17 Measuring mitochondrial membrane potential (MMP)

We conducted the MMP assay using JC-1 (ThermoFisher Scientific, Carlsbad, CA, USA), a mitochondria-specific cationic dye. Cells were seeded in a 96-well plate until they reached 60% confluency. An amount of 10 $\mu\text{g/ml}$ JC-1 was loaded into the wells, and the cells were thoroughly washed twice using PBS before incubating with the tested compounds. The wavelengths of 485 nm/530 nm and 535 nm/590 nm were used to measure fluorescence intensity. The ratio of two wavelengths 590/530 was calculated to determine the changes in the mitochondrial membrane potential.

4.18 Caspase 3/7 assay

Caspase 3/7, which belongs to the caspase family, has a vital role in PCD, especially in apoptosis (Walsh *et al.*, 2008). Caspase-Glo[®] 3/7 Assay is generally utilized to investigate the activation of caspase to determine the specific pathway leading to apoptosis induction. The principle of this assay depends on the release of the luminescent signal. In detail, caspase 3/7 activation cleaves the luminogenic substrate, consisting of a tetrapeptide sequence (DEVD). Luciferase function is to produce the luminescent signal. To perform the assay, the cells were cultured in 96-well plates until they reached 60% confluency. The cells were exposed to the tested compounds at IC_{50} concentration for 5 hours. The cells were maintained at RT for 30 min before mixing with the caspase-Glo reagent. An amount of 100 μl Caspase-Glo reagent was put into the cells and mixed at a speed of 300–500 rpm for 30 sec. The luminescence signal was measured after a 1-hour incubation using the plate reader

(Fluoroskan Ascent FL, Thermo Labsystems). Formula (5) was used to determine the fold increase in caspase 3/7 (Ling *et al.*, 2011).

$$\text{Fold change} = \frac{F_{\text{compound}} - F_{\text{blank}}}{F_{\text{DMSO}} - F_{\text{blank}}} \quad (5)$$

Where F_{compound} is the fluorescence intensity obtained from the wells exposed to the tested compound, F_{DMSO} is the fluorescence intensity obtained from the wells exposed to DMSO, and F_{blank} is the fluorescence intensity obtained from unstained wells.

4.19 Reactive oxygen species assay

Reactive oxygen species (ROS) have a pivotal function in many abnormal pathological processes. Increased ROS in cancer cells could result in stimulating mutation and altering cellular sensitivity to therapeutic reagents (Pelicano, Carney and Huang, 2004; Tominaga *et al.*, 2004; Shi *et al.*, 2014). Therefore, detecting intracellular ROS production would contribute to the characterization of a promising anti-cancer agent.

Several methods can be used to measure the ROS change in mammalian cells. Among these methods, 2',7'-dichlorodihydrofluorescein diacetate (H₂DCFDA) has been widely used in the living cell. Here, the non-fluorescent 2',7'-dichlorodihydrofluorescein (H₂DCF) is transformed into fluorescent 2',7'-dichlorofluorescein in the existence of ROS, when it is oxidized. The form of membrane-permeant diacetate ester of H₂DCF is typically used to load into the cells. Attaching diacetate groups to H₂DCF improves the membrane permeability; thus, the cells can take up the reagent rapidly (Forkink *et al.*, 2010).

Cells were plated in 12-well plates until they reached 60% confluency. The cells were exposed to the tested compounds for 5 hours. After harvesting, the cells were mixed with 2 μM H₂DCFDA (Sigma-Aldrich, St. Louis, MO, USA) for 30 min. The cells were washed with PBS, then maintained in complete medium for recovery for 20 min. We used a microplate reader (Fluoroskan Ascent FL, Thermo Labsystems) to measure the fluorescence intensity at 485 nm excitation and 538 nm emission. Here, hydrogen peroxide (H₂O₂) was utilized as the PC for ROS assay at a concentration of

200 μ M. The fold change in ROS production was determined similarly to that of caspase 3/7, as described in section 4.18.

4.20 Apoptotic proteome profiling assay

To perform an apoptotic proteome profiling assay, a Proteome Profile kit for Human Apoptosis Array was purchased from R&D systems. The array can capture a total protein of 35 different apoptosis antibodies with duplicates on the nitrocellulose membrane.

In this assay, the cells were exposed to the tested compounds for 48 hours before performing cell lysis. The cell lysis and protein array experiments were conducted following the manufacturer's protocol. I used PBS to wash the cells prior to adding the lysis buffer, which came along with the kit. The minimum density of the cells (1×10^7 cells/ml) for the lysis was used. The cell lysate was gently shaken for 30 min under cold conditions at 4 °C. After centrifugation, the supernatant was harvested and kept in a -80 °C freezer until performing the protein array assay. An amount of 250 μ g protein was used for each array. After the assay, the images were acquired by XENOVEN (Vivo Vision IVIS Lumina), and the intensity was analyzed by ImageJ software.

4.21 Animal study

An in vivo study was conducted using a U373-MG tumor-bearing xenograft mice model. Protocols for the study were confirmed by the Institutional Animal Ethics Committee, ACTREC, Tata Memorial Centre, Navi Mumbai (ethical number: 01/2015). The protocols followed CPCSEA guidelines (registration number: 65/GO/ReBiBt/S/99/CPCSEA). In this study, we used in-house bred Balb/c or NOD-SCID mice, six to eight weeks old.

The acute toxicity study was carried out by injecting the drug through intraperitoneal route with six mice in a group. In the study, we considered mortality and weight loss (≥ 4 grams/model) as toxicity. The tested compound with a dosage of 20mg/kg was injected into mice every 7 days within a period of 30 days. We observed the physical characteristics as well as mortality of the mice after 5 days post-injected dose.

There are four groups: untreated control, vehicle DMSO control, positive control TMZ, and treated samples. Tumor measurement was conducted using a digital Vernier caliper (Pro-Max, Electronic Digital Caliper, Fowler-NSK, USA). We observed the mice for their mortality, tumor volume (TV), and body weight at regular intervals within 36 days. Formula (6) was used to determine the tumor volume.

$$TV = [(w1 \times w2 \times w2) \times \pi/6] \quad (6)$$

where w1 is the smallest tumor diameter (cm) while w2 is the largest tumor diameter (cm).

Relative tumor volume (RTV) was considered as tumor volume of the day performing the measurement. T/C, a ratio of the test versus control, can be used to evaluate anti-tumor effectiveness. Formulas (7) and (8) were used to calculate the percentage of T/C ratio and percentage of tumor regression. According to USA guidelines, when T/C values ≤ 0.42 , the biological activity was considered significant.

$$\text{Relative Tumor Volume (RTV)} \frac{T}{C} (\%) = \frac{RTV_{Test}}{RTV_{Control}} \quad (7)$$

$$\text{Tumor Regression (\%)} = 100 - \left(\frac{T}{C} \times 100 \right) \quad (8)$$

where RTV is the mean TV of the model undergoing compound treatment of the day performing the measurement. T is the mean of TV of the model undergoing compound treatment; C is the mean of TV of the control model.

4.22 Statistical analysis

All experiments were conducted in several replicates with n= 3–8. The data were the representation of the mean value of replicates and standard deviation and calculated accordingly. After collecting the raw data in the experiments, these data were analyzed using different statistical tests and validations. The data were calculated as the mean of triplicates of each sample. An ANOVA test was utilized to analyze the data of the biological and chemical experiments with significance levels

at $p < 0.05$ and $p < 0.01$ indicated as * and **, respectively, while *ns* indicates non-significant. The ANOVA test was conducted using SPSS version 16.0. The purpose of using this ANOVA is to evaluate whether the observed results of the tested compounds are different from the control.

5 RESULTS

The chapter describes the results achieved from the methods mentioned above. The chapter has four sections, and the major outcomes were included in four research articles. In the first publication, alkylaminophenols were investigated for their anti-tumor effects on GBM cells. The top compound was selected for further analysis. The properties of the top compound were then intensively studied using GSCs and NSCCs and were presented in publication II. The third publication focuses on the characterization of T0 as a GPR17 agonist that has a crucial role in inhibiting GBM cell growth. The fourth publication describes the effect of combinatorial treatment of alkylaminophenol and GPR17 agonist, which was found to be more potent than TMZ for treating GBM.

5.1 Characterization of alkylaminophenols on GBM cells

As mentioned above, alkylaminophenols possess a strong inhibitory effect on osteosarcoma cells, proving that they are promising candidates for cancer treatment. Here, alkylaminophenols were characterized to evaluate their anti-tumor properties on GBM cells.

5.1.1 Cytotoxicity of alkylaminophenols on GBM cells and non-tumor cells

Three alkylaminophenols (THTMP, THMPP, and HNPMI) were tested for cytotoxicity against multiple GBM cell lines, including LN229, Snb19, and 1321N1. The live and dead cells were evaluated after 24-hour treatment at 100 μ M concentration. Interestingly, all three compounds significantly inhibited LN229 with more than 70% cell growth. Although HNPMI and THTMP significantly induced the inhibition of Snb19 cells, HNPMI and THMPP had less toxicity on the 1321N1 cell line (see Fig. 1C in publication I). Notably, THTMP accounted for approximately 100% cell growth inhibition in all tested GBM cell lines. Thus, THTMP is considered a potent anti-cancer agent against GBM cell growth. Next, we examined the cytotoxicity of THTMP in mouse embryonic fibroblast cells (MEF) and human embryonic kidney 293T cells

(HEK293T). Not surprisingly, at 10 μM concentration, only 1% and 2% cell growth inhibition were observed on MEF and HEK293T cells, respectively, with about 4%, 8%, and 12% of that on 1321N1, Snb19, and LN229, respectively (See Fig. 1D in publication I). These results indicate that THTMP selectively shows the inhibitory effect on glioblastoma cells.

We further evaluated the dose- and time-dependent activity of THTMP on GBM cells. For dose-dependent inhibitory activity, we evaluated the cell viability at a series of dosages of 10 μM , 25 μM , 50 μM , 75 μM , and 100 μM on all the three GBM cell lines. Based on the dose-responsive curve, we calculated the IC_{50} values of each cell line upon THTMP and TMZ treatment (positive control). Upon THTMP treatment, the IC_{50} value of LN229 was found to be $26.5 \pm 0.03 \mu\text{M}$, $75.4596 \pm 2.18 \mu\text{M}$ for Snb19, and $61.9 \pm 0.65 \mu\text{M}$ for 1321N1.

Likewise, the IC_{50} values of GBM cells upon TMZ treatment are $84.389 \pm 2.59 \mu\text{M}$ and 87.7614 ± 6.92 for Snb19 and LN229, respectively (see Fig. 1E in publication I). However, we observed no inhibitory effect of TMZ on 1321N1, which is in line with a previous study (Lee, 2016). We conducted the assay on LN229 and Snb19 cells using the IC_{50} concentration for 24, 48, and 72 hours regarding the time-dependent inhibitory effect. We observed the time-dependent inhibitory effect in LN229 from 24 hours to 48 hour-post treatments while observing the Snb19 inhibitory effect from 24 hours to 72 hour-post treatments (see Fig. 1F in publication I). The results show that THTMP has a strong inhibitory effect on GBM cell lines in both time- and dose-dependent fashion.

5.1.2 Whole-genome profiling of GBM cells treated with THTMP

After evaluating the anti-tumor property of THTMP treatment on GBM cells, we also profiled the expression of the genes in GBM cells upon THTMP and TMZ treatment at IC_{50} concentration. We compared THTMP with DMSO (vehicle control) designated as C1 and THTMP with TMZ (positive control) designated as C2.

In total, 7299 DEGs were observed with a q-value <0.05 and a fold change of >1.5 . We noted that the number of DEGs in LN229 was lower than that in Snb19. Specifically, 1550 DEGs were detected in LN229 while 5749 DEGs were detected in Snb19 (see Fig. 3D in publication I). From the C1 comparison, we identified 3714 DEGs in both the cell lines, with 321 DEGs commonly shared for both cell lines. Similarly, for C2, a total of 3585 DEGs were found, of which 289 DEGs were

commonly shared in both the cell lines (see Fig. 3B in publication I). The total DEGs in C1 were higher than in C2, indicating that these two groups perform their role similarly after exposure to the compounds.

THTMP significantly affected the GBM cell growth, which might be due to the drug's ability to cause DNA damage. Hence, we performed gene ontology to analyze the DEGs associated with DNA damage. GO analysis was conducted to identify the enriched genes in DNA damage, e.g., DNA replication, sister chromatid segregation, chromosome segregation, and sister chromatid cohesion. We found that these biological processes were engaged in both cell lines upon THTMP as well as TMZ treatment (see Fig. 4A in publication I). The GO molecular function revealed the interaction of many genes that are significantly involved in molecular functions related to cadherin binding and damaged DNA binding (see Fig. 4B in publication I). It is well known that cadherin binding can selectively interact with damaged DNA, thus affecting the mechanism of DNA damage (Daido *et al.*, 2005).

We also had a look at the top 20 DEGs related to DNA damage for the two GBM cell lines. Overall, LN229 cells modulated more DEGs than Snb19 (see Fig. 4D in publication I). Here, *CKD1*, an enriched gene in the p53 signaling pathway, was downregulated in either THTMP or TMZ treatment. In addition, *CDKN1A*, a gene coding for p21 protein, was found to be upregulated in THTMP treatment. The p21 and p53 pathways play important roles in inducing numerous stress signals involved in DNA damage, oncogenesis, and cell cycle arrest (Santamaría *et al.*, 2007; Stegh *et al.*, 2010). Thus, our findings imply that THTMP has inhibited GBM cell growth by DNA damage via activating p53 and p21 signaling pathways.

From the whole-genome profiling, we also identified the genes associated with other biological processes of the cells, including cell cycle arrest and apoptosis induction. The details of the up- and down-regulation of these associated genes will be discussed further along with biosensor conducted-assays in the next section.

5.1.3 THTMP induces G1/S cell cycle arrest on GBM cells

DNA damage in mammalian cells could result in cell cycle arrest. Our findings also indicated that THTMP could strongly induce DNA damage in GBM cells. As noted in the whole-genome profile, we observed the downregulation of several genes involved in DNA replication, thereby contributing to the DNA replication inhibition and cell cycle arrest. Indeed, several biological processes correlated with cell cycle

progression were modulated, e.g., cycle at G1/S phase, cell cycle checkpoint, G1/S or G2/M transition of mitotic cell cycle, and cell cycle regulation (see Fig. 4A in publication I). Hence, we had a closer look at DEGs associated with the cell cycle, such as *CCNA2*, *CCNE1*, and *CCNE2* coding to cyclin A2, E1, and E2, respectively. These cyclins are associated with regulating G1/S transition. Our RNA-seq results also revealed that *CCNA2*, *CCNE1*, and *CCNE2* were downregulated upon THTMP treatment (see Fig. 5C in publication I), thus contributing to the G1/S phase arrest of GBM cells. Moreover, *BUB1* and *CDC20* genes, which are associated with mitotic cell cycle and oocyte meiosis pathways, were found to be downregulated. Based on these results, we assert that THTMP could arrest GBM cells at G1/S phase.

We also performed an analysis of the cell cycle to further confirm the arrest of GBM cell cycle upon THTMP treatment at IC_{50} concentration. We conducted a biosensor cell cycle assay using FUCCI analyzed under the fluorescence microscope. Results of the assay revealed that both the cell lines had a similar pattern of cell cycle arrest upon treatment. Notably, the majority of cells were observed in S/G2/M phase upon DMSO condition, while the majority of the cells were observed in G1 phase when treated with THTMP. In TMZ treatment, the cells were found to be varied among S/G2/M and G1/S phase (see Figs. 5A and 5B in publication I). Based on these results, we claim that THTMP arrests the cell cycle of GBM cells at G1/S phase, whereas TMZ arrests the cell cycle at S/G2/M phase.

5.1.4 THTMP induces ROS- and caspase 3/7-mediated apoptosis

The growth of tumor cells and the apoptosis pathway are interconnected in; therefore, disturbance in the apoptosis induction may lead to uncontrolled growth of cancer cells and contribute to the limitation of tumor treatment using chemotherapeutics (Thompson, 1995). Here, we analyzed the whole-genome profile of the THTMP-treated GBM cells to determine the DEGs associated with apoptosis (see Fig. 6B in publication I). Comparing the number of DEGs for both THTMP- and TMZ-treated GBM cells showed that THTMP explored more DEGs than TMZ. Notably, THTMP not only suppressed the anti-apoptotic genes' expression but also increased the pro-apoptotic genes' expression. Particularly, the expression of *BCL2L12*, which belongs to the anti-apoptotic gene family called Bcl-2, was remarkably suppressed. *BCL2L12* in GBM patients is reported to be overexpressed, and it also accounts for apoptosis resistance in GBM therapy (Yang *et al.*, 2015). Besides Bcl-2 family genes, other anti-apoptotic genes were also modulated upon

THTMP treatment, including *TNFRSF2*, *TNFSF10*, *TNFSF12*, *RELA*, *BIRC5*. Regarding pro-apoptotic genes, we observed the modulation of several genes. For instance, *CTNNB1*, coding for β -Catenin protein, was downregulated, while *MAGED1* and *BBC3* were found to be upregulated in GBM cells upon THTMP treatment. Altogether, the gene expression profile also revealed that THTMP could induce apoptosis in GBM cells.

To further confirm the apoptosis induction upon THTMP treatment at IC₅₀ concentration, we conducted double staining (annexin V and PI). The percentage of apoptotic cells was determined by counting the number of cells that were both positive to annexin V-FITC and PI, while the percent of necrotic cells was determined based on the percentage of cells, which were positive to only PI (Vermes *et al.*, 1995; Chen *et al.*, 2008a). More than 45% of the cells were subjected to apoptosis in both the cell lines in this study. Of note, 45.8% and 56.4% apoptotic cells were obtained in LN229 and Snb19, respectively. Thus, the percentage of the cells subjected to the apoptosis process was higher when exposed to THTMP than TMZ (see Fig. 6A in publication I). We also observed a portion of necrotic cells in both cell lines upon THTMP treatment. These results also supported the gene expression profile, representing that apoptosis of GBM cells was induced significantly by THTMP treatment.

Additionally, the increment of ROS also contributes to the activation of the apoptotic pathway (Circu and Aw, 2010). Indeed, the moderate production of ROS in cancerous cells contributes to survival, proliferation, angiogenesis, and metastasis (Clerkin *et al.*, 2008). Hence, we also evaluated the production of ROS upon THTMP treatment. Our results revealed that upon THTMP treatment, ROS production was remarkably higher in comparison to TMZ or H₂O₂ in the GBM cell lines (see Fig. 6C in publication I). These results are in agreement with the whole-genome profile in which the expression of *SOD1* was downregulated (see Supplementary Table S3 in publication I), thus decreasing *SOD1* (superoxide dismutase) production and then inducing apoptosis in GBM (Sharma *et al.*, 2007). Our data suggested that THTMP could induce ROS-mediated apoptosis in GBM cells. In addition to this, we also performed the caspase 3/7 assay to determine whether THTMP could induce apoptosis via caspase cascade. Particularly, we could not observe the deregulation of CASP3 and CASP7 in the gene expression profile, which was also confirmed by the caspase 3/7 assay. Surprisingly, in both cell lines, a very low level of caspase 3/7 activation was found in TMZ and THTMP treatments (see Fig. 6B in publication I). From these data, we claim that induction of apoptosis of

THTMP treatment does not involve the activation of caspase 3/7 due to the presence of other anti-apoptotic genes (Stegh *et al.*, 2008).

5.2 Alkylaminophenol targets glioblastoma cancer stem cell

Cancer stem cells (CSCs) are associated with the initiation and progression of cancer disease. In GBM, CSC is defined as a GBM stem cell (GSC) having a similar phenotype to regular neural stem cells (Singh *et al.*, 2004). CSCs or GSCs are associated with tumor invasion, relapse, metastasis, and establishing resistance to conventional cancer therapy. Given these characteristics, it is needed to find a way to suppress the activation of CSCs or GSCs to prove the hypothesis that alkylaminophenol (THTMP) could target glioblastoma cancer stem cells.

5.2.1 Cytotoxicity of THTMP on GSC and NSCC

In order to evaluate the inhibitory activity of THTMP in GSCs, we first isolated GSCs and NSCCs (non-stem cancer cells) from progenitor glioblastoma cells (LN229 and Snb19) based on the biomarker CD133 using a MicroBead Kit (Miltenyi Biotec). After culturing the isolated population, we used CD133 antibodies to examine the CD133 expression in these populations. The result showed that the GSC population had high CD133 intensity indicating high expression of CD133 compared to NSCC and mixed population in LN229 and Snb19 cells. Higher intensities of CD133 expression in mixed and GSC populations were observed in Snb19 than in the LN229 cell line (see Fig. 1C in publication II).

To determine the targeted GBM cell population of THTMP treatment, we evaluated the percentage of cell growth inhibition of NSCC-LN229, NSCC-Snb19, GSC-LN229, and GSC-Snb19 after 24, 48, and 72 hours of treatment, with TMZ as the positive control. In general, we observed that GSC and NSCC populations responded differently to THTMP and TMZ. The result showed that THTMP had better anti-cancer properties than TMZ in both GSC and NSCC populations. Although cell growth of GSC and NSCC populations of both the cells were inhibited in a time-dependent manner, THTMP exposure resulted in a noticeable increment of cell growth inhibition in NSCC versus GSC population. Indeed, more than 90% of cell death was found in NSCC-Snb19 compared to that of NSCC-LN229, with just 32% at 72 hours post-treatment. THTMP showed a similar anti-cancer effect on the GSC

population, in which approximately 17% of cell death was observed on both GSC-LN229 and GSC-Snb19 at 72 hours post-treatment (see Fig. 1D in publication II).

To investigate the ability of GSC to develop resistance upon THTMP treatment, treatments with THTMP as a single treatment and in combination with temozolomide using the resistant variants (RVS) were conducted. To evaluate the degree of variation in the sensitivity of the RVs induced by THTMP in single and combinatorial treatment, we used the IC_{50} concentration to treat the cells for 24 hours. The cytotoxicity of LR1 and LR2 lines derived from GSC-LN229 were found to be 1.0 and 0.7-fold higher, respectively, than the parent cells. Similarly, SR1 and SR2 cell lines derived from GSC-Snb19 were 0.8- and 2.1-fold higher than the parent cells, respectively (see Fig. 1F in publication II). The inhibitory effect was also analyzed for TMZ, THTMP, and the TMZ+THTMP combination. The variants showed a lower level of resistance to TMZ than THTMP. However, treatment with THTMP showed better cytotoxicity on the variants of both GSC populations. Therefore, THTMP possesses higher activity in inhibiting GBM proliferation of the resistance population than TMZ. Interestingly, it was also noted that THTMP showed a synergistic effect with TMZ on those variants.

5.2.2 Whole-genome profiling of GSC and NSCC population treated with THTMP

Whole-genome profiling of four cell lines, including NSCC-LN229, NSCC-Snb19, GSC-LN229, and GSC-Snb19, was performed to gain an insight into how the gene expression of the cells was modulated upon THTMP treatment. Genes with twofold changes having $P < 0.001$ were defined as differentially expressed genes (DEGs). We found that about 2875 and 3269 DEGs were enriched in GSC and NSCC of the LN229 line, respectively. Likewise, GSC and NSCC of Snb19 cells had 300 and 7974 DEGs, respectively (see Figs. 4A and 4B in publication II). Based on the gene set enrichment analysis, we also determined the various biological processes modulated upon THTMP treatment (see Supplementary Tables S5–S8 in publication II). DEGs of NSCC, GSC, and the progenitor cells (mixed population) were further compared to provide in-depth analysis. We identified that about 154 DEGs were shared with NSCC, GSC, and the progenitor LN229, while Snb19 shared only 52 DEGs among those populations (see Fig. 4A and Supplementary Table S9 and S10 in publication II). The low number of shared DEGs in Snb19 could come from GSC-Snb19 cells. Although a smaller number of DEGs were observed in Snb19, the effect of THTMP in modulating

various cellular processes was observed in both GBM cell lines (see Fig. 4C in publication II).

We found that the number of genes related to DNA damage was significantly enriched, which might be related to the higher inhibitory effect of THTMP. For instance, the expression of *FOXM1* was found to be decreased in all cell lines. *FOXM1* is commonly overexpressed in various cancers and is recognized as a hallmark of cancer progression (Gartel, 2017). In addition, we also observed the strong downregulation of *CDK1* in NSCC-Snb19, which was reported to be enriched in p53 signaling pathway. Moreover, *Plk2*, a p53 target gene (Burns *et al.*, 2003), was downregulated in GSC-LN229, NSCC-LN229, and NSCC-Snb19 (see Fig. 1E in publication II). This observation further concluded that p53 signaling pathway was targeted upon THTMP treatment. We also noticed that a greater number of DEGs were observed in NSCC when compared to GSC, suggesting that THTMP has a more substantial inhibitory effect on NSCC than GSC. The reason for this could be that GSC population might be responsible for the resistant nature of the cells upon treatment.

5.2.3 THTMP induces cell cycle arrest in GSC and NSCC

We also analyzed the DEGs related to the cell cycle process. Our results showed that THTMP modulated and enriched various DEGs involved in significant biological processes associated with the cell cycle. The expression of *CCNB2* was found to be decreased in NSCC-LN229 while *GADD45A* expression was increased. Both *CCNB2* and *GADD45A* are considered downstream target genes of p53, which controls G2 checkpoint, suggesting that THTMP arrests NSCC-LN229 at G2/M phase. Regarding GSC-LN229, GSC-Snb19 and NSCC-Snb19, increased expression of *CDK2* and *CDK6* was observed, revealing their function in controlling G1/S phase transition. The expression of *CCND1*, *CCND2*, *CCNE1*, and *CCNE2*, encoding for cyclin D1, D2, E1, and E2, respectively, was decreased, indicating its role in controlling G2/M phase transition by THTMP in GBM cells. Our results revealed that THTMP arrests GSC and NSCC at different cell cycle phases depending on the specific cell line populations.

The cell cycle assay was conducted to further elucidate the loss of cell viability upon THTMP treatment in GSCs and NSCCs. Separation of cells into specific cell cycle phases was done according to the intensity of the fluorescence. In the representative histogram, the left peak indicates the cells present in G1 phase, the middle peak indicates the cells present in S phase, while the right peak indicates the

cells present in G2/M phase (see Fig. 2A in publication II). We demonstrated that GSC-LN229 and GSC-Snb19 were arrested at the G1/S phase after exposure to THTMP. The majority of the cells were accumulated in G1 before a decline was observed when they entered the S phase. A moderate number of the cells was also recorded in G2/M phase. While the NSCC-LN229 cells were arrested in G2/M, NSCC-Snb19 was arrested at G1/S phase. Thus, it might be possible that the NSCCs of GBM comprise a heterogeneous property, making this difference in triggering the cell cycle arrest.

5.2.4 THTMP induces ROS- and caspase 3/7-mediated apoptosis in GSC and NSCC

The mechanism of the effect of THTMP on NSCC and GSC population was identified by several enriched GO pathways, which are related to apoptosis induction (see Supplementary Tables S5–S8 in publication II). We observed that more of those DEGs were modulated in NSCC than GSC (see Fig. 3B in publication II). This result agrees with the annexin V/PI assay in which NSCCs had more remarkable apoptotic cells than GSCs. Here, we determined that apoptosis induction of GBM cells was confirmed by inducing pro-apoptotic genes such as *MADGED1*, *BCL2A1*, *BCL2L11* (Bim), and *BBC3* and suppressing anti-apoptotic genes including *MCL1*, *BCL2L1*, and *BCL2*. Noticeably, the expression of *BBC3*, a gene associated with p53 modulator (PUMA) (Nakano and Vousden, 2001), was significantly increased in GSC-Snb19, which explored the ability of THTMP targeting p53 through the governance of PUMA. Regarding GSC population, we observed the increase in the expression of *BCL2L11* and *BCL2A1*, demonstrating the ability of THTMP to target apoptosis in GSC populations. However, the increase of *BIRC3* expression coding for BIRC protein, an inhibitor of apoptosis (Wang *et al.*, 2016), was found to prevent apoptosis in GSC and NSCC of the LN229 line (see Fig. 3B in publication II).

We performed a double staining annexin V/ PI assay to further confirm the apoptosis induction of GSC and NSCC population by THTMP. The assay was conducted following 24 hours with THTMP, TMZ, and combinatorial treatments. Cells showing positive for annexin V binding and PI were quantified (Chen *et al.*, 2008b). In agreement with the cytotoxicity assay, NSCCs had more apoptotic cells than the GSCs for both LN229 and Snb19 GBM cell lines. Also, THTMP induced apoptosis better than TMZ in all the cases with more than 40% of apoptotic cells upon THTMP treatment compared to approximately 30% and 25% in TMZ treatment

in Snb19 and LN229, respectively. GSC-Snb19 had a greater number of apoptotic cells than GSC-LN229, especially when treated with THTMP. Indeed, up to 30% of apoptotic cells were observed in GSC-Snb19, while only 10% of that was found in GSC-LN229. In addition to apoptosis, a small number of necrotic cells was also observed in GSCs and NSCCs (see Fig. 3A in publication II). Thus, from all these observations, it is evident that THTMP could induce apoptosis in NSCC and GSC populations.

It is well known that a high level of ROS causes changes in ATP and Ca^{2+} levels leading to cytochrome *c* release, thus inducing apoptosis (Satoh, Ishige and Sagara, 2004; Kuznetsov *et al.*, 2008). Further detailed analysis on the oxidative gene expression signature revealed enrichment of various DEGs associated with ROS, including *TXNRD2*, *FOXM1*, *DUSP1*, and *SOD1* (see Supplementary Tables S1–S4 in publication II). These genes are generally highly expressed in the poor prognosis of several tumor types, including glioblastoma (Leone *et al.*, 2017). ROS levels were significantly increased upon THTMP treatment compared with DMSO (see Fig. 3C in publication II). The highest-fold increase of ROS was found in the NSCC population with 2.3- and 2.5-fold increase in NSCC-Snb19 and NSCC-LN229, respectively. Only a 1.2-fold increase of ROS was recorded in GSC-Snb19, while approximately 2-fold increase of that was observed in GSC-LN229. Notably, ROS production was higher in THTMP treatment than in the TMZ and H_2O_2 control. These results also agree with the previous analysis on apoptosis, in which NSCC showed greater effects than GSC. Thus, we conclude that THTMP might induce cell death through ROS-mediated apoptosis.

The role of caspase-mediated apoptosis was studied to determine the involvement of caspase 3/7 as the mechanism of action of THTMP on GBM cells (see Fig. 3D in publication II). Caspase 3/7 was slightly activated when treated with THTMP/TMZ. However, TMZ was found to have a higher fold increase upon THTMP treatment. GSC-LN229 increased the fold level of caspase in both TMZ- and THTMP-treated conditions. Upon THTMP treatment, GSC-Snb19 had a higher fold increase than NSCC-Snb19 and NSCC-LN229, whereas TMZ showed a higher fold in NSCC-LN229 than GSC-Snb19 and NSCC-Snb19. Hence it was confirmed that THTMP induces apoptosis in GSCs via caspase 3/7 activation better than that in NSCCs.

5.2.5 THTMP inhibits EGFR and cancer stem cell signaling pathways

From the set of genes obtained from sequencing, we found several significant signaling pathways and biological processes affected in those GSC and NSCC populations upon THTMP treatment (see Figs. 4C and 4D in publication II). Various signaling pathways were modulated, and six main targeted signaling pathways and their DEGs were further analyzed (see Fig. 5A in publication II). The highest number of genes modulated was found to be associated with the EGFR signaling pathway, representing its significant role. Only five genes respective to PDGF pathway were modulated in each cell line. Other pathways such as TGF-beta, JAK/STAT, and CSC signaling pathways (Wnt, Notch, and Hedgehog) were additionally significantly modulated by THTMP.

In cancer progression, the EGFR signaling pathway has a crucial function in promoting cancer cell survival. Targeting the EGFR signaling pathway will promote the apoptosis process of tumor cells, or they become more sensitive to chemotherapy (Huang, Xu and White, 2009). In the present study, EGFR signaling becomes the most targeted pathway by THTMP treatment. We observed the modulation of different genes involved in the EGFR signaling pathway. Notably, the expressions of *GAB1*, *AKT1*, *RHOJ*, *MAP3K5*, and *MAP3K4* were decreased in all NCSS and GSC cell lines, including the progenitor cells LN229 and Snb19. In contrast, the expression of *STAT2*, *SPRY4*, *SPRY2*, and *RHOQ* were increased (see Fig. 5B in publication II). The higher number of genes respective to the EGFR pathway were modulated in LN229 cells than the progenitor cells.

In Snb19 cells, although THTMP regulated the EGFR signaling pathway of GSC-Snb19, NSCC and their progenitor cells were found to be more potential targets with a greater number of genes enriched specifically to the EGFR pathway. It was also reported that targeting the EGFR signaling pathway results in disrupting JAK/STAT (Leaman *et al.*, 2015). Here, we observed that the JAK/STAT signaling pathway was modulated upon THTMP treatment in all populations. Our results revealed that JAK/STAT of NSCC-LN229 and NSCC-Snb19 were potentially targeted in GSC and mixed populations. The dysregulation of several genes associated with JAK/STAT signaling, including *STAT5A*, *STAT3*, *STAT1*, *JAK2*, and *JAK1*, was observed (see Fig. 5B in publication II). Besides the JAK/STAT signaling pathway, PDGF signaling also functions in controlling tumor growth, proliferation, and metastasis (Cao *et al.*, 2004; Heldin, 2013). Our study demonstrated that THTMP affected the PDGF signaling pathway of these populations through the upregulation of *PDGFA* in mixed-Snb19, mixed-LN229, NSCC-LN229, and GSC-LN229 cells and downregulation

of *PDGFC* in NSCC-Snb19 and GSC-LN229 cells. The gene expression profile demonstrated the alteration of the TGF-beta signaling pathway through the dysregulation of different genes associated with this pathway, including *TGIF2*, *TGIF1*, *TGFBR1*, *TGFB3*, *TGFB2*, *TGFA*, and *CTGF* (see Fig. 5B in publication II). We could observe a similar pattern in other targeted signaling pathways, signifying the greater potential modulation in NSCC than GSC and mixed population of LN229 and Snb19 cell lines.

In addition to the signaling pathways mentioned above, we found that THTMP targeted CSC signaling pathways by downregulating several genes associated with CSC signaling pathways (see Fig. 5C in publication II). CSC signaling pathways of GSC-LN229 and NSCC-LN229 were more highly regulated than their progenitor cells. However, in Snb19, only a few DEGs were found in GSC compared to NSCC and mixed population, suggesting that GSC-Snb19 has the ability to resist the treatment. In detail, THTMP treatment regulated the Wnt signaling pathway in all populations except GSC-Snb19 by the downregulation of numerous genes such as *CSCR4*, *LGR5*, *EDN1*, *STAT3*, *SOX2*, *HAS2*, and *CTNNB1*. It is noted that *CTNNB1* encoding β -catenin is one of the most important genes, which reveals the inhibition of Wnt signaling. The second CSC signaling pathway, which was significantly affected by THTMP is the Hh signaling pathway. This pathway was found to be modulated by the downregulation of *GLI1*, *GLI3*, and *MTBP* genes.

Similarly, the reduced expression of *NOTCH1*, *NOTCH2*, and *JAG1*, showed the inhibition of Notch signaling by THTMP. Although only a few genes were found to be regulated in these populations, this is the only CSC signaling pathway targeted in GSC-Snb19. In LN229 cells, only two DEGs were found in the progenitor, while four and eight DEGs were found in NSCC and GSC populations, respectively.

Although only one DEG was enriched in GSC-Snb19, all three CSC signaling pathways were modulated in NSCC-Snb19, while only two of them (Wnt and Hh) were found to be modulated in the progenitor. According to these results mentioned above, it is notable that separating the GBM into GSCs and NSCCs makes them more accessible targets for the treatment than their progenitors. Hence, it suggests that GSCs and NSCCs might have a strong connection supporting each other's proliferation and forming a strong resistance to the drugs.

5.3 Characterization of GPR17 agonist on GBM

Recently, GPR17 has been highlighted as a potential target for developing a novel therapy for demyelinating and ischemic diseases (I Eberini *et al.*, 2011). In addition, it has been shown that GPR17 bound with agonists reduces the formation of glioma spheres and negatively affects tumor self-renewal and proliferation (Dougherty *et al.*, 2012). This chapter aims to determine whether T0 could serve as a GPR17 agonist in GBM cells. To achieve this purpose, we have determined the expression of GPR17 in GBM and non-GBM cells. Further experiments were performed to confirm the agonism of T0.

5.3.1 GPR17, a potential biomarker for low-grade glioma and glioblastoma

We examined the expression of GPR17 in different cancer datasets using the GEPIA portal in publicly available RNA-seq gene expression. GPR17 expression was detected in low-grade glioma (LGG) and glioblastoma (GBM), even though GPR17 expression in GBM was less detected compared to its normal tissue (see Fig. 1A in publication III). By comparing the histology of oligodendroglioma, oligoastrocytoma, and astrocytoma, we observed the elevated GPR17 expression in oligodendroglioma, which is supposed to have an oligodendroglial phenotype (see Fig. 1B in publication III). Also, we investigated the correlation between overall survival and GPR17 expression in LGG and GBM. GBM cells are classified into three subgroups, including classical, mesenchymal, and proneural GBM cells. Our finding showed that proneural GBM has a higher expression of GPR17, followed by mesenchymal GBM cells with the least expression in classical GBM cells (see Fig. 1B in publication III). We also examined the correlation of survival time with the expression level of GPR17. Interestingly, the high expression of GPR17 corresponded to the low survival time in all types of GBM cells (see Fig. 1C in publication III). The results revealed that GPR17 expression is considered an essential predictive biomarker for improving survival rate based on CGGA and TCGA datasets. Taken together, these RNA-seq profiles revealed that GPR17 is highly expressed in both LGG and GBM, and GPR17 could be used as a potential biomarker for LGG and might also be for GBM.

5.3.2 T0 can be recognized as a potential GPR17 agonist

To evaluate the ability of T0 to be a potential GPR17 agonist, molecular modeling was executed to build the protein-protein interaction of three different signal molecules (GPR17, Gαi, and βAR). According to the result of the ClusPro docking program, the best 50 docked structures were established successfully. Based on the simulation, we observed that GPR17, Gαi, and βAR established a stable complex through different interactions in which the Gαi signal molecule binds to the carboxy-terminal region of the GPR17 receptor while the βAR signal molecule binds to the central region of GPR17 (see Fig. 2A in publication III). From these 50 different structures, the one with the least binding energy of about -1285.6 Kcal/mol was selected for further simulation. We then performed a protein-ligand docking simulation of T0 with the previously established protein-protein complex to understand the modulation of receptors induced by the ligand in activating various intracellular cascades. We performed the docking simulation of the GPR17 receptor complex with T0 and the GPR17 receptor complex with MDL 29,951, which is considered to be the known GPR17 agonist.

Our results indicated that T0 has better interaction with the GPR17 complex compared to the MDL 29,951 compound. Particularly, 5 hydrogen bonds, 134 poses, and -18.5 Kcal/mol were established due to the interaction of T0 with the GPR17 complex. In comparison, MDL 29,951 and the GPR17 complex formed 4 hydrogen bonds, 124 poses, and -13.4 Kcal/mol. Based on the 2D protein-ligand illustrating interaction, we found that 22 interactions were created when MDL 29,951 binds to a receptor while up to 34 interactions were found in the GPR17-T0 protein-ligand docking simulation (see Fig. 2B in publication III). We then determined the expression of GPR17 on GBM cells by analyzing RNA and protein expression. The results revealed that both the cell lines highly expressed GPR17 (see Figs. 2C and 2D in publication III); thus, they are considered suitable models for further studies of GPR17 ligands.

As mentioned, cAMP and calcium influx are two crucial secondary messengers that are involved in the GPR17 signaling pathway. Here, we performed two classical secondary messenger assays to confirm T0 as a GPR17 agonist for glioblastoma cells. Our results showed that T0 decreased the forskolin-stimulated intracellular cAMP depending on the increase of compound concentration (see Fig. 2E in publication III). The results implied that T0 inhibited the activation of adenylyl cyclase via Gαi/o-

mediated activity. Regarding calcium influx, T0 led to decreased calcium levels in both LN229 and Snb19 cell lines (see Fig. 2F in publication III). Also, T0 modulated calcium influx in a time-dependent manner (see Fig. 2G in publication III). All these data suggested that T0 inhibits calcium influx in GBM cells, implying that Gαq might not be involved in the activation of GPR17 of T0.

5.3.3 Cytotoxicity of T0 on GBM cells

The cytotoxicity activity of T0 was characterized on LN229 and Snb19 GBM cell lines. T0 showed the strongest inhibitory effect on GBM compared to TMZ and MDL 29,951 at 10 μM. At 100 μM, T0 also possessed higher cytotoxicity activity than MDL 29,951; however, TMZ had a better inhibitory effect on Snb19 than T0. Notably, 57% cell growth inhibition was achieved in Snb19 at 100 μM concentration of T0, while 65% of that was observed in LN229 cells. The cell growth inhibition percentage was remarkably less than the cells treated with MDL 29,951 (approximately 1–2%) (see Figs. 3A and 3B in publication III). Thereby, the results suggested that T0 has a better inhibitory effect on GBM cells (especially in LN229 compared to Snb19) while MDL has no cytotoxic effect on these two cell lines. We also evaluated the inhibitory activity of T0 on mouse embryonic fibroblast cells (MEF) to evaluate its cytotoxicity on normal cells. T0 more significantly induced cell growth inhibition on GBM cells than MEF cells with less than 15% at 100 μM (see Fig. 3C in publication III). This result indicates that T0 could target GBM cells rather than the normal cells.

Dose- and time-dependent inhibiting effects of T0 on glioblastoma cells were evaluated using 10 μM, 25 μM, 50 μM, 75 μM, and 100 μM concentrations and for 24 hours, 48 hours, and 72 hours treatment. T0 increased the growth inhibition of the cells in both dose- and time-dependent manners. Compared to Snb19 cells, LN229 cells showed a better effect at 100 μM with 100% cell death at 48 and 72 hours post-treatment, while approximately 60% cell death was observed in Snb19 in the same conditions. IC₅₀ concentrations of these cell lines were found to be 98 μM and 86 μM for Snb9 and LN229, respectively.

We also performed RNA sequencing analysis to understand the whole-genome expression profile associated with GBM cell death mechanism when exposed to T0. We noted that DNA damage of GBM cells was due to the upregulation of *DDIT3* and *DDIT4* in both cell lines (see Fig. 3F in publication III). In addition, the downregulation of *CDK1* in LN229 cells further confirmed the DNA damage of GBM cells by T0

agonist. Other DEGs related to DNA damage in LN229 and Snb19 were represented (see Figure 3E in publication III).

5.3.4 T0 induces apoptosis and cell cycle arrest on GBM

The whole-genome profiling reveals that several DEGs associated with the apoptosis process were also enriched significantly. For instance, *BIR5*, which is correlated with apoptosis induction, was downregulated in both cell lines. The same trend was also observed in the expression of *API5*. We also observed other DEGs, which were differently enriched specifically for each cell line. In LN229, the expression of *BCLAF1*, a pro-apoptotic gene that belongs to the Bcl-2 family, was decreased, whereas the expression of *TBBIM6*, a Bax inhibitor, was decreased with increased expression of *BBC3* expression in Snb19 cells (see Fig. 3I in publication III). This suggests that T0 could induce apoptosis in GBM cells. We also noticed the suppression of *CASP2*, *CASP3*, and *CASP7* in these cell lines, demonstrating that the caspase pathway was not involved in apoptosis induction upon T0 treatment.

To confirm the ability of T0 to induce GBM, we conducted an apoptosis assay using annexin V/PI staining. We demonstrated that T0 induced a significant percentage of apoptotic cells upon TMZ and T0 treatment compared to DMSO control. Approximately 32% and 21.9% of apoptotic cells were recorded in LN229 when treated with T0 and TMZ, respectively. Likewise, either T0 or TMZ also led to 35% of apoptotic cells in Snb19. We also noticed a small portion of necrotic cells in these two cell lines; however, TMZ produced a greater number of necrotic cells than T0 (see Fig. 3G and 3H in publication III).

Cell cycle assay was also performed to analyze how T0 affects GBM cell cycle phases in-depth. We first observed the change of genes associated with the cell cycle process through the gene expression profile. It was observed that T0 might arrest the GBM cell cycle at G1/S phase because of the downregulation of *CDK2* (see Fig. 3L in publication III). The downregulation of *CDK2* leads to p53 and p21 signaling activation. The change of several cyclin-related genes supports these observations. Indeed, there was a declined cyclin E2 in LN229 and cyclin D1 and D3 in Snb19 through the downregulation of *CCNE1*, *CCND1*, and *CCND3* genes. The expression of cyclin A2, B1, and B2 was also decreased in these two cell lines by the decreased expression of *CCNA2*, *CCNB1*, and *CCNB2* expression (see Fig. 3L in publication III). These results suggested that GBM cell growth was arrested at G2/M phase. The propidium iodide assay was performed to check the cell cycle arrest, which revealed

that the majority of cells in G1 phase was upon T0 treatment, particularly 59% and 68.2% cells for LN229 and Snb19, respectively (see Figs. 3J and 3K in publication III). Thus, all these data revealed that T0 arrests the GBM cell cycle at G1 phase.

5.3.5 T0 modulated various GBM signaling pathways

By performing the gene expression profile and G0 analysis, we have identified the potential signaling pathway that T0 could target in GBM cells. T0 altered different signaling pathways, e.g., NF- κ B, PI3K-Akt, STAT, and MAPK. Regarding the PI3K-Akt pathway, the modulations of various PI3K-Akt-associated genes have been observed via downregulation of *MCL1* and upregulation of *PTPN23* (see Fig. 4A in publication III). It is noted that *MCL1* associates to PI3K-Akt mediated by CREB, a downstream transcription factor of PI3K-Akt (Wu *et al.*, 2019), while *PPTN23* is reported as a tumor suppressor gene (Zhang *et al.*, 2017). Therefore, it suggests that T0 could target GBM cells via the inhibition of the PI3K-Akt pathway. *MCL1* is not only involved in PI3K-Akt but also is associated with the STAT signaling pathway that inhibits cell growth, reduces invasion, and enhances apoptosis of GBM cells.

We also noted the decreased expression of *TGFA* (see Fig. 4B in publication III), a gene associated with several tumor growths, including glioblastoma (Tang, Steck and Yung, 1997). The inhibition of the NF- κ B signaling pathway was detected upon T0 treatment due to the increased expression of *NFKBIA* and *RELA* in LN229, while the expression of *CTNNB1* and *MDM2* was found to be decreased in Snb19 cells (see Fig. 4C in publication III). It is well-known that *NFKBIA* is normally deleted in grade IV gliomas (approximately 25%), resulting in reduced patient survival (Bredel *et al.*, 2011). Furthermore, reconstructing the expression of *NFKBIA* helps increase the sensitivity of chemotherapy (Kinker *et al.*, 2016). The actual performance of *RELA* is still under debate, given the evidence that *RELA* overexpression leads to TRAIL-mediated apoptosis inhibition as well as tumorigenesis correlation (Chen, Kandasamy and Srivastava, 2003; Yu *et al.*, 2003). It is also reported that β -catenin, encoded by *CNNB1*, could be involved in driving tumorigenesis by the cross-regulation of NF- κ B (Deng *et al.*, 2002). Aberrant accretion of β -catenin leads to many cancers particularly; downregulation of β -catenin leads to decreasing tumorigenicity (Cai *et al.*, 2014) and inducing apoptosis (Yang *et al.*, 2017). Downregulation of *MDM2* also supported the involvement of the NF- κ B signaling pathway since *MDM2* is a co-transcription factor of NF- κ B at the cytokine promoters, thus suppressing tumor cell growth (Thomasova *et al.*, 2012).

The results of this study also showed the effect of T0 in modulating the MAPK signaling pathway by increased expression of *DUSP3* and *DUSP4* in both LN229 and Snb19 cell lines (see Fig. 4D in publication III). It is reported that either *DUSP3* or *DUSP4* regulates the MAPK family (Kondoh and Nishida, 2007; Huang and Tan, 2012). Also, we observed the increase of *SPRY1*, implying the inhibitory effect on the Ras/MAPK signaling pathway in LN229 and Snb19 upon T0 treatment (Hanafusa *et al.*, 2002). Thus, T0 could successfully bind to the GPR17 receptor, leading to Gai/o activation that inhibits adenylyl cyclase and subsequently decreases the cAMP level. cAMP plays a vital role in regulating protein kinase A (PKA), resulting in inhibiting NF- κ B, STAT, PI3K-Akt, and MAPK/ERK signaling pathways (see Fig. 4E in publication III).

5.3.6 T0 can cross the blood-brain barrier (BBB) and its inhibitory effect on xenograft mice model

Although many conventional and novel therapies have been developed for GBM treatment, delivery into the brain through the BBB is the main obstacle limiting the efficacy of these therapies at the target site (Jue and McDonald, 2016). Here, we used the wild mice model to evaluate the ability of T0 crossing the BBB by HPLC analysis. As a result, T0 had a retention time of 6.043 min, thus confirming the ability of T0 to penetrate the BBB in wild mice (see Fig. 5A in publication III). According to histological analysis of the brain tissues, there were no changes in brain cells' morphology (see Fig. 5B in publication III). In addition, we found no significant pathological changes in the heart, kidney, liver, uterus, and ovary in weight (mg) of T0-treated mice. Other biochemical nephrotoxicity indicators such as sugar, urea, and creatinine of T0-treated mice were also investigated. The results revealed that no significant differences in these indicators were observed compared to control mice (see Fig. 5C in publication III). Taken together, we conclude that T0 has an ability to cross the BBB, which still maintains metabolic homeostasis in wild mice.

We also evaluated the activity of T0 against the growth of the cells derived from GBM patients (PdG), including RN1, MMK1, and JK2, which were collected from different age groups and features (see Fig. 6A in publication III). We first performed a microarray analysis to evaluate the expression of GPR17 in these cells. MMK1 was found to have the highest expression of GPR17, followed by RN1 and JK2. We also found that T0 led to a significant percentage of cell death in MMK1, RN1, and JK2 with 86%, 80%, and 73%, respectively (see Fig. 6B in publication III). Notably, TMZ

had a mild cytotoxic effect on these cell lines with lower than 21% cell growth inhibition. In addition, in this study, we noted a positive correlation between GPR17 expression of PdG cells and the percentage of cell death.

To further investigate the potency of T0 in clinical application, we conducted *in vivo* anti-tumor efficacy test of T0 using xenograft mouse models derived from GBM cells (see Figs. 6C and 6D in publication III). Our results revealed that the tumor volume was decreased from the 8th day to the 36th day of treatment in both T0 and TMZ treatment compared to untreated and DMSO control.

5.4 Combinatorial treatment of alkylaminophenol and GPR17 agonist on PdG cells

Several studies reveal that combining two different compounds could improve the anti-tumor effect in cancer, especially in glioblastoma cells. Therefore, in this section, we present the results of using dual compounds (THTMP and T0) against PdG cells, mesenchymal GBM subtype.

5.4.1 Cytotoxicity of THTMP and T0 single treatment on PdG cells

Since GBM cells have a strong heterogeneity property, we used four GBM cell lines, namely JK2, MMK1, RN1, and PB1, obtained from GBM patients (Stringer *et al.*, 2019). Single treatments of THTMP, T0, and TMZ were performed on these cell lines with a series of concentrations of 5 μ M, 10 μ M, 25 μ M, 50 μ M, 75 μ M, and 100 μ M for 48 hours. At 100 μ M upon TMZ treatment, JK2, MMK1, RN1, and PB1 revealed only 12% of cell growth inhibition; thus, they are classified as TMZ-resistant. Interestingly, at 75 μ M of THTMP, these four cell lines were strongly inhibited up to 90% of cell growth thus, grouping them as THTMP-sensitive cells. RN1 and PB1 cells were resistant to T0 because only 12.5%–37.5% of cell growth inhibition was observed at 75 μ M, thus classifying them as T0-resistant cells. At the same time, JK2 and MMK1 were grouped as T0-sensitive cells with 73.4% cell growth inhibition at 75 μ M (see Figs. 1A and 1B in publication IV). Upon THTMP treatment, the IC₅₀ of MMK1, JK2, RN1, and PB1 were 51.9 μ M, 51.1 μ M, 40.4 μ M, and 32.7 μ M, respectively, while 69.8 μ M, 50.0 μ M, 81.4 μ M, and 101.6 μ M, respectively, upon T0 treatment (see Fig. 1C in publication IV). According to the sensitivity of the cell lines and the IC₅₀ value, we observed that MMK1 and JK2 were more sensitive to THMTP

and T0. Thus, these two cell lines were selected for further analysis of combinatorial treatments, using THTMP, T0, and TMZ against GBM cells.

We performed combinatorial treatment of THTMP+TMZ, THTMP+T0, and T0+TMZ. Our results revealed that TMZ did not improve the inhibitory effect when combined with T0, which showed less than 50% of growth inhibition in MMK1 at the ratio of 70 μM :100 μM . A similar result was recorded in JK2, showing the least effect of TMZ when combined with T0. On the other hand, combining TMZ (10 μM) with THTMP (10 μM) improved the cytotoxicity activity of THTMP on MMK1 and JK2, especially at higher concentrations of THTMP (30 μM –50 μM), resulting in approximately 80% cell growth inhibition. Notably, the combination of THTMP and T0 significantly inhibited, with approximately 90% cell growth inhibition at the ratio of 50 μM :10 μM (see Figs. 1D and 1E in publication IV).

5.4.2 Synergistic effect of THTMP and T0 on PdG cells

Although we observed the increased inhibitory effect with the combinatorial treatment of THTMP with either TMZ or T0, a detailed study of synergism needs to be evaluated. Here, the synergistic effect of these combinations was assessed by quantifying the coefficient of drug interaction (CDI) value using the COMPUSYN method (Chou, 2010). According to Chou's method, if $\text{CDI} > 1$, the combination has antagonism, while synergism is confirmed when $\text{CDI} < 1$. The additive effect was reported when CDI is equal to 1. Our results indicated that combinatorial treatments of THTMP with either TMZ or T0 possessed synergism with lower CDI values in which THTMP+T0 had more synergistic effect than THTMP+TMZ. Also, we noticed that increasing THTMP concentration led to increased synergism with the lower CDI obtained in this combination. In contrast, increased concentration of T0 did not show any significant differences in CDI (see Figs. 2A and 2B in publication IV). According to our results, the combination of 50 μM THTMP and 10 μM T0 had the best synergistic effect due to the lowest CDI value; however, we chose the ratio of 3:1 (30 μM THTMP and 10 μM T0) for further studies, since 50% of cell growth inhibition was obtained when the cells were treated at this ratio.

5.4.3 Effect of combinatorial treatment on migration, invasion, and colony formation properties of PdG cells

Cell invasion is considered a crucial characteristic of cancer. It is associated with cell migration and significantly influences metastasis (Albini *et al.*, 1987). The Transwell technique was conducted to evaluate the effect of THTMP and T0 individually and in combination. Remarkably, both THTMP and T0 decreased the migration ability of MMK1 and JK2 cells in the single treatment. The combination of THTMP and T0 strongly inhibited the GBM migration, with less than 10% of migrated cells found in both cell lines (see Fig. 3A in publication IV). Likewise, THTMP and T0 strongly inhibited the invasion of GBM cells upon combinatorial treatment. THTMP treatment led to 44.3% and 61.1% of cell invasion in MMK1 and JK2, respectively, whereas, 57.5% and 48.7% invaded cells in MMK1 and JK2, respectively, upon T0 treatment. Upon combinatorial treatment, only 27.2% and 20.7% invaded cells were observed in MMK1 and JK2, respectively (see Fig. 3B in publication IV). Thus, we could conclude that THTMP and T0 strongly decrease the movement and invasion properties of GBM cells either in single or in combination treatment.

Besides the migration and invasion ability, colony-forming ability contributes to establishing tumor cell progression. We investigated the colony-forming ability of MMK1 and JK2 after treating them with THTMP and T0 individually and in combination for 48 hours. Even though THTMP and T0 in single treatment led to a remarkable decline in colony formation, a massive decrease in the number of colonies was observed at 48 hours post-treatment upon combinatorial treatment. Approximately 47.9% and 55.5% reduction on MMK1 and JK2, respectively, were recorded. These results indicated that the colony-forming ability of GBM cells was decreased depending on the exposure time of THTMP and combinatorial treatment, while no significant differences were observed when exposure time for T0 was increased. The lowest percentage of the relative colony-forming unit was found at 96 hours (approximately 10%) of exposure followed by 72 hours and finally 48 hours of exposure (see Fig. 4 in publication IV). These data confirmed that the colony-forming property of GBM cells was strongly affected upon THTMP and T0 treatment either individually or in combination, thus effectively targeting the stem cell population in GBM patient tumors.

5.4.4 Combinatorial treatment induces PdG cell cycle arrest at S phase

Our findings have indicated that THTMP and T0 individually and in combination have the ability to induce cell death significantly; hence, we sought to evaluate their effect on the GBM cell cycle using PI staining (see Fig. 5A in publication IV). The fluorescence intensity was quantified to identify the percentage of cells in each phase. The cell number in G2/M phase was similar regardless of their treatments, with 3.5%–6.5% and 14.0%–19.3% in MMK1 and JK2, respectively. An increased percentage of cells in S phase was recorded in comparison with DMSO-treated cells. Particularly in MMK1, 23.7%, 13.5%, and 22.1% of cells were noted in S phase upon THTMP, T0, and combination treatment, respectively, while only 10.0% of that was observed in DMSO control. In JK2, the number of cells in S phase varied upon the treatment, which showed 66.4%, 50.7%, and 69.6% upon THTMP, T0, and combinatorial treatment. Approximately 40.8% of the cells were observed in the case of DMSO. Here, we concluded that both THTMP and T0 individually as well in combination could arrest the GBM cell cycle at S phase before entering the G2/M phase.

5.4.5 Combinatorial treatment induces intrinsic ROS-mediated and mitochondrial apoptosis

To further evaluate the mechanism of action of cell death upon treatment, the apoptosis induction assay was conducted. The highest percentage of apoptotic cells (approximately 35%) was observed in MMK1 and JK2 after being treated with the combination of THTMP and T0. THTMP-treated cells showed approximately 20% and 30% in MMK1 and JK2, respectively. T0 had the lower effect on inducing apoptosis with approximately 15% and 20% of apoptotic cells for MMK1 and JK2 cells, respectively. In addition to apoptosis, we noticed a small proportion of cells subjected to the necrosis process, especially upon T0 treatment (see Fig. 6A in publication IV). The results here are in line with the cytotoxicity results, where the combination of THTMP and T0 resulted in an increased effect on GBM cells.

Calcium signaling also relatively to cell death progression; therefore, intracellular calcium using Fura-2 was measured. Our results showed that the concentration of intracellular calcium ($[Ca^{2+}]_i$) was increased over time up to 120 min when treated with THTMP and T0 individually and in combination (see Fig. 6B in publication IV). In MMK1, THTMP and combinatorial treatment increased $[Ca^{2+}]_i$ better than T0. In JK2 cells, THTMP induced $[Ca^{2+}]_i$ significantly higher than T0 and combination and

remarkably higher than in MMK1. These data suggested that THTMP and T0 in single or combination treatment induce calcium influx, suggesting the involvement of calcium signaling pathway-mediated apoptosis.

It is reported that an accumulation of $[Ca^{2+}]_i$ rapidly leads to the overload of mitochondrial calcium, subsequently damaging mitochondrial membranes. When the mitochondrial membrane is damaged, apoptogenic factors are released, thus triggering the intrinsic apoptosis pathway (Kruman, Guo and Mattson, 1998; Orrenius, Zhivotovsky and Nicotera, 2003; Hajnóczky *et al.*, 2006). In order to demonstrate the mitochondrial integrity affected by these compounds, we performed the MMP assay using JC-1 dye. A sustained decrease of MMP upon THTMP, and combinatorial treatment was observed while T0 slightly increased the MMP over 100 min (see Fig. 6C in publication IV). Despite the increase of MMP upon T0 treatment within 100 min, we noticed the decrease of MMP upon treatment after 24 hours of exposure (see Fig. 6D in publication IV). The results are also in accordance with the calcium influx data, where T0 showed less impact on GBM cells at a shorter exposure time. These data also suggested that apoptosis is triggered by combinatorial treatment through the mitochondrion-dependent pathway.

To further evaluate the effect of our compounds on the mechanism of action of cell death, the ROS assay was performed. ROS is considered to be responsible for many characteristics of cancer cells. It is also involved in various signaling cascades specific to different behaviors of cancer cells like proliferation, survival, metastasis, and angiogenesis (Giles, 2006; Wu and Hua, 2007; Clerkin *et al.*, 2008; Ushio-Fukai and Nakamura, 2008). ROS is also known as an important factor causing the death of cancer cells (Toler, Noe and Sharma, 2006; Circu and Aw, 2010). Our data revealed the production of a higher fold level of ROS upon THTMP and T0 upon single and combinatorial treatment in both cell lines. Approximately 3.5- and 3.0-fold increases were recorded in MMK1 and JK2, respectively, upon combination treatment, and they were significantly higher than the single treatments and H_2O_2 -ROS (positive control) (see Fig. 6E in publication IV). These results suggested that ROS-mediated apoptosis is involved in response to the combinatorial treatment of THTMP and T0. Thus, the loss of MMP leads to the intrinsic apoptotic pathway.

The protein profiling array was performed to determine the modulation of apoptosis-related proteins upon combination treatment. A human apoptosis proteome array containing 35 apoptosis-related proteins was used that represented intrinsic and extrinsic apoptotic pathways (see Fig. 7A in publication IV). Our results revealed the modulation of various apoptosis-related proteins upon combinatorial

treatment, which are involved in intrinsic pathway such as XIAP, p53, cIAP-1, cIAP-2, HSP27, cytochrome *c*, cleaved caspases-3, and Bcl-2. A significant decrease of the anti-apoptotic protein family, Bcl-2, was observed in MMK1 and JK2. Moreover, cytochrome *c* and cleaved caspase-3 expression was also found to be upregulated. The expression of survivin and HSP27, which are known as a caspase 9 inhibitor and cytochrome *c* inhibitor, respectively, decreased significantly. Interestingly, p53-related protein expression strongly decreased upon treatment when compared to DMSO. The decrease of cIAP-1 as well as cIAP-2 expression was found in MMK1, while they were maintained at the same level in JK2 cells. XIAP, which is recognized as the inhibitor of apoptosis protein, decreased significantly, indicating the promising apoptosis induction ability upon treatment (see Figs. 7B and 7C in publication IV). In addition, regarding the intrinsic apoptotic pathway, we also demonstrated that combinatorial treatment inhibited GBM cell growth through an extrinsic pathway due to the modulation of phospho-p53 in JK2 and MMK1. Protein expressions of death receptors such as Fas, FADD, TRAIL R1, TRAIL R2, and TNFR in treated cells were upregulated compared to the control (see Figs. 7B and 7C in publication IV). These results suggested that the combinatorial treatment could activate the intrinsic apoptotic pathway but exclude the involvement of the extrinsic apoptotic pathway of GBM cells.

5.4.6 In vivo study of combinatorial treatment on xenograft model

The anti-tumor efficacy of THTMP+T0 was investigated on the xenograft mouse model for 36 days after the treatment (see Fig. 8A in publication IV). Our results revealed that the relative tumor volume of the therapeutic groups was notably decreased compared to the untreated and the DMSO control. The inhibitory effect of TMZ was higher than the combinatorial treatment. The same pattern was also observed in the percentage of tumor regression value (see Fig. 8B in publication IV). Here, we also observed that in all the conditions, the animal body weight did not change. The result indicates the non-systemic toxicity of the compounds throughout the experimentation period.

6 DISCUSSION

This chapter aims to rationalize the results described in Chapter 5. It focuses on the comparison of the achieved results with the knowledge acquired from previous studies. This chapter shows the significance of the work. It demonstrates the potential anti-tumor activity of alkylaminophenols and GPR17 agonist in single and combinatorial treatment that might help develop GBM treatment in the future.

6.1 The anti-tumor activity of alkylaminophenols, especially THTMP, on glioblastoma cell growth and proliferation

This work is to characterize the anti-tumor activity of alkylaminophenols (publication I). Among three alkylaminophenols, HNPMI structure has a 2-(indolin-1-yl(aryl)methyl)-4-nitrophenol core while THMPP and THTMP have a 2-((1,2,3,4-tetrahydroquinolin-1-yl)(aryl)methyl)phenol core. Amongst these, THTMP showed the strongest inhibitory effect against multiple GBM cell lines, suggesting that the 2-((1,2,3,4-tetrahydroquinolin-1-yl)(aryl)methyl)phenol is an attractive scaffold for developing GBM anti-cancer drugs. By replacing the 4-OMe substituent of the aryl ring with a methyl group in THTMP, it increases its cytotoxicity more than THMPP. This result agrees with the previous study that the lower IC₅₀ value of THTMP is effective against osteosarcoma cell growth, thus reflecting the potency of THTMP as an anti-cancer agent.

We also determined that THTMP induces cell inhibition through DNA damage in a dose- and time-dependent manner. By performing RNA sequencing, the modulation of the gene expression network was explored upon THTMP treatment. Various genes related to DNA damage, DNA replication, apoptosis, and cell cycle were modulated significantly. Interestingly, according to the higher inhibitory effect, alkylaminophenol, THTMP, modulated a greater number of DEGs than TMZ.

THTMP arrested the GBM cell cycle at G1/S phase that is correlated with the modulation of several genes associated with the cell cycle biological pathway. For instance, *CCNA2*, a gene coding for cyclin A2 function in controlling the cell cycle at

G1/S transition point, was significantly modulated upon THTMP treatment. In addition to *CCNA2*, other genes associated with G1/S transition, *BUB1* and *CDC20*, were modulated. The decreased expression of *BUB1* indicates the G1/S phase arrest, revealing its role in the mitosis process. Tang et al. have reported that "the accumulation of *BUB1* at unattached kinetochores affects the recruitment of mitotic arrest deficient dimers" (Tang *et al.*, 2006). Therefore, our results imply that the inhibition of GBM cell growth upon THTMP treatment might cause deregulation in the mitotic cell cycle. In addition to *BUB1*, the decrease of *CDC20* expression further confirms the strong inhibitory effect of THTMP since *CDC20* is reported to be overexpressed in several cancers, including glioblastoma (Marucci *et al.*, 2008; Rajkumar *et al.*, 2011).

Regarding apoptosis induction activity of THTMP, our results reveal that THTMP induces apoptosis in GBM cell lines through upregulated pro-apoptotic genes and downregulated anti-apoptotic genes. We also observed that the number of DEGs associated with apoptosis is higher in Snb19 than LN229 upon THTMP treatment. Also, the sets of anti-apoptotic genes are different in these two cell lines. Thus, the result implies that THTMP could induce apoptosis in GBM cells through the mechanisms specific for each cell line. The result of our work also demonstrated the apoptosis induction activity of TMZ; however, the gene expression profile is limited when compared to THTMP treatment. Therefore, THTMP might possess higher potential activity in inducing GBM apoptosis than TMZ.

6.2 Role of THTMP in GSC and NSCC growth and proliferation by modulating selective signaling pathways:

The focus of this study is to find out the potential mechanism of the activity of THTMP in reducing the growth of GSC and NSCC cells. GSC and NSCC cells from the progenitor LN229 and Snb19 cells were isolated based on the CD133 biomarker. THTMP increased the inhibitory effect of GSC and NSCC over time by damaging the DNA of the cells. The inhibitory activity of THTMP supports the cell cycle data showing that THTMP arrests GSC and NSCC at G1/S and G2/M phase depending on the cell lines. The whole-genome sequencing result strongly confirms the inhibitory activity of THTMP on GSC and NSCC populations. Particularly, decreased expression of *FOXM1* in GSCs and NSCCs indicated strong inactivation and inhibition of THTMP on GBM because *FOXM1* is found to be upregulated in brain cancer (Gong and Huang, 2012), and it is associated with various cellular processes, e.g., cell

proliferation, DNA damage repair, cell cycle progress and cell renewal (Zona *et al.*, 2014).

THTMP showed a better effect on LN229 cells since the downregulation of *Plk2* was found in both NSCC-LN229 and GSC-LN229. Although the exact function of *Plk2* is still in debate, the high expression of *Plk2* is proved to be linked with the chemotherapy resistance in colorectal cancer. Also, the overexpression of *Plk2* leads to an anti-apoptotic effect (Xie *et al.*, 2018). Thus, our findings reveal that THTMP could induce apoptosis of GBM cells due to the decreased *Plk2* expression. An apoptosis induction assay confirmed that THTMP induced apoptosis, especially in an NSCC population. Also, apoptosis induction was mediated by ROS, while caspase 3/7 might not be a significant contributor in inducing apoptosis. In addition to these results, the gene expression profile indicated the modulation of several pro-apoptotic genes and anti-apoptotic genes upon THTMP treatment in both GSC and NSCC populations. Thus, it further confirms that THTMP induces apoptosis in GSC and NSCC populations, yet the in-depth action mechanisms might vary for the specific cell line. Also, it was observed that NSCCs were more highly targeted than GSCs. This result agrees with the previous finding that CSC is highly challenging for chemotherapy.

CSCs have followed two approaches to control the cell cycle in order to prevent tumor progression. One of them is to induce the entry of CSC into the cell cycle, thereby increasing their sensitivity to chemotherapy. Another approach is to force CSC dormancy to avoid generating new cells (Takeishi and Nakayama, 2016). Since the expression of the *Skp2* gene, which is coding for S-phase kinase associated protein 2, remained unmodulated, we could conclude that THTMP does not promote the dormancy of CSCs. On the other hand, the modulation of *CXCR4* (CXC chemokine receptor 4 signaling) was observed, thus targeting CSCs through the first approach, which is inducing the entry of CSC into the cell cycle. Indeed, our PI assay confirmed the cell cycle arrest of those GSCs and NSCCs. In addition, RNA-seq results showed overexpression of numerous genes involved in altering signaling of growth factors and their corresponding signaling pathways. Here, we found several signaling pathways related to growth factors and membrane receptors, such as EGFR, TGF- β , JAK/STAT, and PDGF signaling pathways that were modulated. Our result is in line with a previous study showing that curcumin, a natural phenol, has inhibitory activity on CSCs through the downregulation of *STAT3*. Among the pathways mentioned above, EGF and PDGF were found to be highly targeted

pathways based on the p-value. This suggests that THTMP can play a key role as an EGF and PDGF inhibitor; however, it requires further validation.

One of the most interesting findings of this work is the ability of THTMP to target CSC signaling pathways both in NSCC and in GSC populations. The compound has proven to inhibit CSC signaling pathways Wnt, Notch, and Hh. Wnt signaling was mostly targeted in both GSC and NSCC populations. The expression of a non-degradable β -catenin could widen the CSC population and activate the Wnt signaling pathway, thus leading to the accumulation of β -catenin. We observed a strong downregulated *CTNNB1* gene encoded for β -catenin in GSC-LN229, NSCC-LN229, NSCC-Snb19, and their progenitors. In addition to *CTNNB1*, we observed the deregulated expression of other genes associated with the Wnt signaling pathway upon THTMP treatment. For example, *LGR5*, which can bind to the Wnt receptor, contributes to CSC initiation (Schepers *et al.*, 2012); thus, downregulation of *LGR5* in NSCC-Snb19 has indicated that THTMP prevents CSC initiation. Also, *EDN1* is proven to support the persistence of CSC (Lu *et al.*, 2014); thus, downregulation of *EDN1* in NSCC and mixed-Snb19 has shown the potential ability of the compound to prevent CSC persistence. CSC's invasion and metastasis are also affected due to the downregulation of *MMP7*, *HAS2*, and *CXCR4*, implying that our compound can inhibit invasion and metastasis of GSCs (Gustavson *et al.*, 2004; Choe and Pleasure, 2012; Kretschmer *et al.*, 2016). One interesting group of genes involved in the Hh pathway is GLI, including *GLI1*, *GLI2*, and *GLI3* (Jiang and Hui, 2008). A recent study indicates that *GLI2* has a crucial function in promoting glioma cell growth, proliferation, and migration through the mediation of *ARHGEF16* (Huang *et al.*, 2018). There was no modulation of *GLI2*, but *GLI1* and *GLI3* were modulated in GSC-LN229, NSCC-LN229, NSCC-snb19, and mixed-Snb19. We also noticed that *ARHGEF16* was found to be downregulated in NSCC-Snb19; thus, it might be the target for *GLI3* in GBM cells, yet further validation is needed. It is noted that Wnt had a significant effect on GBM populations, except GSC-Snb19. The same result was also observed in the Hh pathway. Only the Notch pathway was modulated on GSC-Snb19 through the downregulation of *JAG1*. Moreover, only limited deregulated genes were enriched in the mixed-LN229 and Snb19 than their GSCs and NSCCs. Therefore, it suggests that separating the GBM into GSC and NSCC makes them more accessible for targeted therapy than their progenitors.

6.3 T0 as GPR17 agonist and its anti-tumor activity on GBM cells

Recently, GPR17 has been reported as a promising therapeutic target in treating multiple sclerosis and traumatic brain injury in humans (Lecca *et al.*, 2008). A study has reported that a small agonist, MDL 29,951, positively impacts the oligodendrocyte maturation process by activating G α i and G α q protein, resulting in alteration of cAMP and Ca²⁺ concentrations in intact cells, respectively (Hennen *et al.*, 2013). In the present work, the known agonist MDL 29,951 and the novel agonist T0510.3657 were examined for their role in glioblastoma treatment by targeting the GPR17 signaling pathway. Previously, T0 was reported to inhibit cAMP level successfully; however, its cytotoxic activity on cancerous cells still needs investigation (Saravanan *et al.*, 2018). Besides, although MDL 29,951 is reported to be a GPR17 agonist, its inhibitory activity on glioma has not been revealed. Therefore, we have focused on the characterization of T0 to evaluate its ability to serve as a GPR17 agonist and potential chemotherapy for GBM treatment. We also performed the comparative study with MDL 29,951 to check which compound could be more potent.

GPR17 has been reported to be found in brain injury, spinal cord injury and oligodendrocyte differentiation (Li, Zhang and Huang, 2012). It is reported that galinex, a GPR17 agonist, has an ability to delay the development of autoimmune encephalomyelitis (Parravicini *et al.*, 2020). In addition, *in silico* analysis showed that there is upregulation of GPR17 in pediatric diffuse midline glioma clustering to olig1 and olig2 genes (Loveson *et al.*, 2018). Moreover, several genes were explored to play a role in controlling the proliferation of low-grade glioma (LGG) such as LHX2, ARX, CXCL14, and GPR17 (Mascelli *et al.*, 2013). Indeed, our results showed that there was integral expression of GPR17 in LGG as well as in GBM. Our dataset also revealed the there is a link between the expression of GPR17 and the survival time, thus indicating GPR17 as the predictive biomarker for LGG as well as for GBM.

Our results indicated T0 as a potential GPR17 agonist via the inhibition of cAMP level. As predicted, the cAMP level was reduced as G α i was coupled to the C terminal of the GPR17 located in glioma cells upon binding of its agonist T0. It is in line with a previous study stating that the intracellular forskolin induces cAMP level depending on the dose concentration (K Simon *et al.*, 2016). This study was conducted on oligodendrocyte cells by treating them with MDL 29,951, thus inhibiting the oligodendrocyte differentiation. cAMP induction was achieved by triggering the downstream process through the activation of GPR17 by MDL 29,951

through the $G_{\alpha i}$ signaling pathway. The Ca^{2+} assay in our experiment discovered interesting results. We found that the Ca^{2+} was decreased as the concentration of T0 decreased from 100 μ M to 10 μ M. This result contrasts with the previous report, where MDL 29,951, a known agonist of GPR17, significantly induced Ca^{2+} release from rat oligodendrocytes. Thus, the result implies that $G_{\alpha q}$ might not activate the GPR17 signaling pathway upon T0 treatment. As discussed by Ciana et al., only 30% of the hGPR17-transfected cells can couple to PLC in the $G_{\alpha q}$ pathway (Ciana, Fumagalli and Trincavelli, 2006). Another study also reveals a similar pattern in which no effect on calcium level is observed, but the cAMP level is reduced significantly. It further confirms that GPR17 is not strongly associated with the $G_{\alpha q}$ subunit (Fumagalli, Lecca and Abbracchio, 2011). Although T0 decreased calcium influx, which implies that $G_{\alpha q}$ might not be involved in the activation of GPR17 receptor, T0 may have a role in acting as a cannabinoid receptor (Lauckner *et al.*, 2008). Cytotoxicity results concluded that T0 significantly inhibits GBM cell growth after 24 hours of treatment compared to TMZ and MDL 29,951. Therefore, T0 seems to have better performance than the known agonist MDL 29,951. These results indicate that T0 can potentially induce glioblastoma cell growth inhibition, one of the essential criteria for developing anti-tumor drugs.

The study on the kinetic and dynamic effect of T0 on LN229 and Snb19 demonstrated that T0 increases cell death percentage in a dose- and time-dependent manner. We also explored several genes associated with DNA damage that are enriched upon T0 treatment. The study on apoptosis-induced cell death was carried out to confirm whether cell death occurred due to apoptosis induction by T0 or other mechanisms. Our result suggested that T0 induces apoptosis-mediated cell death in GBM cells. The percentage of apoptosis induced by T0 was remarkably higher than that of TMZ. However, it is shown that T0 induces apoptosis-mediated cell death via effectively activating the GPR17 signaling pathway. From the cell cycle assay result, it was clearly understood that both cell lines treated with T0 were arrested at G1 phase. The arrest in G1 indicates the unfavorable condition inside the cells, which makes them stop at G1 phase. It allows cells to enter G0 phase and stay there until everything is back to normal condition. The delay in G1 phase indicates the DNA damage, which prevents the cells from entering M phase. Once the cells have been arrested in G1 phase for a longer time, they might undergo necrosis. The whole-genome profiling further confirmed the in-depth gene expression change linked with the cell cycle and apoptosis progression. Therefore, we conclude that T0 has a stronger ability to inhibit GBM cell growth via apoptosis induction and cell cycle arrest at G1 phase.

Finding a new strategy for GBM treatment has grasped the scientific attention to a greater extent. Some of the anticancer agents were found to be approved by FDA including temozolomide, carmustine, lomustine, and bevacizumab. However, only three of them (temozolomide, carmustine and lomustine) have been found to have ability to partially penetrate to the brain, whereas the bevacizumab does not show significant improvement on the survival of GBM patient (Chinot *et al.*, 2011; Gilbert *et al.*, 2014; Taal *et al.*, 2014). Also, various compounds were identified that targets GPR17 acting as a potential agonist and antagonist (Ivano Eberini *et al.*, 2011; Baqi *et al.*, 2014; Köse *et al.*, 2014). None of them entered into the clinical trials. However, our results showed that T0 not only has an ability to cross the BBB but also has a strong cytotoxic effect against GBM xenograft animal models as well as against GBM patient-derived cells. Thus, T0, GPR17 agonist can open a new gateway for finding successful therapy for glioblastoma treatment.

Overall, even though the pharmacological characterization of GPR17 is still controversial, the result from this study has marked the new goal in generating GPR17-targeted novel signaling molecules. Therefore, it develops the potential approach for therapeutic intervention for GBM treatment. The study results validated the hypothesis that the novel agonist T0 possesses the ability to couple to GPR17 via Gai subunit, thus resulting in the cell apoptosis process and cell cycle arrest at G1 phase.

6.4 The synergistic effect of THTMP and T0 and the use of combinatorial treatment as novel therapeutic agent for glioblastoma

This work evaluates the synergistic effect of THTMP and T0 in combination and the promising anti-tumor property of this combination against multiple PdG cells. This study was initiated by the results of our previous study showing that THTMP single treatment has a strong inhibitory effect on GBM cells while T0 is a potential GPR17 agonist that successfully binds to the GPR17 receptor triggering cell death (Saravanan *et al.*, 2018; Doan *et al.*, 2019, 2020). Given the advantage of combinatorial chemotherapy, we hypothesized that the combination of THTMP and T0 could open a new door to developing a promising therapy for GBM.

Our initial results revealed that all four GBM cell lines were sensitive to THTMP while resistant to TMZ. This finding could be explained by the unmethylation of the MGMT promoter in these cell lines (Stringer *et al.*, 2019), leading to less efficacy of

TMZ in treating GBM (Hegi *et al.*, 2005). Even though less efficacy of TMZ on these cell lines was found, there was increased cell growth inhibition when TMZ was combined with THTMP. This finding suggests that THTMP could be used along with TMZ to increase the efficacy of chemotherapy on the subset of patients. Although combining THTMP with TMZ could improve the inhibitory effect of TMZ, the best combination for the strongest inhibition is the combination of THTMP and T0. It was reported that activation of the GPR17 receptor leads to the inhibition of cAMP level, thereby enhancing the efficacy of chemotherapeutic reagents in glioblastoma (Friesen *et al.*, 2014). Hence, combinatorial treatment of THTMP and T0 possesses a higher inhibitory effect on glioblastoma cells than THTMP and T0 single treatment.

Based on the CDI value, we found that the ratio 50 μ M THTMP and 10 μ M T0 resulting in the best synergism effect. Nevertheless, we selected the ratio of 30 μ M THTMP and 10 μ M T0 for further studies, which gives approximately 50% of cell growth inhibition. It is well known that cell invasion and migration are considered the hallmarks of cancer because they have an essential function in metastasis. The cell invasion mechanisms can help to restrict tumor advancement (Vicente-Manzanares and Horwitz, 2011). We observed that combinatorial treatment significantly reduced migration and invasion properties of GBM cells compared to THTMP and T0 single treatment. These findings are in line with previous reports indicating that phenol derivatives affect the growth of cancerous cells such as breast, colon, and lung cancer cells (Hashim *et al.*, 2008; Sharma *et al.*, 2012; Gupta *et al.*, 2017). Also, the ability to form colonies of GBM cells decreased remarkably, implying the ability of combinatorial treatment in targeting CSC population (Carney *et al.*, 1982; Gou *et al.*, 2007).

In pharmacology, cell growth, proliferation, and apoptosis strongly correlate to developing a new chemotherapeutic treatment. Indeed, cell proliferation remains unchanged when apoptosis is not activated (Ouyang *et al.*, 2012). This study revealed that the combination of THTMP and T0 induced cell cycle arrest remarkably at S phase and induced apoptosis by activating several apoptotic factors better than THTMP and T0 single treatment. Here, we observed that THTMP single treatment resulted in higher cytotoxicity and higher apoptosis induction than T0. Thus, the strong effect of THTMP and T0 in combination might be rooted in the ability to inhibit cAMP level upon activation of the GPR17 signaling pathway by T0, since cAMP is acting as an inhibitor for apoptosis and cell cycle arrest (Boucher *et al.*, 2001).

Furthermore, we also identified the involvement of calcium, mitochondria, and ROS signaling, which are involved in inducing apoptosis due to the modulation of intracellular calcium influx, MMP, and ROS upon the treatments. The mechanism of action of apoptosis activation was further identified by evaluating the change in expression of the apoptotic-related protein. Taken together, our findings suggest that combinatorial treatment activates the apoptosis pathway by accumulating apoptotic mediators, Bax, in mitochondria, leading to increased mitochondrial permeability. This event further releases cytochrome *c*, subsequently activating caspase 3/7 (Douglas R and John C, 1998; Tait and Green, 2010). In addition, the combinatorial treatment also regulated other downstream caspases. For example, the treatment decreased the expression of Survivin, thus inhibiting the activation of caspase 3/7. Moreover, the treatment also triggered the extrinsic apoptotic pathway activation via modulating phosphorylation of p53 (Haupt *et al.*, 2003; Mancini *et al.*, 2009; Seo *et al.*, 2012). However, several dead receptors were found to be the upregulation that does not support the involvement of the extrinsic apoptosis pathway. Hence, these results suggest that the combinatorial treatment more likely activates the intrinsic rather than extrinsic apoptotic pathway. Our results strongly support the apoptosis induction in GBM cells upon combinatorial treatments; however, the involvement of autophagy is still missing. Recently, the study of chemotherapy targeting autophagy has grasped much attention since GBM cells have the ability to inhibit apoptosis (Yan *et al.*, 2016; Taylor, Das and Ray, 2018). Therefore, the study of autophagy of GBM upon the combination of THTMP and T0 should be considered in the future.

Our *in vivo* xenograft model results demonstrated that the combination of THTMP and T0 is a promising strategy against GBM cell growth. TMZ seems to reduce tumor volume better than in combinatorial treatment. However, TMZ has been reported to exert resistance to prolonged therapy, leading to severe consequences such as pneumocystis pneumonia (Tentori and Graziani, 2008), oral ulceration, hepatotoxicity (Kim *et al.*, 2015), acute cardiomyopathy (Huang *et al.*, 2008), and hematological toxicity (Berrocal *et al.*, 2010). No toxic effect of combinatorial treatment in wild mice versus strong mice inhibitory effect against PdG cells indicates the possible development of a therapeutic treatment. Therefore, the combinatorial treatment can potentiate survival through targeted GBM therapy.

7 SUMMARY AND CONCLUSIONS

The study sheds light on the mechanism of action of alkylaminophenol and T0 GPR17 agonist in single and combinatorial treatment against GBM. In the present study, different GBM cells were used, including primary GBM cells (LN229, Snb19, and 1321N1), glioma cancer stem cells (GSC-LN229 and GSC-Snb19), non-stem cancer cells (NSCC-LN229 and NSCC-Snb19), and patient-derived GBM cells (MMK1, JK2, RN1, and PB1). A GBM xenograft mouse model was also utilized to demonstrate the potency of combinatorial treatment for developing novel GBM therapy. The main findings and conclusions are listed below.

1. Among the three phenolic compounds, HNPMI, THMPP, and THTMP, THTMP was found to be a potential derivative possessing a robust inhibitory effect against GBM cells. In comparison with TMZ, THTMP causes greater DNA damage via the modulation of p53, thereby inducing cell death. In addition, THTMP arrests the cell cycle at G1/S phase and induces ROS-mediated apoptosis.
2. THTMP sensitizes TMZ variance of GBM cancer stem cells, thus increasing the percentage of cell growth inhibition. A similar mechanism of action of THTMP was found in GSC and NSCC populations in comparison with the parental GBM population in which the compound targets the cells through ROS-mediated apoptosis. In addition, THTMP possesses the ability to modulate various genes involved in EGFR and CSC signaling pathways.
3. GBM has a high expression of GPR17; thus, it could be used as a target for developing GBM treatment. The GPR17 agonist, T0, selectively binds to the GPR17 receptor in GBM cells and activates downstream signaling pathways, resulting in inhibiting cAMP. T0 also possesses a potential inhibitory effect against GBM cells by arresting the cell cycle at S phase and inducing ROS-mediated apoptosis. Notably, T0 was found to pass across the BBB and thus reduce the tumor volume in GBM xenograft mice models, indicating its ability to serve as a promising agent for GBM treatment.

4. Combinatorial treatment of THTMP and T0 has shown the potential inhibitory effect on multiple patient-derived GBM cell lines by arresting the cell cycle at S phase and inducing cell death through ROS- and caspase-mediated apoptosis. The combinatorial therapy has the ability to reduce migration, invasion, and colony formation of patient-derived GBM cells. Preclinical evaluation of the combinatorial drug has shown promising anti-tumor efficacy in GBM xenograft model by reducing the tumor volume. This work suggests the combinatorial drug as a potential treatment for GBM.

8 REFERENCES

Albain, K.S. *et al.* (2008) "Gemcitabine plus paclitaxel versus paclitaxel monotherapy in patients with metastatic breast cancer and prior anthracycline treatment," *Journal of Clinical Oncology*, 26(24), pp. 3950–3957. doi:10.1200/JCO.2007.11.9362.

Albini, a *et al.* (1987) "A Rapid in Vitro Assay for Quantitating the Invasive Potential of Tumor Cells," *Cancer Research*, 47(12), pp. 3239–3245.

Alvandi, F. *et al.* (2014) "U.S. Food and Drug Administration Approval Summary: Omacetaxine Mepesuccinate as Treatment for Chronic Myeloid Leukemia," *The Oncologist*, 19(1), p. 94. doi:10.1634/theoncologist.2013-0077.

Anders, S., Pyl, P.T. and Huber, W. (2015) "HTSeq – A Python framework to work with high-throughput sequencing data HTSeq – A Python framework to work with high-throughput sequencing data," *Bioinformatics.*, 31(2), pp. 166–169. doi:10.1093/bioinformatics/btu638.

Ashburner, M. *et al.* (2000) "Gene ontology: Tool for the unification of biology," *Nature Genetics*, 25(1), pp. 25–29. doi:10.1038/75556.

Ashkenazi, A. and Dixit, V.M. (1998) "Death receptors: signaling and modulation.," *Science (New York, N.Y.)*, 281(5381), pp. 1305–1308. doi:10.1126/science.281.5381.1305.

Axelsson, M. *et al.* (2013) "U.S. Food and Drug Administration approval: vismodegib for recurrent, locally advanced, or metastatic basal cell carcinoma.," *Clinical cancer research : an official journal of the American Association for Cancer Research*, 19(9), pp. 2289–93. doi:10.1158/1078-0432.CCR-12-1956.

Ayob, A.Z. and Ramasamy, T.S. (2018) "Cancer stem cells as key drivers of tumour progression," *Journal of biomedical science*, 25(1), pp. 1–18.

Badrinath, N. and Yoo, S.Y. (2019) "Recent advances in cancer stem cell-targeted immunotherapy," *Cancers*, 11(3), p. 310. doi:10.3390/cancers11030310.

Baqi, Y. *et al.* (2014) "Improved synthesis of 4-/6-substituted 2-carboxy-1 H-indole-3-propionic acid derivatives and structure–activity relationships as GPR17 agonists," *MedChemComm*, 5(1), pp. 86–92.

Barnum, K.J. and O'Connell, M.J. (2014) "Cell cycle regulation by checkpoints," *Methods in Molecular Biology*, 1170, pp. 29–40. doi:10.1007/978-1-4939-0888-2_2.

Baron, R. and Gori, F. (2018) "Targeting WNT signaling in the treatment of osteoporosis," *Current Opinion in Pharmacology*, 40, pp. 134–141.

Van Den Bent, M.J. *et al.* (2009) "Randomized phase II trial of erlotinib versus temozolomide or carmustine in recurrent glioblastoma: EORTC brain tumor group study 26034," *Journal of Clinical Oncology*, 27(8), pp. 1268–1274. doi:10.1200/JCO.2008.17.5984.

Bernhaus, A. *et al.* (2009) "Digalloylresveratrol, a new phenolic acid derivative induces apoptosis and cell cycle arrest in human HT-29 colon cancer cells," *Cancer Letters*, 274(2), pp. 299–304. doi:10.1016/j.canlet.2008.09.020.

Berrocal, A. *et al.* (2010) "Extended-schedule dose-dense temozolomide in refractory gliomas," *Journal of Neuro-Oncology*, 96(3), pp. 417–422. doi:10.1007/s11060-009-9980-7.

Bieging, K.T., Mello, S.S. and Attardi, L.D. (2014) "Unravelling mechanisms of p53-mediated tumour suppression," *Nature Reviews Cancer*, 14(5), pp. 359–370. doi:10.1038/nrc3711.

Biersack, B. *et al.* (2018) "Recent developments concerning the application of the Mannich reaction for drug design," *Expert Opinion on Drug Discovery*, 13(1), pp. 39–49. doi:10.1080/17460441.2018.1403420.

Bloch, O. *et al.* (2012) "Impact of extent of resection for recurrent glioblastoma on overall survival: Clinical article," *Journal of Neurosurgery*, 117(6), pp. 1032–1038. doi:10.3171/2012.9.JNS12504.

Boucher, M.J. *et al.* (2001) "cAMP protection of pancreatic cancer cells against apoptosis induced by ERK inhibition," *Biochemical and Biophysical Research Communications*, 285(2), pp. 207–216. doi:10.1006/bbrc.2001.5147.

Brechbiel, J., Miller-Moslin, K. and Adjei, A.A. (2014) "Crosstalk between hedgehog and other signaling pathways as a basis for combination therapies in cancer," *Cancer Treatment Reviews*, 40(6), pp. 750–759. doi:10.1016/j.ctrv.2014.02.003.

- Bredel, M. *et al.* (2011) "NFKBIA deletion in glioblastomas," *New England Journal of Medicine*, 364(7), pp. 627–637. doi:10.1056/NEJMoa1006312.
- Brown, T.J. *et al.* (2016) "Association of the extent of resection with survival in glioblastoma a systematic review and meta-Analysis," *JAMA Oncology*, 2(11), pp. 1460–1469. doi:10.1001/jamaoncol.2016.1373.
- Brugarolas, J. *et al.* (1995) "Radiation-induced cell cycle arrest compromised by p21 deficiency," *Nature*, 377(6549), pp. 552–557. doi:10.1038/377552a0.
- Buccioni, M. *et al.* (2011) "Innovative functional cAMP assay for studying G protein-coupled receptors: application to the pharmacological characterization of GPR17," *Purinergic signalling*, 7(4), pp. 463–468.
- Burns, T.F. *et al.* (2003) "Silencing of the Novel p53 Target Gene Snk/Plk2 Leads to Mitotic Catastrophe in Paclitaxel (Taxol)-Exposed Cells," *Molecular and Cellular Biology*, 23(16), p. 5556. doi:10.1128/mcb.23.16.5556-5571.2003.
- Cadigan, K.M. and Waterman, M.L. (2012) "TCF/LEFs and Wnt signaling in the nucleus," *Cold Spring Harbor Perspectives in Biology*, 4(11), p. a007906. doi:10.1101/cshperspect.a007906.
- Cai, K. *et al.* (2014) "Downregulation of β -catenin decreases the tumorigenicity, but promotes epithelial-mesenchymal transition in breast cancer cells," *Journal of Cancer Research and Therapeutics*, 10(4), p. 1063. doi:10.4103/0973-1482.139378.
- Cai, Y. *et al.* (2004) "Antioxidant activity and phenolic compounds of 112 traditional Chinese medicinal plants associated with anticancer," *Life Sciences*, 74(17), pp. 2157–2184. doi:10.1016/j.lfs.2003.09.047.
- Cao, R. *et al.* (2004) "PDGF-BB induces intratumoral lymphangiogenesis and promotes lymphatic metastasis," *Cancer Cell*, 6(4), pp. 333–345. doi:10.1016/j.ccr.2004.08.034.
- Carneiro, B.A. and El-Deiry, W.S. (2020) "Targeting apoptosis in cancer therapy," *Nature reviews Clinical oncology*, 17(7), pp. 395–417.
- Carney, D.N. *et al.* (1982) "Demonstration of the stem cell nature of clonogenic tumor cells from lung cancer patients.," *Stem cells*, 1(3), pp. 149–164.
- Carocho, M. and CFR Ferreira, I. (2013) "The role of phenolic compounds in the fight against cancer—a review," *Anti-Cancer Agents in Medicinal Chemistry (Formerly Current Medicinal Chemistry-Anti-Cancer Agents)*, 13(8), pp. 1236–1258.

Casaburi, I. *et al.* (2013) "Potential of olive oil phenols as chemopreventive and therapeutic agents against cancer: A review of in vitro studies," *Molecular Nutrition and Food Research*, 57(1), pp. 71–83. doi:10.1002/mnfr.201200503.

Casey, L.M. *et al.* (2006) "Jag2-Notch1 signaling regulates oral epithelial differentiation and palate development," *Developmental Dynamics*, 235(7), pp. 1830–1844. doi:10.1002/dvdy.20821.

Ceruti, S. *et al.* (2011) "Expression of the new P2Y-like receptor GPR17 during oligodendrocyte precursor cell maturation regulates sensitivity to ATP-induced death," *GLIA*, 59(3), pp. 363–378. doi:10.1002/glia.21107.

Chaichana, K.L., Jusue-Torres, I., Navarro-Ramirez, R., *et al.* (2014) "Establishing percent resection and residual volume thresholds affecting survival and recurrence for patients with newly diagnosed intracranial glioblastoma," *Neuro-Oncology*, 16(1), pp. 113–122. doi:10.1093/neuonc/not137.

Chaichana, K.L., Jusue-Torres, I., Lemos, A.M., *et al.* (2014) "The butterfly effect on glioblastoma: is volumetric extent of resection more effective than biopsy for these tumors?," *Journal of Neuro-Oncology*, 120(3), pp. 625–634. doi:10.1007/s11060-014-1597-9.

Chen, K., Huang, Y.H. and Chen, J.L. (2013) "Understanding and targeting cancer stem cells: Therapeutic implications and challenges," *Acta Pharmacologica Sinica*, 34(6), pp. 732–740. doi:10.1038/aps.2013.27.

Chen, S. *et al.* (2008a) "Detection of apoptosis induced by new type gosling viral enteritis virus in vitro through fluorescein annexin V-FITC/PI double labeling," *World Journal of Gastroenterology*, 14(14), pp. 2174–2178. doi:10.3748/wjg.14.2174.

Chen, S. *et al.* (2008b) "Detection of apoptosis induced by new type gosling viral enteritis virus in vitro through fluorescein annexin V-FITC/PI double labeling," *World Journal of Gastroenterology*, 14(14), pp. 2174–2178. doi:10.3748/wjg.14.2174.

Chen, X., Kandasamy, K. and Srivastava, R.K. (2003) "Differential roles of RelA (p65) and c-Rel subunits of nuclear factor κ B in tumor necrosis factor-related apoptosis-inducing ligand signaling," *Cancer Research*, 63(5), pp. 1059–1066.

Chen, Z. and Duan, X. (2018) "hsa_circ_0000177-miR-638-FZD7-Wnt signaling cascade contributes to the malignant behaviors in glioma," *DNA and cell biology*, 37(9), pp. 791–797.

Chicheportiche, Y. *et al.* (1997) "TWEAK, a new secreted ligand in the tumor necrosis factor family that weakly induces apoptosis," *Journal of Biological Chemistry*, 272(51), pp. 32401–32410. doi:10.1074/jbc.272.51.32401.

Chinnaiyan, A.M. (1999) "The apoptosome: heart and soul of the cell death machine.," *Neoplasia (New York, N.Y.)*, 1(1), pp. 5–15.
doi:http://dx.doi.org/10.1038/sj.neo.7900003.

Chinot, O.L. *et al.* (2011) "AVAglio: Phase 3 trial of bevacizumab plus temozolomide and radiotherapy in newly diagnosed glioblastoma multiforme," *Advances in Therapy*, 28(4), pp. 334–340. doi:10.1007/s12325-011-0007-3.

Choe, Y. and Pleasure, S.J. (2012) "Wnt signaling regulates intermediate precursor production in the postnatal dentate gyrus by regulating Cxcr4 expression," *Developmental Neuroscience*, 34(6), pp. 502–514. doi:10.1159/000345353.

Chou, T.C. (2010) "Drug combination studies and their synergy quantification using the chou-talalay method," *Cancer Research*, 70(2), pp. 440–446.
doi:10.1158/0008-5472.CAN-09-1947.

Chung, I. *et al.* (2010) "Spatial control of EGF receptor activation by reversible dimerization on living cells," *Nature*, 464(7289), pp. 783–787.
doi:10.1038/nature08827.

Chung, K.Y. *et al.* (2005) "Cetuximab shows activity in colorectal cancer patients with tumors that do not express the epidermal growth factor receptor by immunohistochemistry," *Journal of Clinical Oncology*, 23(9), pp. 1803–1810.
doi:10.1200/JCO.2005.08.037.

Ciana, P., Fumagalli, M. and Trincavelli, M. (2006) "The orphan receptor GPR17 identified as a new dual uracil nucleotides/cysteinyl-leukotrienes receptor," *The EMBO*, 25(19), pp. 4615–4627. doi:10.1038/sj.emboj.7601341.

Circu, M.L. and Aw, T.Y. (2010) "Reactive oxygen species, cellular redox systems, and apoptosis.," *Free radical biology & medicine*, 48(6), pp. 749–62.
doi:10.1016/j.freeradbiomed.2009.12.022.

Clarke, A.R. *et al.* (1993) "Thymocyte apoptosis induced by p53-dependent and independent pathways," *Nature*, 362(6423), pp. 849–852. doi:10.1038/362849a0.

Clerkin, J.S. *et al.* (2008) "Mechanisms of ROS modulated cell survival during carcinogenesis," *Cancer Letters*, 266(1), pp. 30–36.
doi:10.1016/j.canlet.2008.02.029.

- Cohen, D.J. (2012) "Targeting the Hedgehog Pathway. Role in Cancer and Clinical Implications of Its Inhibition," *Hematology/Oncology Clinics of North America*, 26(3), pp. 565–588. doi:10.1016/j.hoc.2012.01.005.
- Cole, G.M. *et al.* (2005) "Prevention of Alzheimer's disease: Omega-3 fatty acid and phenolic anti-oxidant interventions," in *Neurobiology of Aging*, pp. 133–136. doi:10.1016/j.neurobiolaging.2005.09.005.
- Comeau, S.R. *et al.* (2004) "ClusPro: A fully automated algorithm for protein-protein docking," *Nucleic Acids Research*, 32(suppl_2), pp. W96–W99. doi:10.1093/nar/gkh354.
- Cooper, G.M. and Hausman, R.E. (2007) *The Cell: A Molecular Approach 2nd Edition*, Sinauer Associates. doi:NBK9839.
- Della Corte, C.M. *et al.* (2015) "SMO gene amplification and activation of the hedgehog pathway as novel mechanisms of resistance to anti-epidermal growth factor receptor drugs in human lung cancer," *Clinical Cancer Research*, 21(20), pp. 4686–4697. doi:10.1158/1078-0432.CCR-14-3319.
- Cory, S. and Adams, J.M. (2002) "The Bcl2 family: regulators of the cellular life-or-death switch," *Nature Reviews Cancer*, 2(9), pp. 647–656. doi:10.1038/nrc883.
- Creemers, G.J. *et al.* (1996) "Topotecan, an active drug in the second-line treatment of epithelial ovarian cancer: results of a large European phase II study.," *J. Clin. Oncol.*, 14(12), pp. 3056–61. doi:10.1200/JCO.1996.14.12.3056.
- Cui, H. *et al.* (2013) "Notch3 functions as a tumor suppressor by controlling cellular senescence," *Cancer Research*, 73(11), pp. 3451–3459. doi:10.1158/0008-5472.CAN-12-3902.
- Cunningham, D. *et al.* (2004) "Cetuximab monotherapy and cetuximab plus irinotecan in irinotecan- refractory metastatic colorectal cancer," *New England Journal of Medicine*, 351(4), pp. 337–345. doi:10.1056/NEJMoa033025.
- Dai, J. and Mumper, R.J. (2010) "Plant phenolics: Extraction, analysis and their antioxidant and anticancer properties," *Molecules*, 15(10), pp. 7313–7352. doi:10.3390/molecules15107313.
- Daido, S. *et al.* (2005) "Inhibition of the DNA-dependent protein kinase catalytic subunit radiosensitizes malignant glioma cells by inducing autophagy," *Cancer Research*, 65(10), pp. 4368–4375. doi:10.1158/0008-5472.CAN-04-4202.

- Davis, M.E. (2016) "Glioblastoma: Overview of disease and treatment," *Clinical Journal of Oncology Nursing*, 20(5), pp. 1–8. doi:10.1188/16.CJON.S1.2-8.
- Day, B.W. *et al.* (2013) "EphA3 Maintains Tumorigenicity and Is a Therapeutic Target in Glioblastoma Multiforme," *Cancer Cell*, 23(2), pp. 238–248. doi:10.1016/j.ccr.2013.01.007.
- Dean, M., Fojo, T. and Bates, S. (2005) "Tumour stem cells and drug resistance," *Nature Reviews Cancer*, 5(4), pp. 275–284. doi:10.1038/nrc1590.
- Deng, J. *et al.* (2002) "β-catenin interacts with and inhibits NF-κB in human colon and breast cancer," *Cancer Cell*, 2(4), pp. 323–334. doi:10.1016/S1535-6108(02)00154-X.
- Dhillon, A.S. *et al.* (2007) "MAP kinase signalling pathways in cancer," *Oncogene*, 26(22), pp. 3279–3290. doi:10.1038/sj.onc.1210421.
- Doan, P. *et al.* (2016) "Synthesis and Biological Screening for Cytotoxic Activity of N- substituted Indolines and Morpholines," *European Journal of Medicinal Chemistry*, 120, pp. 296–303. doi:10.1017/CBO9781107415324.004.
- Doan, P. *et al.* (2017) "Effect of alkylaminophenols on growth inhibition and apoptosis of bone cancer cells," *European Journal of Pharmaceutical Sciences*, 107, pp. 208–216. doi:10.1016/j.ejps.2017.07.016.
- Doan, P. *et al.* (2019) "Alkylaminophenol induces G1/S phase cell cycle arrest in glioblastoma cells through p53 and cyclin-dependent kinase signaling pathway," *Frontiers in pharmacology*, 10, p. 330. doi:10.3389/fphar.2019.00330.
- Doan, P. *et al.* (2020) "Glioblastoma Multiforme Stem Cell Cycle Arrest by Alkylaminophenol through the Modulation of EGFR and CSC Signaling Pathways," *Cells*, 9(3), p. 681. doi:10.3390/cells9030681.
- Dobin, A. *et al.* (2013) "STAR: Ultrafast universal RNA-seq aligner," *Bioinformatics*, 29(1), pp. 15–21. doi:10.1093/bioinformatics/bts635.
- Dorsam, R.T. and Gutkind, J.S. (2007) "G-protein-coupled receptors and cancer," *Nature Reviews Cancer*, 7(2), pp. 79–94. doi:10.1038/nrc2069.
- Dougherty, J.D. *et al.* (2012) "Candidate pathways for promoting differentiation or quiescence of oligodendrocyte progenitor-like cells in glioma," *Cancer Research*, 72(18), pp. 4856–4868. doi:10.1158/0008-5472.CAN-11-2632.

Douglas R, G. and John C, R. (1998) "Mitochondria and Apoptosis," *Science*, 281, pp. 1309–1312. doi:10.1126/science.281.5381.1309.

Dragu, D.L. *et al.* (2015) "Therapies targeting cancer stem cells: Current trends and future challenges.," *World journal of stem cells*, 7(9), p. 1185. doi:10.4252/wjsc.v7.i9.1185.

Duan, J. *et al.* (2020) "Phenolic compound ellagic acid inhibits mitochondrial respiration and tumor growth in lung cancer," *Food & Function*, 11(7), pp. 6332–6339.

Duvoix, A. *et al.* (2005) "Chemopreventive and therapeutic effects of curcumin," *Cancer Letters*, pp. 181–190. doi:10.1016/j.canlet.2004.09.041.

Eberini, I *et al.* (2011) "In silico identification of new ligands for GPR17: a promising therapeutic target for neurodegenerative diseases," *Journal of Computer-Aided Molecular Design*, 25(8), pp. 743–752. doi:10.1007/s10822-011-9455-8.

Elmore, S. (2007) "Apoptosis: a review of programmed cell death.," *Toxicologic pathology*, 35(4), pp. 495–516. doi:10.1080/01926230701320337.

Emmert-Streib, F. and Glazko, G. V. (2011) "Pathway analysis of expression data: Deciphering functional building blocks of complex diseases," *PLoS Computational Biology*, 7(5), p. e1002053. doi:10.1371/journal.pcbi.1002053.

Enari, M. *et al.* (1998) "A caspase-activated DNase that degrades DNA during apoptosis, and its inhibitor ICAD.," *Nature*, 391(6662), pp. 43–50. doi:10.1038/34112.

Erasimus, H. *et al.* (2016) "DNA repair mechanisms and their clinical impact in glioblastoma," *Mutation Research/Reviews in Mutation Research*, 769, pp. 19–35. doi:10.1016/j.mrrev.2016.05.005.

Eseonu, C.I. *et al.* (2017) "Comparative volumetric analysis of the extent of resection of molecularly and histologically distinct low grade gliomas and its role on survival," *Journal of Neuro-Oncology*, 134(1), pp. 65–74. doi:10.1007/s11060-017-2486-9.

Faghfuri, E. *et al.* (2018) "Mitogen-activated protein kinase (MEK) inhibitors to treat melanoma alone or in combination with other kinase inhibitors," *Expert Opinion on Drug Metabolism and Toxicology*, 14(3), pp. 317–330. doi:10.1080/17425255.2018.1432593.

Fernandez-L, A. *et al.* (2009) "YAP1 is amplified and up-regulated in hedgehog-associated medulloblastomas and mediates Sonic hedgehog-driven neural precursor proliferation," *Genes and Development*, 23(23), pp. 2729–2741. doi:10.1101/gad.1824509.

Fine, H.A. *et al.* (1993) "Meta-analysis of radiation therapy with and without adjuvant chemotherapy for malignant gliomas in adults," *Cancer*, 71(8), pp. 2585–2597. doi:10.1002/1097-0142(19930415)71:8<2585::AID-CNCR2820710825>3.0.CO;2-S.

Fischer, U. and Schulze-Osthoff, K. (2005) "New approaches and therapeutics targeting apoptosis in disease," *Pharmacological reviews*, 57(2), pp. 187–215. doi:10.1124/pr.57.2.6.

Fiuza, S.M. *et al.* (2004) "Phenolic acid derivatives with potential anticancer properties--a structure-activity relationship study. Part 1: methyl, propyl and octyl esters of caffeic and gallic acids," *Bioorganic & medicinal chemistry*, 12(13), pp. 3581–3589. doi:10.1016/j.bmc.2004.04.026.

Flaherty, K.T. *et al.* (2012) "Combined BRAF and MEK inhibition in melanoma with BRAF V600 mutations," *New England Journal of Medicine*, 367(18), pp. 1694–1703. doi:10.1056/NEJMoa1210093.

Forkink, M. *et al.* (2010) "Detection and manipulation of mitochondrial reactive oxygen species in mammalian cells.," *Biochimica et biophysica acta*, 1797(6–7), pp. 1034–44. doi:10.1016/j.bbabi.2010.01.022.

Franke, H. *et al.* (2013) "Changes of the GPR17 receptor, a new target for neurorepair, in neurons and glial cells in patients with traumatic brain injury," *Purinergic Signalling*, 9(3), pp. 451–462. doi:10.1007/s11302-013-9366-3.

Franken, N.A.P. *et al.* (2006) "Clonogenic assay of cells in vitro," *Nature Protocols*, 1(5), pp. 2315–2319. doi:10.1038/nprot.2006.339.

Friedl, P. and Bröcker, E.B. (2000) "The biology of cell locomotion within three-dimensional extracellular matrix," *Cellular and Molecular Life Sciences*, 57(1), pp. 41–64. doi:10.1007/s000180050498.

Friedl, P. and Wolf, K. (2003) "Tumour-cell invasion and migration: diversity and escape mechanisms," *Nature reviews. Cancer*, 3(5), pp. 362–74. doi:10.1038/nrc1075.

- Friedman, H.S. *et al.* (2009) "Bevacizumab alone and in combination with irinotecan in recurrent glioblastoma," *Journal of Clinical Oncology*, 27(28), pp. 4733–4740. doi:10.1200/JCO.2008.19.8721.
- Friesen, C. *et al.* (2014) "Opioid receptor activation triggering downregulation of cAMP improves effectiveness of anti-cancer drugs in treatment of glioblastoma," *Cell Cycle*, 13(10), pp. 1560–1570. doi:10.4161/cc.28493.
- Fumagalli, M., Lecca, D. and Abbracchio, M.P. (2011) "Role of purinergic signalling in neuro-immune cells and adult neural progenitors," *Frontiers in Bioscience*, 16(2326), pp. 10–2741. doi:10.2741/3856.
- Gan, H.K., Cvrljevic, A.N. and Johns, T.G. (2013) "The epidermal growth factor receptor variant III (EGFRvIII): Where wild things are altered," *FEBS Journal*, 280(21), pp. 5350–5370. doi:10.1111/febs.12393.
- Gartel, A.L. (2017) "FOXM1 in cancer: Interactions and vulnerabilities," *Cancer Research*, 77(12), pp. 3135–3139. doi:10.1158/0008-5472.CAN-16-3566.
- Gavai, A. V. *et al.* (2015) "Discovery of clinical candidate BMS-906024: A potent pan-notch inhibitor for the treatment of leukemia and solid tumors," *ACS Medicinal Chemistry Letters*, 6(5), pp. 523–527. doi:10.1021/acsmchemlett.5b00001.
- Gerstner, E.R. *et al.* (2011) "Phase I trial with biomarker studies of vatalanib (PTK787) in patients with newly diagnosed glioblastoma treated with enzyme inducing anti-epileptic drugs and standard radiation and temozolomide," *Journal of Neuro-Oncology*, 103(2), pp. 325–332. doi:10.1007/s11060-010-0390-7.
- Gilbert, M.R. *et al.* (2014) "A randomized trial of bevacizumab for newly diagnosed glioblastoma," *New England Journal of Medicine*, 370(8), pp. 699–708.
- Giles, G.I. (2006) "The redox regulation of thiol dependent signaling pathways in cancer.," *Current pharmaceutical design*, 12(34), pp. 4427–4443. doi:10.2174/138161206779010549.
- Giono, L.E. and Manfredi, J.J. (2006) "The p53 tumor suppressor participates in multiple cell cycle checkpoints," *Journal of Cellular Physiology* [Preprint]. doi:10.1002/jcp.20689.
- Gomes, C.A. *et al.* (2003) "Anticancer Activity of Phenolic Acids of Natural or Synthetic Origin: A Structure-Activity Study," *Journal of Medicinal Chemistry*, 46(25), pp. 5395–5401. doi:10.1021/jm030956v.

Gong, A. and Huang, S. (2012) "FoxM1 and Wnt/ β -catenin signaling in glioma stem cells," *Cancer Research*, 72(22), pp. 5658–5662. doi:10.1158/0008-5472.CAN-12-0953.

González-Espinosa, C. and Guzmán-Mejía, F. (2013) "Basic Elements of Signal Transduction Pathways Involved in Chemical Neurotransmission," in *Identification of Neural Markers Accompanying Memory*, pp. 121–133. doi:10.1016/B978-0-12-408139-0.00008-0.

Gopinathan, L., Ratnacaram, C.K. and Kaldis, P. (2011) "Established and novel Cdk/Cyclin complexes regulating the cell cycle and development," *Results and Problems in Cell Differentiation*, 53, pp. 365–389. doi:10.1007/978-3-642-19065-0_16.

Gottschling, S. *et al.* (2012) "Are we missing the target? - Cancer stem cells and drug resistance in non-small cell lung cancer," *Cancer Genomics and Proteomics*, 9(5), pp. 275–286.

Gou, S. *et al.* (2007) "Establishment of clonal colony-forming assay for propagation of pancreatic cancer cells with stem cell properties," *Pancreas*, 34(4), pp. 429–435. doi:10.1097/MPA.0b013e318033f9f4.

Gryniewicz, G., Poenie, M. and Tsien, R.Y. (1985) "A new generation of Ca²⁺ indicators with greatly improved fluorescence properties," *Journal of Biological Chemistry*, 260(6), pp. 3440–3450.

Gupta, E. *et al.* (2017) "Anticancer potential of steviol in MCF-7 human breast cancer cells," *Pharmacognosy Magazine*, 13(51), p. 345. doi:10.4103/pm.pm_29_17.

Gustavson, M.D. *et al.* (2004) "Tcf binding sequence and position determines β -catenin and Lef-1 responsiveness of MMP-7 promoters," *Molecular Carcinogenesis*, 41(3), pp. 125–139. doi:10.1002/mc.20049.

Hajnóczky, G. *et al.* (2006) "Mitochondrial calcium signalling and cell death: Approaches for assessing the role of mitochondrial Ca²⁺ uptake in apoptosis," *Cell Calcium*, 40(5–6), pp. 553–560. doi:http://dx.doi.org/10.1016/j.ceca.2006.08.016.

Halperin, E.C. *et al.* (1989) "Radiation therapy treatment planning in supratentorial glioblastoma multiforme: An analysis based on post mortem topographic anatomy with ct correlations," *International Journal of Radiation Oncology, Biology, Physics*, 17(6), pp. 1347–1350. doi:10.1016/0360-3016(89)90548-8.

- Hamm, H.E. (1998) "The many faces of G protein signaling.," *The Journal of biological chemistry*, 273(2), pp. 669–72. doi:10.1074/jbc.273.2.669.
- Han, M. *et al.* (2001) "Crystal structure of beta-arrestin at 1.9 Å: possible mechanism of receptor binding and membrane Translocation," *Structure*, 9(9), pp. 869–880. doi:S096921260100644X [pii].
- Han, X. *et al.* (2018) "Kaempferol suppresses proliferation but increases apoptosis and autophagy by up-regulating microRNA-340 in human lung cancer cells," *Biomedicine & Pharmacotherapy*, 108, pp. 809–816.
- Hanafusa, H. *et al.* (2002) "Sprouty1 and Sprouty2 provide a control mechanism for the Ras/MAPK signalling pathway," *Nature Cell Biology*, 4(11), pp. 850–858. doi:10.1038/ncb867.
- Hanif, F. *et al.* (2017) "Glioblastoma Multiforme: A Review of its Epidemiology and Pathogenesis through Clinical Presentation and Treatment," *Asian Pacific journal of cancer prevention : APJCP*, 18(1), pp. 3–9. doi:10.22034/APJCP.2017.18.1.3.
- Harandi, A. *et al.* (2009) "Clinical efficacy and toxicity of anti-EGFR therapy in common cancers," *Journal of Oncology* [Preprint]. doi:10.1155/2009/567486.
- Harbour, J.W. *et al.* (1999) "Cdk phosphorylation triggers sequential intramolecular interactions that progressively block Rb functions as cells move through G1," *Cell*, 98(6), pp. 859–869. doi:10.1016/S0092-8674(00)81519-6.
- Hashim, Y.Z.H.-Y. *et al.* (2008) "Inhibitory effects of olive oil phenolics on invasion in human colon adenocarcinoma cells in vitro.," *International journal of cancer. Journal international du cancer*, 122(3), pp. 495–500. doi:10.1002/ijc.23148.
- Hassan, K.A. *et al.* (2013) "Notch pathway activity identifies cells with cancer stem cell-like properties and correlates with worse survival in lung adenocarcinoma," *Clinical Cancer Research*, 19(8), pp. 1972–1980. doi:10.1158/1078-0432.CCR-12-0370.
- Haupt, S. *et al.* (2003) "Apoptosis - The p53 network," *Journal of Cell Science*, 116(20), pp. 4077–4085. doi:10.1242/jcs.00739.
- He, X. *et al.* (2004) "LDL receptor-related proteins 5 and 6 in Wnt/ β -catenin signaling: Arrows point the way," *Development*, 131(8), pp. 1663–1677. doi:10.1242/dev.01117.

Hegi, M.E. *et al.* (2005) "MGMT Gene Silencing and Benefit from Temozolomide in Glioblastoma," *New England Journal of Medicine*, 352(10), pp. 997–1003. doi:10.1056/NEJMoa043331.

Hegi, M.E. *et al.* (2008) "Correlation of O6-methylguanine methyltransferase (MGMT) promoter methylation with clinical outcomes in glioblastoma and clinical strategies to modulate MGMT activity," *Journal of Clinical Oncology*, 26(25), pp. 4189–4199. doi:10.1200/JCO.2007.11.5964.

Heldin, C.H. (2013) "Targeting the PDGF signaling pathway in tumor treatment," *Cell Communication and Signaling*, 11(1), pp. 1–18. doi:10.1186/1478-811X-11-97.

Hennen, S. *et al.* (2013) "Decoding signaling and function of the orphan G protein-coupled receptor GPR17 with a small-molecule agonist," *Science Signaling*, 6(298). doi:10.1126/scisignal.2004350.

Heuss, S.F. *et al.* (2008) "The intracellular region of Notch ligands Dll1 and Dll3 regulates their trafficking and signaling activity," *Proceedings of the National Academy of Sciences of the United States of America* [Preprint]. doi:10.1073/pnas.0800695105.

Hill, M.M. *et al.* (2004) "Analysis of the composition, assembly kinetics and activity of native Apaf-1 apoptosomes.," *The EMBO journal*, 23(10), pp. 2134–45. doi:10.1038/sj.emboj.7600210.

Hsu, H., Xiong, J. and Goeddel, D. V. (1995) "The TNF receptor 1-associated protein TRADD signals cell death and NF-kappa B activation," *Cell*, 81(4), pp. 495–504. doi:10.1016/0092-8674(95)90070-5.

Hu, Y. and Fu, L. (2012) "Targeting cancer stem cells: a new therapy to cure cancer patients.," *American journal of cancer research*, 2(3), p. 340.

Huang, C.Y. and Tan, T.H. (2012) "DUSPs, to MAP kinases and beyond," *Cell and Bioscience*, 2(1), pp. 1–10. doi:10.1186/2045-3701-2-24.

Huang, D. *et al.* (2018) "GLI2 promotes cell proliferation and migration through transcriptional activation of ARHGEF16 in human glioma cells," *Journal of Experimental and Clinical Cancer Research*, 37(1), pp. 1–17. doi:10.1186/s13046-018-0917-x.

Huang, G. *et al.* (2008) "Solid lipid nanoparticles of temozolomide: Potential reduction of cardiac and nephric toxicity," *International Journal of Pharmaceutics*, 355(1–2), pp. 314–320. doi:10.1016/j.ijpharm.2007.12.013.

Huang, P.H., Xu, A.M. and White, F.M. (2009) "Oncogenic EGFR signaling networks in glioma," *Science Signaling*, 2(87). doi:10.1126/scisignal.287re6.

Hulkower, K.I. and Herber, R.L. (2011) "Cell Migration and Invasion Assays as Tools for Drug Discovery," *Pharmaceutics*, 3(4), pp. 107–124. doi:10.3390/pharmaceutics3010107.

Igney, F.H. and Krammer, P.H. (2002) "Death and anti-death: tumour resistance to apoptosis.," *Nature reviews. Cancer*, 2(4), pp. 277–88. doi:10.1038/nrc776.

Infante, P. *et al.* (2015) "Gli1/ DNA interaction is a druggable target for Hedgehog-dependent tumors," *The EMBO Journal*, 34(2), pp. 200–217. doi:10.15252/embj.201489213.

Javelaud, D. *et al.* (2011) "TGF- β /SMAD/GLI2 signaling axis in cancer progression and metastasis," *Cancer Research*, 71(17), pp. 5606–5610. doi:10.1158/0008-5472.CAN-11-1194.

Ji, T.H., Grossmann, M. and Ji, I. (1998) "G protein-coupled receptors I. Diversity of receptor-ligand interactions," *Journal of Biological Chemistry*, 273(28), pp. 17299–17302. doi:10.1074/jbc.273.28.17299.

Jiang, J. and Hui, C. chung (2008) "Hedgehog Signaling in Development and Cancer," *Developmental Cell*, 15(6), pp. 801–812. doi:10.1016/j.devcel.2008.11.010.

Jones, R.J., Matsui, W.H. and Smith, B.D. (2004) "Cancer stem cells: Are we missing the target?," *Journal of the National Cancer Institute*, 96(8), pp. 583–585. doi:10.1093/jnci/djh095.

Jue, T.R. and McDonald, K.L. (2016) "The challenges associated with molecular targeted therapies for glioblastoma," *Journal of Neuro-Oncology*, pp. 427–434. doi:10.1007/s11060-016-2080-6.

Justilien, V. and Fields, A.P. (2015) "Molecular pathways: Novel approaches for improved therapeutic targeting of hedgehog signaling in cancer stem cells," *Clinical Cancer Research*, 21(3), pp. 505–513. doi:10.1158/1078-0432.CCR-14-0507.

Kam, P.C.A. and Ferch, N.I. (2000) "Apoptosis: mechanisms and clinical implications," *Anaesthesia*, 55(11), pp. 1081–1093. doi:10.1046/j.1365-2044.2000.01554.x.

Kamoto, D. *et al.* (2015) "Structure, Function, Pharmacology, and Therapeutic Potential of the G Protein, Galpha/q,11," *Front Cardiovasc Med*, 2, p. 14. doi:10.3389/fcvm.2015.00014.

Kampa, M. *et al.* (2004) "Antiproliferative and apoptotic effects of selective phenolic acids on T47D human breast cancer cells: potential mechanisms of action.," *Breast Cancer Research*, 6(2), pp. 63–74. doi:10.1186/bcr752.

Karjalainen, A. *et al.* (2017) "Synthesis of phenol-derivatives and biological screening for anticancer activity," *Anti-Cancer Agents in Medicinal Chemistry*, 17(999), pp. 1–1. doi:10.2174/1871520617666170327142027.

Katoh, Masuko and Katoh, Masaru (2006) "Notch ligand, JAG1, is evolutionarily conserved target of canonical WNT signaling pathway in progenitor cells," *International Journal of Molecular Medicine*, 17(4), pp. 681–685. doi:10.3892/ijmm.17.4.681.

Kerr, J.F.R., Wyllie, A.H. and Currie, A.R. (1972) "Apoptosis : a Basic Biological Phenomenon With Wide Ranging Implications in Tissue Kinetics," *Br. J. Cancer*, 26, pp. 239–257. doi:10.1038/bjc.1972.33.

Kim, H.A. *et al.* (2012) "Notch1 counteracts WNT/ β -catenin signaling through chromatin modification in colorectal cancer," *Journal of Clinical Investigation*, 122(9), pp. 3248–3259. doi:10.1172/JCI61216.

Kim, J.H. *et al.* (2017) "Roles of Wnt target genes in the journey of cancer stem cells," *International Journal of Molecular Sciences*, 18(8), p. 1604. doi:10.3390/ijms18081604.

Kim, S.S. *et al.* (2015) "Encapsulation of temozolomide in a tumor-targeting nanocomplex enhances anti-cancer efficacy and reduces toxicity in a mouse model of glioblastoma," *Cancer Letters*, 369(1), pp. 250–258. doi:10.1016/j.canlet.2015.08.022.

Kimple, R.J. *et al.* (2002) "Structural determinants for GoLoco-induced inhibition of nucleotide release by G α subunits," *Nature*, 416(6883), pp. 878–881. doi:10.1038/416878a.

Kinker, G.S. *et al.* (2016) "Deletion and low expression of NFKBIA are associated with poor prognosis in lower-grade glioma patients," *Scientific Reports*, 6(1), pp. 1–9. doi:10.1038/srep24160.

- Kischkel, F.C. *et al.* (1995) "Cytotoxicity-dependent APO-1 (Fas/CD95)-associated proteins form a death-inducing signaling complex (DISC) with the receptor.," *The EMBO journal*, 14(22), pp. 5579–5588.
- Kobayashi, T. and Kageyama, R. (2010) "Hes1 regulates embryonic stem cell differentiation by suppressing Notch signaling," *Genes to Cells*, 15(7), pp. 689–698. doi:10.1111/j.1365-2443.2010.01413.x.
- Kondoh, K. and Nishida, E. (2007) "Regulation of MAP kinases by MAP kinase phosphatases," *Biochimica et Biophysica Acta - Molecular Cell Research*, 1773(8), pp. 1227–1237. doi:10.1016/j.bbamcr.2006.12.002.
- Köse, M. *et al.* (2014) "Development of [(3)H]2-Carboxy-4,6-dichloro-1H-indole-3-propionic Acid [(3)H]PSB-12150): A Useful Tool for Studying GPR17.," *ACS medicinal chemistry letters*, 5(4), pp. 326–30. doi:10.1021/ml400399f.
- Kozasa, T. *et al.* (1998) "p115 RhoGEF, a GTPase activating protein for Gα12 and Gα13," *Science*, pp. 2109–2111. doi:10.1126/science.280.5372.2109.
- Kretschmer, I. *et al.* (2016) "Esophageal squamous cell carcinoma cells modulate chemokine expression and hyaluronan synthesis in fibroblasts," *Journal of Biological Chemistry*, 291(8), pp. 4091–4106. doi:10.1074/jbc.M115.708909.
- Kruman, I., Guo, Q. and Mattson, M.P. (1998) "Calcium and reactive oxygen species mediate staurosporine-induced mitochondrial dysfunction and apoptosis in PC12 cells," *Journal of Neuroscience Research*, 51(3), pp. 293–308. doi:10.1002/(SICI)1097-4547(19980201)51:3<293::AID-JNR3>3.0.CO;2-B.
- Kuehne, P. and Hesse, M. (1993) "Simple synthesis of (±)-(E)-3-(4-hydroxyphenyl)-N-[4-(3-methyl-2,5-dioxo-1-pyrrolidinyl)butyl]-2-propenamide, a novel phenolic amide derivative from the bulbs of *Lilium regale* WILSON," *Tetrahedron*, 49(21), pp. 4575–4580. doi:10.1016/S0040-4020(01)81286-2.
- Kurosaka, K. *et al.* (2003) "Silent cleanup of very early apoptotic cells by macrophages," *Journal of immunology (Baltimore, Md. : 1950)*, 171, pp. 4672–4679. doi:10.4049/jimmunol.171.9.4672.
- Kuznetsov, A. V. *et al.* (2008) "Survival Signaling by C-RAF: Mitochondrial Reactive Oxygen Species and Ca²⁺ Are Critical Targets," *Molecular and Cellular Biology*, 28(7), p. 2304. doi:10.1128/mcb.00683-07.

Labrecque, L. *et al.* (2005) "Combined inhibition of PDGF and VEGF receptors by ellagic acid, a dietary-derived phenolic compound," *Carcinogenesis*, 26(4), pp. 821–826. doi:10.1093/carcin/bgi024.

Lacroix, M. *et al.* (2001) "A multivariate analysis of 416 patients with glioblastoma multiforme: Prognosis, extent of resection, and survival," *Journal of Neurosurgery*, 95(2), pp. 190–198. doi:10.3171/jns.2001.95.2.0190.

Lam, F.C. *et al.* (2018) "Enhanced efficacy of combined temozolomide and bromodomain inhibitor therapy for gliomas using targeted nanoparticles," *Nature Communications*, 9(1), pp. 1–11. doi:10.1038/s41467-018-04315-4.

Lauckner, J.E. *et al.* (2008) "GPR55 is a cannabinoid receptor that increases intracellular calcium and inhibits M current," *Proceedings of the National Academy of Sciences of the United States of America*, 105(7), pp. 2699–2704. doi:10.1073/pnas.0711278105.

Leaman, D.W. *et al.* (2015) "Roles of JAKs in activation of STATs and stimulation of c-fos gene expression by epidermal growth factor.," *Molecular and Cellular Biology*, 16(1), p. 369. doi:10.1128/mcb.16.1.369.

Lecca, D. *et al.* (2008) "The recently identified P2Y-like receptor GPR17 is a sensor of brain damage and a new target for brain repair," *PLoS ONE*, 3(10), p. e3579. doi:10.1371/journal.pone.0003579.

Lee, S., Rauch, J. and Kolch, W. (2020) "Targeting MAPK signaling in cancer: Mechanisms of drug resistance and sensitivity," *International Journal of Molecular Sciences*, 21(3), p. 1102. doi:10.3390/ijms21031102.

Lee, S.Y. (2016) "Temozolomide resistance in glioblastoma multiforme," *Genes and Diseases*, 3(3), pp. 198–210. doi:10.1016/j.gendis.2016.04.007.

Leone, A. *et al.* (2017) "Oxidative Stress Gene Expression Profile Correlates with Cancer Patient Poor Prognosis: Identification of Crucial Pathways Might Select Novel Therapeutic Approaches," *Oxidative Medicine and Cellular Longevity* [Preprint]. doi:10.1155/2017/2597581.

Levine, A.J. (1997) "p53, the cellular gatekeeper for growth and division," *Cell*, 88(3), pp. 323–331. doi:10.1016/S0092-8674(00)81871-1.

Levoye, A. *et al.* (2006) "Do orphan G-protein-coupled receptors have ligand-independent functions? New insights from receptor heterodimers," *EMBO Reports*, 7(11), pp. 1094–1098. doi:10.1038/sj.embor.7400838.

- Lewis, K.L. *et al.* (2011) "Notch2 receptor signaling controls functional differentiation of dendritic cells in the spleen and intestine," *Immunity*, 35(5), pp. 780–791. doi:10.1016/j.immuni.2011.08.013.
- Li, H. *et al.* (2009) "The Sequence Alignment/Map format and SAMtools," *Bioinformatics*, 25(16), pp. 2078–2079. doi:10.1093/bioinformatics/btp352.
- Li, J. *et al.* (2007) "CBP/p300 are bimodal regulators of Wnt signaling," *EMBO Journal*, 26(9), pp. 2284–2294. doi:10.1038/sj.emboj.7601667.
- Li, Y., Zhang, S. and Huang, S. (2012) "FoxM1: A potential drug target for glioma," *Future Oncology* [Preprint]. doi:10.2217/fon.12.1.
- Li, Y.Z. *et al.* (1999) "Release of mitochondrial cytochrome C in both apoptosis and necrosis induced by beta-lapachone in human carcinoma cells.," *Molecular medicine (Cambridge, Mass.)*, 5(4), pp. 232–239. doi:10.1007/BF03402120.
- Liang, C.-C., Park, A.Y. and Guan, J.-L. (2007) "In vitro scratch assay: a convenient and inexpensive method for analysis of cell migration in vitro.," *Nature protocols*, 2(2), pp. 329–33. doi:10.1038/nprot.2007.30.
- Ling, L.-U. *et al.* (2011) "The role of reactive oxygen species and autophagy in safingol-induced cell death.," *Cell death & disease*, 2, p. e129. doi:10.1038/cddis.2011.12.
- Locksley, R.M., Killeen, N. and Lenardo, M.J. (2001) "The TNF and TNF receptor superfamilies: Integrating mammalian biology," *Cell*, pp. 487–501. doi:10.1016/S0092-8674(01)00237-9.
- Love, M.I., Huber, W. and Anders, S. (2014) "Moderated estimation of fold change and dispersion for RNA-seq data with DESeq2," *Genome Biology*, 15(12). doi:10.1186/s13059-014-0550-8.
- Loveson, K. *et al.* (2018) "DIPG-15. The Role of the G-Protein-Coupled Receptor, GPR17 in Paediatric Diffuse Midline Glioma," *Neuro-oncology*, 20(Suppl 2), p. i51.
- Lowe, S.W., Schmitt, E.M., *et al.* (1993) "P53 is required for radiation-induced apoptosis in mouse thymocytes," *Nature*, 362(6423), pp. 847–849. doi:10.1038/362847a0.
- Lowe, S.W., Ruley, H.E., *et al.* (1993) "p53-dependent apoptosis modulates the cytotoxicity of anticancer agents," *Cell*, 74(6), pp. 957–967. doi:10.1016/0092-8674(93)90719-7.

Lowe, S.W. and Lin, a W. (2000) "Apoptosis in cancer.," *Carcinogenesis*, 21(3), pp. 485–495. doi:10.1093/carcin/21.3.485.

Lu, J.W. *et al.* (2014) "Overexpression of endothelin 1 triggers hepatocarcinogenesis in zebrafish and promotes cell proliferation and migration through the AKT pathway," *PLoS ONE*, 9(1), p. e85318. doi:10.1371/journal.pone.0085318.

Lv, S. *et al.* (2015) "The Clinical Implications of Chemokine Receptor CXCR4 in Grade and Prognosis of Glioma Patients: A Meta-Analysis," *Molecular Neurobiology*, 52(1), pp. 555–561. doi:10.1007/s12035-014-8894-3.

Mahapatra, D.K., Asati, V. and Bharti, S.K. (2017) "MEK inhibitors in oncology: a patent review (2015-Present)," *Expert Opinion on Therapeutic Patents*, 27(8), pp. 887–906. doi:10.1080/13543776.2017.1339688.

Malumbres, M. and Barbacid, M. (2009) "Cell cycle, CDKs and cancer: A changing paradigm," *Nature Reviews Cancer*, 9(3), pp. 153–166. doi:10.1038/nrc2602.

Manach, C. *et al.* (2004) "Polyphenols: Food sources and bioavailability," *American Journal of Clinical Nutrition*, 79(5), pp. 727–747. doi:10.1093/ajcn/79.5.727.

Mancini, F. *et al.* (2009) "MDM4 (MDMX) localizes at the mitochondria and facilitates the p53-mediated intrinsic-apoptotic pathway," *EMBO Journal*, 28(13), pp. 1926–1939. doi:10.1038/emboj.2009.154.

Manthey, J. a, Grohmann, K. and Guthrie, N. (2001) "Biological properties of citrus flavonoids pertaining to cancer and inflammation.," *Current medicinal chemistry*, 8(2), pp. 135–153. doi:10.2174/0929867013373723.

Mao, J. *et al.* (2001) "Low-density lipoprotein receptor-related protein-5 binds to Axin and regulates the canonical Wnt signaling pathway," *Molecular Cell*, 7(4), pp. 801–809. doi:10.1016/S1097-2765(01)00224-6.

Martinelli, E. *et al.* (2009) "Anti-epidermal growth factor receptor monoclonal antibodies in cancer therapy," *Clinical and Experimental Immunology*, 158(1), pp. 1–9. doi:10.1111/j.1365-2249.2009.03992.x.

Marucci, G. *et al.* (2008) "Gene expression profiling in glioblastoma and immunohistochemical evaluation of IGFBP-2 and CDC20," *Virchows Archiv*, 453(6), pp. 599–609. doi:10.1007/s00428-008-0685-7.

Mascelli, S. *et al.* (2013) "Molecular fingerprinting reflects different histotypes and brain region in low grade gliomas," *BMC Cancer* [Preprint]. doi:10.1186/1471-2407-13-387.

Mathieu, V. *et al.* (2008) "Combining bevacizumab with temozolomide increases the antitumor efficacy of temozolomide in a human glioblastoma orthotopic xenograft model," *Neoplasia*, 10(12), pp. 1383–1392. doi:10.1593/neo.08928.

McGirt, M.J. *et al.* (2009) "Independent association of extent of resection with survival in patients with malignant brain astrocytoma," *Journal of Neurosurgery*, 110(1), pp. 156–162. doi:10.3171/2008.4.17536.

Memi, F., Zecevic, N. and Radonjić, N. (2018) "Multiple roles of Sonic Hedgehog in the developing human cortex are suggested by its widespread distribution," *Brain Structure and Function*, 223(5), pp. 2361–2375. doi:10.1007/s00429-018-1621-5.

Merchant, A.A. and Matsui, W. (2010) "Targeting Hedgehog - A cancer stem cell pathway," *Clinical Cancer Research*, 16(12), pp. 3130–3140. doi:10.1158/1078-0432.CCR-09-2846.

Mi, H. *et al.* (2009) "PANTHER version 7: Improved phylogenetic trees, orthologs and collaboration with the Gene Ontology Consortium," *Nucleic Acids Research*, 38(Suppl_1), p. D204_D210. doi:10.1093/nar/gkp1019.

Michałowicz, J. and Duda, W. (2007) "Phenols - Sources and toxicity," *Polish Journal of Environmental Studies*, 16(3), pp. 347–362.

Miller, K. *et al.* (2007) "Paclitaxel plus Bevacizumab versus Paclitaxel Alone for Metastatic Breast Cancer," *New England Journal of Medicine*, 357(26), pp. 2666–2676. doi:10.1056/NEJMoa072113.

Modjtahedi, H. and Essapen, S. (2009) "Epidermal growth factor receptor inhibitors in cancer treatment: Advances, challenges and opportunities," *Anti-Cancer Drugs*, 20(10), pp. 851–855. doi:10.1097/CAD.0b013e3283330590.

Mokhtari, R.B. *et al.* (2013) "Combination of carbonic anhydrase inhibitor, acetazolamide, and sulforaphane, reduces the viability and growth of bronchial carcinoid cell lines," *BMC cancer*, 13(1), p. 378. doi:10.1186/1471-2407-13-378.

Mokhtari, R.B. *et al.* (2017) "Combination therapy in combating cancer," *Oncotarget*, 8(23), p. 38022. doi:10.18632/oncotarget.16723.

- Najafi, M., Farhood, B. and Mortezaee, K. (2019) "Cancer stem cells (CSCs) in cancer progression and therapy," *Journal of cellular physiology*, 234(6), pp. 8381–8395.
- Nakano, K. and Vousden, K.H. (2001) "PUMA, a novel proapoptotic gene, is induced by p53," *Molecular Cell*, 7(3), pp. 683–694. doi:10.1016/S1097-2765(01)00214-3.
- Nandi, S., Vracko, M. and Bagchi, M.C. (2007) "Anticancer activity of selected phenolic compounds: QSAR studies using ridge regression and neural networks.," *Chemical biology & drug design*, 70(5), pp. 424–36. doi:10.1111/j.1747-0285.2007.00575.x.
- Neto, Í., Andrade, J., Fernandes, A. S., *et al.* (2016) "Multicomponent Petasis-borono Mannich Preparation of Alkylaminophenols and Antimicrobial Activity Studies," *ChemMedChem*, 11(18), pp. 2015–2023. doi:10.1002/cmde.201600244.
- Neto, Í., Andrade, J., Fernandes, A S, *et al.* (2016) "Multicomponent Petasis-borono Mannich Preparation of Alkylaminophenols and Antimicrobial Activity Studies," *ChemMedChem*, 11(18), pp. 2015–2023. doi:10.1002/cmde.201600244.
- Nicolas, M. *et al.* (2003) "Notch1 functions as a tumor suppressor in mouse skin," *Nature Genetics*, 33(3), pp. 416–421. doi:10.1038/ng1099.
- Norbury, C.J. and Hickson, I.D. (2001) "Cellular responses to DNA damage.," *Annual review of pharmacology and toxicology*, 41, pp. 367–401. doi:10.1146/annurev.pharmtox.41.1.367.
- Olliaro, P. *et al.* (1996) "Systematic review of amodiaquine treatment in uncomplicated malaria.," *Lancet (London, England)*, 348(9036), pp. 1196–1201. doi:10.1016/S0140-6736(96)06217-4.
- Orrenius, S., Zhivotovsky, B. and Nicotera, P. (2003) "Calcium: Regulation of cell death: the calcium-apoptosis link," *Nat Rev Mol Cell Biol*, 4(7), pp. 552–565. doi:10.1038/nrm1150.
- Osanyingbemi-Obidi, J. *et al.* (2011) "Notch signaling contributes to lung cancer clonogenic capacity in vitro but may be circumvented in tumorigenesis in vivo," *Molecular Cancer Research*, 9(12), pp. 1746–1754. doi:10.1158/1541-7786.MCR-11-0286.

- Ostrom, Q.T. *et al.* (2014) "CBTRUS statistical report: Primary brain and central nervous system tumors diagnosed in the United States in 2007–2011," *Neuro-Oncology*, 16(suppl_4), pp. iv1–iv63. doi:10.1093/neuonc/nou223.
- Ouyang, L. *et al.* (2012) "Programmed cell death pathways in cancer: A review of apoptosis, autophagy and programmed necrosis," *Cell Proliferation*, 45(6), pp. 487–498. doi:10.1111/j.1365-2184.2012.00845.x.
- Park, J. *et al.* (2019) "Effect of combined anti-PD-1 and temozolomide therapy in glioblastoma," *Oncolmmunology*, 8(1), p. e1525243. doi:10.1080/2162402X.2018.1525243.
- Parravicini, C. *et al.* (2016) "A promiscuous recognition mechanism between GPR17 and SDF-1: Molecular insights," *Cellular Signalling*, 28(6), pp. 631–642. doi:10.1016/j.cellsig.2016.03.001.
- Parravicini, C. *et al.* (2020) "Development of the first in vivo GPR17 ligand through an iterative drug discovery pipeline: a novel disease-modifying strategy for multiple sclerosis," *PloS one*, 15(4), p. e0231483.
- Von Pawel, J. *et al.* (1999) "Topotecan versus cyclophosphamide, doxorubicin, and vincristine for the treatment of recurrent small-cell lung cancer," *Journal of Clinical Oncology*, 17(2), pp. 658–658. doi:10.1200/JCO.1999.17.2.658.
- Pelicano, H., Carney, D. and Huang, P. (2004) "ROS stress in cancer cells and therapeutic implications," *Drug Resistance Updates*, 7(2), pp. 97–110. doi:10.1016/j.drug.2004.01.004.
- Periasamy, V.S. *et al.* (2015) "Time Lapse Microscopy Observation of Cellular Structural Changes and Image Analysis of Drug Treated Cancer Cells to Characterize the Cellular Heterogeneity," *Environmental toxicology*, 30(6), pp. 724–734. doi:10.1002/tox.
- Pfeffer, C.M. and Singh, A.T.K. (2018) "Apoptosis: a target for anticancer therapy," *International journal of molecular sciences*, 19(2), p. 448.
- Pisano, M. *et al.* (2007) "Antiproliferative and pro-apoptotic activity of eugenol-related biphenyls on malignant melanoma cells.," *Molecular cancer*, 6, p. 8. doi:10.1186/1476-4598-6-8.
- Pollard, S.M. *et al.* (2009) "Glioma Stem Cell Lines Expanded in Adherent Culture Have Tumor-Specific Phenotypes and Are Suitable for Chemical and Genetic Screens," *Cell Stem Cell*, 4(6), pp. 568–580. doi:10.1016/j.stem.2009.03.014.

- Pommier, Y. (2006) "Topoisomerase I inhibitors: Camptothecins and beyond," *Nature Reviews Cancer*, 6(10), pp. 789–802. doi:10.1038/nrc1977.
- Prados, M.D. *et al.* (2009) "Phase II study of erlotinib plus temozolomide during and after radiation therapy in patients with newly diagnosed glioblastoma multiforme or gliosarcoma.," *Journal of Clinical Oncology*, 27(4), pp. 579–84. doi:10.1200/JCO.2008.18.9639.
- Rad, E.B. *et al.* (2016) "Notch4 signaling induces a mesenchymal- Epithelial-like transition in melanoma cells to suppress malignant behaviors," *Cancer Research*, 76(7), pp. 1690–1697. doi:10.1158/0008-5472.CAN-15-1722.
- Raff, M.C. (1992) "Social controls on cell survival and cell death," *Nature*, 356(6368), pp. 397–400. doi:10.1038/356397a0.
- Rajkumar, T. *et al.* (2011) "Identification and validation of genes involved in cervical tumorigenesis," *BMC Cancer*, 11. doi:10.1186/1471-2407-11-80.
- Rappoport, Z. (2003) *The Chemistry of Phenols*, John Wiley & Sons. John Wiley & Sons. doi:10.1002/0470857277.
- Reithmeier, T. *et al.* (2010) "BCNU for recurrent glioblastoma multiforme: efficacy, toxicity and prognostic factors," *BMC Cancer*, 10(1), p. 30. doi:10.1186/1471-2407-10-30.
- Ren, H., Yang, B. and Rainov, N. (2008) "Receptor Tyrosine Kinases as Therapeutic Targets in Malignant Glioma," *Reviews on Recent Clinical Trials*, 2(2), pp. 87–101. doi:10.2174/157488707780599384.
- Rezatabar, S. *et al.* (2019) "RAS/MAPK signaling functions in oxidative stress, DNA damage response and cancer progression," *Journal of cellular physiology*, 234(9), pp. 14951–14965.
- Rode, H.-J. (2008) *Apoptosis, Cytotoxicity and Cell Proliferation*, Roche Diagnostics GmbH. Roche Diagnostics GmbH. doi:05242134001.
- Rajo, F. *et al.* (2015) "Targeted therapies in breast cancer," *Seminars in Diagnostic Pathology*, 25(4), pp. 245–261. doi:10.1053/j.semmp.2008.08.001.
- Roman, G. (2015) "Mannich bases in medicinal chemistry and drug design," *European Journal of Medicinal Chemistry*, 89, pp. 743–816. doi:10.1016/j.ejmech.2014.10.076.

- Ronkainen, J. and Tervonen, O. (2006) "Cost analysis of an open low-field (0.23T) MRI unit: Effect of procedure shares in combined imaging, interventional, and neurosurgical use," *Acta Radiologica*, 47(4), pp. 359–365. doi:10.1080/02841850500537698.
- Rosholm, T. *et al.* (2015) "Glycerol as an efficient medium for the petasis borono-mannich reaction.," *ChemistryOpen*, 4(1), pp. 39–46. doi:10.1002/open.201402066.
- Roskoski, R. (2014) "The ErbB/HER family of protein-tyrosine kinases and cancer," *Pharmacological Research*, 79, pp. 34–74. doi:10.1016/j.phrs.2013.11.002.
- Roskoski, R. (2018) "Targeting oncogenic Raf protein-serine/threonine kinases in human cancers," *Pharmacological Research*, 135, pp. 239–258. doi:10.1016/j.phrs.2018.08.013.
- Saelens, X. *et al.* (2004) "Toxic proteins released from mitochondria in cell death.," *Oncogene*, 23(16), pp. 2861–2874. doi:10.1038/sj.onc.1207523.
- Salentin, S. *et al.* (2017) "From malaria to cancer: Computational drug repositioning of amodiaquine using PLIP interaction patterns," *Scientific Reports*, 7(1), pp. 1–13. doi:10.1038/s41598-017-11924-4.
- Sansom, O.J. *et al.* (2004) "Loss of Apc in vivo immediately perturbs Wnt signaling, differentiation, and migration," *Genes and Development*, 18(12), pp. 1385–1390. doi:10.1101/gad.287404.
- Santamaría, D. *et al.* (2007) "Cdk1 is sufficient to drive the mammalian cell cycle," *Nature*, 448(7155), pp. 811–815. doi:10.1038/nature06046.
- Saravanan, K.M. *et al.* (2018) "Identification of novel GPR17-agonists by structural bioinformatics and signaling activation," *International Journal of Biological Macromolecules*, 106, pp. 901–907. doi:10.1016/j.ijbiomac.2017.08.088.
- Satoh, T., Ishige, K. and Sagara, Y. (2004) "Protective effects on neuronal cells of mouse afforded by ebselen against oxidative stress at multiple steps," *Neuroscience Letters*, 371(1), pp. 1–5. doi:10.1016/j.neulet.2004.04.055.
- Schepers, A.G. *et al.* (2012) "Lineage tracing reveals Lgr5+ stem cell activity in mouse intestinal adenomas," *Science*, 337(6095), pp. 730–735. doi:10.1126/science.1224676.

van Schie, E.H. and van Amerongen, R. (2020) "Aberrant WNT/CTNNB1 Signaling as a Therapeutic Target in Human Breast Cancer: Weighing the Evidence," *Frontiers in Cell and Developmental Biology*, 8, p. 25. doi:10.3389/fcell.2020.00025.

Schneider, E., Montenarh, M. and Wagner, P. (1998) "Regulation of CAK kinase activity by p53," *Oncogene*, 17(21), pp. 2733–2741. doi:10.1038/sj.onc.1202504.

Schulze-Osthoff, K. *et al.* (1998) "Apoptosis signaling by death receptors.," *European journal of biochemistry / FEBS*, 254(3), pp. 439–459. doi:10.1046/j.1432-1327.1998.2540439.x.

Seeram, N.P. *et al.* (2006) "Blackberry, black raspberry, blueberry, cranberry, red raspberry, and strawberry extracts inhibit growth and stimulate apoptosis of human cancer cells in vitro," *Journal of Agricultural and Food Chemistry*, 54(25), pp. 9329–9339. doi:10.1021/jf061750g.

Selassie, C.D. *et al.* (1999) "On the toxicity of phenols to fast growing cells. A QSAR model for a radical-based toxicity," *Journal of the Chemical Society, Perkin Transactions 2*, (12), pp. 2729–2733. doi:10.1039/a905764a.

Sensi, C. *et al.* (2014) "Oxysterols act as promiscuous ligands of class-A GPCRs: In silico molecular modeling and in vitro validation," *Cellular Signalling*, 26(12), pp. 2614–2620. doi:10.1016/j.cellsig.2014.08.003.

Seo, H.S. *et al.* (2012) "Apigenin induces apoptosis via extrinsic pathway, inducing p53 and inhibiting STAT3 and NFκB signaling in HER2-overexpressing breast cancer cells," *Molecular and Cellular Biochemistry*, 366(1), pp. 319–334. doi:10.1007/s11010-012-1310-2.

Shankar, S., Ganapathy, S. and Srivastava, R.K. (2007) "Green tea polyphenols: biology and therapeutic implications in cancer.," *Frontiers in bioscience : a journal and virtual library*, 12(51), pp. 4881–4899. doi:10.2741/2435.

Shapiro, W.R. *et al.* (1989) "Randomized trial of three chemotherapy regimens and two radiotherapy regimens in postoperative treatment of malignant glioma," *Journal of Neurosurgery*, 71(1), pp. 1–9. doi:10.3171/jns.1989.71.1.0001.

Sharma, V. *et al.* (2007) "Kaempferol induces apoptosis in glioblastoma cells through oxidative stress.," *Molecular cancer therapeutics*, 6(9), pp. 2544–53. doi:10.1158/1535-7163.MCT-06-0788.

- Sharma, V. *et al.* (2012) "Synthesis and cytotoxic evaluation of substituted 3-(3'-indolyl-/3'-pyridyl)-isoxazolidines and bis-indoles," *Acta Pharmaceutica Sinica B*, 2(1), pp. 32–41. doi:10.1016/j.apsb.2011.12.009.
- Shi, J. *et al.* (2014) "An IDH1 mutation inhibits growth of glioma cells via GSH depletion and ROS generation," *Neurological Sciences*, 35(6), pp. 839–845. doi:10.1007/s10072-013-1607-2.
- Shukuya, T. *et al.* (2011) "Efficacy of gefitinib for non-adenocarcinoma non-small-cell lung cancer patients harboring epidermal growth factor receptor mutations: A pooled analysis of published reports," *Cancer Science*, 102(5), pp. 1032–1037. doi:10.1111/j.1349-7006.2011.01887.x.
- Sigismund, S., Avanzato, D. and Lanzetti, L. (2018) "Emerging functions of the EGFR in cancer," *Molecular Oncology*, 12(1), pp. 3–20. doi:10.1002/1878-0261.12155.
- Simon, K *et al.* (2016) "The Orphan G Protein-coupled Receptor GPR17 Negatively Regulates Oligodendrocyte Differentiation via Gα_q/o and Its Downstream Effector Molecules," *J Biol Chem*, 291(2), pp. 705–718. doi:10.1074/jbc.M115.683953.
- Simon, Katharina *et al.* (2016) "The orphan G protein-coupled receptor GPR17 negatively regulates oligodendrocyte differentiation via Gα_q/o and its downstream effector molecules," *Journal of Biological Chemistry*, 291(2), pp. 705–718. doi:10.1074/jbc.M115.683953.
- Singh, S.K. *et al.* (2004) "Identification of human brain tumour initiating cells," *Nature*, 432(7015), pp. 369–401. doi:10.1038/nature03128.
- Skoda, J. *et al.* (2016) "Co-expression of cancer stem cell markers corresponds to a pro-tumorigenic expression profile in pancreatic adenocarcinoma," *PLoS ONE*, 11(7), p. e0159255. doi:10.1371/journal.pone.0159255.
- Soares, S. *et al.* (2013) "Different phenolic compounds activate distinct human bitter taste receptors," *Journal of agricultural and food chemistry*, 61(7), pp. 1525–1533.
- Song, L.L. and Miele, L. (2005) "Role of Notch signaling in cell-fate determination of human mammary stem/progenitor cells," *Women's Oncology Review*, 6(6), pp. 1–11. doi:10.1080/14733400500089633.

Sörensen, I., Adams, R.H. and Gossler, A. (2009) "DLL1-mediated Notch activation regulates endothelial identity in mouse fetal arteries," *Blood*, 113(22), pp. 5680–5688. doi:10.1182/blood-2008-08-174508.

Sorich, M.J. *et al.* (2015) "Extended RAS mutations and anti-EGFR monoclonal antibody survival benefit in metastatic colorectal cancer: A meta-analysis of randomized, controlled trials," *Annals of Oncology*, 26(1), pp. 13–21. doi:10.1093/annonc/mdu378.

Stea, B. *et al.* (2003) "Time and dose-dependent radiosensitization of the glioblastoma multiforme U251 cells by the EGF receptor tyrosine kinase inhibitor ZD1839 ('Iressa')," *Cancer Letters*, 202(1), pp. 43–51. doi:10.1016/j.canlet.2003.07.006.

Stegh, A.H. *et al.* (2008) "Bcl2L12-mediated inhibition of effector caspase-3 and caspase-7 via distinct mechanisms in glioblastoma," *Proceedings of the National Academy of Sciences*, 105(31), pp. 10703–10708. doi:10.1073/pnas.0712034105.

Stegh, A.H. *et al.* (2010) "Glioma oncoprotein Bcl2L12 inhibits the p53 tumor suppressor," *Genes and Development*, 24(19), pp. 2194–2204. doi:10.1101/gad.1924710.

Stewart, B.W. and Wild, C.P. (2014) "World cancer report 2014," *World Health Organization*, pp. 1–2. doi:9283204298.

Stringer, B.W. *et al.* (2019) "A reference collection of patient-derived cell line and xenograft models of proneural, classical and mesenchymal glioblastoma," *Scientific Reports*, 9(1), pp. 1–14. doi:10.1038/s41598-019-41277-z.

Stupp, R. *et al.* (2005) "Radiotherapy plus Concomitant and Adjuvant Temozolomide for Glioblastoma," *The New England Journal of Medicine*, 352(10), pp. 987–996. doi:10.1056/NEJMoa043330.

Su, P. *et al.* (2019) "A ginger derivative, zingerone—a phenolic compound—induces ROS-mediated apoptosis in colon cancer cells (HCT-116)," *Journal of biochemical and molecular toxicology*, 33(12), p. e22403.

Taal, W. *et al.* (2014) "Single-agent bevacizumab or lomustine versus a combination of bevacizumab plus lomustine in patients with recurrent glioblastoma (BELOB trial): a randomised controlled phase 2 trial," *The lancet oncology*, 15(9), pp. 943–953.

Tait, S.W.G. and Green, D.R. (2010) "Mitochondria and cell death: Outer membrane permeabilization and beyond," *Nature Reviews Molecular Cell Biology*, 11(9), pp. 621–632. doi:10.1038/nrm2952.

Takahashi-Yanaga, F. and Kahn, M. (2010) "Targeting Wnt signaling: Can we safely eradicate cancer stem cells?," *Clinical Cancer Research*, 16(12), pp. 3153–3162. doi:10.1158/1078-0432.CCR-09-2943.

Takeishi, S. and Nakayama, K.I. (2016) "To wake up cancer stem cells, or to let them sleep, that is the question," *Cancer Science*, 107(7), pp. 875–881. doi:10.1111/cas.12958.

Tamimi, A.F. and Juweid, M. (2017) "Epidemiology and Outcome of Glioblastoma," in *Glioblastoma*. doi:10.15586/codon.glioblastoma.2017.ch8.

Tang, P., Steck, P.A. and Yung, W.K.A. (1997) "The autocrine loop of TGF- α /EGFR and brain tumors," *Journal of Neuro-Oncology*, 35(3), pp. 303–314. doi:10.1023/A:1005824802617.

Tang, Z. *et al.* (2006) "PP2A Is Required for Centromeric Localization of Sgo1 and Proper Chromosome Segregation," *Developmental Cell*, 10(5), pp. 575–585. doi:10.1016/j.devcel.2006.03.010.

Tanoue, L.T. (2009) "EGFR Antagonists in Cancer Treatment," *Yearbook of Pulmonary Disease* [Preprint]. doi:10.1016/s8756-3452(08)79180-1.

Taussig, R., Iñiguez-Lluhi, J.A. and Gilman, A.G. (1993) "Inhibition of adenylyl cyclase by G α_i ," *Science*, 261(5118), pp. 218–221. doi:10.1126/science.8327893.

Taylor, M.A., Das, B.C. and Ray, S.K. (2018) "Targeting autophagy for combating chemoresistance and radioresistance in glioblastoma," *Apoptosis*, 23(11), pp. 563–575. doi:10.1007/s10495-018-1480-9.

Tentori, L. and Graziani, G. (2008) "Recent Approaches to Improve the Antitumor Efficacy of Temozolomide," *Current Medicinal Chemistry*, 16(2), pp. 245–257. doi:10.2174/092986709787002718.

Theeler, B.J. and Gilbert, M.R. (2015) "Advances in the treatment of newly diagnosed glioblastoma," *BMC Medicine*, 13(1), pp. 1–11. doi:10.1186/s12916-015-0536-8.

Thomasova, D. *et al.* (2012) "p53-independent roles of MDM2 in NF- κ B signaling: Implications for cancer therapy, wound healing, and autoimmune diseases," *Neoplasia*, 14(12), pp. 1097–1101. doi:10.1593/neo.121534.

Thompson, C.B. (1995) "Apoptosis in the pathogenesis and treatment of disease.," *Science*, 267(5203), pp. 1456–1462. doi:10.1126/science.7878464.

Thompson, D.C. *et al.* (1993) "Biological and toxicological consequences of quinone methide formation," *Chemico-Biological Interactions*, 86(2), pp. 129–162. doi:10.1016/0009-2797(93)90117-H.

Todaro, G.J., Lazar, G.K. and Green, H. (1965) "The initiation of cell division in a contact-inhibited mammalian cell line," *Journal of Cellular and Comparative Physiology*, 66(3), pp. 325–333. doi:10.1002/jcp.1030660310.

Toler, S., Noe, D. and Sharma, a (2006) "Selective enhancement of cellular oxidative stress by chloroquine: implications for the treatment of glioblastoma multiforme.," *Neurosurgical focus*, 21(6), p. E10. doi:10.3171/foc.2006.21.6.1.

Tominaga, H. *et al.* (2004) "Involvement of reactive oxygen species (ROS) in the induction of genetic instability by radiation.," *Journal of radiation research*, 45(2), pp. 181–8. doi:JST.JSTAGE/jrr/45.181 [pii].

Torres de Pinedo, A., Peñalver, P. and Morales, J.C. (2007) "Synthesis and evaluation of new phenolic-based antioxidants: Structure–activity relationship," *Food Chemistry*, 103(1), pp. 55–61. doi:10.1016/j.foodchem.2006.07.026.

Ushio-Fukai, M. and Nakamura, Y. (2008) "Reactive oxygen species and angiogenesis: NADPH oxidase as target for cancer therapy," *Cancer Letters*, 266(1), pp. 37–52. doi:10.1016/j.canlet.2008.02.044.

Vermes, I. *et al.* (1995) "A novel assay for apoptosis. Flow cytometric detection of phosphatidylserine expression on early apoptotic cells using fluorescein labelled Annexin V," *Journal of Immunological Methods*, 184(1), pp. 39–51. doi:10.1016/0022-1759(95)00072-I.

Vermeulen, K., Berneman, Z.N. and Van Bockstaele, D.R. (2003) "Cell cycle and apoptosis," *Cell Proliferation*, 36(3), pp. 165–175. doi:10.1046/j.1365-2184.2003.00267.x.

Vicente-Manzanares, M. and Horwitz, A.R. (2011) "Cell migration: An overview," *Methods in Molecular Biology*, 769, pp. 1–24. doi:10.1007/978-1-61779-207-6_1.

Vijendra Kumar, N. *et al.* (2014) "Synthesis and quorum sensing inhibitory activity of key phenolic compounds of ginger and their derivatives," *Food Chemistry*, 159, pp. 451–457. doi:10.1016/j.foodchem.2014.03.039.

Visvader, J.E. and Lindeman, G.J. (2008) "Cancer stem cells in solid tumours: accumulating evidence and unresolved questions.," *Nature reviews. Cancer*, 8(10), pp. 755–68. doi:10.1038/nrc2499.

Vousden, K.H. and Lane, D.P. (2007) "p53 in health and disease," *Nature Reviews Molecular Cell Biology* [Preprint]. doi:10.1038/nrm2147.

Vousden, K.H. and Prives, C. (2009) "Blinded by the Light: The Growing Complexity of p53," *Cell*, 137(3), pp. 413–431. doi:10.1016/j.cell.2009.04.037.

De Vries, S.J., Van Dijk, M. and Bonvin, A.M.J.J. (2010) "The HADDOCK web server for data-driven biomolecular docking," *Nature Protocols*, 5(5), pp. 883–897. doi:10.1038/nprot.2010.32.

Wajant, H. (2002) "The Fas signaling pathway: more than a paradigm.," *Science*, 296(5573), pp. 1635–1636. doi:10.1126/science.1071553.

Walsh, J.G. *et al.* (2008) "Executioner caspase-3 and caspase-7 are functionally distinct proteases.," *Proceedings of the National Academy of Sciences of the United States of America*, 105(35), pp. 12815–12819. doi:10.1073/pnas.0707715105.

Wang, D. *et al.* (2016) "BIRC3 is a novel driver of therapeutic resistance in Glioblastoma," *Scientific Reports*, 6(1), pp. 1–13. doi:10.1038/srep21710.

Wang, N. *et al.* (2012) "Ellagic acid, a phenolic compound, exerts anti-angiogenesis effects via VEGFR-2 signaling pathway in breast cancer," *Breast cancer research and treatment*, 134(3), pp. 943–955.

Weinert, E.E. *et al.* (2006) "Substituents on quinone methides strongly modulate formation and stability of their nucleophilic adducts," *Journal of the American Chemical Society*, 128(36), pp. 11940–11947. doi:10.1021/ja062948k.

Weinert, T. (1997) "A DNA damage checkpoint meets the cell cycle engine," *Science*, pp. 1450–1451. doi:10.1126/science.277.5331.1450.

Wellbrock, J. *et al.* (2015) "Expression of hedgehog pathway mediator GLI represents a negative prognostic marker in human acute myeloid leukemia and its inhibition exerts Antileukemic effects," *Clinical Cancer Research*, 21(10), pp. 2388–2398. doi:10.1158/1078-0432.CCR-14-1059.

Williams, C.K. *et al.* (2006) "Up-regulation of the Notch ligand Delta-like 4 inhibits VEGF-induced endothelial cell function," *Blood*, 107(3), pp. 931–939. doi:10.1182/blood-2005-03-1000.

Wu, D. and Pan, W. (2010) "GSK3: a multifaceted kinase in Wnt signaling," *Trends in Biochemical Sciences*, 35(3), pp. 161–168. doi:10.1016/j.tibs.2009.10.002.

Wu, D.M. *et al.* (2019) "MCL1 gene silencing promotes senescence and apoptosis of glioma cells via inhibition of the PI3K/Akt signaling pathway," *IUBMB Life*, 7(1), pp. 81–92. doi:10.1002/iub.1944.

Wu, P.K. and Park, J.I. (2015) "MEK1/2 Inhibitors: Molecular Activity and Resistance Mechanisms," *Seminars in Oncology*, 42(6), pp. 849–862. doi:10.1053/j.seminoncol.2015.09.023.

Wu, X.J. and Hua, X. (2007) "Targeting ROS: Selective killing of cancer cells by a cruciferous vegetable derived pro-oxidant compound," *Cancer Biology and Therapy*, 6(5), pp. 646–647. doi:10.4161/cbt.6.5.4092.

Xie, Y. *et al.* (2018) "Polo-like kinase 2 promotes chemoresistance and predicts limited survival benefit from adjuvant chemotherapy in colorectal cancer," *International Journal of Oncology*, 52(5), pp. 1401–1414. doi:10.3892/ijo.2018.4328.

Yan, Y. *et al.* (2016) "Targeting autophagy to sensitive glioma to temozolomide treatment," *Journal of Experimental and Clinical Cancer Research*, 35(1), pp. 1–14. doi:10.1186/s13046-016-0303-5.

Yang, C.-M. *et al.* (2017) "β-Catenin promotes cell proliferation, migration, and invasion but induces apoptosis in renal cell carcinoma," *OncoTargets and therapy*, 10, pp. 711–724. doi:10.2147/OTT.S117933.

Yang, F. *et al.* (2010) "Sorafenib Induces Growth Arrest and Apoptosis of Human Glioblastoma Cells through the Dephosphorylation of Signal Transducers and Activators of Transcription 3," *Molecular Cancer Therapeutics*, 9(4), pp. 953–962. doi:10.1158/1535-7163.MCT-09-0947.

Yang, M.C. *et al.* (2015) "Bcl2L12 with a BH3-like domain in regulating apoptosis and TMZ-induced autophagy: A prospective combination of ABT-737 and TMZ for treating glioma," *International Journal of Oncology*, 46(3), pp. 1304–1316. doi:10.3892/ijo.2015.2838.

Yarmolinsky, M.B. (1995) "Programmed cell death in bacterial populations," *Science*, 267(5199), pp. 836–837. doi:10.1126/Science.7846528.

Y.Benjamini and Y.Hochberg (1995) "Controlling the False Discovery Rate: A Practical and Powerful Approach to Multiple Testing," *Journal of the Royal*

Statistical Society. Series B (Methodological), 57(1), pp. 289–300.
doi:10.2307/2346101.

Yen, W.C. *et al.* (2015) “Targeting notch signaling with a Notch2/Notch3 antagonist (Tarextumab) inhibits tumor growth and decreases tumor-initiating cell frequency,” *Clinical Cancer Research*, 21(9), pp. 2084–2095. doi:10.1158/1078-0432.CCR-14-2808.

Yoshida, T. *et al.* (2008) “Kaempferol sensitizes colon cancer cells to TRAIL-induced apoptosis,” *Biochemical and Biophysical Research Communications*, 375(1), pp. 129–133.

You, S. *et al.* (2010) “PTCH1, a receptor of Hedgehog signaling pathway, is correlated with metastatic potential of colorectal cancer,” *Upsala Journal of Medical Sciences*, 115(3), pp. 169–175. doi:10.3109/03009731003668316.

Youle, R.J. and Strasser, A. (2008) “The BCL-2 protein family: Opposing activities that mediate cell death,” *Nature Reviews Molecular Cell Biology*, 9(1), pp. 47–59. doi:10.1038/nrm2308.

Yu, H.G. *et al.* (2003) “Increased expression of RelA/nuclear factor- κ B protein correlates with colorectal tumorigenesis,” *Oncology*, 65(1), pp. 37–45. doi:10.1159/000071203.

Zhang, B. *et al.* (2018) “Antineoplastic activity of isoliquiritigenin, a chalcone compound, in androgen-independent human prostate cancer cells linked to G2/M cell cycle arrest and cell apoptosis,” *European Journal of Pharmacology*, 821, pp. 57–67. doi:10.1016/j.ejphar.2017.12.053.

Zhang, S. *et al.* (2017) “Suppression of protein tyrosine phosphatase N23 predisposes to breast tumorigenesis via activation of FYN kinase,” *Genes and Development*, 31(19), pp. 1939–1957. doi:10.1101/gad.304261.117.

Zhang, Y. *et al.* (2008) “Isolation and identification of strawberry phenolics with antioxidant and human cancer cell antiproliferative properties,” *Journal of Agricultural and Food Chemistry*, 56(3), pp. 670–675. doi:10.1021/jf071989c.

Zhao, C. *et al.* (2007) “Loss of β -Catenin Impairs the Renewal of Normal and CML Stem Cells In Vivo,” *Cancer Cell*, 12(6), pp. 528–541. doi:10.1016/j.ccr.2007.11.003.

Zona, S. *et al.* (2014) “FOXM1: An emerging master regulator of DNA damage response and genotoxic agent resistance,” *Biochimica et Biophysica Acta - Gene*

Regulatory Mechanisms, 1839(11), pp. 1316–1322.
doi:10.1016/j.bbagr.2014.09.016.

Zörnig, M. *et al.* (2001) "Apoptosis regulators and their role in tumorigenesis,"
Biochimica et Biophysica Acta - Reviews on Cancer, 1551(2), pp. F1–F37.
doi:10.1016/S0304-419X(01)00031-2.

PUBLICATIONS

I



Alkylaminophenol Induces G1/S Phase Cell Cycle Arrest in Glioblastoma Cells Through p53 and Cyclin-Dependent Kinase Signaling Pathway

Phuong Doan^{1,2}, Aliyu Musa^{2,3}, Nuno R. Candeias⁴, Frank Emmert-Streib^{2,3}, Olli Yli-Harja^{2,5,6} and Meenakshisundaram Kandhavelu^{1,2*}

¹ Molecular Signaling Lab, Faculty of Medicine and Health Technology, Tampere University and BioMediTech, Tampere, Finland, ² Institute of Biosciences and Medical Technology, Tampere, Finland, ³ Predictive Medicine and Data Analytics Lab, Faculty of Medicine and Health Technology, Tampere University and BioMediTech, Tampere, Finland, ⁴ Faculty of Engineering and Natural Sciences, Tampere University, Tampere, Finland, ⁵ Computational Systems Biology Group, Faculty of Medicine and Health Technology, Tampere University and BioMediTech, Tampere, Finland, ⁶ Institute for Systems Biology, Seattle, WA, United States

OPEN ACCESS

Edited by:

Carmen Alvarez-Lorenzo,
University of Santiago
de Compostela, Spain

Reviewed by:

Wei-jiang Zhao,
Shantou University Medical College,
China
Joseph Louis Lasky,
Cure 4 The Kids, United States

*Correspondence:

Meenakshisundaram Kandhavelu
meenakshisundaram.kandhavelu@
tuni.fi

Specialty section:

This article was submitted to
Pharmacology of Anti-Cancer Drugs,
a section of the journal
Frontiers in Pharmacology

Received: 19 August 2018

Accepted: 19 March 2019

Published: 02 April 2019

Citation:

Doan P, Musa A, Candeias NR,
Emmert-Streib F, Yli-Harja O and
Kandhavelu M (2019)
Alkylaminophenol Induces G1/S
Phase Cell Cycle Arrest
in Glioblastoma Cells Through p53
and Cyclin-Dependent Kinase
Signaling Pathway.
Front. Pharmacol. 10:330.
doi: 10.3389/fphar.2019.00330

Glioblastoma (GBM) is the most common type of malignant brain tumor in adults. We show here that small molecule 2-[(3,4-dihydroquinolin-1(2H)-yl)(p-tolyl)methyl]phenol (THTMP), a potential anticancer agent, increases the human glioblastoma cell death. Its mechanism of action and the interaction of selective signaling pathways remain elusive. Three structurally related phenolic compounds were tested in multiple glioma cell lines in which the potential activity of the compound, THTMP, was further validated and characterized. Upon prolonged exposure to THTMP, all glioma cell lines undergo p53 and cyclin-dependent kinase mediated cell death with the IC₅₀ concentration of 26.5 and 75.4 μM in LN229 and Snb19, respectively. We found that THTMP strongly inhibited cell growth in a dose and in time dependent manner. THTMP treatment led to G1/S cell cycle arrest and apoptosis induction of glioma cell lines. Furthermore, we identified 3,714 genes with significant changes at the transcriptional level in response to THTMP. Further, a transcriptional analysis (RNA-seq) revealed that THTMP targeted the p53 signaling pathway specific genes causing DNA damage and cell cycle arrest at G1/S phase explained by the decrease of cyclin-dependent kinase 1, cyclin A2, cyclin E1 and E2 in glioma cells. Consistently, THTMP induced the apoptosis by regulating the expression of Bcl-2 family genes and reactive oxygen species while it also changed the expression of several anti-apoptotic genes. These observations suggest that THTMP exerts proliferation activity inhibition and pro-apoptosis effects in glioma through affecting cell cycle arrest and intrinsic apoptosis signaling. Importantly, THTMP has more potential at inhibiting GBM cell proliferation compared to TMZ, the current chemotherapy treatment administered to GBM patients; thus, we propose that THTMP may be an alternative therapeutic option for glioblastoma.

Keywords: phenol, anticancer, cytotoxicity, apoptosis induction, gene expression, cell cycle

INTRODUCTION

Glioblastoma (GBM) is known as the most aggressive primary brain tumor. Although different treatments have been combined such as surgical operation, chemotherapy, or radiotherapy, no standard treatment has been proven to be effective for treating brain tumor. It is noted that patients with glioblastoma have an average survival of 12–15 months. For chemotherapy, temozolomide (TMZ) is one of the drugs accepted to be used in combination with radiotherapy to treat brain tumor (Stupp et al., 2005). However, some limitations related to use of TMZ such as the over expression of O6-methylguanine-DNA methyltransferase (MGMT) and/or lacking of a DNA repair pathway in GBM cells (Hegi et al., 2005) still need to be addressed; therefore, effective recurrence needs to be explored further.

A comprehensive understanding of the response of glioblastomas to chemotherapy and detailed chemotherapy resistance analysis of gliomas may help to identify effective agents for the treatment of this disease. Currently, many chemical compounds including sorafenib (Yang et al., 2010), bevacizumab (Friedman et al., 2009), and kaempferol (Sharma et al., 2007) have been studied for anti-glioma ability, especially for inducing GBM growth arrest and apoptosis. In the past few decades, many efforts have been made in understanding chemotherapy-induced DNA damage response (DDR) such as activation of checkpoint, repair and cell death pathways. It is reported that GBM responds to DNA damage induced by genotoxic drugs by activating DNA repair machinery (Erasmus et al., 2016). Thereby, improving chemotherapy response should be made to address this issue. Beside the DNA damage, targeting cell cycle arrest and apoptosis also grasped the attention for GBM treatment. In glioma cells, several key regulatory elements of cell cycle and apoptosis alter the expression of cyclin-dependent kinases such as Bcl-2 protein family, p53 protein, inhibitor of apoptosis proteins (IAPs) or receptor tyrosine kinases like the epidermal growth factor receptor (EGFR) and their down-stream signaling cascade. Among these signaling pathways, p53 plays an essential role in cellular responses to DNA damage and regulation of cell cycle and apoptosis. It is well known that p53 functions as a transcription factor for genes relevant for the regulation of the cell cycle (e.g., p21) or apoptosis (e.g., BAX, BAK, PUMA, Bcl-2). Furthermore, p53 may also promote apoptosis through transcription-independent mechanisms and direct interactions with members of the Bcl-2 family of proteins in the cytosol or mitochondria.

In the past decades, many advances have been made in understanding the ability of phenolic compounds in acting as effective chemopreventive agents especially throughout the properties of inducing cell cycle arrest and apoptosis in tumor cells (Wu et al., 2009). Several mechanisms were studied explaining the effectiveness of these compounds as chemopreventive agents for cancer treatment. These compounds can suppress the overexpression of pro-oxidant enzymes implicated in the development of cancer. They are also able to inhibit the transcriptional factor activation, thus regulating target genes correlated with cell survival, apoptosis and proliferation (Wcislo et al., 2013). For instance, polyphenols have the ability

to modulate various targets of apoptosis pathways including the expression of regulatory proteins, cytochrome *c*, activation of caspase 9 and caspase 3 (Selvendiran et al., 2006), increase of caspases-8 and t-Bid levels (Selvendiran et al., 2006), increase of Bax and Bak expression (Selvendiran et al., 2006), down-regulation of Bcl-2 and Bcl-XL expression, and modulation of transcription factor NF- κ B (Gong et al., 2003). In addition, a study of resveratrol, a natural phenol, revealed the ability to prevent or delay the onset of several types of cancers because they can regulate multiple cellular processes associated with carcinogenesis. In detail, this compound can inhibit cell proliferation and induce apoptosis by dysregulating cell cycle (Gali-Muhtasib et al., 2015), increasing caspase activity (Kim et al., 2003), and decreasing Bcl-2 and Bcl-XL levels.

Alkylaminophenols, being Mannich bases, are a particular kind of phenols (Roman, 2015). Although reported as precursors of quinone methides (Weinert et al., 2006), which can react with biomacromolecules (Thompson et al., 1993), alkylaminophenol moiety is also found in some FDA-approved drugs namely, amodiaquine, used for malaria treatment (Olliaro et al., 1996) and in topotecan, a topoisomerase inhibitor chemotherapeutic agent (Pommier, 2006). Previously, we reported the potential anticancer activity as apoptosis inducer of several alkylaminophenols on osteosarcoma cells, namely: *N*-[2-hydroxy-5-nitrophenyl(4'-methylphenyl)methyl]indoline (HNPMI) (Doan et al., 2016), 2-[(1,2,3,4-tetrahydroquinolin-1-yl)(4-methoxyphenyl)methyl]phenol (THMPP) (Karjalainen et al., 2017) and 2-[(3,4-dihydroquinolin-1(2H)-yl)(p-tolyl)methyl]phenol (THTMP) (Neto et al., 2016). To our knowledge, the anticancer activity of various phenolic derivatives have been evaluated on several human cancer cell lines but the effect as well as the in depth mechanism of phenols on brain cancer are not well investigated. Motivated by the numerous reports on the anticancer properties of phenolic compounds and our previous studies on alkylaminophenols, we recently examine the effect of HNPMI, THMPP, and THTMP on multiple glioblastoma cell lines (1321N1, LN229, and Snb19). Several *in vitro* preclinical assays were performed to indicate the cytotoxicity of this derivative on GBM. Specifically, the ability to kill GBM cells.

In spite of the multiple mechanisms have been proposed for chemotherapeutic resistance in glioblastoma cells, the analysis of molecular signaling events is still not comprehensive. To date, advances in high-throughput sequencing methodology have provided a large amount of information regarding gene expression at the transcriptome level, as well as the underlying molecular events in response to chemotherapeutic drugs. Hence, the RNA-seq technique was used in this work to investigate alkylaminophenol -responsive genes in GBM cells. Here, we compared the gene expression profile of GMB cells between an alkylaminophenol and temozolomide. After determining the gene expression profile, we focused on the cell cycle arrest and the apoptosis pathway activated by our alkylaminophenol and investigated the significant of cell cycle genes as well as pro-apoptosis and anti-apoptosis genes in gliomas chemotherapeutic resistance. The cell cycle arrest was then validated by FUCCI biosensor and the apoptosis induction validation was performed

using Annexin V and PI double staining. Moreover, ROS production and caspase 3/7 activation measurements were conducted to reconfirm the involvement of apoptosis pathway when the GBM cells were treated with phenolic derivatives.

MATERIALS AND METHODS

GBM Cell Lines and Chemical Preparation

1321N1 is a human astrocytoma cell line isolated as a sub clone of the cell line 1181N1 which in turn was isolated from the parent line U-118 MG (one of a number of cell lines derived from malignant gliomas). LN229 cell line was taken from a patient with right frontal parieto-occipital glioblastoma. The cells exhibit mutated p53 (TP53) and possible homozygous deletions in the p16 and p14ARF tumor suppressor genes. Snb19 is a malignant glioblastoma cell line initiated from the surgical resection of a left parietooccipital glioblastoma multiforme tumor. This line has been shown by DNA profiling studies to be a derivative of the U-373 cell line.

Synthesis and spectral characterization of compounds HNPMI (18), THMPP (19), and THTMP (20) were previously reported. These compounds and TMZ (Sigma-Aldrich, United States) were dissolved in dimethyl sulphoxide (DMSO, Sigma-Aldrich, St. Louis, MO, United States) to obtain a stock of 100 mM, from which, intermediate dilutions were prepared. The final concentrations used were 100, 75, 50, 25, and 10 μ M, in the culture medium.

Cell Culture

The human glioma cell lines Snb19, LN229, and mouse embryonal fibroblast (MEF) cell lines were cultured in Dulbecco's Modified Eagle Medium (DMEM) supplemented with 10% FBS, 0.1 mg/ml Streptomycin, 100 U/ml Penicillin, and 0.025 mg/ml Amphotericin B. For 1321N1 cell line, the culture medium was prepared as previously but it was supplemented with 2 mM sodium pyruvate. HEK293T cells were cultured in DMEM supplemented with 10% FBS, 0.1 mg/ml Streptomycin, 100 U/ml Penicillin, 2 mM sodium pyruvate, and 0.025 mg/ml Amphotericin B. The culture was maintained at 37°C in a humidified atmosphere containing 5% CO₂. All of the components for cell culture were purchased from Sigma-Aldrich, St. Louis, MO, United States.

In vitro Cytotoxicity Assay

Cytotoxicity assay was performed to evaluate cell growth inhibition of the three compounds HNPMI, THMPP, and THTMP at 100 μ M concentration on three glioblastoma cell lines (1321N1, Snb19, and LN229). Cells were seeded with an initial density of 1×10^5 cells/well in 12-well plates containing appropriate medium for each cell line. When the cells reach 60–70% of confluence, the cells were then treated with the three compounds at 100 μ M and incubated for 24 h at culture conditions. Treated cells were collected using centrifugation at 3000 rpm for 10 min. Number of live and dead cells

were determined using trypan blue solution and Countess II FL Automated Cell Counter (Thermo Fisher Scientific). Inhibition percentage was calculated using the formula (1). In this experiment, biological and technical replicates were conducted for each condition. Temozolomide (TMZ, Sigma-Aldrich, St. Louis, MO, United States) and DMSO 2% were used as positive and negative control, respectively.

Inhibition (%) =

$$\frac{\text{Mean No. of untreated cells (DMSO control)} - \text{Mean No. of treated cells}}{\text{Mean No. of untreated cells (DMSO control)}} \times 100 \quad (1)$$

The cytotoxicity of the top compound was evaluated on multiple GBM cell lines, 1321N1, LN229, Snb19, and HEK293T (immortal cells) human embryonic kidney and normal brain cells MEF. Ten micromolar concentration of the top compound was used to treat the cells followed by trypan blue exclusion assay to quantify the percentage of live and dead cells. The inhibition percentage was calculated as described above.

Inhibitory Kinetic Study

The inhibitory kinetic study was performed for 24 h exposure time using different concentrations 100, 75, 50, 25, 10 μ M of the top compound on 1321N1, Snb19, and LN229 cells. After treatment, the cells were collected as described in the cytotoxicity assay. The positive control TMZ was also utilized. After that the dose-response curves were plotted. Half maximal inhibitory concentration (IC₅₀) was calculated based on the curves fit. The two cell lines with best IC₅₀ were selected for further time-dependent study. In this study, the cells were treated with IC₅₀ concentration of the top compound and incubated for 48 and 72 h. The time-dependent graph was plotted.

Illumina Sequencing and Bioinformatics Analysis

To perform the RNA-seq, RNA of samples had to be isolated. LN229 and Snb19 cells were seeded into 6 well-plate and incubated overnight. The cells were treated with THTMP and TMZ for 24 h at IC₅₀ concentration. The total RNA of the cells were isolated using GeneJET RNA Purification Kit (Thermo Fisher Scientific) following the manufacture's instructions. Then, the total RNA of 18 samples of LN229 and Snb19 cells (including triplicates of THTMP treated, TMZ treated and untreated samples) were sent to whole transcriptome sequencing by Biomedicum Functional Genomics Unit (FuGU, University of Helsinki, Finland) using Illumina NextSeq 500. The sequencing produced data in bcl format which was converted into FASTQ file format.

RNASeq Data Analysis Pipeline

FastQC (Andrews, 2010) (version 0.11.2) was used for quality control to ensure that the quality value was above Q30. The Human (homo sapiens) genome FASTA file¹ and gene annotation

¹ http://ftp.ensembl.org/pub/release-92/fasta/homo_sapiens/dna/

GTF file (Homo sapiens human release 92²) were obtained from Ensembl. Although RNA-seq is a popular research tool, there is no gold standard for analyzing RNA-seq data. Among the available tools, we chose up-to-date open source tools for mapping, retrieving read counts, and differential expression analysis. We used STAR (Dobin et al., 2013) (version 2.6) to generate indexes and to map reads to the human genome. For assembly, we chose SAMtools (Li et al., 2009) (version 1.2) and the “union” mode of HTSeq (Anders et al., 2014) (version 0.9.1), as the gene-level read counts could provide more flexibility in the differential expression analysis. Both STAR and HTSeq analyses were conducted using the high-performance research computing resources provided by TUT TCSC Merop computing cluster³ in the Linux operating system (version 2.6.32). Differential expression (DE) and statistical analysis were performed using DESeq2 (Love et al., 2014) (release 3.3) in R (version 3.2.4). DESeq2 was chosen as a leading statistical method⁴. DESeq2 internally corrects for library size, so it is important to provide un-normalized raw read counts as input. We used variance stabilizing transformation to account for differences in sequencing depth. *P*-values were adjusted for multiple testing using the Benjamini-Hochberg procedure (Benjamini and Hochberg, 1995). A false discovery rate adjusted *p*-value (i.e., *q*-value) <0.05 was set for the selection of DE genes.

Gene Ontology (GO) and Pathway Analysis

Gene ontology (Ashburner et al., 2000) and KEGG pathway (Kanehisa and Goto, 2000) analyses were performed with the PANTHER over-representation Test (released on Feb 03, 2018) in PANTHER version 13.1⁵ (Mi et al., 2009; Emmert-Streib and Glazko, 2011). This program supports the human genome. PANTHER uses a binomial test and a Bonferroni correction for multiple testing and displays *z*-scores to indicate whether a potential regulator is activated or inhibited. We used the default settings for statistical analysis in both the PANTHER pathway and GO terms. In the analyses, only pathways and GO terms with *p*-value <0.05 and fold change of 1.5 were set as cutoff values.

Analysis of Cell Cycle Progression

The Snb19 and LN229 cells were cultured in 96-well plates with the initial density of 1×10^5 cells/well. Cells were incubated overnight with appropriate culture conditions. When the cell confluence reached 60%, they were treated with the IC₅₀ concentration of the top compound for 8 h. Then Premo FUCCI Cell Cycle Sensor *BacMam 2.0* (Thermo Fisher Scientific) was added into each well and incubated for 16 h following the manufacture’s protocol. The cells were then captured using confocal microscope. The analysis of images was done based on different fluorescent colors of the cells in which red fluorescent cells were the cells in G1 phase, green fluorescent cells means the

cells in S, G2, M phase and the overlaid red and green fluorescent cells are the cells in G1/S phase (Zielke and Edgar, 2015).

Annexin V-FITC/PI Apoptotic Assay

To determine the apoptosis and/or necrosis of the top compound on Snb19 and LN229 cell lines, the Dead Cell Apoptosis Kit with Annexin V FITC and PI (Thermo Fisher Scientific) was used. The apoptosis determination was performed followed by the standard protocol from the manufacture. Briefly, the cells were cultured in 6 well-plate with the initial density of 5×10^5 cells/well. The cells were treated with IC₅₀ concentration of the top compound, TMZ and negative control (DMSO) were harvested and washed in cold PBS. The cell pellets were then resuspended in $1 \times$ annexin-binding buffer provided in the kit. Then, 5 μ L of FITC conjugated Annexin V and 1 μ L of the 100 μ g/mL PI working solutions were added to the 100 μ L of cell suspension. The cells were incubated at room temperature for 15 min prior to the fluorescence measurements. The image acquisition was done by using EVOS imaging system (Thermo Fisher Scientific) with $20 \times$ objective magnification.

Detection of Intracellular Reactive Oxygen Species

The Snb19 and LN229 cells were cultured in 12-well plates with the initial density of 1×10^5 cells/well. Cells were incubated overnight with appropriate culture conditions then treated with the IC₅₀ concentration of the top compound and TMZ for 5 h. After that, cells were harvested by centrifugation at 3000 rpm for 10 min and transferred into 96-well plate. Cells were incubated with 2 μ M 2',7'-dichlorodihydrofluorescein diacetate (H2DCFDA), known as dichlorofluorescein diacetate (Sigma-Aldrich, St. Louis, MO, United States), for 30 min at cell culture conditions. The cells were then washed with pre-warm PBS and recovered in pre-warmed completed medium for 20 min prior to the fluorescence measurement. Fluorescence intensity was measured using plate reader (Fluoroskan Ascent FL, Thermo LabSystems) at excitation 485 nm and emission 538 nm. DMSO and hydrogen peroxide 200 μ M were used as the negative and positive controls. The fold increase in ROS production was calculated using the following formula (2).

$$\text{Fold increase} = \frac{F_{\text{test}} - F_{\text{blank}}}{F_{\text{control}} - F_{\text{blank}}} \quad (2)$$

Where: F_{test} is the fluorescence readings from the treated wells, F_{control} is the fluorescence readings from the untreated wells, and F_{blank} is the fluorescence readings from the unstained wells.

Caspases 3/7 Activities Assay

Snb19 and LN229 cells were seeded on 96 well-plates at the initial density of 1×10^4 cells/well with appropriate medium. After culturing for 24 h, cells were treated with TMZ and the top compound at IC₅₀ concentration for 5 h. Determination of caspase activity was performed using Caspase-Glo 3/7 Assay kit (Promega, Madison United States) followed by the standard protocol from the manufacture. Briefly, the plate containing cells were removed from incubator and allowed to equilibrate to room

² ftp://ftp.ensembl.org/pub/release-92/gtf/homo_sapiens

³ <https://wiki.eduuni.fi/display/tutsn/TUT+Narvi+Cluster>

⁴ <https://bioconductor.org/packages/release/bioc/vignettes/DESeq2/inst/doc/DESeq2.html>

⁵ <http://www.pantherdb.org/>, released on October 24, 2016

temperature for 30 min. An amount of 100 μ l of Caspase-Glo reagent was added to the plate containing 100 μ l of treated cell, untreated cell, blank or TMZ. After that, content of wells was gently mixed using a plate shaker at 300–500 rpm for 30 s. The plate was incubated for further 1 h before measuring the luminescence using a plate-reading luminometer (Fluoroskan Ascent FL, Thermo LabSystems). The fold increase in caspase 3/7 was calculated using formula (2) as described in ROS assay.

Statistical Analysis

All of the experiments were conducted with three biological repeats and technical repeats. The data was analyzed using SPSS 20.0. For comparison between the tested groups, statistical significant differences were evaluated with the *t*-test using a threshold of $P < 0.001$ and $P < 0.05$. For comparison of more than two groups, statistical significance was determined with a one-way ANOVA test with the level of significance at $p < 0.05$.

RESULTS

Characterization of Human Glioma Cells Treated With Alkylaminophenols

Three GBM cell lines were treated with 100 μ M HNPMI, THMP, and THTMP (Figure 1A). After 24 h of treatment, the cells lost the proliferative activity with dramatic changes in morphology, losing attachment property and incrementing granularity (Figure 1B). Delightfully, THTMP strongly inhibited the growth of GBM cells 1321N1, LN229, and Snb19 (Figure 1C). At 100 μ M, THTMP was responsible for almost 100% cell death of 1321N1 and LN229 and approximately 80% cell death of Snb19. HNPMI also showed high cytotoxicity on LN229 and Snb19 with more than 80% cell death while it had little effect on 1321N1 with only 23% cell death. THMP has the least cytotoxicity effect compared to THTMP and HNPMI (Figure 1C).

From the above results, it is concluded that THTMP is a potent inhibitor of GBM cell growth. Here, we also used an immortal cell line, HEK293T and a non-tumorous cell line, MEF to examine the effect of THTMP. In general, THTMP has higher cytotoxicity effect on GBM cells compared with immortal and non-tumorous cells. In which, approximately 3 to 12% cell death were found in different GBM cell lines whilst only 2 and 1% growth inhibition were observed in HEK293T and MEF cells, respectively (Figure 1D). Thus, this result suggests that THTMP has the selectivity on GBM cells and was hence selected for further studies.

The dose-dependent inhibitory effect of THTMP against GBM cells was studied at 10, 25, 50, 75 and 100 μ M concentrations (Figure 1E). Among three cell lines, LN229 was the most affected by THTMP with an IC_{50} concentration of 26.5 ± 0.03 μ M, followed by 1321N1 with an IC_{50} of 61.9 ± 0.65 μ M and least inhibited cell line was Snb19 with an IC_{50} of 75.5 ± 2.18 . Besides, TMZ showed better effect on Snb19 than LN229 while seemingly no effect was observed in 1321N1. This is in an agreement with the previous findings (Lee, 2016).

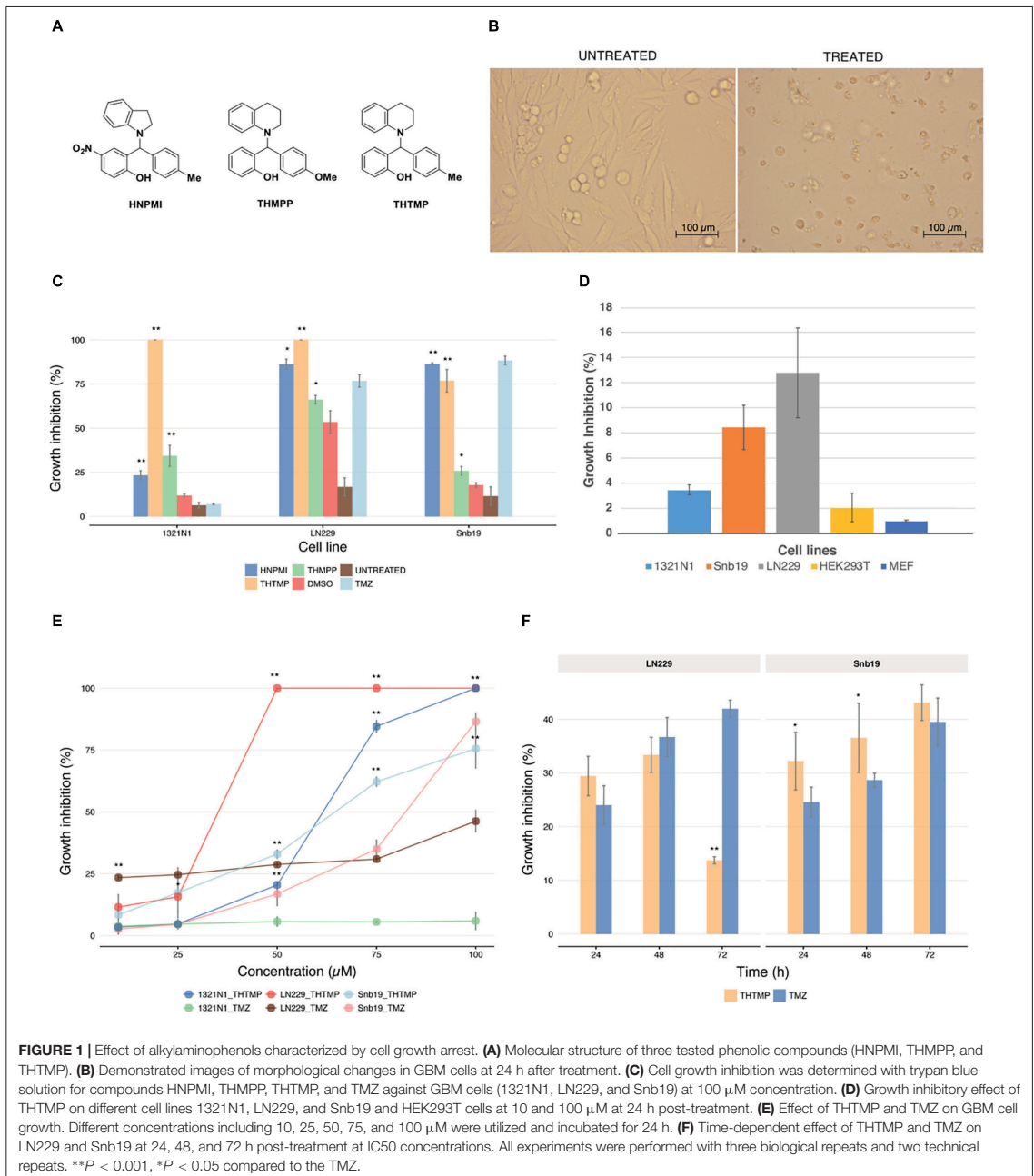
Based on the results obtained for THTMP and TMZ in dose response curve, further studies were performed on LN229 and Snb19 to understand the compound action mode as anticancer drug. To observe the effect of THTMP over the hours on cell viability, LN229 and Snb19 cells were treated for 24, 48, and 72 h with IC_{50} concentration (Figure 1F). The result showed that there was a time-dependent effect on Snb19 from 24 to 72 h and on LN229 from 24 to 48 h. In details, the growth inhibition of Snb19 was increased from 32.2 to 36.5% and to 43.1% at 24, 48, and 72 h post-treatment, respectively. The growth inhibition of LN229 was increased from 29.4% at 24 h treatment to 33.4% at 48 h treatment and was decreased to 13.7% at 72 h treatment.

Global Change in Gene Expression in Response to Top Compound Principal Component Analysis (PCA) and Hierarchical Clustering Analysis

We performed PCA at each sample to determine whether samples in each cell line group clustered with each other or other groups. First, we used HTSeq to count reads that uniquely aligned to one gene, and these data were then imported into DESeq2 to generate PCA plots (Figure 2A). Furthermore, PCA scree plots confirmed that principal components 1 (PC1) and 2 (PC2) accounted for 70–80% of the total variation in gene expression at each time point (Figure 2B). To further investigate the cell-type dependent nature of the DEGs, we performed hierarchical clustering of the top 100 DEGs (i.e., those with the smallest *q*-values identified in the cell line analysis in DESeq2). In agreement with the PCA plots, this analysis demonstrated clustering of almost all sample groups from each cell line forming two clusters (Figure 2D).

Differentially Expressed Genes (DEGs)

In average, 20,090 genes were mapped by at least one read in each of the two cell line samples. Overall, 7,299 DEGs with a *q*-value < 0.05 and fold change > 1.5 (LN229 1,550; Snb19 5,749) were detected over the two comparisons (C1: THTMP vs. Untreated; C2: THTMP vs. TMZ) in the cell type analysis of DESeq2 (Supplementary Tables S1–S4). The results of plot analysis of gene expression in two cell lines of the GBM after treatment are shown in Figure 2C. The numbers of differentially expressed genes with more than 1.5-fold change were higher in Snb19 than in LN229 (Figure 3D). Indeed, there were higher number of differentially expressed genes in these Snb19 cell line when compared with LN229 cell line as shown in Figure 2C. We applied the MA plot function in DESeq2 to visualize the top genes with the smallest *q*-values (Figure 3A). We investigated the similarity in differential gene expression profiles regulated LN229 and Snb19. The fold-changes in overlapped genes filtered by the *q*-value < 0.05 were plotted for LN229 and Snb19 cell lines. Comparison of gene expression profiles showed correlations between LN229 and Snb19 cell lines ($R^2 > 0.10$, Figure 3C left in C1; $R^2 > 0.12$, Figure 3C right in C2). Venn diagrams indicated overlap in genes whose expression was regulated in the same direction (Figure 3B). We identified 3,714 DEGs between THTMP and untreated (negative control) samples among the cell lines (*q*-value < 0.05) (Supplementary Tables S1–S4 and Figure 3B top). In this comparison, Snb19 demonstrated the



most DEGs, with 321 of the 3,714 DEGs common to both LN229 and Snb19. We also compared the THTMP and TMZ samples as a positive control group, both individually and combined as a single “affected” group. In these comparisons,

3,585 number of DEGs were identified, with the largest number of DEGs identified in Snb19 cell line, and 289 out of 3,585 DEGs common in both cell lines (**Supplementary Tables S1–S4** and **Figure 3B** down).

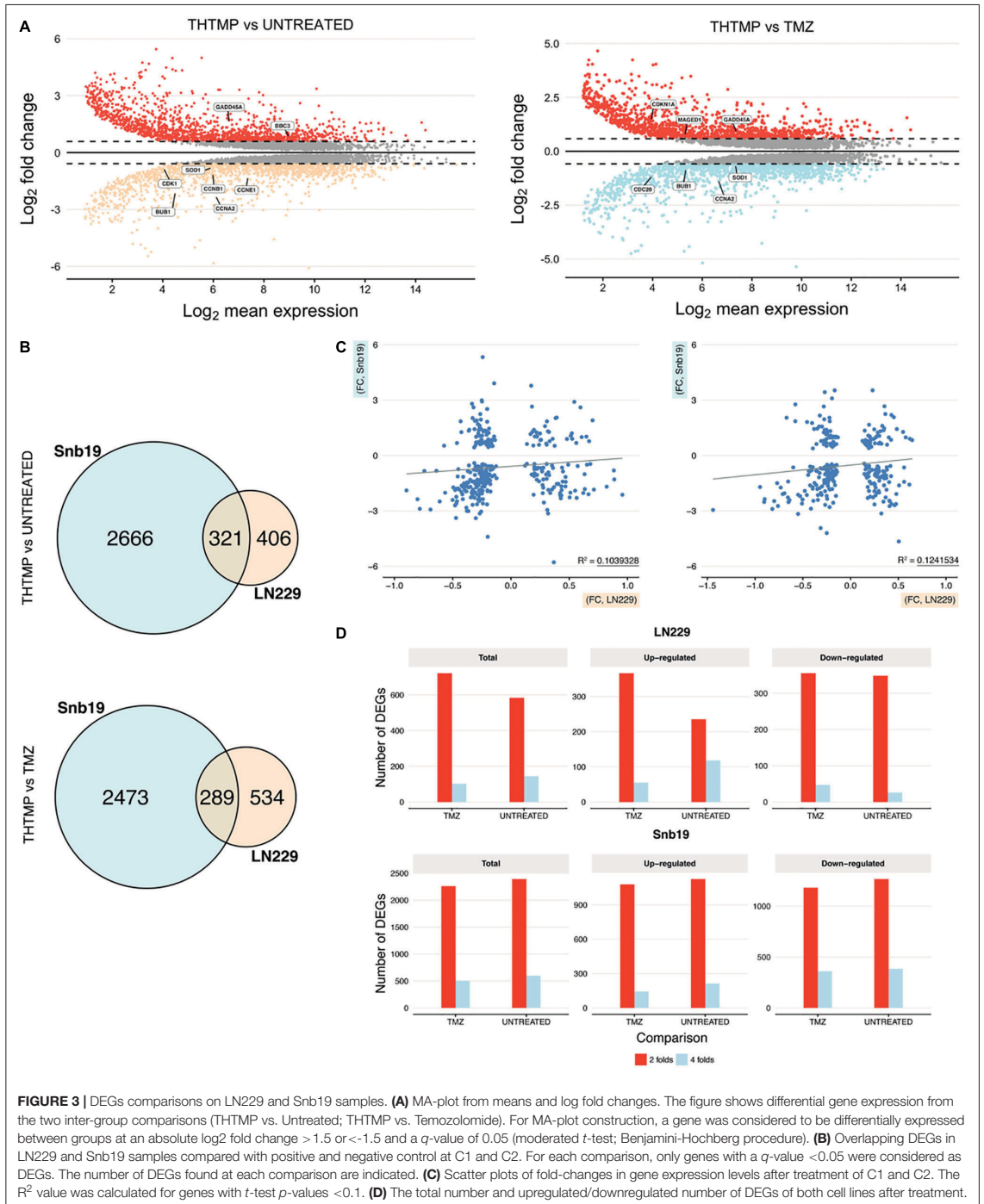


FIGURE 3 | DEGs comparisons on LN229 and Snb19 samples. **(A)** MA-plot from means and log fold changes. The figure shows differential gene expression from the two inter-group comparisons (THTMP vs. Untreated; THTMP vs. Temozolomide). For MA-plot construction, a gene was considered to be differentially expressed between groups at an absolute log₂ fold change > 1.5 or < -1.5 and a *q*-value of 0.05 (moderated *t*-test; Benjamini-Hochberg procedure). **(B)** Overlapping DEGs in LN229 and Snb19 samples compared with positive and negative control at C1 and C2. For each comparison, only genes with a *q*-value < 0.05 were considered as DEGs. The number of DEGs found at each comparison are indicated. **(C)** Scatter plots of fold-changes in gene expression levels after treatment of C1 and C2. The R² value was calculated for genes with *t*-test *p*-values < 0.1. **(D)** The total number and upregulated/downregulated number of DEGs of both cell lines after treatment.

A substantial overlap of DEGs was present when comparing LN229 and Snb19 samples with the control group at C1 and C2. The overlapping DEGs between the cell line were higher at C1 (3,714 DEGs) than at C2 (3,585 DEGs), supporting the two groups behave similarly at the end-stage of the treatment, as expected based on **Figure 3B**. Both cell lines shared appreciable proportions of gene expression profiles (21.23% of genes in LN229; 78.76% of genes in Snb19). The complete lists of DEGs from the cell line analysis and all pairs of comparisons appear in **Supplementary Tables S1–S4**.

Dynamic Cellular Damage Responses Induced by THTMP

The gene ontology was conducted to analyze up and down regulated genes regarded to DNA damage. GO analysis identified the list of genes that were enriched in DNA replication, sister chromatid segregation, DNA-dependent DNA replication, chromosome segregation, sister chromatid cohesion, and nuclear chromosome segregation process. These biological processes are involved in the DNA replication pathway in both cell lines when they were treated with THTMP and TMZ (**Figure 4A**). Enrichment analysis for GO molecular function and pathways clearly demonstrated related phenotypes associated with GBM (**Figures 4B,C**). GO terms cadherin binding, damaged DNA binding for molecular function appeared to be significantly overrepresented, and none significantly underrepresented. Cadherin binding, a type I membrane protein involved in cell adhesion and damaged DNA binding, interacting selectively and non-covalently with damaged DNA have coordinated effect on regulation and function in DNA damage (Daido et al., 2005). Previous studies have shown that GBMs are highly resistant to single inhibitor, suggesting that combinational strategies involving standard chemotherapies like TMZ and pathway inhibitors might be a possible future direction for treating GBM (Jacinto and Esteller, 2007).

Genes associated with the DNA damage were listed in **Figure 4D**. In general, more DEGs were observed in Snb19 when they were treated with THTMP and TMZ. Here, the top 20 DEGs were listed in **Figure 4D**. In LN229, eight DEGs were expressed when they were treated with THTMP and six DEGs were found in TMZ treatment. CDK1 gene is downregulated when the cells were treated with THTMP and TMZ in both cell types. It is reported that CDK1 was observed to be enriched in the p53 signaling pathway, which is induced by a number of stress signals, including DNA damage, oxidative stress and activated oncogenes. It is noted that p53 signaling network is an integral tumor suppressor pathway in GBM pathogenesis that affects cellular processes, including cell cycle control and cell death execution (Stegh et al., 2010). Moreover, CDKN1A was found to be upregulated in Snb19 when they were treated with THTMP (**Figure 4D**). It is noted that CDKN1A is a gene encoding for p21 protein which contributes to the cell response to DNA damage not only by inactivating G1-phase cyclins/CDKs complexes, but also through other processes, which possibly include direct interaction with PCNA to inhibit DNA replication, and indirect effects mediated by interaction with other cell cycle regulators.

Thereby, our result suggests that DNA damage has been confirmed by the downregulation of CDK1 as well as upregulation of CDKN1A leading to activation of p53 and p21 signaling; thus, inhibiting the growth of glioblastoma. Moreover, CDK1 also plays an important role in cell cycle control (Santamaría et al., 2007). Here, the downregulation of CDK1 expression was identified in THTMP treated conditions confirming cyclin-dependent kinase mediated cell cycle arrest. Detailed investigation of cell cycle arrest was performed using biosensor and gene expression profiling.

THTMP Induces G1/S DNA Damage Checkpoint

It has been demonstrated that DNA damage induced the cell cycle arrest in proliferating mammalian cells (Erasmus et al., 2016). At first, cell cycle progression was imaged using FUCCI fluorescent biosensor and microscopy. Different phases of the cell cycle were determined based on different fluorescence signals, red signal corresponding to G1 phase, yellow signal corresponding to G1/S phase and green signal corresponding to S/G2/M phase (**Figure 5A**). In this study, similar results were observed in both cell lines after the treatment. In DMSO condition, the highest number of cells were present in S/G2/M phase, moderate number of the cells were present in G1 phase, and least number of the cells were present in G1/S phase. Upon THTMP treatment, the majority of the cells were present in G1 phase, following is the G1/S phase and small number of cells were in S/G2/M phase. In TMZ condition, the percentage of cells in different phases varied between G1/S and S/G2/M phase. According to these results, it is to conclude that GBM cells were arrested at G1/S phase when they were treated with THTMP and were arrested at S/G2/M phase when they were under TMZ treatment (**Figure 5B**).

Here, we show that THTMP induced the downregulation of many genes related to DNA replication, thereby, inhibiting the process of DNA replication and cell cycle progression. Next, genes associated with cell cycle progression were selectively analyzed (**Figure 5C**). There are several biological processes involved in cell cycle pathway that have been activated by the treatment. It includes cell cycle G1/S phase, G1/S transition of mitotic cell cycle, G2/M transition of mitotic cell cycle, cell cycle G2/M phase transition, cell cycle checkpoint and positive regulation of cell cycle (**Figure 4A**). Regarding the expression of various genes involved in cell cycle, genes in Snb19 have higher fold change compared to those in LN229 (**Figure 5C**). For example, the fold change of CCNA2 gene is -0.4 and -2.5 in LN229 and Snb19, respectively, when they were treated with THTMP. The fold change of CCNB2 gene is -0.3 and -2.1 in LN229 and Snb19, respectively, when they were treated with TMZ.

Here, the genes associated with G1 phase and G1/S checkpoint were first selectively analyzed (**Figure 5C**). CCNA2 gene coding to cyclin A2 protein was found to be downregulated in both cell lines when they were treated with THTMP. In Snb19, genes CCNE1 and CCNE2 coding to Cyclin E1 and E2 proteins were found to be decreased in THTMP treatment. It is noted that overexpression of Cyclin A and Cyclin E has the function to

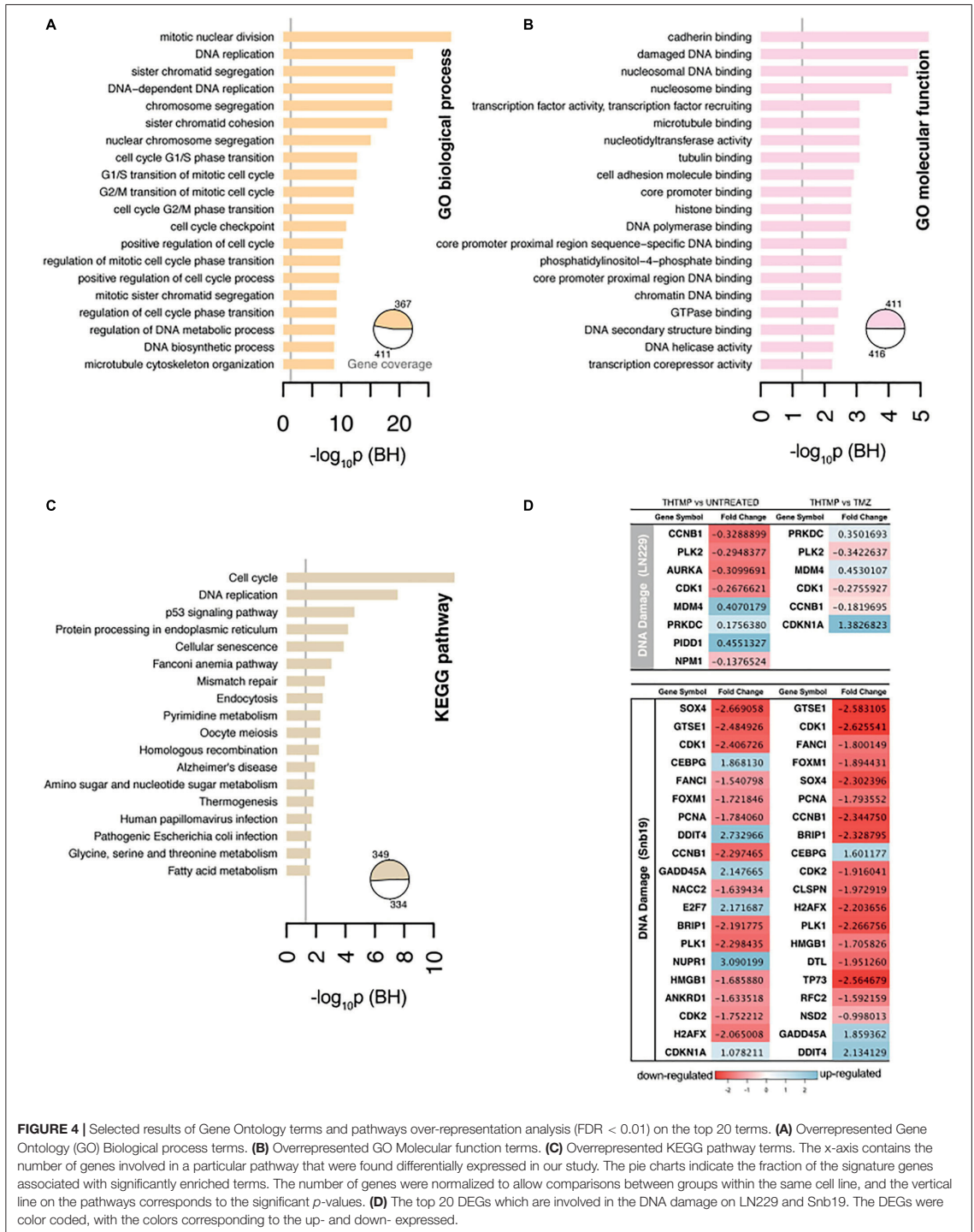


FIGURE 4 | Selected results of Gene Ontology terms and pathways over-representation analysis (FDR < 0.01) on the top 20 terms. **(A)** Overrepresented Gene Ontology (GO) Biological process terms. **(B)** Overrepresented GO Molecular function terms. **(C)** Overrepresented KEGG pathway terms. The x-axis contains the number of genes involved in a particular pathway that were found differentially expressed in our study. The pie charts indicate the fraction of the signature genes associated with significantly enriched terms. The number of genes were normalized to allow comparisons between groups within the same cell line, and the vertical line on the pathways corresponds to the significant p -values. **(D)** The top 20 DEGs which are involved in the DNA damage on LN229 and Sbn19. The DEGs were color coded, with the colors corresponding to the up- and down- expressed.

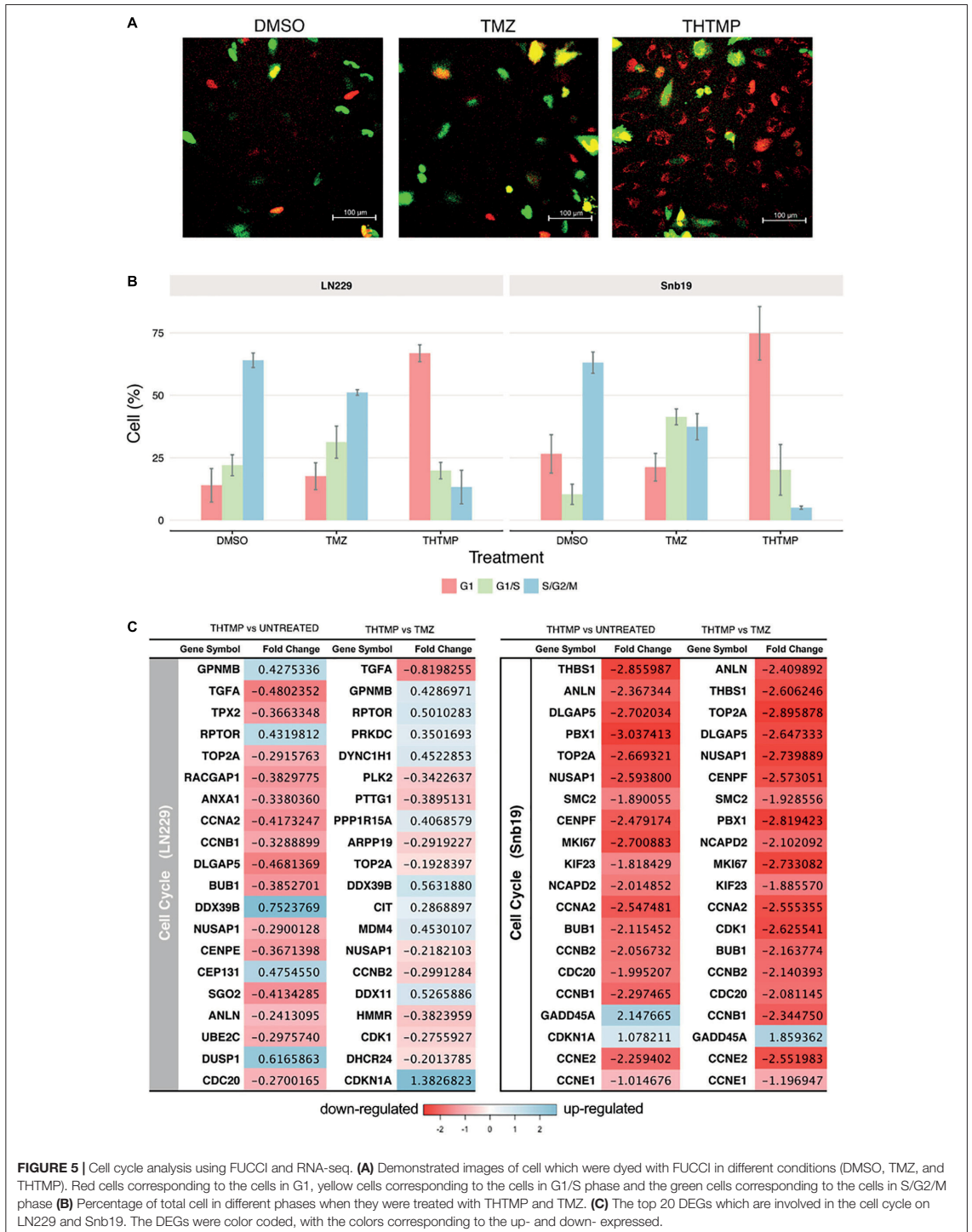


FIGURE 5 | Cell cycle analysis using FUCCI and RNA-seq. **(A)** Demonstrated images of cell which were dyed with FUCCI in different conditions (DMSO, TMZ, and THTMP). Red cells corresponding to the cells in G1, yellow cells corresponding to the cells in G1/S phase and the green cells corresponding to the cells in S/G2/M phase **(B)** Percentage of total cell in different phases when they were treated with THTMP and TMZ. **(C)** The top 20 DEGs which are involved in the cell cycle on LN229 and Snb19. The DEGs were color coded, with the colors corresponding to the up- and down- expressed.

regulate G1/S transition when they complex with CDK2; thus, decreased expression level of CCNA2, CCNE1, and CCNE2 could lead to mediate the G1/S arrest. Moreover, BUB1 was identified to be downregulated in this study and was enriched in biological processes associated with the mitotic cell cycle, including cell cycle chromatid segregation, G1/S transition of mitotic cells and DNA replication. CDC20 appears to act as a regulator protein interacting with several other proteins at multiple points in the cell cycle. We found that CDC20 gene was downregulated and enriched in cell cycle and oocyte meiosis pathways.

In case of TMZ treatment, FUCCI analysis shows that both Snb19 and LN229 cells were arrested at S/G2/M phase. It is in accordance with our gene expression analysis. Genes CCNB1, CCNB2, CCNA2, which relate to Cyclin B1 and Cyclin A2, were found to be decreased. These two cyclins have the function to regulate G2/M transition when they complex with CDK1. Moreover, CDKN1A (p21) and GADD45A, two downstream target genes of p53 in the G2 checkpoint, were found to be increased in LN229 and Snb19, respectively, at the transcriptional level. Previous studies have reported that increased p21 expression led to the repression of cyclin B1 and Cdc2 promoters and that increased GADD45A expression inhibits Cdc2 activity, thereby mediating G2/M arrest (Jin et al., 2000; Yang et al., 2000).

The results show that THTMP induced cell cycle arrest at G1/S phase while TMZ induced cell cycle arrest at G2/M phase in both cell lines. This result implies that THTMP has inhibited synthesis of GBM cells before they can entry to replication and division periods; therefore, strongly preventing cell proliferation. Moreover, G1/S phase arrest of cell cycle progression provides an opportunity for cells to either undergo repair mechanisms or follow the apoptotic pathway (Bartek and Lukas, 2001).

THTMP Increases ROS Production and Induces Pro-apoptotic and Anti-apoptotic Genes

Apoptosis induction assay was performed using Annexin V/PI double staining. Here, the percentage of apoptosis was calculated based on the cells with Annexin V-FITC positive and PI negative and both Annexin V-FITC and PI positive. The percentage of necrosis was defined based on the cells with Annexin V-FITC negative and PI positive (Chen et al., 2008). **Figure 6A** shows the live, apoptosis and necrosis of LN229 and Snb19 when they were treated with THTMP and TMZ. Generally, apoptosis induction was observed in both cell lines compared with positive control and untreated conditions. The apoptosis percentage of LN229 cells treated with THTMP is 45.8% while only 21.9 and 11.2% were obtained when they were treated with TMZ and DMSO, respectively. In case of Snb19 cells, 56.4% of apoptotic cells were found in THTMP treated condition whilst TMZ and untreated conditions exhibit only 36.2 and 11.5% apoptotic cells. Beside the apoptotic cells, necrotic cells were also observed in both cell lines. However, necrosis percentage is less than 10% in case of Snb19 while in LN229, 27.0 and 7.6% were found to be necrotic cells when they were treated with TMZ and THTMP, respectively.

The results above are in accordance with the gene expression profile showing the enrichment of apoptosis pathways including neuron apoptotic process, positive regulation of neuron apoptotic process, regulation of apoptotic signaling pathway, regulation of neuron apoptotic process, intrinsic apoptotic signaling pathway and extrinsic apoptotic signaling pathway. Genes involved in regulation of apoptotic process were presented in **Figure 6B**. Moreover, the gene expression profile indicates lower number of the DEGs related to apoptosis process in TMZ treatment compared to THTMP treatment (**Figure 6B**). The expression changes showing in **Figure 6B** revealed that THTMP tended to induce pro-apoptotic genes, reduce anti-apoptotic genes and also induce some anti-apoptotic genes.

Among pro-apoptotic genes, CTNBN1 gene coding for β -catenin protein was downregulated in LN229 cells when they were treated with THTMP. It is reported that abnormal accumulation of β -catenin contributes to most cancers and repressed CTNBN1 also leads to inducing apoptosis in some tumor cells (Yang et al., 2017). Interestingly, the pro-apoptotic Bcl-2 family gene MAGED1 was also found to be upregulated in LN229 whereas BBC3 (PUMA) gene was upregulated in Snb19 when they were treated with THTMP. Moreover, BCL2L12, an anti-apoptotic gene, was found to be downregulated in Snb19 cells. It is noted that BCL2L12 expression is upregulated in most human glioblastomas. Expression of Bcl2L12 results in resistance to apoptosis (Yang et al., 2015). Our findings demonstrated that THTMP has shown the ability to induce apoptosis of Snb19 and LN229 via mitochondrial pathway throughout the upregulation of pro-apoptotic and downregulation of anti-apoptotic Bcl-2 family genes.

Although the altered expression of genes described above could confirm apoptosis, genes involved in anti-apoptosis were expressed when the cells were treated with THTMP. The anti-apoptotic characteristics of Snb19 cells were identified by the downregulation of several genes from the membrane stress receptors, such as TNFSF10, TNFSF12, and TNFRSF2. Moreover, the upregulation of RELA, a member of NF κ B family, suggested a decline in inflammatory processes and strong anti-apoptotic properties for this cell line. In LN229 cells, the regulation of the TNF receptor pathway as well as NF κ B signaling pathway was not significantly affected, but there was a modest upregulation of BIRC6 encoded for BIRC protein, a member of the inhibitor of apoptosis (IAP) gene family preventing apoptotic cell death. Interestingly, the BIRC5 was suppressed in Snb19.

In addition to the activation of apoptotic pathways in the treated cells, reactive oxygen species (ROS) could lead to cell cycle arrest and induces apoptosis in anticancer treatment (Circu and Aw, 2010). It is well known that ROS is produced in both normal and abnormal cells especially in cancer cells. ROS plays an important role in proliferation, survival, metastasis and angiogenesis (Clerkin et al., 2008). In this study, the effects of THTMP, TMZ and H₂O₂, a positive control in the levels of ROS on GBM cells, was assessed using ROS production assay. **Figure 6C** shows an increase of ROS level when the cells were treated with THTMP and TMZ. Interestingly, the fold increase of ROS of Snb19 and LN229 cells treated with THTMP were higher than H₂O₂. As seen in **Figure 6C**, Snb19 cells have higher level of

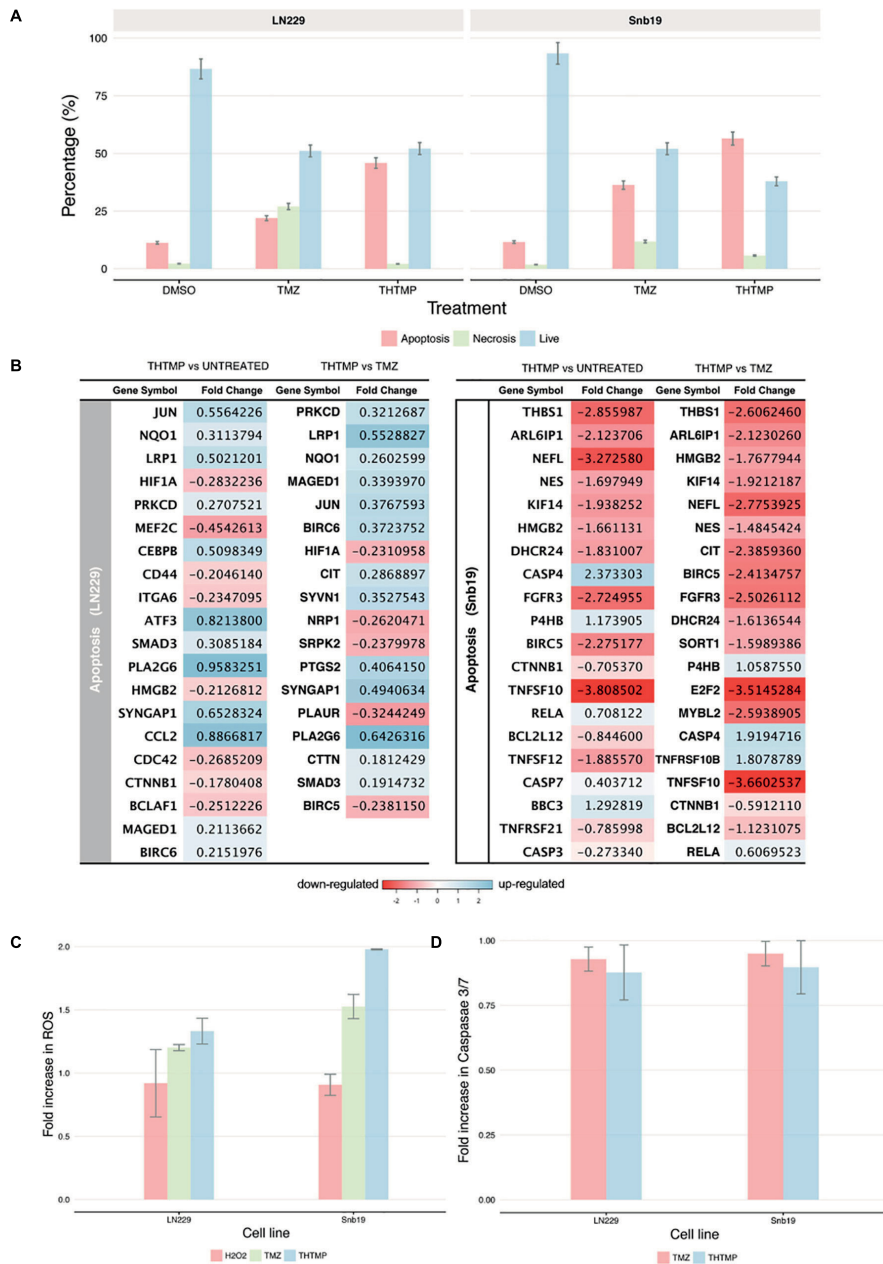


FIGURE 6 | Apoptosis induction determination using double stains Annexin V and Propidium iodide and RNA-seq. **(A)** Percentage of apoptosis, necrosis and live cell using Dead Cell Apoptosis Kit with Annexin V-FITC and PI of untreated cell (DMSO control) and compound TMZ and compound THTMP at 24 h post-treatment on Snb19 and LN229. **(B)** The top 20 DEGs which are involved in apoptosis of LN229 and Snb19. The DEGs were color coded, with the colors corresponding to the up- and down- expressed. **(C)** Effect of THTMP and TMZ on intracellular ROS production. Fluorescence intensity of ROS was determined by activity of 2 μ M H₂DCFDA (30 min), fluorescent probe. H₂O₂ was used as the positive control. **(D)** Activity of caspases 3/7 in LN229 and Snb19. Caspase 3/7 was determined using luminescence plate reader. Fold increase in ROS and caspases 3 and 7 activity of LN229 and Snb19 cell lines was calculated when they were treated with THTMP and PC at IC₅₀ concentration. Triplicates were performed for each condition.

ROS compared to LN229 in all of the conditions. In which, up to 2 fold increase was found in THTMP treatment of Snb19 while only 1.3 fold increase was observed in LN229. The same trend was observed for the TMZ treatment in which 1.5 fold and 1.2 fold were obtained in Snb19 and LN229, respectively. Thus, ROS were significantly produced when GBM cells were affected with THTMP. This suggests that higher ROS level could be interlinked with the observed apoptotic cell death of cancer cells upon treatment with compound THTMP. Moreover, in mammalian cells, ROS are produced by normal oxidative metabolism and cellular antioxidants such as superoxide dismutase (SOD1) and thioredoxin (TRX1) detoxify these species (Covarrubias et al., 2008). A study indicated that decreasing SOD1 and TRX1 could lead to apoptosis induction in glioma cells when they were treated with kaempferol, a natural phenolic compound, via elevation of ROS (Sharma et al., 2007). In agreement, we also found out that while THTMP treatment had no effect on TRX1, a decrease in SOD1 was observed in Snb19 cells (**Supplementary Table S3**). Thus, THTMP induced ROS-mediated apoptosis.

According to **Figure 6D**, caspase 3/7 was not significantly increased in both cell lines when they were treated with THTMP and TMZ. This is also in agreement with the gene expression profile where we could not find the significant expression of CASP3 and CASP7 in LN229 cells (**Figure 6B**). In case of Snb19 cells, although the CASP3 and CASP7 were expressed, the CASP3 was downregulated and CASP7 was upregulated when they were treated with THTMP (**Figure 6B**). This result interprets the no change in caspase 3/7 activation assay results (**Figure 6C**). The repression of caspase genes might be caused from the activation of anti-apoptotic genes (Stegh et al., 2008). Thus, apoptosis inductions of GBM cells by THTMP and TMZ were not via caspase 3/7. Instead of CASP3 and CASP7, CASP4 was found to be upregulated in Snb19 when they were treated with both THTMP and TMZ. Therefore, the result implies the involvement of caspase 4 in Snb19 when they were treated with THTMP and TMZ.

DISCUSSION

DNA damage response induced by THTMP was validated and shown to be dose- and time-dependent. A detailed analysis of global molecular expression profiling is required in order to understand the complex cellular responses. Here, by combining biochemical studies with high-throughput RNA sequencing, the changes in gene expression in glioma cells induced by THTMP was explored. Our results show that genes involved in DNA damage, DNA replication, cell cycle arrest and apoptosis induction were transcriptionally modulated and highly enriched when GBM cells were treated with THTMP.

Firstly, our study demonstrated a THTMP induced activation of various genes associated with DNA damage and cell cycle arrest. The cell cycle arrest in GBM when they were treated with THTMP and TMZ may be explained by transcriptional expression change of some crucial genes that are listed in **Figure 5B**. CCNA2 gene was found in both Snb19 and LN229 when they were treated with THTMP compound. This gene

belongs to a highly conserved cyclin family and the encoded protein of this gene is crucial in the control of the cell cycle at G1/S and G2/M transition points. Here, several important genes in control cell cycle at G1/2 and G2/M such as CCNA2, BUB1, CDC20 are selected for further discussion in order to understand their mechanism in controlling cell cycle of GBM.

In previous studies, it is reported that overexpression of CCNA2 is involved in tumor transformation and progression in numerous types of cancer (Uhlen et al., 2010). As expected, our results show that CCNA2 was downregulated, which is in accordance with the function of cyclin A2 protein in cell cycle indicating that CCNA2 inhibits the growth of GBM. BUB1 was also found to be downregulated that can explain the G1/S transition arrest since the BUB family of genes encode proteins that are involved in large multi-protein kinetochore complex, and are reported to be key component of the checkpoint regulator pathway. BUB1 encodes a serine/threonine protein kinase which plays an important role in mitosis (Tang et al., 2006), and BUB1 accumulates at unattached kinetochores where it mediates the recruitment of mitotic arrest deficient (Mad) dimers. Combination of Mad and BUB1 leads to prevention of premature separation of sister chromatids until all chromosomes are correctly attached to kinetochores; thus, correctly chromosome segregation achieved (Ricke et al., 2011). This suggests that GBM cell growth may be inhibited by regulating the mitotic cell cycle in THTMP treated conditions (Grabsch et al., 2003). In addition, previous reports indicate that CDC20 is highly expressed in various type of human tumors including breast, cervical and glioblastoma cancer (Marucci et al., 2008; Jiang et al., 2011; Rajkumar et al., 2011). It is also reported that expression level of CDC20 is correlated with the grade of glioblastoma and it is expressed at different levels in patients at different ages (Bie et al., 2011). In the study CDC20 was downregulated, which leads to conclude that CDC20 may inhibit GBM growth. According to the biological process enrichment results, CCNA2 was enriched in cell cycle and oocyte meiosis pathways, in which CDK1, BUB1 and CDC20 were also involved. These genes are also known as key genes playing a crucial role in promoting GBM growth (Chen et al., 2016). Repression of these genes when the cells were treated with THTMP indicates that this compound strongly inhibits the growth of GBM throughout cell cycle arrest.

Secondly, we detected apoptotic effects induced by THTMP. Analysis of apoptosis genes subsequently revealed that the progress of apoptosis was accompanied by changes in both pro-apoptotic and anti-apoptotic gene expression, consistent with the observation in other chemotherapeutic therapies in cancer cells (Kim et al., 2003). It is noted that BCL2L12 is overexpressed in primary GBM and functions to inhibit post-mitochondrial apoptosis signaling (Stegh et al., 2007). This study shows that THTMP has induced apoptosis via mitochondrial pathway in both LN229 and Snb19 cell lines due to the suppression of Bcl-2 family, BCL2L12. The study also shows that a large number of genes of Snb19 was expressed compared to LN229 when they were treated with THTMP. The anti-apoptotic genes expressed in LN229 and Snb19 are different. This result implies that apoptosis pathways of GBM cells will be executed in different mechanisms when they were treated with THTMP. This study

shows that TMZ also induced apoptosis in GBM cells as explored by Annexin V/PI double staining; however, the gene profile of this condition is still limited. Here, the absence of caspase 3/7 activation indicates that THTMP has not induced apoptosis via caspase 3 and 7 of LN229 and Snb19, but the caspase 4 might be involved in the apoptosis pathway of Snb19 cells.

CONCLUSION

Overall, the effect of THTMP on GBM cells is relatively much stronger than TMZ in all aspects. This study provides experimental evidence that THTMP is capable of inhibiting the growth of GBM cells. THTMP has the ability to induce DNA damage through the p53 signaling pathway leading to cell cycle arrest. The G1/S checkpoint arrest depends on the decrease of cyclin A2 in both Snb19 and LN229 cells-treated with THTMP. Moreover, the decrease of cyclin E1 and E2 in Snb19 in THTMP treatment also contributes to the G1/S checkpoint arrest. This result suggests that THTMP facilitates cancer cells to undergo programmed cell death pathways, apoptosis in glioblastoma cells. The induction of apoptosis of GBM in THTMP treated conditions is associated with increasing pro-apoptotic factor of Bcl-2. In addition, it is indicated that caspase 4 may play a role in this apoptosis induction instead of caspase 3/7.

The findings on inhibition of GBM proliferation and downregulation of cell cycle genes in the G1/S phase not only provide a better understanding of the mechanisms of THTMP, a phenolic compound, as anticancer agent, but also open an avenue for investigating the role of oxidative stress in GBM involving cell cycle and apoptosis regulation. However, testing THTMP on glioma animal model and computational pharmacogenomics approaches (Musa et al., 2018) will allow this compound to be used as a potential chemotherapeutic drug for glioma treatment.

REFERENCES

- Anders, S., Pyl, P. T., and Huber, W. (2014). HTSeq – a python framework to work with high-throughput sequencing data HTSeq – a python framework to work with high-throughput sequencing data. *Bioinformatics* 31, 166–169. doi: 10.1093/bioinformatics/btu638
- Andrews, S. (2010). *FastQC: A Quality Control Tool for High Throughput Sequence Data*. Available at: <http://www.bioinformatics.babraham.ac.uk/projects/fastqc/> (Retrieved October 21, 2018).
- Ashburner, M., Ball, C. A., Blake, J. A., Botstein, D., Butler, H., Cherry, J. M., et al. (2000). Gene ontology: tool for the unification of biology. *Nat. Genet.* 25, 25–29. doi: 10.1038/75556
- Bartek, J., and Lukas, J. (2001). Pathways governing G1/S transition and their response to DNA damage. *FEBS Lett.* 490, 117–122. doi: 10.1016/S0014-5793(01)02114-7
- Benjamini, Y., and Hochberg, Y. (1995). Controlling the false discovery rate: a practical and powerful approach to multiple testing. *J. R. Stat. Soc. Ser. B* 57, 289–300. doi: 10.2307/2346101
- Bie, L., Zhao, G., Cheng, P., Rondeau, G., Porwollik, S., Ju, Y., et al. (2011). The accuracy of survival time prediction for patients with glioma is improved by measuring mitotic spindle checkpoint gene expression. *PLoS One* 6:e25631. doi: 10.1371/journal.pone.0025631
- Chen, C., Sun, C., Tang, D., Yang, G., Zhou, X., and Wang, D. (2016). Identification of key genes in glioblastoma-associated stromal cells using

AUTHOR CONTRIBUTIONS

PD executed experiments and data analysis. AM analyzed the RNAseq data. NC prepared and characterized the compounds. FE-S contributed in development of the project. OY-H contributed in development of the project, conceived and managed the project. MK designed and supervised the experiments of the biological assays, data analysis, conceived and managed the project. All authors involved in the manuscript write up and approved the final version of the manuscript.

FUNDING

This study was supported by Academy of Finland (Nr.297200) and TUT presidents grant.

ACKNOWLEDGMENTS

We thank Biomedicum Functional Genomics Unit (FuGU, University of Helsinki, Finland) for helping us to perform RNA-seq. We also thank Prof. Ville Santala for providing access to the plate reader instrument for reactive oxygen species and Caspase measurements at TUT.

SUPPLEMENTARY MATERIAL

The Supplementary Material for this article can be found online at: <https://www.frontiersin.org/articles/10.3389/fphar.2019.00330/full#supplementary-material>

bioinformatics analysis. *Oncol. Lett.* 11, 3999–4007. doi: 10.3892/ol.2016.4526

Chen, S., Cheng, A. C., Wang, M. S., and Peng, X. (2008). Detection of apoptosis induced by new type gosling viral enteritis virus in vitro through fluorescein annexin V-FITC/PI double labeling. *World J. Gastroenterol.* 14, 2174–2178. doi: 10.3748/wjg.14.2174

Circu, M. L., and Aw, T. Y. (2010). Reactive oxygen species, cellular redox systems, and apoptosis. *Free Radic. Biol. Med.* 48, 749–762. doi: 10.1016/j.freeradbiomed.2009.12.022

Clerkin, J. S., Naughton, R., Quiney, C., and Cotter, T. G. (2008). Mechanisms of ROS modulated cell survival during carcinogenesis. *Cancer Lett.* 266, 30–36. doi: 10.1016/j.canlet.2008.02.029

Covarrubias, L., Hernández-García, D., Schnabel, D., Salas-Vidal, E., and Castro-Obregón, S. (2008). Function of reactive oxygen species during animal development: passive or active? *Dev. Biol.* 320, 1–11. doi: 10.1016/j.ydbio.2008.04.041

Daido, S., Yamamoto, A., Fujiwara, K., Sawaya, R., Kondo, S., and Kondo, Y. (2005). Inhibition of the DNA-dependent protein kinase catalytic subunit radiosensitizes malignant glioma cells by inducing autophagy. *Cancer Res.* 65, 4368–4375. doi: 10.1158/0008-5472.CAN-04-4202

Doan, P., Karjalainen, A., Chandraseelan, J., Sandberg, O., Yli-Harja, O., Rosholm, T., et al. (2016). Synthesis and biological screening for cytotoxic activity of N- substituted indolines and morpholines. *Eur. J. Med. Chem.* 120, 296–303. doi: 10.1017/CBO9781107415324.004

- Doan, A., Davis, C. A., Schlesinger, F., Drenkow, J., Zaleski, C., Jha, S., et al. (2013). STAR: ultrafast universal RNA-seq aligner. *Bioinformatics* 29, 15–21. doi: 10.1093/bioinformatics/bts635
- Emmert-Streib, F., and Glazko, G. V. (2011). Pathway analysis of expression data: deciphering functional building blocks of complex diseases. *PLoS Comput. Biol.* 7:e1002053. doi: 10.1371/journal.pcbi.1002053
- Erasimus, H., Gobin, M., Niclou, S., and Van Dyck, E. (2016). DNA repair mechanisms and their clinical impact in glioblastoma. *Mutat. Res. Mutat. Res.* 769, 19–35. doi: 10.1016/j.mrr.2016.05.005
- Friedman, H. S., Prados, M. D., Wen, P. Y., Mikkelsen, T., Schiff, D., Abrey, L. E., et al. (2009). Bevacizumab alone and in combination with irinotecan in recurrent glioblastoma. *J. Clin. Oncol.* 27, 4733–4740. doi: 10.1200/JCO.2008.19.8721
- Gali-Muhtasib, H., Hmadi, R., Kareh, M., Tohme, R., and Darwiche, N. (2015). Cell death mechanisms of plant-derived anticancer drugs: beyond apoptosis. *Apoptosis* 20, 1531–1562. doi: 10.1007/s10495-015-1169-2
- Gong, L., Li, Y., Nedeljkovic-Kurepa, A., and Sarkar, F. H. (2003). Inactivation of NF-kappaB by genistein is mediated via Akt signaling pathway in breast cancer cells. *Oncogene* 22, 4702–4709. doi: 10.1038/sj.onc.1206583
- Grabsch, H., Takeno, S., Parsons, W. J., Pomjanski, N., Boecking, A., Gabbert, H. E., et al. (2003). Overexpression of the mitotic checkpoint genes BUB1, BUBR1, and BUB3 in gastric cancer-association with tumour cell proliferation. *J. Pathol.* 200, 16–22. doi: 10.1002/path.1324
- Hegi, M. E., Diserens, A.-C., Gorlia, T., Hamou, M.-F., de Tribolet, N., Weller, M., et al. (2005). MGMT gene silencing and benefit from temozolomide in glioblastoma. *N. Engl. J. Med.* 352, 997–1003. doi: 10.1056/NEJMoa043331
- Jacinto, F. V., and Esteller, M. (2007). MGMT hypermethylation: a prognostic foe, a predictive friend. *DNA Repair* 6, 1155–1160. doi: 10.1016/j.dnarep.2007.03.013
- Jiang, J., Jedinak, A., and Sliva, D. (2011). Ganodermanontriol (GDNT) exerts its effect on growth and invasiveness of breast cancer cells through the down-regulation of CDC20 and uPA. *Biochem. Biophys. Res. Commun.* 415, 325–329. doi: 10.1016/j.bbrc.2011.10.055
- Jin, S., Antinore, M. J., Lung, F. D. T., Dong, X., Zhao, H., Fan, F., et al. (2000). The GADD45 inhibition of Cdc2 kinase correlates with GADD45-mediated growth suppression. *J. Biol. Chem.* 275, 16602–16608. doi: 10.1074/jbc.M000284200
- Kanehisa, M., and Goto, S. (2000). KEGG: key to encyclopedia of genes and genomes. *Nucleic Acids Res.* 28, 27–30. doi: 10.1093/nar/28.1.27
- Karjalainen, A., Doan, P., Sandberg, O., Chandraseelan, J., Yli-Harja, O., Candeias, N., et al. (2017). Synthesis of phenol-derivatives and biological screening for anticancer activity. *Anticancer Agents Med. Chem.* 17, 1710–1720. doi: 10.2174/1871520617666170327142027
- Kim, Y. A., Lee, W. H., Choi, T. H., Rhee, S. H., Park, K. Y., and Choi, Y. H. (2003). Involvement of p21WAF1/CIP1, pRB, Bax and NF-kappaB in induction of growth arrest and apoptosis by resveratrol in human lung carcinoma A549 cells. *Int. J. Oncol.* 23, 1143–1149.
- Lee, S. Y. (2016). Temozolomide resistance in glioblastoma multiforme. *Genes Dis.* 3, 198–210. doi: 10.1016/j.gendis.2016.04.007
- Li, H., Handsaker, B., Wysoker, A., Fennell, T., Ruan, J., Homer, N., et al. (2009). The sequence alignment/map format and SAMtools. *Bioinformatics* 25, 2078–2079. doi: 10.1093/bioinformatics/btp352
- Love, M. I., Huber, W., and Anders, S. (2014). Moderated estimation of fold change and dispersion for RNA-seq data with DESeq2. *Genome Biol.* 15:50. doi: 10.1186/s13059-014-0550-8
- Marucci, G., Morandi, L., Magrini, E., Farnedi, A., Franceschi, E., Miglio, R., et al. (2008). Gene expression profiling in glioblastoma and immunohistochemical evaluation of IGFBP-2 and CDC20. *Virchows Arch.* 453, 599–609. doi: 10.1007/s00428-008-0685-7
- Mi, H., Dong, Q., Muruganujan, A., Gaudet, P., Lewis, S., and Thomas, P. D. (2009). PANTHER version 7: improved phylogenetic trees, orthologs and collaboration with the gene ontology consortium. *Nucleic Acids Res.* 38, D204–D210. doi: 10.1093/nar/gkp1019
- Musa, A., Ghorraie, L. S., Zhang, S. D., Glazko, G., Yli-Harja, O., Dehmer, M., et al. (2018). A review of connectivity map and computational approaches in pharmacogenomics. *Brief. Bioinform.* 19, 506–523. doi: 10.1093/bib/bbw112
- Neto, Í, Andrade, J., Fernandes, A. S., Pinto Reis, C., Salunke, J. K., Priimagi, A., et al. (2016). Multicomponent petasis-borono mannich preparation of alkylaminophenols and antimicrobial activity studies. *ChemMedChem* 11, 2015–2023. doi: 10.1002/cmdc.201600244
- Olliaro, P., Nevill, C., LeBras, J., Ringwald, P., Mussano, P., Garner, P., et al. (1996). Systematic review of amodiaquine treatment in uncomplicated malaria. *Lancet* 348, 1196–1201. doi: 10.1016/S0140-6736(96)06217-4
- Pommier, Y. (2006). Topoisomerase I inhibitors: camptothecins and beyond. *Nat. Rev. Cancer* 6, 789–802. doi: 10.1038/nrc1977
- Rajkumar, T., Sabitha, K., Vijayalakshmi, N., Shirley, S., Bose, M. V., Gopal, G., et al. (2011). Identification and validation of genes involved in cervical tumorigenesis. *BMC Cancer* 11:80. doi: 10.1186/1471-2407-11-80
- Ricke, R. M., Jegathanan, K. B., and van Deursen, J. M. (2011). Bub1 overexpression induces aneuploidy and tumor formation through Aurora B kinase hyperactivation. *J. Cell Biol.* 193, 1049–1064. doi: 10.1083/jcb.201012035
- Roman, G. (2015). Mannich bases in medicinal chemistry and drug design. *Eur. J. Med. Chem.* 89, 743–816. doi: 10.1016/j.ejmech.2014.10.076
- Santamaria, D., Barrière, C., Cerqueira, A., Hunt, S., Tardy, C., Newton, K., et al. (2007). Cdk1 is sufficient to drive the mammalian cell cycle. *Nature* 448, 811–815. doi: 10.1038/nature06046
- Selvendiran, K., Koga, H., Ueno, T., Yoshida, T., Maeyama, M., Torimura, T., et al. (2006). Luteolin promotes degradation in signal transducer and activator of transcription 3 in human hepatoma cells: An implication for the antitumor potential of flavonoids. *Cancer Res.* 66, 4826–4834. doi: 10.1158/0008-5472.CAN-05-4062
- Sharma, V., Joseph, C., Ghosh, S., Agarwal, A., Mishra, M. K., and Sen, E. (2007). Kaempferol induces apoptosis in glioblastoma cells through oxidative stress. *Mol. Cancer Ther.* 6, 2544–2553. doi: 10.1158/1535-7163.MCT-06-0788
- Stegh, A. H., Brennan, C., Mahoney, J. A., Forloney, K. L., Jenq, H. T., Luciano, J. P., et al. (2010). Glioma oncoprotein Bcl2L12 inhibits the p53 tumor suppressor. *Genes Dev.* 24, 2194–2204. doi: 10.1101/gad.1924710
- Stegh, A. H., Kesari, S., Mahoney, J. E., Jenq, H. T., Forloney, K. L., Protopopov, A., et al. (2008). Bcl2L12-mediated inhibition of effector caspase-3 and caspase-7 via distinct mechanisms in glioblastoma. *Proc. Natl. Acad. Sci.* 105, 10703–10708. doi: 10.1073/pnas.0712034105
- Stegh, A. H., Kim, H., Bachoo, R. M., Forloney, K. L., Zhang, J., Schulze, H., et al. (2007). Bcl2L12 inhibits post-mitochondrial apoptosis signaling in glioblastoma. *Genes Dev.* 21, 98–111. doi: 10.1101/gad.1480007
- Stupp, R., Mason, W., van den Bent, M. J., Weller, M., Fisher, B. M., Taphoorn, M. J. B., et al. (2005). Radiotherapy plus concomitant and adjuvant temozolomide for glioblastoma. *N. Engl. J. Med.* 352, 987–996. doi: 10.1056/NEJMoa043330
- Tang, Z., Shu, H., Qi, W., Mahmood, N. A., Mumby, M. C., and Yu, H. (2006). PP2A is required for centromeric localization of sgo1 and proper chromosome segregation. *Dev. Cell* 10, 575–585. doi: 10.1016/j.devcel.2006.03.010
- Thompson, D. C., Thompson, J. A., Sugumaran, M., and Mouldén, P. (1993). Biological and toxicological consequences of quinone methide formation. *Chem. Biol. Interact.* 86, 129–162. doi: 10.1016/0009-2797(93)90117-H
- Uhlen, M., Oksvold, P., Fagerberg, L., Lundberg, E., Jonasson, K., Forsberg, M., et al. (2010). Towards a knowledge-based human protein atlas. *Nat. Biotechnol.* 28, 1248–1250. doi: 10.1038/nbt1210-1248
- Wcislo, G., Korniluk, J., and Szarlej-Wcislo, K. (2013). Cancer chemoprevention by resveratrol treatment. *Polyphenols Hum. Health Dis.* 2, 1323–1330. doi: 10.1016/B978-0-12-398456-2.00099-2
- Weinert, E. E., Dondi, R., Colloredo-Melz, S., Frankenfeld, K. N., Mitchell, C. H., Freccero, M., et al. (2006). Substituents on quinone methides strongly modulate formation and stability of their nucleophilic adducts. *J. Am. Chem. Soc.* 128, 11940–11947. doi: 10.1021/ja062948k
- Wu, Y.-S., Coumar, M. S., Chang, J.-Y., Sun, H.-Y., Kuo, F.-M., Kuo, C.-C., et al. (2009). Synthesis and evaluation of 3-aryloindoles as anticancer agents: metabolite approach. *J. Med. Chem.* 52, 4941–4945. doi: 10.1021/jm900060s
- Yang, C.-M., Ji, S., Li, Y., Fu, L.-Y., Jiang, T., and Meng, F.-D. (2017). β -Catenin promotes cell proliferation, migration, and invasion but induces apoptosis in renal cell carcinoma. *Oncotargets Ther.* 10, 711–724. doi: 10.2147/OTT.S117933
- Yang, F., Brown, C., Buettner, R., Hedvat, M., Starr, R., Scuto, A., et al. (2010). Sorafenib induces growth arrest and apoptosis of human glioblastoma cells through the dephosphorylation of signal transducers and activators of transcription 3. *Mol. Cancer Ther.* 9, 953–962. doi: 10.1158/1535-7163.MCT-09-0947

- Yang, M. C., Loh, J. K., Li, Y. Y., Huang, W. S., Chou, C. H., Cheng, J. T., et al. (2015). Bcl2L12 with a BH3-like domain in regulating apoptosis and TMZ-induced autophagy: a prospective combination of ABT-737 and TMZ for treating glioma. *Int. J. Oncol.* 46, 1304–1316. doi: 10.3892/ijo.2015.2838
- Yang, Q., Manicone, A., Coursen, J. D., Linke, S. P., Nagashima, M., Forgues, M., et al. (2000). Identification of a functional domain in a GADD45-mediated G2/M checkpoint. *J. Biol. Chem.* 275, 36892–36898. doi: 10.1074/jbc.M005319200
- Zielke, N., and Edgar, B. A. (2015). FUCCI sensors: Powerful new tools for analysis of cell proliferation. *Wiley Interdiscip. Rev. Dev. Biol.* 4, 469–487. doi: 10.1002/wdev.189



Conflict of Interest Statement: The authors declare that the research was conducted in the absence of any commercial or financial relationships that could be construed as a potential conflict of interest.

Copyright © 2019 Doan, Musa, Candeias, Emmert-Streib, Yli-Harja and Kandhavelu. This is an open-access article distributed under the terms of the Creative Commons Attribution License (CC BY). The use, distribution or reproduction in other forums is permitted, provided the original author(s) and the copyright owner(s) are credited and that the original publication in this journal is cited, in accordance with accepted academic practice. No use, distribution or reproduction is permitted which does not comply with these terms.

II

Article

Glioblastoma Multiforme Stem Cell Cycle Arrest by Alkylaminophenol through the Modulation of EGFR and CSC Signaling Pathways

Phuong Doan ^{1,2,3}, Aliyu Musa ^{1,4} , Akshaya Murugesan ^{1,2,5}, Vili Sipilä ^{1,2}, Nuno R. Candeias ⁶ , Frank Emmert-Streib ^{4,7}, Pekka Ruusuvaori ², Kirsi Granberg ^{2,3}, Olli Yli-Harja ^{2,3,8,9} and Meenakshisundaram Kandhavelu ^{1,2,3,*}

¹ Molecular Signaling Lab, Faculty of Medicine and Health Technology, Tampere University, P.O. Box 553, 33101 Tampere, Finland; phuong.doan@tuni.fi (P.D.); aliyu.musa@tuni.fi (A.M.); akshaya.murugesan@tuni.fi (A.M.); vili.sipila@tuni.fi (V.S.)

² BioMediTech Institute and Faculty of Medicine and Health Technology, Tampere University, Arvo Ylpön katu 34, 33520 Tampere, Finland; pekka.ruusuvaori@tuni.fi (P.R.); kirsi.granberg@tuni.fi (K.G.); olli.yli-harja@tuni.fi (O.Y.-H.)

³ Science Center, Tampere University Hospital, Arvo Ylpön katu 34, 33520 Tampere, Finland

⁴ Predictive Society and Data Analytics Lab, Faculty of Information Technology and Communication Sciences, Tampere University, 33101 Tampere, Finland; frank.emmert-streib@tuni.fi

⁵ Department of Biotechnology, Lady Doak College, Thallakulam, Madurai 625002, India

⁶ LAQV-REQUIMTE, Department of Chemistry, University of Aveiro, 3810-193 Aveiro, Portugal; ncandeias@ua.pt

⁷ Institute of Biosciences and Medical Technology, 33101 Tampere, Finland

⁸ Computational Systems Biology Group, Faculty of Medicine and Health Technology, Tampere University, P.O. Box 553, 33101 Tampere, Finland

⁹ Institute for Systems Biology, 1441N 34th Street, Seattle, WA 98103-8904, USA

* Correspondence: meenakshisundaram.kandhavelu@tuni.fi; Tel.: +35-8417-4887-72

Received: 19 February 2020; Accepted: 9 March 2020; Published: 10 March 2020



Abstract: Cancer stem cells (CSCs), a small subpopulation of cells existing in the tumor microenvironment promoting cell proliferation and growth. Targeting the stemness of the CSC population would offer a vital therapeutic opportunity. 3,4-Dihydroquinolin-1(2H)-yl(*p*-tolyl)methylphenol (THTMP), a small synthetic phenol compound, is proposed to play a significant role in controlling the CSC proliferation and survival. We assessed the potential therapeutic effects of THTMP on glioblastoma multiforme (GBM) and its underlying mechanism in various signaling pathways. To fully comprehend the effect of THTMP on the CSCs, CD133⁺ GBM stem cell (GSC) and CD133⁻ GBM Non-stem cancer cells (NSCC) population from LN229 and SNB19 cell lines was used. Cell cycle arrest, apoptosis assay and transcriptome analysis were performed for individual cell population. THTMP strongly inhibited NSCC and in a subtle way for GSC in a time-dependent manner and inhibit the resistance variants better than that of temozolomide (TMZ). THTMP arrest the CSC cell population at both G1/S and G2/M phase and induce ROS-mediated apoptosis. Gene expression profiling characterize THTMP as an inhibitor of the p53 signaling pathway causing DNA damage and cell cycle arrest in CSC population. We show that the THTMP majorly affects the EGFR and CSC signaling pathways. Specifically, modulation of key genes involved in Wnt, Notch and Hedgehog, revealed the significant role of THTMP in disrupting the CSCs' stemness and functions. Moreover, THTMP inhibited cell growth, proliferation and metastasis of multiple mesenchymal patient-tissue derived GBM-cell lines. THTMP arrests GBM stem cell cycle through the modulation of EGFR and CSC signaling pathways.

Keywords: GBM stem cells; non-stem cancer cells; resistance population; cell cycle arrest; alkylaminophenol and cell death

1. Introduction

Glioblastoma multiforme or simply glioblastoma (GBM) is the most common malignant primary tumor. GBM is a grade IV astrocytoma that accounts for up to 60% of gliomas and carries the worst prognosis of all the cancers [1]. The current treatment of GBM using an alkylating agent, temozolomide (TMZ) combined with radiotherapy, shows their transient effect in only a few subsets of patients [2–4]. Hence, there is an urgent need for exploring effective therapeutics for GBM. To achieve this goal, many efforts have been made in understanding the complicated mechanisms that control GBM growth.

The initiation and progression of cancer is governed by a small subset of tumor-initiating cells termed cancer stem cells (CSC), whereas in GBM, GBM stem cells (GSCs) have a similar phenotype to the normal neural stem cells [5]. CSCs accounts for a rare fraction of a certain tumor that is responsible for tumor characteristics such as invasion, metastasis and relapse. The self-renewal ability of those differentiated cells allows them to become resistant to the current modern medicine involving radiation and chemotherapy [6]. Hence, research centering to hamper the activation of CSC via modulation of signaling pathway is much appreciated. Molecules such as CD133, CD44, ABCG2 and ALDH are believed to function as a biomarkers in some kind of CSCs [7–10]. Furthermore, several signaling pathway have been associated in the self-renewal behavior of cancer stem cells including Wingless-Int (Wnt), Notch and Hedgehog (Hh) pathways [11–14]. In addition to the CSC signaling pathways, EGFR signaling is also reported as a primary contributor to GBM initiation and progression. Oncogenic role of EGFR driving to GBM tumorigenesis has been validated both in *in vivo* and *in vitro* models [15–19]. Thus, targeting important downstream signaling pathways in CSC is important for identifying novel GBM therapy.

In the past decades, several phenolic compounds have been approved by FDA as anticancer agent including vincristine for small-cell lung cancer [20], paclitaxel for metastatic breast cancer [21], omacetaxine for chronic myeloid leukemia [22] etc. Among various phenolic compounds, alkylaminophenol moiety is found in some FDA-approved drugs such as amodiaquine and hycamtin (topotecan) is used as a promising chemotherapeutic agents [23,24]. Earlier reports from our research group have shown that several alkylaminophenols functions as an inducer of apoptosis on osteosarcoma and GBM [25–28]. Although anticancer activity of phenolic derivatives has been well reported on various cancers, their effect on GBM is not well investigated. Hence, the present study is aimed at evaluating the effect of alkylaminophenols on GSC and non-stem cancer cells (NSCC) derived from two different GBM cell lines (LN229 and SNB19). The profound investigation on the cellular mechanisms has been performed, which revealed the cytotoxic effect of alkylaminophenols on GSC. The multiple patient-derived GBM cell lines were also used to further confirm the potential of the compound as an effective chemotherapeutic agent for GBM.

2. Materials and Methods

2.1. Chemical Preparation

Synthesis and spectral characterization of compounds HNPMI [25], THMPP [26] and THTMP [29] (Figure 1A) were previously reported. These compounds and temozolomide (Sigma-Aldrich, St. Louis, MO, USA) were dissolved in dimethyl sulphoxide (DMSO, Sigma-Aldrich) to obtain a stock solution of 100 mM. Intermediate dilutions were prepared using stock solution.

2.2. Cell Viability and Heterogeneity from Dose-Response Curves

The cell viability assay was performed to determine the inhibitory effect of the compounds against the growth of GBM cells, LN229 and SNB19. The cell lines were gifted by Dr.Kirsi Granberg, Faculty of Medicine and Health Technology, Tampere, Finland). LN229 was originated from a patient with right frontal parieto-occipital glioblastoma with mutated p53 and homozygous deletions in the p16 and p14ARF tumor suppressor genes. SNB19 was derived from a patient with the left parietooccipital glioblastoma tumor. The cells were cultured in Dulbecco's Modified Eagle Medium

(DMEM) full medium (DMEM, 10% FBS, 0.1 mg/mL streptomycin, 100 U/mL penicillin, and 0.025 mg/mL amphotericin B). The concentrations of 100 μ M, 75 μ M, 50 μ M, 25 μ M, and 10 μ M of each compound (HNPMI, THMPP, and THTMP) were used to determine the cell viability. After 24 h exposure, the cells were collected by centrifugation at 3000 rpm for 5 min. Cell viability was determined by trypan blue and Countess II FL Automated Cell Counter (ThermoFisher Scientific, Carlsbad, CA, USA). Half-maximal inhibitory concentration (IC_{50}) values were calculated based on the sigmoidal dose-response curves, which were generated in the Matlab 2013a software using logistic function. Then, the half-maximal effective concentration (EC_{50}) of cell death inducing compounds were calculated from these dose-response curves as suggested previously [30] by using the following formula:

$$EC_{50} = Y_b + \frac{Y_t - Y_b}{1 + 10^{(LogEC_{50} - X) * HS}} \quad (1)$$

where, Y_b is the Y value at the bottom plateau, Y_t is the Y value at the top plateau, $LogEC_{50}$ is the X value when the response is halfway between bottom plateau and top plateau, and HS is the Hill coefficient [31].

2.3. Isolation of Glioblastoma Stem Cells (GSC) and Non-Stem Cancer Cell (NSCC) and Cell Culture

In GBM, CD133 has been accepted as a marker for CSCs which was isolated using CD133 MicroBead Kit (Miltenyi Biotec, Lund, Sweden). The cells containing CD133 enrichment are classified as GBM stem cells (GSC) and the cells containing CD133 depletion are defined as GBM non-stem cancer cells (NSCC). The procedure for the isolation of the GSC and NSCC was followed as instructed by the manufacturer. Briefly, after harvesting the cells, 300 μ L of buffer was added to 1×10^8 total cells. Then, 100 μ L of the FcR blocking reagent and CD133 MicroBeads were added into the buffer containing cells. The mixture was mixed, incubated for 30 min at 4 $^{\circ}$ C and the cells were then washed with buffer to remove the reagents. The cells are subjected for magnetic separation using columns supplied with the kit and MACS separator.

In this study, we used LN229 and SNB19 GBM cells for GSC and NSCC isolation. GSC-LN229 and GSC-SNB19 cells were cultured in StemPro hESC SFM medium (Life Technologies, Pleasanton, CA, USA) while NSCC-LN229 and NSCC-SNB19 cells were cultured in DMEM full medium. The cells were maintained at 37 $^{\circ}$ C in a humidified atmosphere containing 5% CO_2 . All of the components of the cell culture were purchased from Sigma-Aldrich.

2.4. Pharmacodynamics Study

The time-dependent study was performed using IC_{50} concentration of THTMP on LN229 and SNB19 as described previously [28]. GSC and NSCC are treated with THTMP for 24, 48 and 72 h. Treated cells were collected using centrifugation at 3000 rpm for 10 min. Number of live and dead cells were determined using trypan blue solution and Countess II FL Automated Cell Counter (ThermoFisher Scientific). Inhibition percentage was calculated using Equation (2). Biological and technical replicates were conducted for each condition. TMZ and DMSO vehicle were used as positive and negative control, respectively.

$$\text{Inhibition (\%)} = \frac{\text{Mean No. of untreated cells (DMSO control)} - \text{Mean No. of treated cells}}{\text{Mean No. of untreated cells (DMSO control)}} \times 100 \quad (2)$$

2.5. Resistance Variants

The response rate to current chemotherapies for cancer depends on the availability of various chemotherapy regimens. However, multidrug resistance (MDR) still develops nearly in all patients with cancers and leads to chemotherapy failure [32,33]. We tested the ability of THTMP and TMZ on creating drug-resistant tumor cells. The THTMP-resistant and TMZ-resistant variants of GSC-LN229 and GSC-SNB19 cells were obtained by exposing the cells to THTMP/TMZ as follows. GSC-LN229 and

GSC-SNB19 cells were cultured at an initial density of 5×10^5 cells per 25-cm² flask containing 10 mL medium for 3 days. The cells were then treated with 5 μ M of compound (THTMP/TMZ) for 24 h. The cells were then cultured in the compound-free medium for 2 weeks to recover the cell density. The above treatment was repeated five times. The variants that survived THTMP and TMZ exposure were designated as R1 and R2, respectively. After obtaining R1 and R2, cytotoxicity assay was performed by exposing the cells to the IC₅₀ concentration of THTMP and/or TMZ for 24 h. The cell viability assay and the cell growth inhibition were carried out as described in Section 2.4.

2.6. Illumina Sequencing, RNA-Seq Data and Gene Ontology Analysis

To perform Illumina sequencing, RNA samples were isolated from GSC and NSCC. GSC-LN229, NSCC-LN229, GSC-SNB19 and NSCC-SNB19 cells were cultured as described in Section 2.3. The cells were then treated with the IC₅₀ concentration of THTMP/TMZ for 24 h. RNA of treated GSC and NSCC was isolated using GeneJET RNA Purification Kit (ThermoFisher Scientific, Waltham, MA, USA) following the manufacturer's instruction. Whole transcriptome sequencing of the total RNA samples of GSC-LN229, NSCC-LN229, GSC-SNB19 and NSCC-SNB19 cells (including triplicates of THTMP treated, TMZ treated and untreated samples) were performed by the Biomedicum Functional Genomics Unit (FuGU, University of Helsinki, Helsinki, Finland) using Illumina NextSeq 500. The sequencing produced data in bcl format, which was converted into FASTQ file format. The RNA-seq data analysis pipeline, gene ontology and pathway analysis was performed as described previously [28]. In this analysis, only pathways and GO term with *p*-value <0.05 and fold change of 1.5 were set as cutoff values.

2.7. Cell Cycle Analysis

GSC-LN229, NSCC-LN229, GSC-SNB19 and NSCC-SNB19 cells were cultured in 6 well-plate at an initial density of 5×10^5 cells/well. The cells were treated with the IC₅₀ concentration of the compounds (THTMP or TMZ) for 24 h. The cells were then harvested, washed in ice cold PBS and fixed in 70% ice-cold ethanol for 30 min at 4 °C. After washing in cold PBS, the cells were suspended in 200 μ L PBS containing 20 μ g/mL propidium iodide (PI), 0.2 mg/mL RNase and 0.1% triton X-100 and incubated for 30 min at 37 °C. Fluorescence images were captured using EVOS imaging system (ThermoFisher Scientific, Waltham, MA, USA) with 10 \times objective magnification. The cell cycle phases were analyzed using CellProfiler [34,35].

2.8. Annexin V-Fluorescein Isothiocyanate (FITC)/Propidium Iodide (PI) Labelling (V-FITC/PI) Double Staining Assay

Apoptosis induction assay was performed using Dead Cell Apoptosis Kit with Annexin V-fluorescein isothiocyanate (FITC) and propidium iodide (PI) (ThermoFisher Scientific, Waltham, MA, USA) followed by the manufacturer's protocol. Briefly, GSC-LN229, NSCC-LN229, GSC-SNB19 and NSCC-SNB19 cells were seeded in 6 well-plate with the initial density of 5×10^5 cells/well. The cells were treated with the IC₅₀ concentration of THTMP for 24 h, and then harvested and washed in ice-cold PBS. The cell pellets were then resuspended in 1X annexin-binding buffer provided along with the kit. Then, 5 μ L of FITC conjugated Annexin V and 1 μ L of the 100 μ g/mL PI were added to 100 μ L of the cell suspension. The cells were incubated at RT for 15 min prior to the fluorescence measurements. The image acquisition was done by using EVOS imaging system (ThermoFisher Scientific, Waltham, MA, USA) with 20 \times objective magnification. The positive control (TMZ) and negative control (DMSO) were also included in the study.

2.9. Detection of Intracellular Reactive Oxygen Species (ROS) and Caspase 3/7 Activity

GSC-LN229, NSCC-LN229, GSC-SNB19 and NSCC-SNB19 cells were cultured overnight in the appropriate culture conditions. The cells were then treated with the IC₅₀ concentration of THTMP/TMZ for 5 h. Cells were harvested by centrifugation at 3000 rpm for 10 min. For ROS detection, the cells

were incubated with 2 μM 2',7'-dichlorodihydrofluorescein diacetate (H2DCFDA) (Sigma-Aldrich), for 30 min at cell culture condition. The cells were then washed and recovered in pre-warmed complete medium for 20 min prior to the fluorescence measurement at the excitation wavelength of 485 nm and emission wavelength of 538 nm by Fluoroskan Ascent FL (Thermo Labsystems; St. Louis, MO, USA). DMSO and hydrogen peroxide (200 μM) were used as the negative and positive controls. For caspase 3/7 detection, we used Caspase-Glo®3/7 Assay kit (Promega, Madison, WI, USA) following the standard protocol of the manufacturer. Caspase-Glo reagent was added to the plate containing treated cell, untreated cell, blank or TMZ with the ratio of 1:1 (*v/v*). After that, the cells were gently mixed and incubated for 1 h. The luminescence was measured using Fluoroskan Ascent FL (Thermo Labsystems).

The fold increase in ROS production and caspase 3/7 were calculated using Equation (3):

$$\text{Fold increase} = \frac{F_{\text{test}} - F_{\text{blank}}}{F_{\text{control}} - F_{\text{blank}}} \quad (3)$$

where, F_{test} is the fluorescence/luminescence readings from the treated wells, F_{control} is the fluorescence/luminescence readings from the untreated wells, and F_{blank} is the fluorescence/luminescence readings from the unstained wells.

2.10. In Vitro Cytotoxicity in Patient-Derived (GBM) Cells

Three cell lines from low-passage patient-derived primary GBMs (MMK1, RN1 and PB1), display the phenotype of GBM, were a gift from Dr. Brett Stringer (QIMR Berghofer, Medical Research Institute, QLD, Australia). The generation of these low-passage primary patients' GBMs was done by isolating the patient's tumor, which was approved by the human ethics committee of the Queensland Institute of Medical Research and Royal Brisbane and Women's Hospital (ethical approval number: P3420, HREC/17/QRBW/577 Novel Therapies for Brain Cancer) [36]. These cells were then cultured in the serum-free medium using 1% matrigel-coated flasks, as previously described [37]. The cells were maintained in an incubator at 37 °C in humidified air with 5% CO₂. MMK1, RN1 and PB1 cell lines were plated in 12-well plates (1 \times 10⁵ cells/well), treated with THTMP/TMZ (100 and 10 μM) for 24 h. The cell viability assay and the cell growth inhibition were carried out as described in the Section 2.4.

2.11. Wound Healing Assay on Patient-Derived (GBM) Cells

Initial density of 3 \times 10⁵ cells/well was plated in 12-well plate. MMK1, RN1 and PB1 cells were cultured as described in Section 2.10 until reaching the monolayer confluency. A scratch was made in each well using a thin tip. The edges were smoothed and washed with the phosphate-buffered saline (PBS). The cells were then treated with 30 μM of THTMP/TMZ. The scratched area was visualized under a light microscope every 2 h for a total period of 10 h.

2.12. Statistical Analysis

The following experiments such as, cell viability assay, pharmacodynamics study, Illumina sequencing, cell cycle progression, annexin V-FITC/PI staining, ROS and caspase assay, in-vitro cytotoxicity in patient derived GBM cells and wound healing assay, were conducted with five biological repeats and technical repeats. The data were shown as means \pm S.D and analysed using IBM SPSS (Statistics for Windows version 20.0). For comparison between the tested groups, statistical significant differences were evaluated using the *t*-test. For comparison of more than two groups, statistical significance was determined using a one-way ANOVA test. $p < 0.05$ was considered statistically significant.

3. Results

3.1. Effect of Alkylaminophenol in Glioblastoma Multiforme (GBM) Cell Lines

A series of alkylaminophenols, HNPMI, THMPP and THTMP, were investigated for their induction of cell death on multiple GBM cancer cell lines. THTMP has the highest inhibitory effect on the GBM cells at a concentration of 100 μM (Figure 1A) compared with HNPMI and THMPP. Although these three compounds have shown promising cell growth inhibition on GBM cell lines, LN229 and SNB19, the presence of methyl group in the place of 4-OMe in THTMP improved the percentage of cytotoxicity. THTMP shows 0% and 23.13% cell viability on LN229 and SNB19, respectively. HNPMI shows a similar effect on both GBM cell lines, whereas THMPP has varying cell death effect. The top lead compound, THTMP potentially inhibited the GBM cell proliferation in a dose-dependent manner (Figure 1B) in which the IC_{50} values were about 26.5 μM and 87.8 μM for LN229 and SNB19, respectively. We also previously reported that, THTMP has selectively inhibited the growth of GBM cells than the non-cancerous cells (Supplementary Figure S1) [28]. IC_{50} of positive drug control, TMZ on these two cell lines was also calculated to be 75.4 μM and 84.4 μM , respectively. Sigmoidal dose-response curve was used to calculate the EC_{50} . The EC_{50} values of THTMP and TMZ for the respective cell lines were about 30.1 μM and 88.2 μM (LN229) as well as 69.3 μM and 82.3 μM (SNB19), respectively. Thus, the improved EC_{50} values were observed for THTMP than the TMZ on both the cell lines.

3.2. Glioblastoma Stem Cells (GSC) and Non-Stem Cancer Cell (NSCC) Show a Heterogeneous Sensitivity to 3,4-Dihydroquinolin-1(2H-yl)(p-tolyl)methylphenol (THTMP) and Temozolomide (TMZ) Treatment in Time-Dependent Manner

There are evidences affirming that tumor-specific stem cell populations are the key contributor to the failure in chemotherapy and radiotherapy. The eradication of CSC population is the necessity that could support the therapies for the efficient reduction in the progression of the tumor. Thus, to pursue this insight, we have evaluated the efficacy of THTMP and TMZ on GSCs and NSCCs derived from LN229 and SNB19. The expression of CD133 in each population was tested using CD133 antibody. The intensity of CD133 was found to be higher in GSC than in the NSCC and its mixed population (Figure 1C). Also, the CD133 was found to be overexpressed in the GSC and mixed population of SNB19 than LN229.

In order to identify the effect of THTMP/TMZ on the GBM sub-population, GSC-LN229, GSC-SNB19, NSCC-LN229 and NSCC-LN229, we have examined the growth-inhibitory effect using the IC_{50} concentration after 24, 48 and 72 h of THTMP/TMZ exposure. GSCs and NSCCs responded heterogeneously on THTMP and TMZ exposure (Figure 1D). We noticed a gradual increase in the percentage of cell death upon THTMP treatment, while TMZ induced varying cell death in GSC population of both cell lines over the time. THTMP has higher growth inhibition than the TMZ in NSCC population of both cell lines. Time dependent treatment of THTMP has shown a considerable increase of cell death in NSCC than GSC. NSCC-SNB19 has cell death by 90%, whereas NSCC-LN229 has 32%, after 72 h of treatment.

To further explore the underlying mechanism on the effect of THTMP at 24 h post treatment, the differential expression of genes (DEGs) involved in the DNA damage was analysed. DEGs with two-fold changes or greater ($p < 0.001$) upon THTMP treatment were quantitatively analysed (Supplementary Tables S1–S4). Totally twelve DEGs associated with the DNA damage were listed (Figure 1E). *FOXM1* and *CDK1* overexpression induces carcinogenesis and disease progression in GBM. *FOXM1* upregulation regulates G2/M phase in cell cycle and P53 signaling pathway [38]. Upon THTMP treatment, *FOXM1* was downregulated in GSC and NSCC populations of both cell lines. Besides *FOXM1*, we also noticed the downregulation of *p53* target genes, *PLK2* in GSC-LN229, and NSCC-LN229. Thus, THTMP can target p53 signaling pathway in GBM cells.

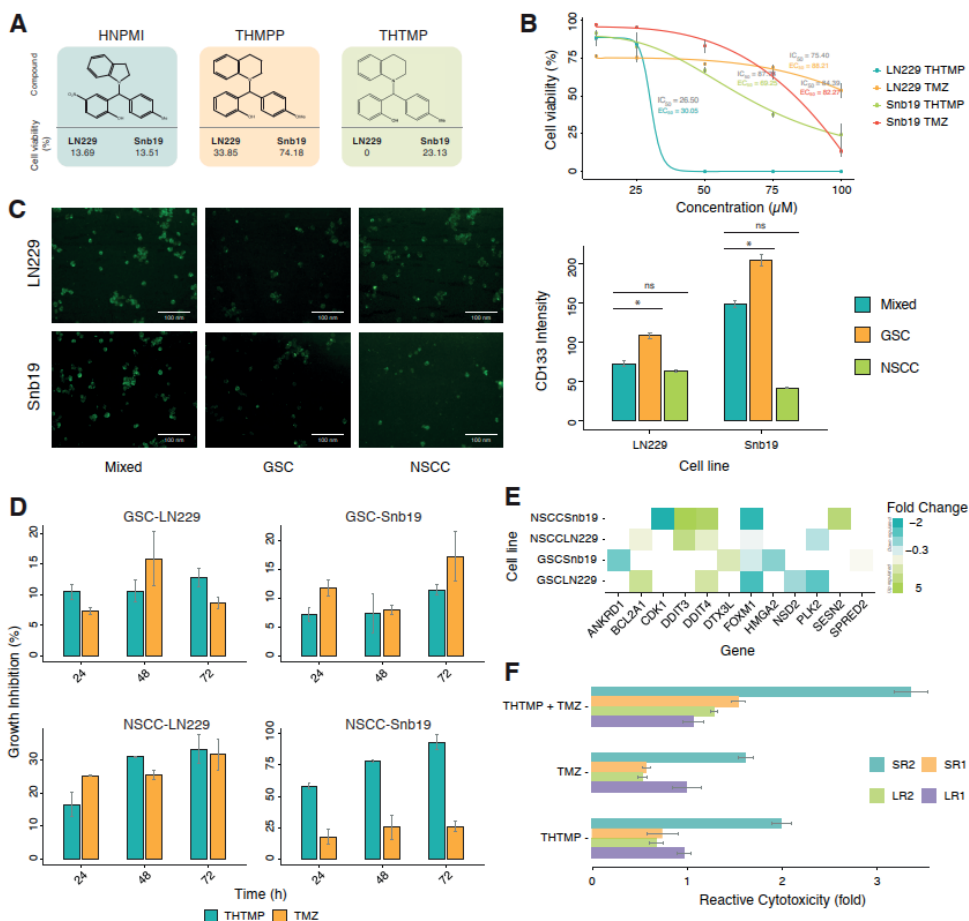


Figure 1. Effect of 3,4-Dihydroquinolin-1(2*H*)-yl(*p*-tolyl)methyl)phenol (THTMP) treatment on cell survival in GBM cells. (A) Molecular structure of three tested alkylaminophenols (HNPMP, THMP and THTMP) and % cell viability of those compounds on LN229 and SNB19 cell lines at 100 μM concentration. (B) Percentage of cell viability for LN229 and SNB19 cell lines upon treatment with THTMP/TMZ in the dilution series from 10 μM to 100 μM. (C) Representative image and intensity of CD133 on GSC, NSCC and mixed population of LN229 and SNB19. (D) Time-dependent effect of THTMP on GSC and NSCC cells. The results were normalized to DMSO control. One-way ANOVA was conducted ($P < 0.05$) to determine the statistical significance in all the conditions compared to DMSO control. (E) The top DEGs involved in DNA damage on GSC-LN229, GSC-SNB19, NSCC-LN229 and NSCC-SNB19. The DEGs were color coded corresponding to the up- and down- expressed genes. (F) Relative cytotoxicity of resistant variants, LR1, LR2 (derived from GSC-LN229) and SR1, SR2 (derived from GSC-SNB19) to THTMP and/or TMZ. The results were normalized to DMSO control. One-way ANOVA was done ($P < 0.05$) to determine the statistical significance in all the conditions compared to DMSO control. All experiments were performed with $N = 5$. * $p < 0.05$, ns—non significant.

Upon THTMP treatment, more DEGs were found in NSCC than in GSC population. This may be due to the ability of GSC to resist the effect upon THTMP on due course of treatment. Since the development of resistant GSC cells prevented them from being subjective for THTMP and/or TMZ treatment, we investigated the mechanism of alteration in the sensitivity of resistant variants. GSC resistant variants were developed upon treatment with THTMP and/or TMZ as described in the

method section. On treatment with THTMP, the cytotoxicity effect of GSC-LN229 derived cells, LR1 and LR2 were 1.0 and 0.7-fold higher than the respective parent cells, whereas GSC-SNB19 derived cells SR1 and SR2 were 0.8 and 2.1-fold higher, respectively. In parallel, the cytotoxic effect of TMZ and combination of THTMP/TMZ on the resistant variants was also analysed. These results substantiated the above findings that there was higher cytotoxic potential of THTMP than the TMZ. Thus, synergy of THTMP with TMZ on both GSC variants showed higher cytotoxicity (i.e., % of cell death in THTMP treated cells <THTMP + TMZ; % of cell death in TMZ treated cells <THTMP + TMZ).

3.3. THTMP Triggers Cell Cycle Arrest in GSCs and NSCCs

To gain more insights into the effect of THTMP/TMZ on the cell viability and cell proliferation, we examined the cell cycle phases in GSCs and NSCCs. Cells in G1, S and G2/M phase were separated based on the linear fluorescence intensity of propidium iodide stain. The large initial peak (left) represents the cells in G1, the intervening area represents cells in S phase and the final tail/small peak (right) represents cells in G2/M phase. THTMP treatment induced the cell cycle arrest at G1/S phase in both GSC-LN229 and GSC-SNB19 cells (Figure 2A). This inference is made by comparing the proportion of cells present in each phase. As shown in Figure 2A, we could observe the majority of cells in G1 phase, with significant reduction of cells in S phase and with further loss in G2/M phase. Subsequently, cell cycle analysis of NSCC-LN229 revealed that most of the cells arrested in G2/M phase, whereas SNB19 arrest happens in G1/S phase of NSCC-SNB19 cells.

The arrest in the different phases of the cell cycle is possible due to the presence of heterogeneous cell populations in NSCCs. As shown in Figure 2B, upon THTMP treatment, both GSC-LN229 and GSC-SNB19 have ~70% of cells in G1 phase while ~15% in S phase and G2/M phase. Most of the cells were arrested in G1 phase, suggesting the smaller number of cells entering into the S phase and G2/M phase. Although the same pattern was observed in DMSO conditions of NSCC of both cell lines, the percentage of NSCCs found to be fluctuating on THTMP treated conditions.

THTMP treatment leads to 44%, 23.9% and 32.1% of cells in G2/M phase, S phase and G1 phase, respectively in NSCC-LN229, whilst 27.3%, 17.8% and 54.9% of the cells were observed in G2/M, S phase and G1 phase, respectively in NSCC-SNB19. Thus, NSCC-LN229 cells were arrested at G2/M phase and NSCC-SNB19 cells at G1/S phase.

The results obtained from cell cycle assay were substantiated by the transcriptome profiling. The THTMP could induce several biological processes involved in cell cycle pathways such as cell cycle G1/S phase transition, G1/S transition of mitotic cell cycle, mitotic cell cycle checkpoint, cell cycle DNA replication, cell cycle G2/M phase transition, G2/M transition of mitotic cell cycle, cell cycle arrest (Supplementary Tables S5–S8).

As shown in Figure 2C, number of genes were significantly enriched that corresponds to the cell cycle pathway. In NSCC-LN229, there occurs downregulation of *CCNB2* coding to cyclin B2, and an upregulation of *GADD45A* which is a downstream target gene of *p53* in G2 checkpoint. This suggests that NSCC-LN229 cells were arrested at G2/M phase. Meanwhile, NSCC-SNB19, GSC-LN229 and GSC-SNB19 showed the upregulation of *CDK2* and *CDK6* that are associated with G1/S arrest, whereas genes coding for cyclin D1, D2, E1, and E2 such as *CCND1*, *CCND2*, *CCNE1* and *CCNE2* respectively, were downregulated. These cyclins are essential for triggering and regulating G2/M transition in complex with *CDK1*. In addition, the most significant event observed was the downregulation of *BUB1* gene expression, which played vital role in G1/S transition of mitotic cells and DNA replication. Thus, transcriptome data revealed that, THTMP induced cell cycle arrest at G1/S or G2/M phase, which is explicitly specific for different cell line populations. Taken together the cell cycle arrest and gene expression analysis, THTMP could possibly inhibit the synthesis before they enter the synthesis phase or mitotic phase and thus potentially prevents cell proliferation.

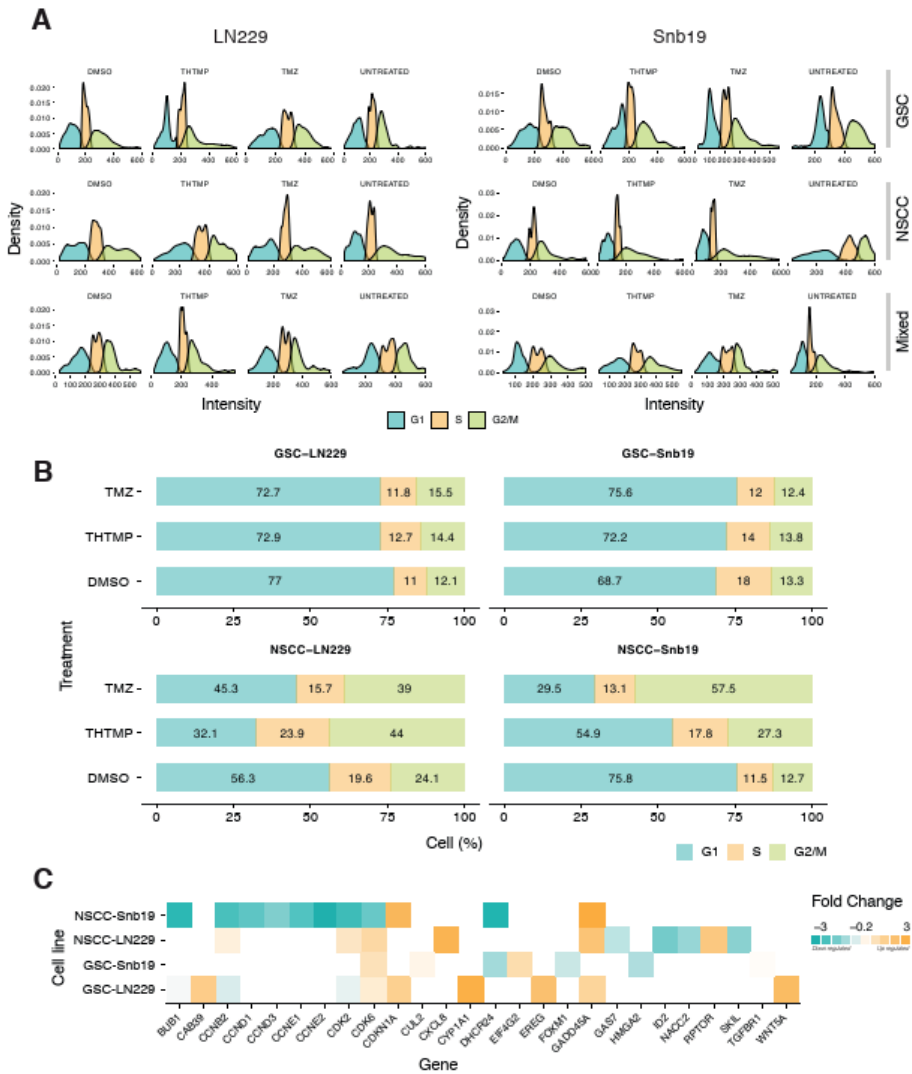


Figure 2. THTMP triggers GSC and NSCC cell cycle arrest. (A) Graphs represented the distribution of cells in different phases of cell cycle (B) The bar diagram representing the percentage of total cells in different cell cycle phases treated with THTMP/TMZ. (C) The top DEGs involved in the cell cycle in GSC and NSCC population. The DEGs were color coded corresponding to the up- and down- expressed genes. Five biological and technical repeats were used in cell cycle and gene expression analysis. All experiments were performed with N = 5.

3.4. THTMP Induces the Apoptosis via ROS and Caspase 3/7 Activation

The potential of THTMP causing apoptosis in GBM cells was analysed based on the differences in plasma membrane integrity and permeability using Annexin V/PI dual staining. Figure 3A shows the percentage of apoptotic and necrotic cells in THTMP/TMZ treatment in GSC and NSCC of LN229 and SNB19 cells. Exposure of GSC and NSCC of LN229 and SNB19 with THTMP/TMZ induced the apoptosis and necrosis. NSCCs have a greater percentage of apoptotic cells compared to GSCs in both cell lines, in agreement with the cytotoxicity results. THTMP exposed GSC-SNB19 has higher apoptosis

than GSC-LN229, which was about 30% and 10%, respectively. Meanwhile, THTMP treated NSCC population showed 40% of apoptosis in both cell lines, while TMZ showed 25% and 30% apoptosis in LN229 and SNB19, respectively (Figure 3A). This suggests the better potentiality of THTMP to induce apoptosis both in NSCC and GSC population.

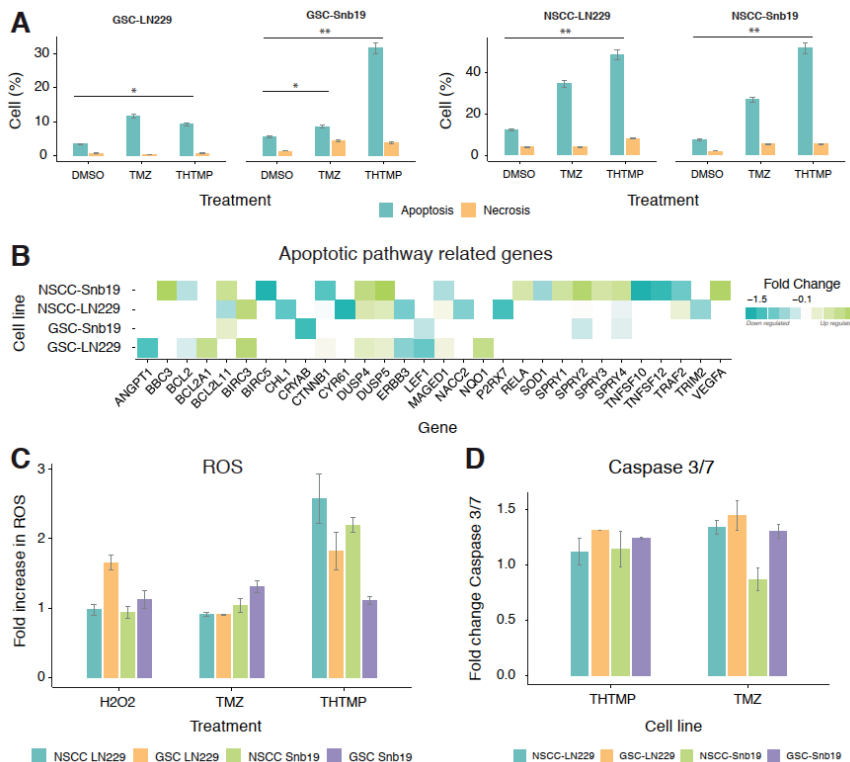


Figure 3. THTMP induces apoptosis in NSCCs and GSCs. (A) Percentage of apoptotic cells and necrotic cells upon THTMP/TMZ treatment at 24 h, stained with Annexin V-FITC/PI. (B) The top DEGs which are involved in apoptosis induction on GSCs and NSCCs. The DEGs were color coded that corresponds to the up- and down-expressed genes. (C) Effect of THTMP/TMZ on NSCCs and GSCs intracellular ROS production. (D) Activity of caspases 3/7 on NSCCs and GSCs in THTMP/TMZ treatment. Fold increase in ROS and caspases 3/7 activity of cells was calculated with triplicates for each condition. The data were normalized against DMSO control (C,D). * $p < 0.05$, ** $p < 0.01$.

To explore the genes involved in inducing the apoptosis on THTMP treatment, gene expression profiling of GSC and NSCC was also performed. GO term enrichment analysis was conducted to detect the biological significance of genes in cell death, programmed cell death and apoptosis process (Supplementary Tables S5–S8). It is figured out that a greater number of DEGs related to apoptotic signaling pathway was enriched in THTMP treated condition than in the control (Figure 3B). Among them, we found that NSCC was modulated more than GSC, which is also evidenced from the previous data of apoptosis assay. It is further validated by observing the upregulation of the pro-apoptotic genes (*BBC3*, *BCL2L11* (*Bim*), *BCL2A1*, *MADGED1*) and as well downregulation of a few pro-survival genes (*BCL2*, *BCL2L1* and *MCL1*).

Notably, *BBC3*, a p53 upregulated modulator of apoptosis (*PUMA*) was significantly upregulated in GSC-SNB19. *PUMA* is induced in cells following p53 activation by binding to Bcl-2 and further localizes to mitochondria that induces cytochrome *c* release and finally activates programmed cell

death. Thus, in GSC, upregulation of *BCL2A1* and *BCL2L11* was observed, indicating the role of THTMP in p53 inducible apoptosis. In contrast, the upregulation of *BIRC3* which encodes for BIRC protein, a member of the inhibitor of apoptosis gene (IAPs) unfortunately prevents apoptosis in GSC-LN229 and NSCC-LN229 cells. Nevertheless, a strong downregulation of *BIRAC5* was observed in NSCC-SNB19 cells.

Accumulation of reactive oxygen species (ROS) at the mitochondria is one of the apoptotic stimuli in the intrinsic death pathway. High level of ROS might damage proteins, nucleic acids, resulting in oxidative stress and cellular dysfunctions [39–42]. To study the ROS mediated apoptosis on treatment with THTMP/TMZ, ROS assay was performed using H2DCFDA. THTMP exposed cells showed increased apoptosis due to the higher ROS production which is directly proportional to H2DCFDA-flourescence intensity. THTMP treatment significantly produced higher fold level of ROS with 2.5 and 2.3 in NSCC-LN229 and NSCC-SNB19, respectively. However, 2-fold increase of ROS was noticed in GSC-LN229 while only with 1.2-fold in GSC-SNB19 (Figure 3C). ROS level was found to be higher in THTMP treated cells than in TMZ, DMSO control and H₂O₂ control. Furthermore, oxidative gene expression signatures confirmed several DEGs related to ROS such as *FOXM1*, *TXNRD2*, *DUSP1*, and *SOD1* were also enriched (Supplementary Tables S1–S4). These genes are associated with poor patient prognosis in several tumor types including glioblastoma [43,44].

In addition to the ROS mediated apoptosis, we have also analysed the possible role of caspase mediated apoptosis. It is been evident that, there seems to be a least level of caspase 3/7 activation on treatment with both THTMP and TMZ (Figure 3D). Yet, TMZ has highest fold increase in caspase activity than in THTMP. GSC-LN229, GSC-SNB19 has higher caspase activity in TMZ than THTMP treatment. NSCC-LN229 has higher caspase activity than NSCC-SNB19 in TMZ and vice versa in THTMP. This could be a possible reason for higher cytotoxicity in NSCC-SNB19 upon THTMP treatment than other conditions (Figure 1D). This endorse that THTMP could selectively induce apoptosis of GSC and NSCC population of both cell lines via caspase 3/7 activation.

3.5. Effect of THTMP on GSC and NSCC Gene Expression

Global gene expression profiling was performed to determine the mechanism of action of THTMP on GSC and NSCC proliferation and survival. Gene set enrichment analysis explored the DEGs of GSC-LN229 and NSCC-LN229 up to 2875 and 3269 respectively, whereas NSCC-SNB19 and GSC-SNB19 has 7974 and 300 DEGs, respectively (Figure 4A). Genes that were enriched either in a upregulation or downregulation fashion (Figure 4B), have been reported to be highly associated with various biological functions such as cellular process, DNA replication, DNA repair, cell cycle, chromatin remodelling, apoptotic process and programmed cell death (Supplementary Tables S5–S8). We also analysed the DEGs of GSC and NSCC with the progenitor cells, namely mixed-LN229 and mixed-SNB19. It is revealed that there are 154 genes shared in common with GSC, NSCC and mixed population, while only 52 genes in SNB19 (Figure 4A, Supplementary Tables S9 and S10). The least sharing of DEGs could be because of the less number of genes expressed in GSC-SNB19. All these data suggest that a few of the biological processes (Figure 4C) and signaling pathways (Figure 4D) were affected in those populations on treatment with THTMP. The influence of THTMP to modulate the cellular process, metabolic process, mitotic cell cycle, apoptotic process, programmed cell death in all the populations of GBM cells was observed (Figure 4C).

3.6. Effect of THTMP on Multiple Signaling Pathways

To identify the association of modulated signaling pathways, six main targeted pathways were selected for the further analysis (Figure 5A). The number of genes represented in each pathway for both cell lines was also listed in Figure 5A. The more number of DEGs was associated with EGFR pathway suggests its significant role in modulating the pathway, while the PDGF pathway even with only five DEGs, identified as the second most significant pathway. Various other pathways like JAK/STAT, TGF-beta, Wnt, Notch and Hh pathways also shows significant modulation when the cell lines are

treated with THTMP. EGFR signaling plays an important role in promoting glioblastoma survival and progression and thus by targeting EGFR pathway, the cancer cells either will undergo apoptosis or becomes sensitized to chemotherapy [15]. Our analysis provides a prime data on understanding the dysregulated genes in EGFR pathways upon THTMP treatment.

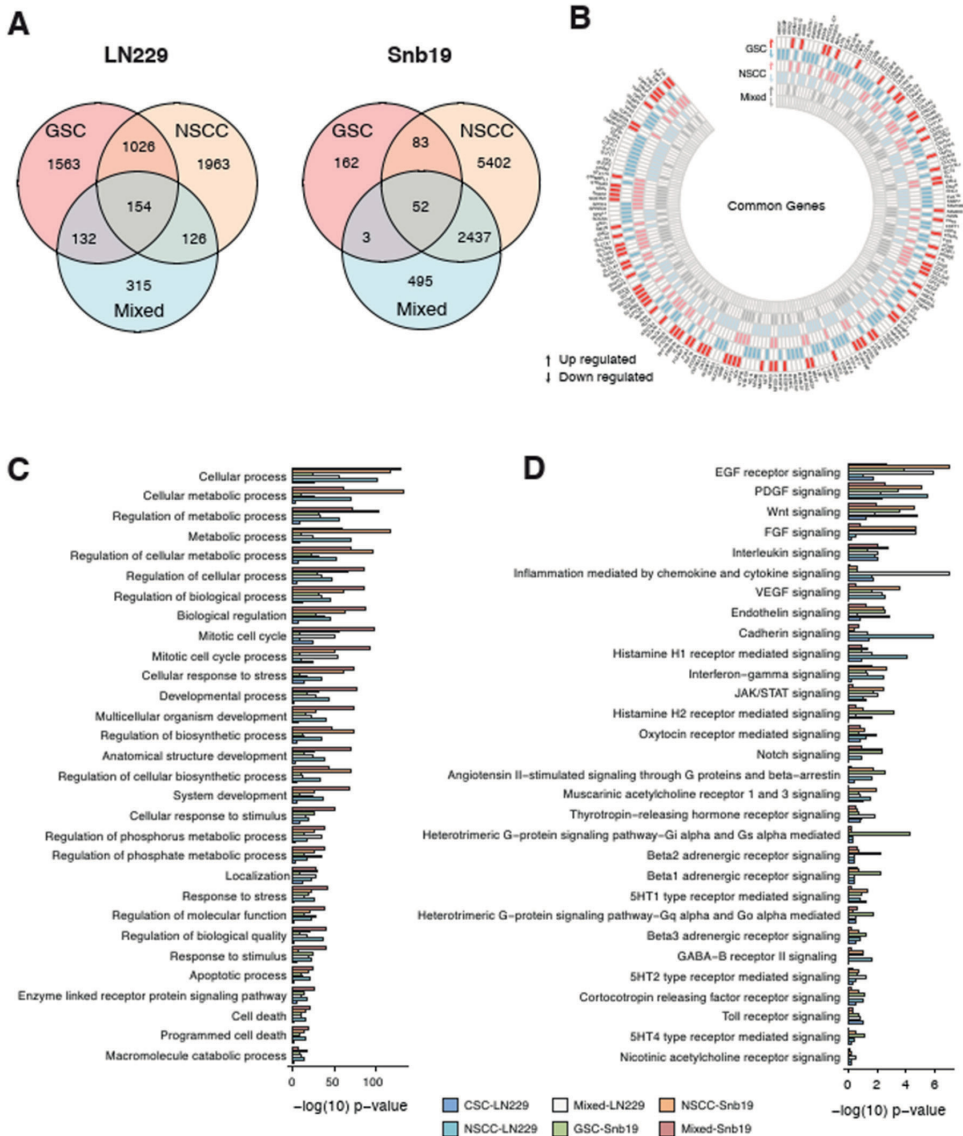


Figure 4. Effect of THTMP on GSC, NSCC and their progenitors gene expression patterns (A) Overlapping DEGs in GSC, NSCC and mixed populations of LN229 and SNB19 cell lines. (B) Circos plot of overlapping up- and down-regulated genes detected in GSC, NSCC and progenitor lines. (C) Common KEGG biological process in GSC, NSCC and progenitor lines. (D) Common signaling pathways in GSC, NSCC and progenitor lines.

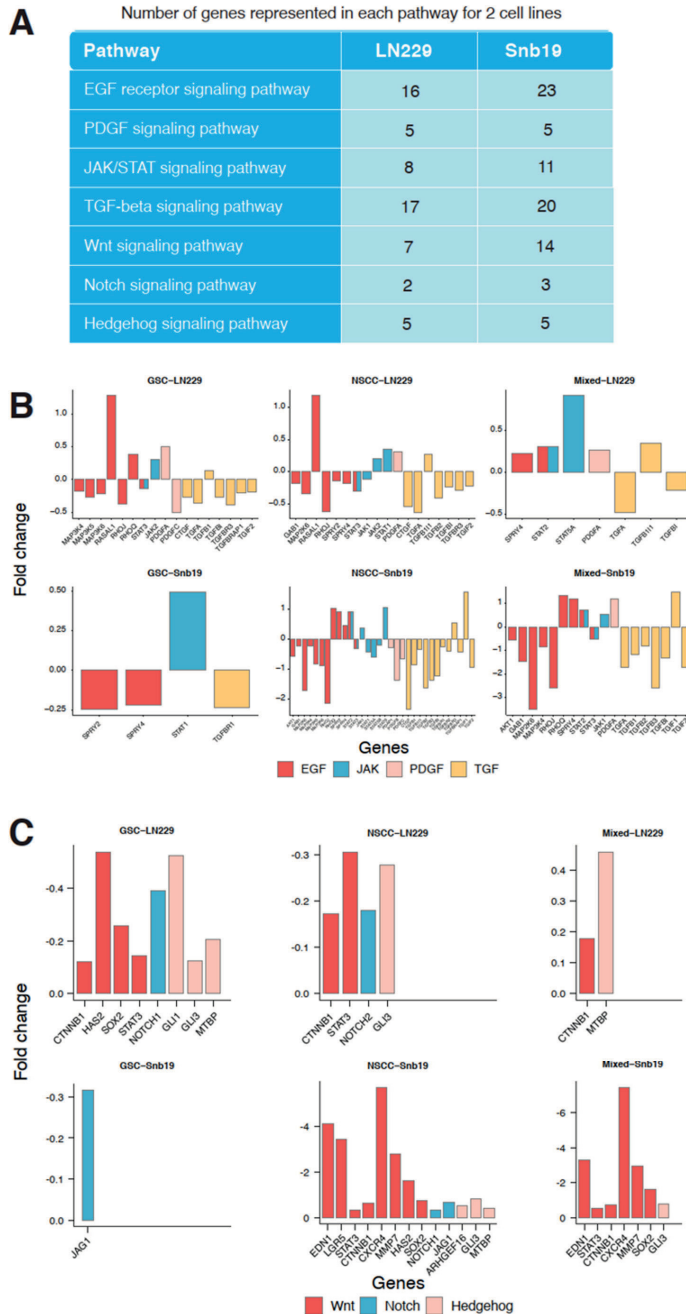


Figure 5. Effect of THTMP on multiple signaling pathways (A) Significant targeted signaling pathways upon THTMP treatment. (B) Comparison of DEGs fold change in EGF, PDGF, JAK/STAT, and TGF- β signaling pathways of GSC, NSCC and mixed populations. (C) Comparison of DEGs fold change in CSC signaling pathways in GSC, NSCC and progenitor lines.

Figure 5B shows the hub genes which are up and down regulated includes *RHOQ*, *SPRY2*, *SPRY4*, *STAT2* and *MAP3K4*, *MAP3K5*, *RHOJ*, *AKT1*, *GAB1* in GSC, NSCC and their progenitor of LN229 and SNB19. More number of genes were regulated in EGFR signaling in GSC and NSCC population of LN229 than the mixed population. Unlike LN229, more number of EGFR signaling genes in SNB19 cells was targeted in GSC, NSCC and mixed population. Targeted EGFR signaling also leads to the interruption of JAK/STAT pathway [45–47]. It was also figured out that JAK/STAT signaling of GSC, NSCC and mixed population was modulated under THTMP treatment.

Figure 5B shows that JAK/STAT signaling was highly targeted in NSCC rather than GSC and mixed populations in both cell lines. JAK/STAT was interrupted throughout the dysregulation of *JAK1*, *JAK2*, *STAT1*, *STAT3* and *STAT5A* genes. In addition, the PDGF signaling interruption was also recorded in those populations. In this study, we determined that *PDGFA* gene was upregulated in GSC-LN229, NSCC-LN229 and mixed-LN229 and mixed-SNB19 cells. A fold change of downregulated *PDGFC* gene was also found in GSC-LN229 and NSCC-SNB19 cells. It is observed that even though the PDGF signaling pathway was modulated by THTMP, different gene sets were regulated depending on different characteristics of the cell population and cell line. In addition to altered signaling of growth factors, we also found the interruption of TGF-beta signaling pathway by THTMP. TGF-beta signaling was affected by a wide range of genes such as *CTGF*, *TGFA*, *TGFB2*, *TGFB3*, *TGFB1*, *TGIF1* and *TGIF2* in all the populations. The pattern shows that the NSCC was highly targeted in this signaling, when compared to the GSC and mixed population in both cell lines.

3.7. GSCs and NSCCs Supports Each Other

Transcriptome profiling evidenced that CSC signaling pathways such as Wnt, Notch and Hh was also targeted by THTMP treatment. Figure 5C shows the downregulation of the genes involved in these three signaling pathways. In LN229, both the GSC and NSCC populations were highly modulated than the mixed cells. The similar result was also observed in NSCC-SNB19 while GSC-SNB19 was quite difficult to be targeted than their mixed populations.

The Wnt signaling pathway was targeted mainly by THTMP in all the cell populations except GSC-SNB19, because of the downregulation of bulk crucial genes, *CTNNB1*, *HAS2*, *SOX2*, *STAT3*, *EDN1*, *LGR5*, *CSCR4* and *MMP7*. To be more specific, *CTNNB1* was down regulated which decipher for β -catenin, thus leading to the inhibition of Wnt signaling. Downregulation of genes such as *GLII*, *GLI3*, *MTBP* of Hh pathway and *JAG1*, *NOTCH1*, *NOTCH2* of Notch pathway, suggest that THTMP significantly inhibits these pathways in all the cell populations. Notably, Notch signaling pathway was only targeted in GSC-SNB19. Thus, it is evident from the data, separating GBM cell lines into individual GSC and NSCC population, makes them more easily targeted than their mixed cells. These observations revealed that GSC and NSCC could possibly have a connection that benefits each others proliferation and provides resistance to the drugs.

3.8. Induction of Cell Death in Patient-Derived GBM Cell Lines by THTMP

Low-passage, serum-free cell lines, MMK1, RN1 and JK2 cultured from mesenchymal patient tumour tissue are used for preclinical study especially for the cell death analysis. The cells were treated with THTMP/TMZ at 10 μ M and 100 μ M for 24 h. Microscopic observation of GBM patient-derived cell lines revealed the loss of adherence property and changes in the morphology under THTMP at 100 μ M (Figure 6A) treatment, remains unaffected in the DMSO treated condition. THTMP strongly inhibited the growth of mesenchymal patient-derived GBM cells compared to TMZ (Figure 6B). Absolute 100% cell death at 100 μ M in all of three cell lines was observed upon treatment with THTMP. At 10 μ M, the higher growth inhibition was found in MMK1 and RN1 approximately with 24% and 23%, respectively and with only 8% in PB1. Similar patterns of cell death were also observed in 10 μ M TMZ treated cells, while around 20% of growth inhibition was observed in MMK1 and RN1 at 100 μ M treatment. However, the growth inhibition percentage of TMZ was remarkably lower when compared

with THTMP treatment. These results indicate THTMP as the promising agent of an inhibitor of patient-derived GBM cells.

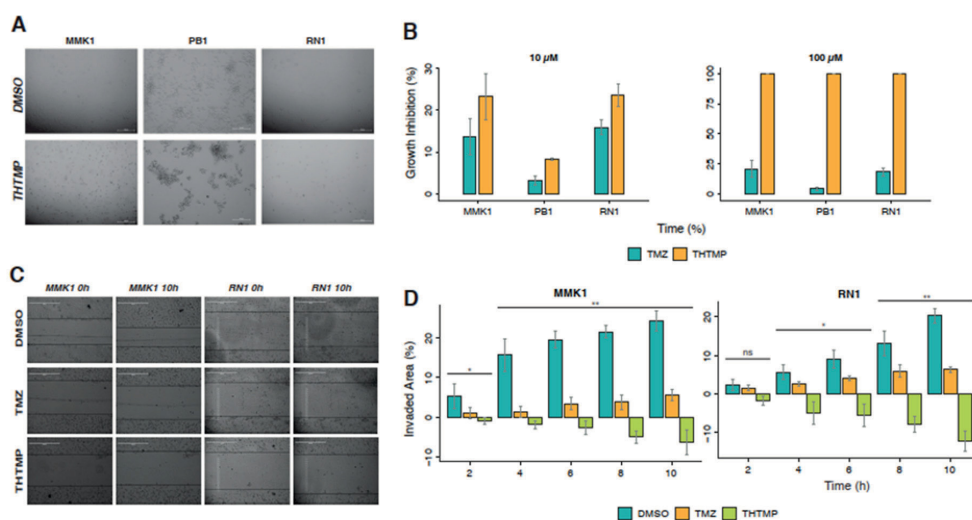


Figure 6. THTMP inhibited cell growth and cell migration of patient-derived mesenchymal subtype of GBM cells. (A) Demonstrated images of morphological changes in patient-derived GBM cells at 24 h after THTMP and DMSO treatment. (B). Growth inhibitory effect of THTMP on different cell lines, MMK1, RN1 and PB1 at 10 and 100 μ M after 24 h post treatment. (C) Example images of scratch assay shows the closing/widening of the scratched area over the time. All images were taken using a light microscope with 10 \times objective. (D) Quantification of the percentage of invading area of MMK1 and RN1 cells for every 2 h over the period of 10 h after the scratch. * $p < 0.05$, ** $p < 0.01$, ns—non significant.

The cell migration and invasion are one of the most important characteristics of malignant tumor cells [48] and indeed, inhibiting cell migration is considered as a potent target for developing new anticancer therapy. Wound healing assay was performed on these three patient-derived mesenchymal cell lines for a period of 10 h upon treatment with THTMP/TMZ. Among these cell lines, PB1 has low adherent ability, and so they are lifted immediately after the scratch and hence the assay was not performed in this particular cell line. The MMK1 and RN1 after THTMP treatment, the invaded areas decreased steadily over time (Figure 6C,D) whilst it increased steadily over time after DMSO and TMZ treatment. After 10 h of post treatment, invaded area of MMK1 cells increased to 20% by DMSO, while only 6% by TMZ and -5% by THTMP. The similar pattern was also observed in RN1. These results confirm that THTMP has the ability to reduce not only the cell proliferation, but also the migration due to enhanced cell death in patient-derived cells, thus further confirming THTMP as a potent drug.

4. Discussion

Tumorigenic cancer stem cells (CSCs) is a fraction of sub population of cells present in all tumor involved in invasion, metastasis and relapse. CSC have self-renewal ability and the capacity to become differentiated cells, thus allowing them to create resistance to current radiation and chemotherapy treatment [6]. In recent years, efforts have been made in elucidation on the molecular mechanisms to suppress the specific CSCs [7–10]. Therefore, many therapeutics have been developed targeting specific signaling pathways in order to inhibit the activation of CSCs [49].

In the present study, we were able to focus on the anticancer property of THTMP against GSC and NSCC population. THTMP inhibits the GSC and NSCC proliferation in a time dependent manner, thereby causing DNA damage, and the cells get arrested at G1/S phase and G2/M phase. Transcriptome

analysis confirms the anti-proliferation activity of THTMP on these populations. *FOXM1*, a major hallmark of cancer was significantly downregulated in GSC and NSCC. *FOXM1* is known as an essential transcription factor that is required for various biological process such as DNA damage repair, cell renewal, cell proliferation and cell cycle progress [50]. Thus, THTMP act as a *FOXM1* inhibitor thereby reducing the CSC proliferation.

Transcriptome analysis revealed that different set of genes associated with apoptosis was enriched in different populations. For example, pro-apoptotic genes like *BCL2L11* and *BBC3* were upregulated in GSC and NSCC of SNB19 while *BCL2A1* and *MAGED1* were found to be upregulated in GSC and NSCC of LN229. The same pattern was also observed in anti-apoptotic genes in these populations. It's been noticed that cluster of genes were highly targeted in NSCC than GSC. Therefore, THTMP could induce cell death by regulating several key genes involved in apoptosis process.

A complete understanding on the biological features of CSCs is essential for the development of a new anticancer therapeutics. Among several mechanisms proposed so far on therapeutic resistance in CSCs, we mainly focused on the cell cycle regulation in CSCs. Two approaches have been proposed to prevent recurrence of the tumor. The first approach is known as induction of the entry of CSCs into cell cycles to increase their sensitivity to anticancer therapy (wake up therapy) whereas the second strategy is to forcefully maintain the CSCs dormancy (hibernation therapy), that prevents the generation of new cells [51]. According to the gene expression profile, *Skp2* gene coding for S-Phase Kinase Associated Protein 2 was not modulated. This protein reduces the frequency of aldehyde dehydrogenase positivity among the cancerous cells which are the indicators of CSC function [52]. This data suggests that THTMP could not promote the dormancy of CSCs, in contrast, we could observe that the CXC chemokine receptor 4 signaling (*CXCR4*) is modulated by THTMP, which confirms its role in the wake-up therapeutic strategy in targeting CSCs [53,54].

The gene expression pattern of several signaling pathways such as EGF, PDGF, JAK/STAT, TGF- β were affected upon THTMP treatment. It is known that PDGF signaling regulates tumor growth and metastasis [55,56]. In GBM, the overexpression of *PDGFA* has a retention motif enhancing its autocrine stimulatory effect, was also found to efficiently promote GBM development [57]. THTMP has the ability to modulate PDGF signaling via downregulation of *PDGFA* in selective population of both the cell lines. The transcription factor signal transducer and activator of transcription STAT3, functions as a double-edged sword that behaves both as an oncogene and as well as onco-suppressor. Earlier research in curcumin, a natural phenol, has inhibited cancer stem cells via downregulation of STAT3 [58,59] which is also observed in the cells that were treated with THTMP.

Despite the consistent association of THTMP in targeting various CSC signaling pathway in both GSC and NSCC population, it has been shown to inhibit Wnt, Notch and Hh pathways. The intricacy mechanism of the Wnt signaling pathway provides various levels of therapeutic intervention and the gene expression analysis provides plethora of approaches being discovered to reduce Wnt/ β -catenin signaling output [11]. Along with *CTNNB1*, other crucial genes of Wnt pathway were also downregulated. Our data presents the ability of THTMP to drive the downregulation of *LGR5* in NSCC-SNB19 that could help the inhibition of precursor CSC. Also, *EDN1* which is secreted by most of the solid tumors for the persistent growth and survival by suppressing apoptosis [60] is also downregulated in NSCC and mixed-SNB19 cell population. Downregulation of a few significant genes creates a cascade of events in modulation and further inhibition of CSC. THTMP modulates MMP7 regulators and consequently inhibits the invasion and metastasis of CSC in GBM cells. It is observed that Wnt has a wide range of effects on different GBM population except, GSC-SNB19 with similar effect in Hh pathway. On the other hand, Notch pathway has been modulated in CSC signaling pathways on GSC-SNB19 through the down-regulation of *JAG1*. Henceforth, limited modulated genes were enriched in the progenitors, LN229 and SNB19 when compared to the GSC and NSCC populations.

Overall data suggest the significant role of THTMP in cell cycle arrest and apoptosis induction via modulating EGFR and CSC signaling pathway. The ability of THTMP in inhibiting the GBM cell proliferation and the TMZ resistant variants, implies THTMP as a clinically potential agent. The

present research reveals that THTMP could also reverse TMZ resistance property in CSC population of GBM cells, by reducing its proliferation and migration. Therefore, THTMP can be considered to develop an adjuvant chemotherapeutic agent for treating GBM.

5. Conclusions

The data concluded the potential implications of THTMP in GBM treatment by inducing DNA damage through ROS-mediated apoptosis in GSC and NSCC population. THTMP sensitizes the TMZ variance and thus inhibits the GBM cell growth and proliferation. THTMP plays crucial role in regulating the genes involved in the major check points in the cell cycle pathways. Additionally, THTMP regulates the tumorigenicity of GBM through the modulation of CSC and EGFR signaling pathway. Thus, our present study unravels the new insights of exploiting THTMP in modulating signaling pathways that targets the cell proliferation and migration. Overall, THTMP based adjuvant chemotherapeutic agent can be developed for the GBM treatment.

Supplementary Materials: The following are available online at <http://www.mdpi.com/2073-4409/9/3/681/s1>, Table S1: The list shows the genes that were differentially expressed in THTMP vs Untreated in GSC-LN229, Table S2: The list shows the genes that were differentially expressed in THTMP vs Untreated in NSCC-LN229, Table S3: The list shows the genes that were differentially expressed in THTMP vs Untreated in GSC-SNB19, Table S4: The list shows the genes that were differentially expressed in THTMP vs Untreated in NSCC-SNB19, Table S5: The list shows the GO biological processes that were differentially modulated in THTMP vs Untreated in GSC-LN229, Table S6: The list shows the GO biological processes that were differentially modulated in THTMP vs Untreated in NSCC-LN229, Table S7: The list shows the GO biological processes that were differentially modulated in THTMP vs Untreated in GSC-SNB19, Table S8: The list shows the GO biological processes that were differentially modulated in THTMP vs Untreated in NSCC-SNB19, Table S9: The list shows the DEGS that were shared in common with GSC, NSCC and mixed population in LN229, Table S10: The list shows the DEGS that were shared in common with GSC, NSCC and mixed population in SNB19, Figure S1: Growth inhibitory effect of THTMP on different cell lines at 10 μ M at 24 h post treatment.

Author Contributions: N.R.C. synthesized and characterized the compounds. P.D. executed the experiments and data analysis. A.M. (Aliyu Musa) analyzed RNA-seq data. V.S. performed single cell images analysis. O.Y.-H. and M.K. conceived and managed all studies. A.M. (Akshaya Murugesan), F.E.-S., P.R., and K.G. involved in project development. All the authors contributed to writing the manuscript. All authors have read and agreed to the published version of the manuscript.

Acknowledgments: P.D., V.S., Aliyu Musa, Akshaya Murugesan, and O.Y.H. acknowledge the Academy of Finland for the project grant support (decision no. 297200) and Tampere University of Technology for Instrumental facility grant support. N.R.C. acknowledges Janne and Aatos Erkkö Foundation and Academy of Finland (Decision 287954) for financial support.

Conflicts of Interest: The authors declare that they have no conflict of interest.

Abbreviations

GBM	Glioblastoma multiforme
CSC	Cancer stem cells
NSCC	Non-stem cancer cells
GSC	GBM stem cells
TMZ	Temozolomide
ROS	Reactive Oxygen Species
RNA-seq	RNA-sequencing
DMEM	Dulbecco's Modified Eagle's Medium
DNA	Deoxyribonucleic acid
FBS	Fetal Bovin Serum
GO	Gene Ontology
DEG	Differentially expressed gene

References

1. Louis, D.N.; Ohgaki, H.; Wiestler, O.D.; Cavenee, W.K.; Burger, P.C.; Jouvet, A.; Scheithauer, B.W.; Kleihues, P. The 2007 WHO classification of tumours of the central nervous system. *Acta Neuropathol.* **2007**, *114*, 97–109. [CrossRef] [PubMed]
2. Hegi, M.E.; Diserens, A.-C.; Gorlia, T.; Hamou, M.-F.; de Tribolet, N.; Weller, M.; Kros, J.M.; Hainfellner, J.A.; Mason, W.; Mariani, L.; et al. MGMT Gene Silencing and Benefit from Temozolomide in Glioblastoma. *N. Engl. J. Med.* **2005**, *352*, 997–1003. [CrossRef] [PubMed]
3. Amarouch, A.; Mazeran, J.J. Radiotherapy plus concomitant and adjuvant Temozolomide for glioblastoma. *Cancer Radiother.* **2005**, *9*, 196–197.
4. Tjendraputra, E.; Tran, V.H.; Liu-Brennan, D.; Roufogalis, B.D.; Duke, C.C. Effect of Ginger Constituents and Synthetic Analogues on Cyclooxygenase-2 Enzyme in Intact Cells. *Bioorg. Chem.* **2001**, *29*, 156–163. [CrossRef] [PubMed]
5. Singh, S.K.; Hawkins, C.; Clarke, I.D.; Squire, J.A.; Bayani, J.; Hide, T.; Henkelman, R.M.; Cusimano, M.D.; Dirks, P.B. Identification of human brain tumour initiating cells. *Nature* **2004**, *432*, 396–401. [CrossRef] [PubMed]
6. Tirino, V.; Desiderio, V.; Paino, F.; De Rosa, A.; Papaccio, F.; La Noce, M.; Laino, L.; De Francesco, F.; Papaccio, G. Cancer stem cells in solid tumors: An overview and new approaches for their isolation and characterization. *FASEB J.* **2013**, *27*, 13–24. [CrossRef]
7. Grosse-Gehling, P.; Fargeas, C.A.; Dittfeld, C.; Garbe, Y.; Alison, M.R.; Corbeil, D.; Kunz-Schughart, L.A. CD133 as a biomarker for putative cancer stem cells in solid tumours: Limitations, problems and challenges. *J. Pathol.* **2013**, *229*, 355–378. [CrossRef]
8. Baumann, M.; Krause, M. CD44: A cancer stem cell-related biomarker with predictive potential for radiotherapy. *Clin. Cancer Res.* **2010**, *16*, 5091–5093. [CrossRef]
9. Ding, X.W.; Wu, J.H.; Jiang, C.P. ABCG2: A potential marker of stem cells and novel target in stem cell and cancer therapy. *Life Sci.* **2010**, *86*, 631–637. [CrossRef]
10. Marcatò, P.; Dean, C.A.; Giacomantonio, C.A.; Lee, P.W. Aldehyde dehydrogenase its role as a cancer stem cell marker comes down to the specific isoform. *Cell Cycle* **2011**, *10*, 1378–1384. [CrossRef]
11. Nusse, R. Wnt signaling in disease and in development. *Cell Res.* **2005**, *15*, 28–32. [CrossRef] [PubMed]
12. Song, L.L.; Miele, L. Role of Notch signaling in cell-fate determination of human mammary stem/progenitor cells. *Women's Oncol. Rev.* **2005**, *5*, 9–11. [CrossRef]
13. Liu, S.; Dontu, G.; Mantle, I.D.; Patel, S.; Ahn, N.S.; Jackson, K.W.; Suri, P.; Wicha, M.S. Hedgehog signaling and Bmi-1 regulate self-renewal of normal and malignant human mammary stem cells. *Cancer Res.* **2006**, *66*, 6063–6071. [CrossRef] [PubMed]
14. Sharifzad, F.; Ghavami, S.; Mardpour, S.; Mollapour, M.; Azizi, Z.; Taghikhani, A.; Łos, M.J.; Verdi, J.; Fakharian, E.; Ebrahimi, M.; et al. Glioblastoma cancer stem cell biology: Potential theranostic targets. *Drug Resist. Updat.* **2019**, *42*, 35–45. [CrossRef] [PubMed]
15. Huang, P.H.; Xu, A.M.; White, F.M. Oncogenic EGFR signaling networks in glioma. *Sci. Signal.* **2009**, *2*, re6. [CrossRef] [PubMed]
16. Ekstrand, A.J.; Sugawa, N.; James, C.D.; Collins, V.P. Amplified and rearranged epidermal growth factor receptor genes in human glioblastomas reveal deletions of sequences encoding portions of the N- and/or C-terminal tails. *Proc. Natl. Acad. Sci. USA* **2006**, *89*, 4309–4313. [CrossRef]
17. Ohgaki, H.; Dessen, P.; Jourde, B.; Horstmann, S.; Nishikawa, T.; Di Patre, P.L.; Burkhard, C.; Schüller, D.; Probst-Hensch, N.M.; Maiorka, P.C.; et al. Genetic pathways to glioblastoma: A population-based study. *Cancer Res.* **2004**, *64*, 6892–6899. [CrossRef]
18. Eskilsson, E.; Røslund, G.V.; Solecki, G.; Wang, Q.; Harter, P.N.; Graziani, G.; Verhaak, R.G.W.; Winkler, F.; Bjerkvig, R.; Miletic, H. EGFR heterogeneity and implications for therapeutic intervention in glioblastoma. *Neuro. Oncol.* **2018**, *20*, 743–752. [CrossRef]
19. Roos, A.; Dhruv, H.D.; Peng, S.; Inge, L.J.; Tuncali, S.; Pineda, M.; Millard, N.; Mayo, Z.; Eschbacher, J.M.; Loftus, J.C.; et al. EGFRvIII–Stat5 signaling enhances glioblastoma cell migration and survival. *Mol. Cancer Res.* **2018**, *16*, 1185–1195. [CrossRef]

20. Von Pawel, J.; Schiller, J.H.; Shepherd, F.A.; Fields, S.Z.; Kleisbauer, J.P.; Chrysson, N.G.; Stewart, D.J.; Clark, P.I.; Palmer, M.C.; Depierre, A.; et al. Topotecan versus cyclophosphamide, doxorubicin, and vincristine for the treatment of recurrent small-cell lung cancer. *J. Clin. Oncol.* **1999**, *17*, 658–667. [CrossRef]
21. Miller, K.; Wang, M.; Gralow, J.; Dickler, M.; Cobleigh, M.; Perez, E.A.; Shenkier, T.; Cella, D.; Davidson, N.E. Paclitaxel plus Bevacizumab versus Paclitaxel Alone for Metastatic Breast Cancer. *N. Engl. J. Med.* **2007**, *357*, 2666–2676. [CrossRef] [PubMed]
22. Alvandi, F.; Kwitkowski, V.E.; Ko, C.-W.; Rothmann, M.D.; Ricci, S.; Saber, H.; Ghosh, D.; Brown, J.; Pfeiler, E.; Chikhale, E.; et al. U.S. Food and Drug Administration Approval Summary: Omacetaxine Mepesuccinate as Treatment for Chronic Myeloid Leukemia. *Oncologist* **2013**, *19*, 94–99. [CrossRef] [PubMed]
23. Creemers, G.J.; Bolis, G.; Gore, M.E.; Scarfone, G.; Lacave, A.J.; Guastalla, J.P.; Despax, R.; Favalli, G.; Kreinberg, R.; Van Belle, S.; et al. Topotecan, an active drug in the second-line treatment of epithelial ovarian cancer: Results of a large European phase II study. *J. Clin. Oncol.* **1996**, *14*, 3056–3061. [CrossRef] [PubMed]
24. Salentin, S.; Adasme, M.F.; Heinrich, J.C.; Haupt, V.J.; Daminelli, S.; Zhang, Y.; Schroeder, M. From malaria to cancer: Computational drug repositioning of amodiaquine using PLIP interaction patterns. *Sci. Rep.* **2017**, *7*, 11401. [CrossRef]
25. Doan, P.; Karjalainen, A.; Chandraseelan, J.; Sandberg, O.; Yli-Harja, O.; Rosholm, T.; Franzen, R.; Candeias, N.R.; Kandhavelu, M. Synthesis and Biological Screening for Cytotoxic Activity of N- substituted Indolines and Morpholines. *Eur. J. Med. Chem.* **2016**, *120*, 296–303. [CrossRef]
26. Karjalainen, A.; Doan, P.; Sandberg, O.; Chandraseelan, J.; Yli-Harja, O.; Candeias, N.; Kandhavelu, M. Synthesis of phenol-derivatives and biological screening for anticancer activity. *Anticancer. Agents Med. Chem.* **2017**, *17*, 1. [CrossRef]
27. Doan, P.; Nguyen, T.; Yli-Harja, O.; Kandhavelu, M.; Yli-Harja, O.; Doan, P.; Nguyen, T.; Yli-Harja, O.; Candeias, N.R. Effect of alkylaminophenols on growth inhibition and apoptosis of bone cancer cells. *Eur. J. Pharm. Sci.* **2017**, *107*, 208–216. [CrossRef]
28. Doan, P.; Musa, A.; Candeias, N.R.; Emmert-Streib, F.; Yli-Harja, O.P.; Kandhavelu, M. Alkylaminophenol induces G1/S phase cell cycle arrest in glioblastoma cells through p53 and cyclin-dependent kinase signaling pathway. *Front. Pharmacol.* **2019**, *10*, 330. [CrossRef]
29. Neto, Í.; Andrade, J.; Fernandes, A.S.; Pinto Reis, C.; Salunke, J.K.; Priimagi, A.; Candeias, N.R.; Rijo, P. Multicomponent Petasis-borono Mannich Preparation of Alkylaminophenols and Antimicrobial Activity Studies. *ChemMedChem.* **2016**, *11*, 2015–2023. [CrossRef]
30. Xia, X.; Owen, M.S.; Lee, R.E.C.; Gaudet, S. Cell-to-cell variability in cell death: Can systems biology help us make sense of it all? *Cell Death Dis.* **2014**, *5*, e1261. [CrossRef]
31. Fallahi-Sichani, M.; Honarnejad, S.; Heiser, L.M.; Gray, J.W.; Sorger, P.K. Metrics other than potency reveal systematic variation in responses to cancer drugs. *Nat. Chem. Biol.* **2013**, *9*, 708–714. [CrossRef] [PubMed]
32. Szakács, G.; Paterson, J.K.; Ludwig, J.A.; Booth-Genthe, C.; Gottesman, M.M. Targeting multidrug resistance in cancer. *Nat. Rev. Drug Discov.* **2006**, *5*, 219–234. [CrossRef] [PubMed]
33. Uribe, D.; Torres, Á.; Rocha, J.D.; Niechi, I.; Oyarzún, C.; Sobrevia, L.; San Martín, R.; Quezada, C. Multidrug resistance in glioblastoma stem-like cells: Role of the hypoxic microenvironment and adenosine signaling. *Mol. Asp. Med.* **2017**, *55*, 140–151. [CrossRef] [PubMed]
34. McQuin, C.; Goodman, A.; Chernyshev, V.; Kamentsky, L.; Cimini, B.A.; Karhohs, K.W.; Doan, M.; Ding, L.; Rafelski, S.M.; Thirstrup, D.; et al. CellProfiler 3.0: Next-generation image processing for biology. *PLoS Biol.* **2018**, *16*, e2005970. [CrossRef] [PubMed]
35. Chowdhury, S.; Kandhavelu, M.; Yli-Harja, O.; Ribeiro, A.S. An interacting multiple model filter-based autofocus strategy for confocal time-lapse microscopy. *J. Microsc.* **2012**, *245*, 265–275. [CrossRef] [PubMed]
36. Day, B.W.; Stringer, B.W.; Al-Ejeh, F.; Ting, M.J.; Wilson, J.; Ensbey, K.S.; Jamieson, P.R.; Bruce, Z.C.; Lim, Y.C.; Offenhäuser, C.; et al. EphA3 Maintains Tumorigenicity and Is a Therapeutic Target in Glioblastoma Multiforme. *Cancer Cell* **2013**, *23*, 238–248. [CrossRef]
37. Pollard, S.M.; Yoshikawa, K.; Clarke, I.D.; Danovi, D.; Stricker, S.; Russell, R.; Bayani, J.; Head, R.; Lee, M.; Bernstein, M.; et al. Glioma Stem Cell Lines Expanded in Adherent Culture Have Tumor-Specific Phenotypes and Are Suitable for Chemical and Genetic Screens. *Cell Stem Cell* **2009**, *4*, 568–580. [CrossRef]

38. Gartel, A.L. FOXM1 in cancer: Interactions and vulnerabilities. *Cancer Res.* **2017**, *77*, 3135–3139. [CrossRef]
39. Satoh, T.; Ishige, K.; Sagara, Y. Protective effects on neuronal cells of mouse afforded by ebselen against oxidative stress at multiple steps. *Neurosci. Lett.* **2004**, *371*, 1–5. [CrossRef]
40. Kuznetsov, A.V.; Smigelskaite, J.; Doblender, C.; Janakiraman, M.; Hermann, M.; Wurm, M.; Scheidl, S.F.; Sucher, R.; Deutschmann, A.; Troppmair, J. Survival Signaling by C-RAF: Mitochondrial Reactive Oxygen Species and Ca²⁺ Are Critical Targets. *Mol. Cell. Biol.* **2008**, *28*, 2304–2313. [CrossRef]
41. Moloney, J.N.; Cotter, T.G. ROS signaling in the biology of cancer. *Semin. Cell Dev. Biol.* **2018**, *80*, 50–64. [CrossRef] [PubMed]
42. Srinivas, U.S.; Tan, B.W.Q.; Vellayappan, B.A.; Jeyasekharan, A.D. ROS and the DNA damage response in cancer. *Redox Biol.* **2019**, *25*, 101084. [CrossRef] [PubMed]
43. Leone, A.; Roca, M.S.; Ciardiello, C.; Costantini, S.; Budillon, A. Oxidative Stress Gene Expression Profile Correlates with Cancer Patient Poor Prognosis: Identification of Crucial Pathways Might Select Novel Therapeutic Approaches. *Oxid. Med. Cell. Longev.* **2017**, *2017*, 2597581. [CrossRef] [PubMed]
44. Su, B.C.; Chen, J.Y. Pharmacological inhibition of p38 potentiates antimicrobial peptide TP4-induced cell death in glioblastoma cells. *Mol. Cell. Biochem.* **2020**, *464*, 1–9. [CrossRef] [PubMed]
45. Leaman, D.W.; Pisharody, S.; Flickinger, T.W.; Commane, M.A.; Schlessinger, J.; Kerr, I.M.; Levy, D.E.; Stark, G.R. Roles of JAKs in activation of STATs and stimulation of c-fos gene expression by epidermal growth factor. *Mol. Cell. Biol.* **1996**, *16*, 369–375. [CrossRef] [PubMed]
46. Song, X.; Liu, Z.; Yu, Z. EGFR Promotes the Development of Triple Negative Breast Cancer Through JAK/STAT3 Signaling. *Cancer Manag. Res.* **2020**, *12*, 703. [CrossRef]
47. Zulkifli, A.A.; Tan, F.H.; Putoczki, T.L.; Stylli, S.S.; Luwor, R.B. STAT3 signaling mediates tumour resistance to EGFR targeted therapeutics. *Mol. Cell. Endocrinol.* **2017**, *451*, 15–23. [CrossRef]
48. Eccles, S.A.; Box, C.; Court, W. Cell migration/invasion assays and their application in cancer drug discovery. *Biotechnol. Annu. Rev.* **2005**, *11*, 391–421.
49. Hu, Y.; Fu, L. Targeting cancer stem cells: A new therapy to cure cancer patients. *Am. J. Cancer Res.* **2012**, *2*, 340–356.
50. Zona, S.; Bella, L.; Burton, M.J.; Nestal de Moraes, G.; Lam, E.W.F. FOXM1: An emerging master regulator of DNA damage response and genotoxic agent resistance. *Biochim. Biophys. Acta* **2014**, *1839*, 1316–1322. [CrossRef]
51. Takeishi, S.; Nakayama, K.I. To wake up cancer stem cells, or to let them sleep, that is the question. *Cancer Sci.* **2016**, *107*, 875–881. [CrossRef] [PubMed]
52. Ma, I.; Allan, A.L. The Role of Human Aldehyde Dehydrogenase in Normal and Cancer Stem Cells. *Stem Cell Rev. Rep.* **2011**, *7*, 292–306. [CrossRef] [PubMed]
53. Rasti, A.; Abolhasani, M.; Zanjani, L.S.; Asgari, M.; Mehrazma, M.; Madjd, Z. Reduced expression of CXCR4, a novel renal cancer stem cell marker, is associated with high-grade renal cell carcinoma. *J. Cancer Res. Clin. Oncol.* **2017**, *143*, 95–104. [CrossRef] [PubMed]
54. Gravina, G.L.; Mancini, A.; Colapietro, A.; Vitale, F.; Vetuschi, A.; Pompili, S.; Rossi, G.; Marampon, F.; Richardson, P.J.; Patient, L.; et al. The novel CXCR4 antagonist, PRX177561, reduces tumor cell proliferation and accelerates cancer stem cell differentiation in glioblastoma preclinical models. *Tumour Biol.* **2017**, *39*, 1010428317695528. [CrossRef] [PubMed]
55. Cao, R.; Björndahl, M.A.; Religa, P.; Clasper, S.; Garvin, S.; Galter, D.; Meister, B.; Ikomi, F.; Tritsaris, K.; Dissing, S.; et al. PDGF-BB induces intratumoral lymphangiogenesis and promotes lymphatic metastasis. *Cancer Cell* **2004**, *6*, 333–345. [CrossRef] [PubMed]
56. Heldin, C.H. Targeting the PDGF signaling pathway in tumor treatment. *Cell Commun. Signal.* **2013**, *11*, 97. [CrossRef]
57. Nazarenko, I.; Hedrén, A.; Sjödin, H.; Orrego, A.; Andrae, J.; Afink, G.B.; Nistér, M.; Lindström, M.S. Brain abnormalities and glioma-like lesions in mice overexpressing the long isoform of PDGF- α in astrocytic cells. *PLoS ONE* **2011**, *6*, e18303. [CrossRef]
58. Chung, S.S.; Vadgama, J.V. Curcumin and epigallocatechin gallate inhibit the cancer stem cell phenotype via down-regulation of STAT3-NF κ B signaling. *Anticancer Res.* **2015**, *35*, 39–46.

59. Khan, A.Q.; Ahmed, E.I.; Elareer, N.; Fathima, H.; Prabhu, K.S.; Siveen, K.S.; Kulinski, M.; Azizi, F.; Dermime, S.; Ahmad, A. Curcumin-Mediated Apoptotic Cell Death in Papillary Thyroid Cancer and Cancer Stem-Like Cells through Targeting of the JAK/STAT3 Signaling Pathway. *Int. J. Mol. Sci.* **2020**, *21*, 438. [CrossRef]
60. Lu, J.W.; Liao, C.Y.; Yang, W.Y.; Lin, Y.M.; Jin, S.L.C.; Wang, H.D.; Yuh, C.H. Overexpression of endothelin 1 triggers hepatocarcinogenesis in zebrafish and promotes cell proliferation and migration through the AKT pathway. *PLoS ONE* **2014**, *9*, e85318. [CrossRef]



© 2020 by the authors. Licensee MDPI, Basel, Switzerland. This article is an open access article distributed under the terms and conditions of the Creative Commons Attribution (CC BY) license (<http://creativecommons.org/licenses/by/4.0/>).

III

Article

Targeting Orphan G Protein-Coupled Receptor 17 with T0 Ligand Impairs Glioblastoma Growth

Phuong Doan ^{1,2,†}, Phung Nguyen ^{1,2,†}, Akshaya Murugesan ^{1,2,3}, Kumar Subramanian ^{1,2}, Saravanan Konda Mani ⁴, Vignesh Kalimuthu ⁵, Bobin George Abraham ⁶, Brett W. Stringer ⁷, Kadalmani Balamuthu ⁵, Olli Yli-Harja ^{8,9} and Meenakshisundaram Kandhavelu ^{1,2,9,*}

- ¹ Molecular Signaling Lab, Faculty of Medicine and Health Technology, Tampere University, P.O. Box 553, 33101 Tampere, Finland; phuong.doan@tuni.fi (P.D.); phunghatien.nguyen@tuni.fi (P.N.); akshaya.murugesan@tuni.fi (A.M.); kumar.subramanian@tuni.fi (K.S.)
- ² BioMediTech Institute and Faculty of Medicine and Health Technology, Tampere University, Arvo Ylpön Katu 34, 33520 Tampere, Finland
- ³ Department of Biotechnology, Lady Doak College, Thallakulam, Madurai 625002, India
- ⁴ Bharath Institute of Higher Education and Research, Chennai 600073, India; saravananbioinform@gmail.com
- ⁵ Department of Animal Science, Bharathidasan University, Tiruchirappalli 620024, India; ksvignesh738@gmail.com (V.K.); kadalmani@bdu.ac.in (K.B.)
- ⁶ Faculty of Medicine and Health Technology, Tampere University, P.O. Box 553, 33101 Tampere, Finland; bobin.george.abraham@tuni.fi
- ⁷ College of Medicine and Public Health, Flinders University, Sturt Rd., Bedford Park, SA 5042, Australia; Brett.W.Stringer@gmail.com
- ⁸ Computational Systems Biology Group, Faculty of Medicine and Health Technology, Tampere University, P.O. Box 553, 33101 Tampere, Finland; olli.yli-harja@tuni.fi
- ⁹ Institute for Systems Biology, 401 Terry Ave N, Seattle, WA 98109, USA
- * Correspondence: meenakshisundaram.kandhavelu@tuni.fi; Tel.: +358-504721724
- † Equal Contribution.



Citation: Doan, P.; Nguyen, P.; Murugesan, A.; Subramanian, K.; Konda Mani, S.; Kalimuthu, V.; Abraham, B.G.; Stringer, B.W.; Balamuthu, K.; Yli-Harja, O.; et al. Targeting Orphan G Protein-Coupled Receptor 17 with T0 Ligand Impairs Glioblastoma Growth. *Cancers* **2021**, *13*, 3773. <https://doi.org/10.3390/cancers13153773>

Academic Editor: Zhixiang Wang

Received: 23 June 2021

Accepted: 22 July 2021

Published: 27 July 2021

Publisher's Note: MDPI stays neutral with regard to jurisdictional claims in published maps and institutional affiliations.



Copyright: © 2021 by the authors. Licensee MDPI, Basel, Switzerland. This article is an open access article distributed under the terms and conditions of the Creative Commons Attribution (CC BY) license (<https://creativecommons.org/licenses/by/4.0/>).

Simple Summary: Glioblastoma multiforme (GBM), or glioblastoma chemotherapy, has one of the poorest improvements across all types of cancers. Despite the different rationales explored in targeted therapy for taming the GBM aggressiveness, its phenotypic plasticity, drug toxicity, and adaptive resistance mechanisms pose many challenges in finding an effective cure. Our manuscript reports the expression and prognostic role of orphan receptor GPR17 in glioma, the molecular mechanism of action of the novel ligand of GPR17, and provides evidence how the T0 agonist promotes glioblastoma cell death through modulation of the MAPK/ERK, PI3K-Akt, STAT, and NF- κ B pathways. The highlights are as follows: GPR17 expression is associated with greater survival for both low-grade glioma (LGG) and GBM; GA-T0, a potent GPR17 receptor agonist, causes significant GBM cell death and apoptosis; GPR17 signaling promotes cell cycle arrest at the G1 phase in GBM cells; key genes are modulated in the signaling pathways that inhibit GBM cell proliferation; and GA-T0 crosses the blood–brain barrier and reduces tumor volume.

Abstract: Glioblastoma, an invasive high-grade brain cancer, exhibits numerous treatment challenges. Amongst the current therapies, targeting functional receptors and active signaling pathways were found to be a potential approach for treating GBM. We exploited the role of endogenous expression of GPR17, a G protein-coupled receptor (GPCR), with agonist GA-T0 in the survival and treatment of GBM. RNA sequencing was performed to understand the association of GPR17 expression with LGG and GBM. RT-PCR and immunoblotting were performed to confirm the endogenous expression of GPR17 mRNA and its encoded protein. Biological functions of GPR17 in the GBM cells was assessed by in vitro analysis. HPLC and histopathology in wild mice and an acute-toxicity analysis in a patient-derived xenograft model were performed to understand the clinical implication of GA-T0 targeting GPR17. We observed the upregulation of GPR17 in association with improved survival of LGG and GBM, confirming it as a predictive biomarker. GA-T0-stimulated GPR17 leads to the inhibition of cyclic AMP and calcium flux. GPR17 signaling activation enhances cytotoxicity against GBM cells and, in patient tissue-derived mesenchymal subtype GBM cells, induces apoptosis and prevents

proliferation by stoppage of the cell cycle at the G1 phase. Modulation of the key genes involved in DNA damage, cell cycle arrest, and in several signaling pathways, including MAPK/ERK, PI3K-Akt, STAT, and NF- κ B, prevents tumor regression. In vivo activation of GPR17 by GA-T0 reduces the tumor volume, uncovering the potential of GA-T0-GPR17 as a targeted therapy for GBM treatment. Conclusion: Our analysis suggests that GA-T0 targeting the GPR17 receptor presents a novel therapy for treating glioblastoma.

Keywords: glioblastoma; GPR17-targeted drug; mode of action; cell death; toxicity; blood-brain barrier; in vivo

1. Introduction

Glioblastoma (GBM) is an aggressive neoplastic tumor, clinically featured by infiltrative high-grade glioma cells into the brain parenchyma with poor response to treatment [1]. Patients have a median survival time of less than 1.5 years, despite surgery, radiation, and chemotherapy [2]. The dynamic microenvironment of GBM is primarily due to the propensity of neoplastic cells to migrate from the primary tumor mass into nearby tissues [3]. GBM is enriched with unique phenotypic properties, including self-renewal [4,5], hypoxic adaptations [6], genetic lesions [7], and resistance to radiation and chemotherapeutic agents [8]. In addition, gene expression analysis of patient tumor tissue has identified phenotypically distinct molecular subtypes of GBM [9–11], based on the chaotic oscillation of tumor cells [12]. Although multiple subtypes can co-exist in the affected individual, transcriptional dominance defines the incidence of the specific tumor type [13]. The complex cellular and molecular heterogeneity in GBM exists both between patients and within the individual's tumor. All these features, along with the genetic, transcriptional, and functional variation inherent to GBM, contribute to treatment failure, and effective therapeutic strategies remain obscure [14,15]. Therefore, designing new approaches to identify promising drugs or targets for GBM treatment is pivotal, especially targeting the signaling receptors envisaged to subvert cellular communication [16] for disease progression and recurrence.

G protein-coupled receptors (GPCRs), a large superfamily of signaling receptor molecules, have been considered an interesting pharmacological target for numerous pathological conditions [17]. They function explicitly by their accessible “druggable receptor” sites at the cell surface [18]. The iterative structure–function relationship revealed through advanced X-ray crystallographic methods has lifted the structural veil of the receptor, signifying a new era of GPCR-based drug discovery. GPCR-targeted drugs are rapidly emerging for cancer treatment and at least 23 GPCR-targeted agents are in clinical trials, representing its therapeutic interest [19].

An orphan GPCR receptor, GPR17, is an enigmatic receptor that respond to both endogenous purinergic and cysteinyl-leukotriene (CysLT) [20,21] and to synthetic ligands, such as pranlukast and MDL29951, which (ant)agonize, respectively [20,22,23]. GPR17 is a sensor of demyelinated tissues caused by inflammatory responses and crucially promotes the differentiation of the precursor oligodendrocyte into mature cells at the site of plaques or lesions [24,25]. GPR17 clustering is associated with the overexpression of transcription factors such as Olig1 and Olig2 in pediatric diffuse midline glioma (pDMG), with the aborted differentiation of the oligodendrocytic lineage of the cells [26]. A similar hypothesis reflects the role of GPR17 as a candidate agonist gene in decreasing the number of neurospheres in primary murine GBM cells [27]. The limited insight [28,29] into GPR17 signaling in GBM and its tumor microenvironment prompted us to investigate the mechanism of GPR17 signaling activation, the downstream effects, its role in cell death and therapeutic applications in GBM treatment.

2. Results

2.1. GPR17 as a Biomarker for LGG and GBM

We investigated GPR17 expression from publicly available RNAseq gene expression cancer datasets using the GEPIA portal. There is conspicuous expression of GPR17 mRNA in LGG and in GBM, although in the latter cases the expression was less than the level detected in matched normal tissue (Figure 1A and Supplementary Figure S1). Consistent with the known expression of GPR17 in oligodendrocyte precursor cells, elevated GPR17 expression in LGG was highest in the histological subtypes with an immature oligodendroglial component (Figure 1B). Likewise, expression of GPR17 was greatest in the proneural subtype GBM (Figure 1B), which is believed to arise from oligodendroglial precursor cells or have an oligodendroglial phenotype. A univariate analysis of the association between GPR17 expression and overall survival in LGG and GBM demonstrated GPR17 expression to be a strong predictive biomarker of improved survival in both the TCGA and CGGA datasets ($p = 6 \times 10^{-4}$ and 0, respectively) (Figure 1C). GPR17 expression was also associated with improved survival in GBM alone ($p = 0.0478$) in the CGGA dataset, although not in the TCGA dataset. Thus, these RNAseq data revealed an association of GPR17 expression with both LGG and GBM and showed GPR17 to be a strong positive predictive biomarker in LGG and possibly also in GBM.

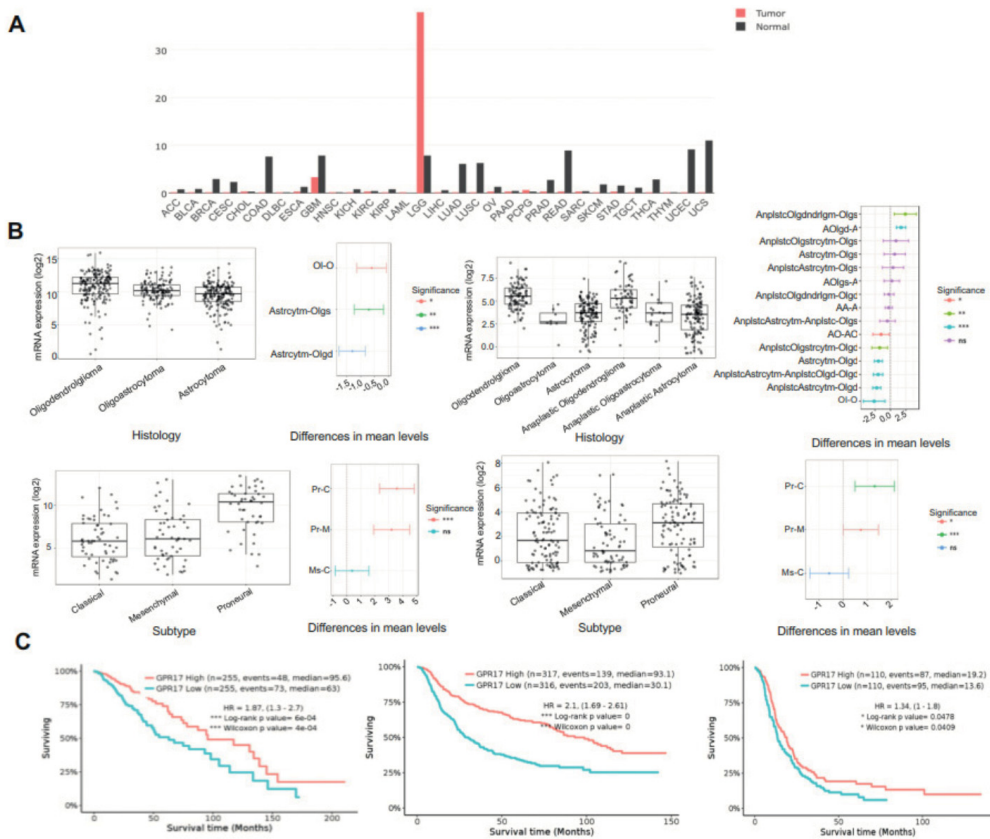


Figure 1. GPR17 as a biomarker in histological subtypes of glioma. **(A)** GPR17 expression profile across all tumor samples and paired normal tissues. **(B)** GPR17 expression in histological subtypes of glioma. **(C)** Overall survival associated with GPR17 expression in the TCGA LGG dataset, CGGA primary glioma dataset, and CGGA primary GBM dataset; survival time is represented in months.

2.2. GA-T0 Activates GPR17 Signaling in GBM Cell Lines

To investigate GPR17 signaling in GBM using a potent ligand, protein–protein-agonist blind docking experiments were performed. Consistent with our previous work on GA-T0 as a novel agonist of GPR17 [30], GPR17–G α I was complexed with GA-T0 (Figure 2A). A two-dimensional protein–ligand interaction plot was generated, which revealed that GA-T0 formed 33 interactions with the amino acid residues of the GPR17 receptor, better than the previously known agonist, MDL 29,951, which exhibits 22 interactions. GA-T0 also exhibited a better binding energy (–18.5 Kcal/mol) than MDL 29,951 (–13.4 Kcal/mol), and 30.76 Å, 59.81 Å, and 8.31 Å are the binding site coordinates (Figure 2B, Supplementary Figure S2). We next investigated GA-T0-mediated GPR17 signaling activation in the GBM cell lines LN229 and SNB19. Endogenous expression of GPR17 mRNA and protein in both cell lines was confirmed by real-time PCR and immunoblotting using GPR17-specific primers and antibodies (Figure 2C,D, Supplementary Figure S4). We further addressed the downstream signaling activation of GPR17 by the GA-T0 agonist in GBM cells by quantifying the level of the secondary messenger cAMP. The GA-T0–GPR17–G α I interaction regulates the decrease in forskolin-stimulated intracellular cAMP by reducing the adenylyl cyclase activity (Figure 2E), with an EC₅₀ of 76.64 μ M and 42.05 μ M for SNB19 and LN229, respectively. Simultaneously, GA-T0 shows inverse agonism for the calcium level in GBM cells, suggesting G α q-independent signaling activation of GPR17 in a dose- (Figure 2F) and time-dependent manner, with an EC₅₀ of 19.64 μ M and 47.33 μ M for SNB19 and LN229, respectively (Figure 2G).

2.3. GPR17 as a Target for Inhibiting GBM Cell Proliferation

To investigate the signaling effect of GPR17 on the proliferation of GBM cells, the percentage of cell growth inhibition was evaluated. At 10 μ M, GA-T0 caused significantly greater inhibition of proliferation of LN229 and SNB19 cells than did MDL 29,951 and TMZ. At 100 μ M, the effect of GA-T0 on GBM cell proliferation was greater still, and again significantly greater than MDL 29,951, although not as great as TMZ against LN229 cells. Interestingly, MDL 29,951 has a negligible cytotoxic effect (1% to 2%) on both GBM cell lines (Figure 3A,B). In contrast to its effect on GBM cells, GA-T0 had a much smaller effect on the proliferation of normal cells (mouse embryonic fibroblasts). Even at a 100 μ M concentration, GA-T0 inhibited the proliferation of MEFs < 15% (Figure 3C). Thus, GA-T0 was found to be a unique agonist inducing GPR17-mediated inhibition of GBM cell proliferation.

Treatment with GA-T0 also strongly reduced GBM cell proliferation in a time-dependent as well as dose-dependent manner, reaching 100% for LN229 cells at 48 h and 60% for SNB19 cells. The IC₅₀ concentrations for LN229 (Figure 3D) were observed to be 86 μ M, 44 μ M, and 43 μ M, and for SNB19 were 98 μ M, 95 μ M, and 95 μ M (Figure 3E) at 24, 48, and 72 h of GA-T0 treatment, respectively, suggesting the cytotoxicity increased over time.

DNA damage can impinge on the proliferation of tumor cells and thus hampers the progression of the disease. To directly assess the genes involved in DNA damage by GA-T0 on GBM cells, we performed total RNA expression analysis of GA-T0-treated LN229 and SNB19 cells. We found upregulation of *DDIT3* [31], *DDIT4* [32,33], and *SQSTM1* [34] in both GBM cell lines, confirming its promising role in DNA damage (Figure 3F).

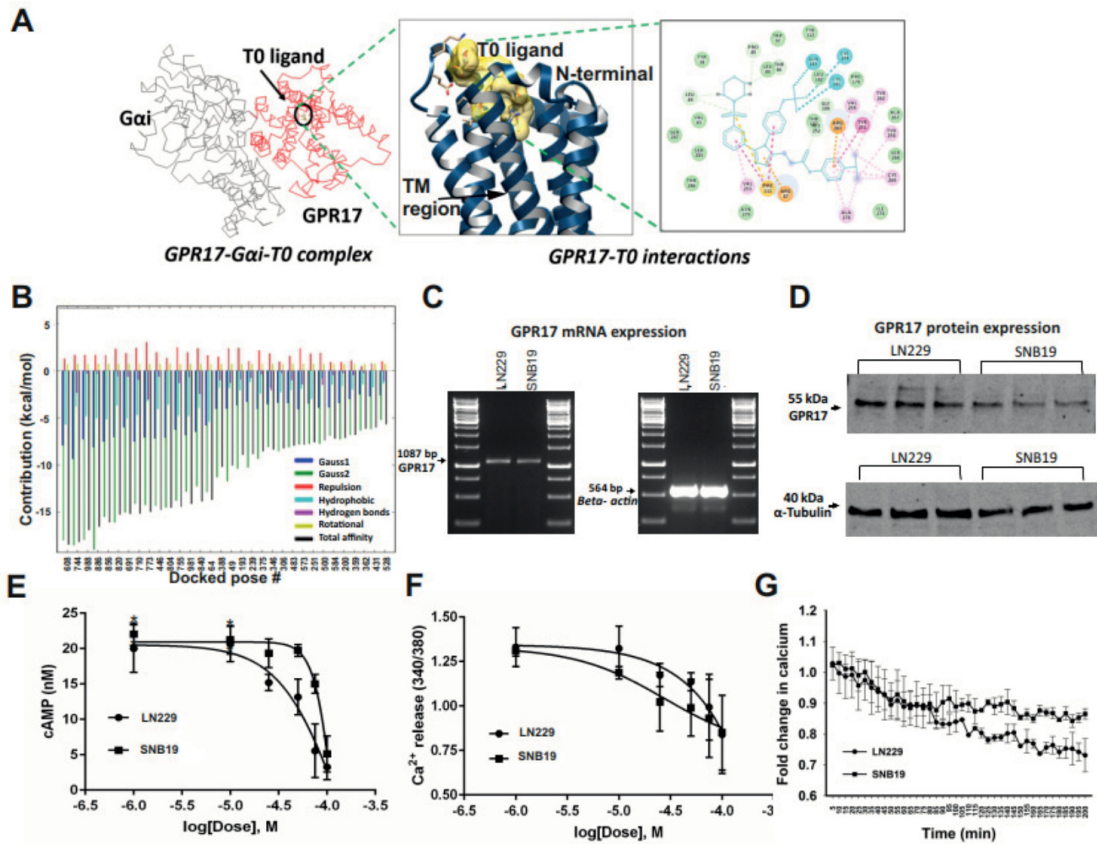


Figure 2. GA-T0 as a potential GPR17 agonist in GBM cells. (A) GPR17–GαI complex obtained from the protein–protein docking where GPR17 is colored red, GαI is grey, and the GA-T0 complex in the black circle. The portion of GPR17–GA-T0 is magnified in the 2-dimensional and 3-dimensional interaction figure. (B) Docked structure of the GPR17–GαI–GA-T0 complex ranked according to binding energy from different interactions, including hydrogen bonds, hydrophobic interaction, ion pair interaction, aromatic interaction, and cation pi interaction. (C) RT-PCR analysis of the GPR17 receptor expression in LN229 and SNB19 cells, using β-actin as a constitutive control. (D) Immunoblot analysis of GPR17 suppressing cell proliferation in LN229 and SNB19 cells with α-tubulin as the loading control. (E) cAMP level (nM) and (F) ratiometric (340/380 nm) analysis of Ca²⁺ release in the SNB19 and LN229 cell lines on treatment with GA-T0. (G) Fold change in the Ca²⁺ level over the time (min) in GBM cells. Data are representative of at least three independent experiments (*n* = 6) using t-test analysis. (E–G) The results are presented as the mean values ± SEM of six experiments. Significant data are denoted by asterisks (*, *p* < 0.05).

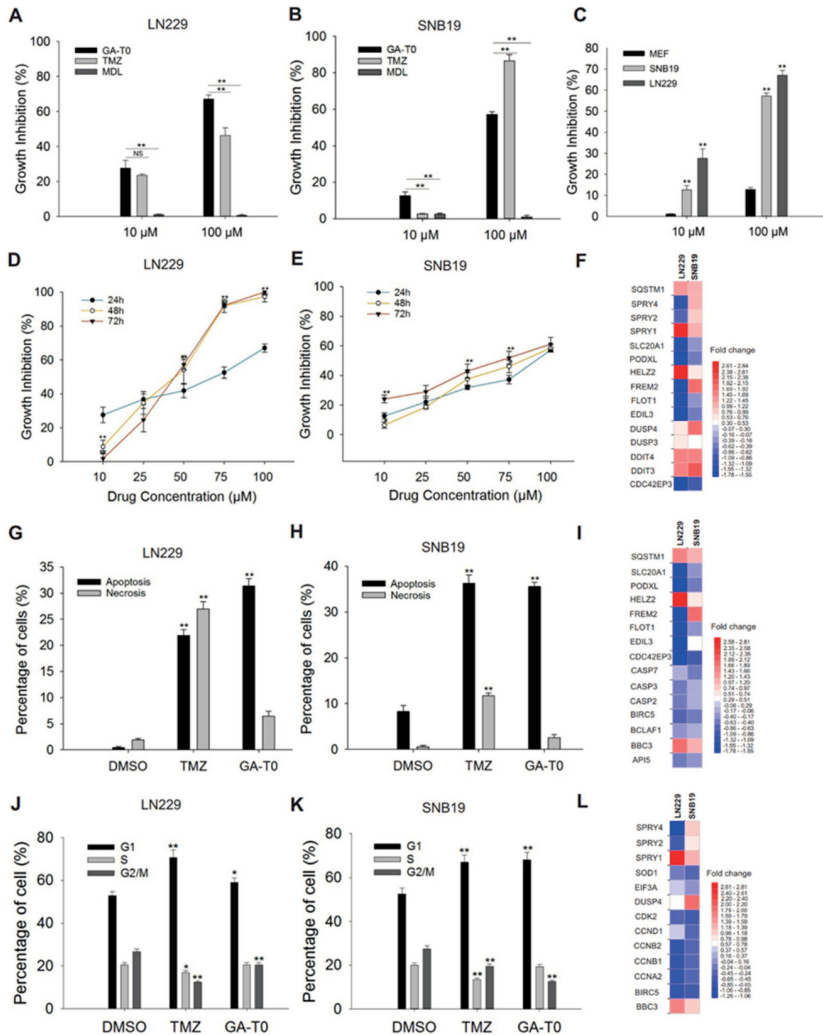


Figure 3. Effect of GA-T0 on glioblastoma cell growth, apoptosis, and the cell cycle. Percentage of cell growth inhibition at 10 μ M and 100 μ M concentrations of GA-T0, MDL 29,951, and TMZ in (A) LN229, (B) SNB19, and (C) non-tumor cells (MEF). Dose- and time-dependent effect of GA-T0 on (D) LN229 and (E) SNB19 at 10, 25, 50, 75, and 100 μ M for 24 h, 48 h, and 72 h, respectively. Top DEGs associated with (F) DNA damage. Percentage of apoptosis and necrosis in (G) LN229 and (H) SNB19 on treatment with DMSO, TMZ, and GA-T0 and (I) DEGs involved in apoptosis. Percentage of cells in different stages of the cell cycle (G1, S, and G2/M phase) in (J) LN229 and (K) SNB19 on treatment with DMSO, TMZ, and GA-T0 and (L) DEGs associated with cell cycle arrest. Data are the mean \pm SD of six experiments using t-test analysis. Non-significant data are denoted by NS and significant data by asterisks (*, $p < 0.05$ and **, $p < 0.01$).

2.4. Apoptosis-Mediated Cell Death Induced by GA-T0

The effect of apoptosis on GBM cells was identified by detecting the externalization of phosphatidylserine (PS) to the outer plasma membrane. GA-T0 shifted nearly 32% of the LN229 cells from viable cells to apoptotic cells (Figure 3G), and 35% of the SNB19

cells (Figure 3H). A similar pattern was observed following TMZ treatment, with 21.9% apoptotic cells for LN229 and 35% for SNB19 cells. In contrast, the percentage of necrotic cells was 7% and 4% for GA-T0 while 27% and 12% for TMZ in the LN229 and SNB19 cell lines, respectively.

We additionally validated the genes involved in apoptosis-mediated cell death through gene expression profiling. Apoptotic inhibitor genes, such as survivin, *BIRC5* [35], and *API5* [36], were downregulated in both GBM cell lines, with the upregulation of the pro-apoptotic gene, *BBC3*, in SNB19 cells, whose expression increases in response to diverse apoptotic stimuli [37] (Figure 3I). *BCLAF1*, an anti-apoptotic Bcl-2 family member, was found to be downregulated in LN229 cells, suggesting a role in GPR17-mediated apoptosis at physiological levels [38,39]. The downregulation of *CASP2* [40] and *CASP3* [41,42] in LN229 cells and *CASP7* [41] in SNB19 cells also supports the likelihood that GPR17 activates a caspase-independent mechanism of apoptosis.

2.5. GA-T0 Promoted Cell Cycle Arrest at the G1 Phase

To determine whether GPR17 signaling promotes cell cycle arrest, the percentage of cells in each phase of the cell cycle was analyzed. Following GA-T0 treatment, we observed significant arrest of GBM cells in the G1 phase, with a concomitant decrease in the percentage of cells in the S and G2/M phase at 24 h ($p < 0.01$ for LN229 and $p < 0.05$ for SNB19). As shown in Figure 3J, GA-T0-treated LN229 cells were found to have 59% arrest at the G1 phase, which increased to 68.2% for SNB19 cells (Figure 3K). Similarly, TMZ also arrested GBM cells in the G1 phase, with 70.7% for LN229 cells and 67% for SNB19 cells.

These results were correlated with the differential expression of genes involved in the cell cycle. Notably, downregulation of the *CDK2* gene was observed in both GBM cell lines, suggesting a pivotal role in cell cycle regulation [43]. This perturbs the p53 signaling pathway, which, in turn, activates the p21 pathway by downregulating several cyclins [44], such as *cyclin E2* in LN229 and *cyclin D1* and *cyclin D3* in SNB19 cells (Supplementary Tables S1 and S2). The downregulation of cyclin-specific genes, such as *CCNE1*, *CCND1* (restricted to SNB19), and *CCND3*, a regulatory subunit of *CDK2*, further suggests potential defects in the transition of the G1 to S phase of the cell cycle. We also noted downregulation of cyclin A2, cyclin B1, and cyclin B2, encoded by *CCNA2*, *CCNB1*, and *CCNB2*, respectively, which potentially prevented the transition of cells from the G2 to M phase (Figure 3L). These results indicated the potential role of the GPR17 signals in maintaining efficient cell cycle progression by inducing cell cycle arrest at the G1 phase.

2.6. Effect of GA-T0 Mediated GPR17 Activation on Signal Transduction Pathways

2.6.1. PI3K–Akt Pathway

MCL1, an anti-apoptotic Bcl-2 family gene that promotes survival of glioma cells by preventing apoptosis [45], was found to be downregulated in both GBM cell lines. *MCL1* inhibition in the PI3K–Akt pathway intriguingly supported our study on the role of GPR17 in arresting the cell cycle at the G1 phase, thus reducing cellular proliferation and in turn increasing senescence and apoptosis [46]. Therefore, silencing *MCL1* by GA-T0 also could target CREB protein [47], a downstream transcription factors of the PI3K/Akt signaling pathway, which is highly regulated in most cancers. Another notable gene, Protein Tyrosine Phosphatase N23, *PTPN23* whose downregulation is correlated with poor survival in breast cancer, was observed to be upregulated in GA-T0 treated GBM cell lines. Also, activation of PI3K/Akt is observed in prostate cancer disease progression upon the loss of *PTP1B* [48], a precedent gene of *PTPN23* (Figure 4A). These observations suggest GPR17 targeting of the PI3K–Akt pathway, thus preventing GBM proliferation.

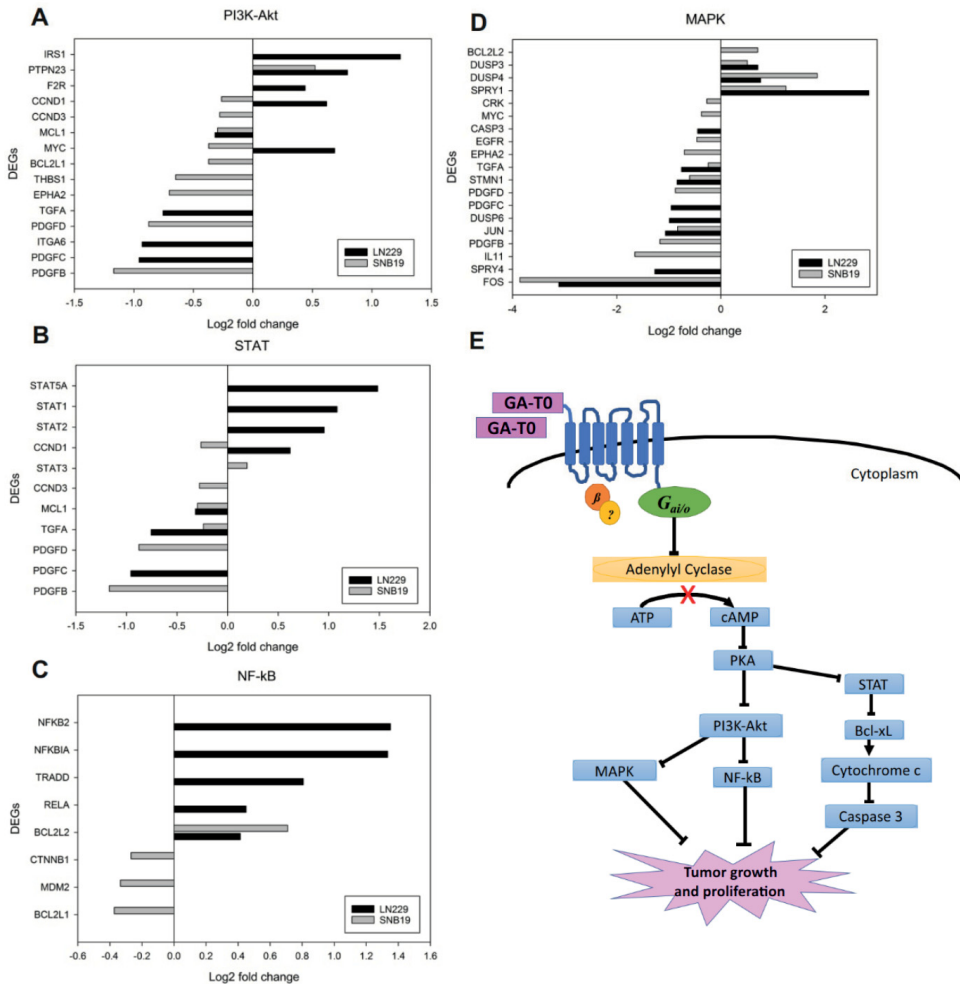


Figure 4. Regulation of signal transduction pathways upon GA-T0 treatment. (A) Key DEGs associated with the PI3K–Akt, (B) STAT, (C), NF-κB, and (D) and MAPK pathways. (E) Schematic overview of signal transduction pathway modulation upon the binding of GA-T0 on the GPR17 receptor in GBM cells.

2.6.2. STAT Pathway

Persistent activation of the STAT pathway contributes to tumor proliferation and survival in the microenvironment and promotes tumor growth [49,50]. The inhibition of *MCL1* activation in the STAT pathway revealed the potential role of GPR17 as a signal transducer in GBM cell lines. The Gαi-mediated reduction in the level of cAMP by GA-T0 (Figures 2F and 4E) supports the fact that the reduced binding of the cAMP response element (CRE) to the promoter region of *MCL1* downregulates its expression [51]. As noted earlier, induced apoptosis by the drug could also transcriptionally downregulate *MCL1* [52]. Likewise, TGFα downregulation, a mitogenic protein, incriminates the agonistic role of GA-T0 in forming autocrine looping, supporting the antiproliferation of human glioma [53] (Figure 4B).

2.6.3. NF- κ B Pathway

The NF- κ B pathway, a prototypical proinflammatory signaling pathway, has been observed to play a key role in cellular adaptation. As shown in Figure 4C, GA-T0 downregulates murine double minute-2 (MDM2), enhancing apoptosis [54] and cell cycle arrest at the G1 phase in SNB19 cells. This effect might involve the role of NF- κ B targeting Bcl3 and NF- κ B kinase subunit beta (*IKK2*) [55] by negatively regulating p53, thus suppressing NF- κ B signaling. GA-T0-treated LN229 cells also showed upregulation of the NF- κ B inhibitor- α (NFKBIA), which prompted our findings on the repression of the NF- κ B pathway. The deletion or downregulation of NFKBIA is well associated with GBM progression and lack of response to therapies [56], in many types of cancers [57], suggesting the role of GA-T0 as a tumor suppressor. CNNB1, encoding β -catenin, was observed to be downregulated in SNB19, whose activation promotes proliferation, migration, and invasion in GBM [58] and oral squamous carcinoma [59].

2.6.4. MAPK Pathway

Augmenting the effects of GA-T0 on the other pathways analyzed, inhibition of the genes related to the MAPK-dependent signaling pathways in both the GBM cell lines was also observed. Notably, *SPRY4*, coding for the sprouty 4 protein, was upregulated in LN229 cells, whose ectopic expression by GA-T0 inhibited the proliferation and migration of GBM cells. Its negative regulation of MAPK activation positions it as a tumor suppressor in GBM [60]. The expression of *STMN1*, coding for stathmin, was also found downregulated in both GBM cell lines, which might be due to the phosphorylation of Ser25 and Ser38 by MAPK [61,62] (Figure 4D). GA-T0 binding to the GPR17 receptor influences the downregulation of the cAMP level by decreasing the adenylyl cyclase activity, which in turn regulates various signaling pathways, such as the PI3K–Akt, Stat, NF- κ B, and MAPK pathways. Thus, GPR17-mediated signaling activation promotes the inhibition of GBM tumor growth and proliferation (Figure 4E).

2.7. GA-T0 Crosses the Blood–Brain Barrier

Being a strong agonist of GBM cell lines, causing potential cell death and cell cycle arrest, we further investigated the ability of GA-T0 to cross the blood–brain barrier (BBB) in wild mice, *Mus musculus*, using HPLC analysis. The retention time of GA-T0 was found to be 6.043, confirming it has the ability to cross the BBB in wild mice (Figure 5A). Histological analysis of the brain tissues showed no morphological or physiological changes in the brain cells (Figure 5B). Analysis of organ histology from GA-T0-treated mice identified no significant pathology in the weight (mg) of the heart, liver, kidney, ovary, and uterus. Assessment of biochemical nephrotoxicity indicators, such as sugar, creatinine, and urea (mg/dL), showed no significant differences compared to the controls, reflecting the ability of GA-T0 to maintain the metabolic homeostasis [63] of the extracellular environment (Figure 5C).

2.8. Preclinical Validation of GA-T0 in Patient-Derived Cell Lines (PDC) and Patient-Derived Xenograft Mouse Models (PDX)

Preclinical validation was performed in patient-derived cell lines (PDC) and patient-derived xenograft mouse models (PDX). Stringer et al. (2019) cultured low-passage primary patient GBM cell lines, such as MMK1, RN1, and JK2, from different age groups, and their demographic features are represented in Figure 6A. Strikingly, microarray analysis revealed the expression variation of GPR17, where MMK1 was implicated as having the highest level of expression followed by RN1 and JK2. This is due to the heterogeneous variation in gene expression exhibited in different GBM patients [64]. Inconsistent with our previous cytotoxicity results, there is no synergy between the action of TMZ in the patient-derived cell lines. Of note, there is less than 21% cell growth inhibition, even at a higher concentration of TMZ, whereas GA-T0 showed significant ($p < 0.01$) cell death of approximately 86%, 80%, and 73% in MMK1, RN1, and JK2, respectively, at a similar

concentration (Figure 6B). There was a positive correlation between GPR17 expression and percentage of cell death in PDC-treated GA-T0 at 100 μ M ($r(9) = 0.680, p = 0.044$) and 10 μ M ($r(9) = 0.777, p = 0.014$) (Supplementary Figure S3). The response of the patients to the GPR17 agonist and TMZ treatment differs widely with host genetic variations and molecular background. The clinical diversity of the tumor cells also influenced its behavior to be distinct for the action of chemotherapy, TMZ.

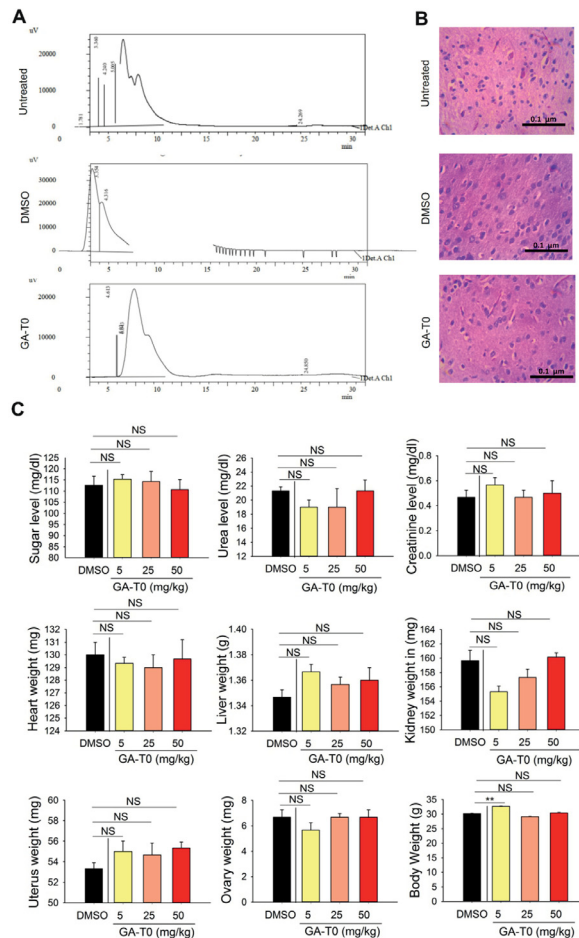


Figure 5. Ability of GA-T0 to cross the BBB in an in vivo model. (A) HPLC analysis showing the retention time in the control, DMSO, and GA-T0-treated *Mus musculus*. (B) Histopathology of the brain tissues from the control, DMSO, and GA-T0-treated wild mice. Photomicrographs of the cerebral cortex of the mice showing a normal architecture of the pyramidal neurons (PYC) in untreated and treated animals. (C) Changes in body weight, organ weight, and biochemical indicators, such as the sugar, creatinine, and urea (mg/dL) level, in wild mice upon GA-T0 treatment at varying concentrations, namely, 5, 25, and 50 mg/kg animal weight. Non-significant data are denoted by NS and significant data by asterisks; biological and technical repeats, $n = 6$, **, $p < 0.01$).

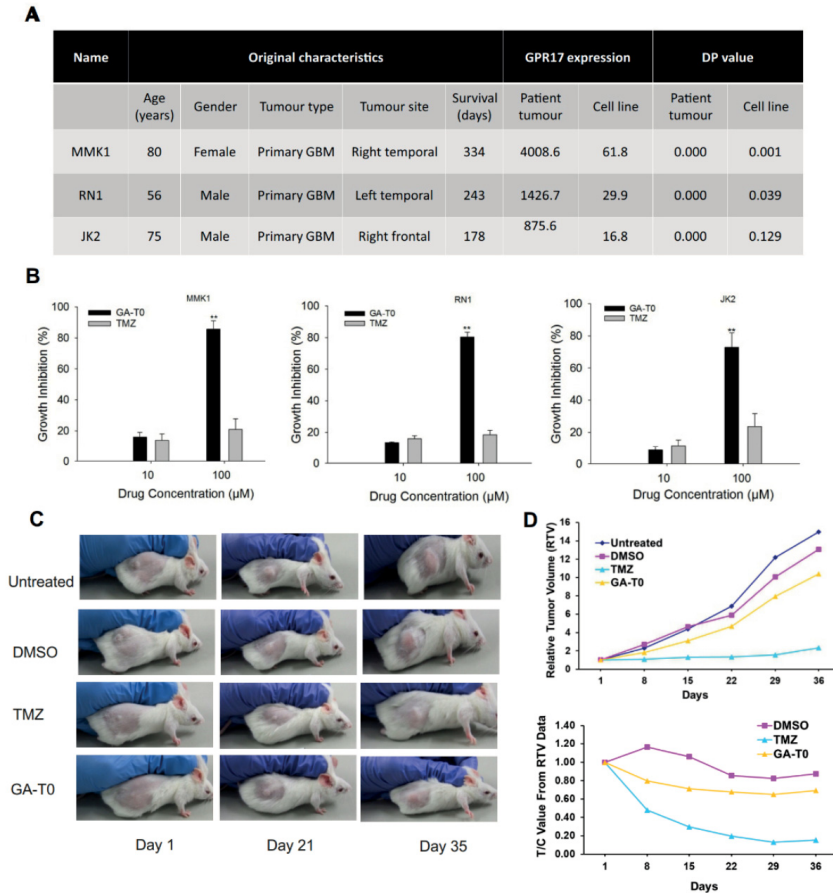


Figure 6. The anti-tumor effect of GA-T0 on patient-tissue-derived GBM cells and PDX animal models. (A) Demographic features of MMK1, RN1, and JK2 cells derived from GBM patients showing differential GPR17 expression. (B) Percentage of growth inhibition on patient-tissue-derived GBM cell lines upon treatment with 10 and 100 μM of GA-T0 and TMZ. (C) Images of xenograft GBM treated with DMSO (vector control), TMZ (positive control), and GA-T0 (Drug) at Day 1, Day 21, and Day 35. (D) Periodical validation of the relative tumor volume (RTV) and relative activity criteria (T/C) in PDX models on treatment with DMSO, TMZ, and GA-T0. (A) DP—detection p -value. Illumina beadchips allow a detection p -value to be calculated as an estimate of gene measurements relative to background. $p < 0.05$ for all samples on a beadchip for a given probe was used as a cut off to compile the gene expression datasets. (B) The results are presented as the mean values \pm SEM of six experiments; significant data are denoted by asterisks (*, $p < 0.05$; **, $p < 0.01$).

To further support the potential clinical application of our results, we used patient-derived xenograft (PDX) mouse models generated from GBM cells. The animals were administered with GA-T0 and TMZ at a dose that exerted only a cytostatic effect (20 mg/kg). The relative tumor volume (RTV) and relative activity criteria (T/C) was periodically measured to validate the role of TMZ and the drug against the control and the vector control. We observed a sudden decrease in the tumor volume for GA-T0 and TMZ till the 8th day of treatment, with a substantial decrease till the 36th day of treatment (Figure 6C,D). The commercial chemotherapeutic agent (TMZ) exerts resistance to prolonged therapy with hematological toxicity [65], acute cardiomyopathy [66], oral ulceration, hepatotoxicity [67], and pneumocystis pneumonia [68], ultimately resulting in the discontinuation of therapy.

The absence of GA-T0 toxicity in wild mice is considered more significant, whereas in PDX models, it is effective against tumor growth, and thus can potentiate progression-free survival through targeted GBM therapy.

3. Discussion

A glioblastoma possessing stable proliferation, invasion, and evasion of apoptosis, with increased angiogenesis, makes it susceptible to escape existing treatment strategies. The currently available drugs also focus only on either controlling inflammation or improving and modulating the patients' immune response, and so no therapies and drugs have been found to provide protective activity against this disease. The potential target for GBM therapeutics has been improved by various comprehensive approaches to reduce its off-tumor toxicity; yet, it remains ambiguous.

GPR17, an orphan G protein-coupled receptor, has been involved in oligodendrocyte differentiation, spinal cord injury, and brain injury [69]. Virtual high-throughput screening technology and in vivo assays identified galinex as a GPR17 agonist that significantly delays the onset of experimental autoimmune encephalomyelitis (EAE) [70]. In silico analysis revealed GPR17 upregulation in pediatric diffuse midline glioma clustering to *olig1* and *olig2* genes [26]. The proliferation rate of infratentorial LGG was controlled by various candidate genes, such as *ARX*, *GPR17*, *LHX2*, and *CXCL14*, where GPR17 is involved in the signal transduction pathway [71]. Our dataset analysis revealed constitutive expression of GPR17 in low-grade glioma (LGG) and GBM, where its expression is not only linked with improved survival but also significantly associated as a predictive biomarker.

Malignant gliomas, being lethal tumors, adjust to the environmental and genotoxic stress and thus promotes proliferation and invasiveness [72]. Our findings established the complex role of GPR17 signaling activation in the increased cytotoxicity against GBM cells, apoptosis, and thereby reduced cell proliferation. Gene expression analysis underscores the multifaceted role of GPR17 activation in the modulation of vital genes in several pathways, such as MAPK/ERK, PI3K–Akt, STAT, and NF- κ B, controlling GBM disease progression. Additional in vivo data are also distinct, showing a reduction in tumor volume without affecting the local cellular environment, suggesting the potential role of GPR17 as a targeted therapy against GBM.

The extensive literature specifies the role of a renewed neurosphere in cultured glioma cells as a potential cause of patients' death due to rapid tumor progression, involvement of proliferative genes, and signals from different pathways for the activation of G1/S phase [73–76]. Intriguingly, in vitro analysis revealed that activation of the GPR17 agonist favored the selective survival of Oligo 2 cells and altered the proliferative ability of glioma cells by decreasing the number of neurospheres [27]. Thus, neurosphere formation in GBM patients is considered as a significant predictor of clinical outcome, independent of tumor grade and patient age, and thus could reflect the clinical severity of glioma. Our work implicated that the PI3K–Akt pathway reduces the proliferation of the neurosphere on arresting the cell cycle at the G1 phase and decreases its number by increased apoptosis. The role of other pathways, such as the STAT, NF- κ B, and MAPK pathways, in specifically regulating the neurogenic proliferation and their activation in GBM tumorigenesis remains to be elucidated.

Identifying the appropriate patient-specific treatment strategy is an unrelenting endeavor in GBM treatment. Lomustine, carmustine, temozolomide, and bevacizumab are the anti-GBM drugs approved by the FDA, out of which the former three drugs only have partial brain penetration, while bevacizumab fails clinical trials and does not show significant impact on patient survival [77–79]. In terms of GPR17-targeted therapy for GBM treatment, there are many novel compounds that are able to interact with the GPR17 receptor [80–82]. Unfortunately, there are no GPR17-targeted compounds under investigation in clinical trials. However, our data revealed that GPR17 signaling activation using GA-T0, observed to arrest cell cycle, induces apoptosis and show a cytotoxic effect against GBM cells, as well as in patient-derived cell lines, with significant tumor cytotoxicity in in vivo PDX animal

models. Thus, abrogation of neural stem cell proliferation, myelin sheath damage, and infiltration to the nearby tissues through the sensor, such as GPR17 signaling activation, could benefit GBM treatment. Taken together, much remains to be discovered about the pharmacological mechanism of GPR17 receptor signaling for multiple subtypes of GBM, which opens the door for new hope in finding successful therapy for glioma treatment.

4. Materials and Methods

4.1. Protein–Protein Docking and Docking Simulations

A comparative molecular interaction study was performed using the computational structured model of GPR17 [30] and X-ray crystallography structure of Guanine Nucleotide Binding Protein [alpha]I1 (GαI) [PDB. ID:1KJY, 2.70 Å] [83]. Cluspro, an FFT web-based docking server, was used to study the binding efficiency of these three interacting signaling proteins [84]. Simultaneously, High Ambiguity Driven protein–protein DOCKing (HADDOCK V.2.2) and *ab-initio* docking methods were also used to achieve the consensus scores [85]. Docking simulation was done for the earlier known GPR17 agonist, 2-carboxy-4,6-dichloro-1H-indole-3-propionic acid (MDL 29,951) [22] and T0510-3657(GA-T0), the recently identified novel agonist by our group via the Blind docking web server [86] (<http://bio-hpc.ucam.edu/webBD/index.php/entry>, accessed on 2 February 2018). For each ligand, 200 binding poses were generated and sorted based on the binding energy and conformation in the protein’s binding site.

4.2. Cell Culture

SNB19 and LN229 human glioma cell lines (gifted by Dr.Kirsi Granberg, Faculty of Medicine and Health Technology, Tampere, Finland) and MEF, the mouse embryonic fibroblast cell line (gifted by Prof. Pasi Kallio, Faculty of Medicine and Health Technology, Tampere, Finland), were cultured in Dulbecco’s Modified Eagle Medium (DMEM) supplemented with 10% FBS, 0.1 mg/mL streptomycin, 100 U/mL penicillin, and 0.025 mg/mL amphotericin B (Sigma-Aldrich, St. Louis, MO, USA) under standard cell culture conditions (37 °C, 5% CO₂).

4.3. Expression Analysis of GPR17 at the mRNA and Protein Level in GBM Cells

Total RNA from LN229 and SNB19 cells was isolated using the GeneJET RNA Purification Kit (ThermoFisher Scientific, Waltham, MA, USA) following the manufacturer’s instruction. RNA was reverse transcribed using High-Capacity cDNA Reverse Transcription Kit (Applied Biosystems™, Waltham, MA, USA). The PCR was carried out to detect the expression of human GPR17 with primers described previously [20] (5'-GACTCCAGCCAAAGCATGAA-3' and 5'-GGGTCTGCTGAGTCTCTAAACA-3'). House-keeping gene β-actin was used as an endogenous control (primers- 5'- CTGGGACGACATG GAGAAAA-3' and 5'-AGGAAGGCTGGAAGAGTGC-3') [87].

To further validate the expression of GPR17 in GBM cell lines at the protein level, an immunoblot assay was performed. For this, LN229 and SNB19 cells were lysed in ice-cold lysis buffer (25 mM Tris, pH 7.4, 150 mM NaCl, 1 mM EDTA, 1% Triton X-100, 1% IGEPAL), supplemented with protease inhibitor mixture (Sigma-Aldrich, St. Louis, MO, USA). The protein was separated by SDS-polyacrylamide gel electrophoresis and transferred to nitrocellulose membrane (Amersham™ Protran™ 0.45 μm NC, GE Healthcare Life Science). The membranes were blocked with BSA and stained with antibodies specific for GPR17 (1:500; sc-514723, Santa Cruz Biotechnology, Dallas, TX, USA) and α-Tubulin (1:1000; sc-8035, Santa Cruz Biotechnology). Signals were visualized using Odyssey CLx (LI-COR Biosciences, Lincoln, NE, USA) after staining the membranes with goat anti-mouse secondary antibody (1:5000; Dylight 800, Thermo Scientific).

4.4. cAMP GloTM Assay

To evaluate the cAMP production in response to the effect of GPR17 agonist, GA-T0, cAMP GloTM Assay was performed. LN229 and SNB19 cells were seeded in a white 96-well

plate (Nuclon, ThermoFisher Scientific, USA) at an initial density of 1×10^4 cell/well. After overnight incubation, the cells were washed with PBS, incubated with 10 μ M Forskolin (FK) (Sigma-Aldrich, St. Louis, MO, USA) for 15 min at 37 °C, and treated with 10 μ M, 25 μ M, 50 μ M, 75 μ M, and 100 μ M of GA-T0 for 2 h. The cells were then harvested, lysed, and assayed for cAMP accumulation using the cAMP-Glo™ Assay kit (Promega, Madison, WI, USA) following the manufacturer's protocol. The luminescence intensity was measured using a Spark plate reader (Spark®, Tecan, Männedorf, Switzerland).

4.5. Measurement of the Intracellular Calcium Concentration

To determine the role of GPR17 in triggering the intracellular Ca^{2+} , a Fura-2 AM assay was performed. GBM cells at 60–70% confluency were cultured in a black, clear bottom 96-well plate (Corning, Sigma-Aldrich), washed with PBS, and treated with 10 μ M, 25 μ M, 50 μ M, 75 μ M, and 100 μ M of GA-T0. After 2 h of incubation at 37 °C, 100 μ L Dulbecco's PBS (Sigma-Aldrich, St. Louis, MO, USA) containing 5 μ M Fura-2 AM (Sigma-Aldrich, St. Louis, MO, USA) and 0.1% Pluronic® F-127 (Sigma-Aldrich, St. Louis, MO, USA) was loaded into each well. Cells were incubated in darkness for 30 min and later washed twice with DPBS. The Ca^{2+} level was measured using a microplate reader (Spark®, Tecan) at two dual excitation/emission wavelengths of 340/510 and 380/310 [88]. The experiments were performed in triplicate for all the conditions.

Similarly, the time-dependent effect of the Ca^{2+} level was also performed as described above, where the fluorescent signals were measured every 5 min in the microplate reader (Spark®, Tecan). The cells were treated with 50 μ L of DPBS for treated condition and 100 μ L of DPBS for untreated condition. At cycle 5 (after 20 min), 50 μ L of GA-T0 (IC_{50}) dissolved in DPBS was added to the treated condition and all the wells were subjected to the fluorescent measurement until it reached cycle 40. The experiment was performed with $n = 6$ in all the conditions and the fluorescent intensity was calculated using the following Equation (1).

$$340/380 \text{ ratio} = (F_{\text{raw } 340} - F_{\text{blank } 340}) / (F_{\text{raw } 380} - F_{\text{blank } 380}) \quad (1)$$

where $F_{\text{raw } 340}$ and $F_{\text{raw } 380}$ are the fluorescent intensities emitted at 510 nm between 340 nm and 380 nm excitation, respectively.

4.6. In Vitro Cell Proliferation Assay

The in vitro cytotoxicity activity of the GPR17 agonist, GA-T0, against SNB19, and LN229 cells was measured. The known GPR17 agonist, MDL 29,951, was used as the positive control and temozolomide (TMZ) as the drug control. An initial density of 1×10^5 cells/well were grown in 12-well plates until 60–70% confluency and the cells were treated with a 10 μ M and 100 μ M concentration of the abovementioned compounds. The cells were incubated for 24 h in the controlled culture conditions and later centrifuged at 3000 rpm for 10 min. Live and dead cells were measured using trypan blue staining using Countless II FL Automated Cell Counter (ThermoFisher Scientific, Waltham, MA, USA). The percentage of inhibition of cell growth [89] was calculated using the following equation (2). Biological and technical replicates were conducted for each condition.

$$\text{Inhibition (\%)} = \frac{\text{Mean No. of untreated cells (control)} - \text{Mean No. of treated cells} \times 100}{\text{Mean No. of untreated cells (control)}} \quad (2)$$

4.7. Pharmacodynamics Study

A pharmacodynamics study was performed to assess the effect of GA-T0 on the relationship between varying drug concentration and time course over cell growth. The study was performed as described previously for the in vitro cytotoxicity assay. The different concentration of GA-T0, 10 μ M, 25 μ M, 50 μ M, 75 μ M, and 100 μ M was used to evaluate the cell viability on SNB19 and LN229 cells. The time-dependent study was

performed for 24 h, 48 h, and 72 h exposure and a half maximal inhibitory concentration (IC_{50}) was calculated from the dose–response curve. The calculated IC_{50} value at 24 h post treatment was used for further analysis.

4.8. Apoptosis Annexin V-FITC/PI Apoptotic Assay

Quantitative assessment of apoptosis and necrosis for GA-T0 against SNB19 and LN229 cells was measured using a Dead Cell Apoptosis Kit using Annexin-V/fluorescein isothiocyanate (FITC) and propidium iodide (PI) (ThermoFisher Scientific, Waltham, MA, USA). Briefly, cells were seeded in 6-well plates at an initial density of 5×10^5 cells/well. Cells were treated then with an IC_{50} concentration of GA-T0 for 24 h. Positive control (TMZ), negative control (DMSO), and untreated samples were also included in the experiment. The cells were collected, washed in ice cold PBS, and the cell pellets were resuspended in $1 \times$ annexin-binding buffer. To 100 μ L of cell suspension, 5 μ L of FITC conjugated annexin-V and 1 μ L of the 100 μ g/mL PI was added and incubated at RT for 15 min. Fluorescent images of the viable, apoptotic, or necrotic cells with differences in plasma membrane integrity and permeability were captured using an EVOS imaging system (ThermoFisher Scientific, Waltham, MA, USA). All the experiments were performed with $n = 6$ in all the experimental conditions.

4.9. Cell Cycle Analysis by Propidium Iodide (PI)

The ability of GA-T0 to arrest cells at the G1 phase, S phase, and G2/M phase of the cell cycle was assessed using PI staining. SNB19 and LN229 cells were cultured in 6 well-plates at an initial density of 5×10^5 cells/well and incubated overnight. The cells were treated with an IC_{50} concentration of GA-T0 and TMZ for 24 h, where DMSO was used as negative control along with the untreated samples. Cells were collected, washed in cold PBS, and fixed in 70% ice-cold ethanol for 30 min at 4 °C. The cells were then suspended in 200 μ L PBS containing 20 μ g/mL PI, 0.2 mg/mL RNase, and 0.1% triton X-100, and incubated for 30 min at 37 °C. Fluorescence images were captured by using an EVOS imaging system (ThermoFisher Scientific, Waltham, MA, USA) and cells arrested at different phases of the cell cycle analyzed using CellProlifer.

4.10. Differential Gene Expression Analysis

High-throughput sequence-based Illumina RNA-seq was used to analyze transcripts for differential expression upon the drug treatment. Total RNA was extracted from GA-T0-treated LN229 and SNB19 cells at their respective IC_{50} concentration for 24 h, using the GeneJET RNA Purification Kit (ThermoFisher Scientific, Waltham, MA, USA). RNA sequencing was done by outsourcing in the Biomedicum Functional Genomics Unit (FuGU, University of Helsinki, Finland) using Illumina NextSeq 500 and the fold change in RNA expression was measured [15]. All the experiments were conducted in triplicates.

4.11. Tumor Samples and Cytotoxicity Effect of GA-T0

The cytotoxicity effect of GA-T0 on patient-derived GBM cell lines, MMK1, RN1, and JK2 (gifted by QIMR Berghofer, Medical Research Institute, 300 Herston Rd, Herston QLD 4006, Australia) was analyzed. The isolation and development of cell lines from the patients were approved by the human ethics committee of the Queensland Institute of Medical Research and Royal Brisbane and Women’s Hospital [90]. The cells were cultured in serum-free conditional medium using 1% Matrigel-coated flasks in a humidified incubator at 37 °C supplied with 5% CO_2 [91]. The cell lines were plated in 12-well plates with the initial density of 1×10^5 cells per well and treated with 100 and 10 μ M of GA-T0 and TMZ for 24 h. The cell growth inhibition was analyzed following the protocol described earlier.

4.12. In Vivo Experiments

4.12.1. Wild Mice

All protocols involving normal mice, *Mus musculus*, were approved by the Institutional animal ethics committee (IAEC) of the department of Animal science at Bharathidasan University, Tiruchirappalli, Tamil Nadu, India (Reg.No:418/GO/Re/S/01/CPCSEA, dt.24.07.2018). Adult female mice weighing 20–25 g were maintained in controlled environmental conditions, including a temperature of 25 ± 2 °C with 12 h dark/light cycle, a standard laboratory diet, and water ad libitum. Grouping of animals ($n = 5$ /group) was done as follows: Treated Groups A, B, and C (GA-T0 with 5 mg, 25 mg, and 50 mg/kg); Group D (vehicle control, 0.1 mL of DMSO/kg); and Group E (control, untreated). The body weight of the animal was recorded periodically at Days 0, 7, and 15. All the mice were immobilized, sacrificed for the recovery of organs (lungs, heart, kidney, ovary, and uterus), and their weight noted before subjecting to further histopathology analysis.

4.12.2. Histopathology Analysis of the Brain Tissues

The brain tissues were dissected after treatment and fixed in Bouin fixative solution for 24 h, processed in ethanol and embedded in paraffin. Microtome sections 5 μ m thick were stained with hematoxylin and eosin and viewed under a light microscope (Olympus BX51, Tokyo, Japan) for any morphological and physiological changes. HPLC was performed with a Shimadzu (model UFLC) HPLC apparatus equipped with a UV-visible detector (235 nm) and Shim-pack GIST-HP C18 column, with an acetonitrile, pH 7.4, phosphate buffer 1:1 (*v/v*) and flow rate of 1.5 mL/min. All compounds were injected as 0.1 mg/mL solutions in DMSO (injection volume—20 μ L). All chromatograms were repeated ($n = 6$), and the mean *k* values were used for further investigations.

4.12.3. Patient-Derived Xenografts (PDXs)

In vivo cancer activity was evaluated against glioblastoma U373-MG Uppsala (https://web.expasy.org/cellosaurus/CVCL_2818, accessed on 24 June 2021) in human tumor xenograft mouse models. All protocols were approved by the Institutional Animal Ethics Committee, ACTREC, Tata Memorial Centre, Navi Mumbai (Ethical number: 01/2015), and adhered to CPCSEA guidelines (Registration Number: 65/GO/ReBiBt/S/99/CPCSEA). In-house bred Balb/c or NOD-SCID mice of six to eight weeks old were used in the experiments. Animals were maintained with utmost human care and all measures were taken to minimize animal suffering before and during the experiments.

Acute toxicity studies

Acute toxicity for GA-T0 by intraperitoneal route was determined using six immunocompetent Balb/c mice per dose. Mortality and weight loss ≥ 4 g/mouse were considered as the toxicity criteria. The dosage of the drug given was 20 mg/kg body weight of the animal and was injected every 7 days for 30 days. The mice were monitored for any of physical sign of morbidity or mortality after 5 days post-dosing of the drug.

Experimental design

All the mice were randomized into the desired experimental groups ($n = 6$ /group). The experimental group comprised of the control (Group A); vehicle control—DMSO (Group B); positive control—temozolomide (Group C); and GA-T0 (Group D). Tumor measurements were carried out to determine the tumor growth and tumor volume using digital Vernier calipers (Pro-Max, Electronic Digital Caliper, Fowler-NSK, USA). Mice were observed at regular intervals for a period of around 36 days for various features, such as the body weight, tumor volume, and mortality.

Statistical calculation for in vivo studies

The data are represented as the relative tumor volume in cubic centimeters (RTV in c.c), T/C (ratio of test versus control), and survival. Tumor volume was calculated using the formula $((w1 \times w1 \times w2) \times (\pi/6))$, where *w1* and *w2* were the smallest and the largest tumor diameter (cm), respectively. RTV was measured as tumor volume on the day of measurement/tumor volume on Day 1. The T/C ratio indicates antitumor effectiveness.

The percentage treatment/control (T/C %) values or percent tumor regression values were calculated using the following equation:

$$(RTV)T/C = RTV_Test/RTV_Control \text{ Tumor Regression \%} = 100 - [T/C * 100] \quad (3)$$

where T = mean tumor volume of the drug-treated group; RTV = mean tumor volume of the drug-treated group on the study day of interest—mean tumor volume of the drug-treated group on the initial day of dosing; and C = mean tumor volume of the control group. As per NCI, USA guidelines, biological activity was considered significant when T/C values were ≤ 0.42 .

5. Conclusions

GPR17 expression is associated with higher survival for both low-grade glioma (LGG) and glioblastoma (GBM). GA-T0, a potent GPR17 receptor agonist, causes significant GBM cell death and apoptosis. Upregulation of *DDIT3*, *DDIT4*, and *SQSTM1* genes showed a significant role in inducing GPR17-activated cell damage. Apoptotic inhibitor genes, such as survivin, *BIRC5*, and *API5*, were downregulated with the upregulation of the proapoptotic genes, such as *BBC3* in SNb19. Downregulation of *CASP2*, *CASP3*, and *CASP7* reveals the GPR17-mediated, caspase-independent mechanism of apoptosis. GPR17 signaling promotes cell cycle arrest at the G1 phase in GBM cells. Key genes are modulated in the signaling pathways such as the MAPK/ERK, PI3K–Akt, STAT, and NF- κ B pathways, which inhibit GBM cell proliferation. GA-T0 crosses the blood–brain barrier and reduces tumor volume in the xenograft model. These results suggest that targeting the GPR17 receptor presents a novel therapeutic target for the treatment of glioblastoma.

Supplementary Materials: The following are available online at <https://www.mdpi.com/article/10.3390/cancers13153773/s1>, Figure S1: GPR17 expression profile across all tumor samples and paired normal tissues. Dots represent expression in individual samples. Figure S2: Two-dimensional interaction diagram for MDL 29,951-protein complex. Figure S3: Correlation between GPR17 expression and percentage of cell death in three Patient derived cell lines treated with 100 μ M and 10 μ M of GA-T0. Spearman's (ρ) and Pearson's (r) correlation between the two values are shown. Figure S4: Western blot analysis of GPR17 receptor protein expression in LN229 and SNB19 cells. Table S1: The list shows the genes that were differentially expressed in GA-T0 vs Untreated in the cell type analysis using DESeq2. Table S2: The list shows the genes that were differentially expressed in GA-T0 vs Untreated in the cell type analysis using DESeq2.

Author Contributions: Conceptualization, O.Y.-H. and M.K.; methodology, P.D., P.N., A.M., K.S., S.K.M., V.K., B.G.A., B.W.S., K.B. and M.K.; validation, P.D., P.N., A.M., K.S., S.K.M., V.K., B.G.A., B.W.S.; formal analysis, P.D., P.N., A.M., S.K.M. and V.K.; investigation, P.D., P.N., A.M., K.S., S.K.M., V.K., B.G.A., B.W.S., and M.K.; resources, B.W.S., K.B., O.Y.-H. and M.K.; data curation, P.D., P.N., A.M., S.K.M., V.K., B.G.A. and B.S.; writing—original draft, P.D., P.N., A.M., S.K.M., B.G.A., B.W.S., K.B. and O.Y.-H., M.K. (with feedback from all authors); writing—review and editing, A.M., B.W.S. and M.K.; visualization, P.D., P.N. and M.K.; supervision, K.B., O.Y.-H. and M.K.; funding acquisition, K.B., O.Y.-H. and M.K. All authors have read and agreed to the published version of the manuscript.

Funding: TUT presidents grant for the salary support of P.D and P.N; Research materials support by Academy of Finland project grant support (decision no. 29720; P.D., P.N., A.K., K.S., O.Y.-H. and M.K.); Also, we thank FIST-SR/FST/LSI/-647/2015 (G) dt. 11/08/2016, DST, NewDelhi, India and EMEQ-SB/EMEQ-184/2013 dt. 09/07/2013, DST, NewDelhi, India, for providing grant support for animal testing.

Institutional Review Board Statement: The study was conducted according to the guidelines of the Declaration of Department of Animal Science, Bharathidasan University, and approved by the IAEC, Bharathidasan University, (protocol code BDU/IAEC/P12/2019 and date of approval is 30.11.2019). The Reg. No. 418/GO/Re/S/01/CPCSEA, dt. 24.07.2018.

Informed Consent Statement: All protocols involving normal mice, *Mus musculus*, were approved by the Institutional animal ethics committee (IAEC) of the department of Animal science at Bharathidasan University, Tiruchirappalli, Tamil Nadu, India (Reg.No:418/GO/Re/S/01/CPCSEA,

dt.24.07.2018). All protocols involving xenograft mouse model were approved by the Institutional Animal Ethics Committee, ACTREC, Tata Memorial Centre, Navi Mumbai (Ethical number: 01/2015) and adhered to CPCSEA guidelines (Registration Number: 65/GO/ReBiBt/S/99/CPCSEA).

Data Availability Statement: The data are available from the corresponding authors upon request.

Acknowledgments: We would like to thank Kirsi Granberg (Faculty of Medicine and Health Technology, Tampere, Finland) for providing the SNB19 and LN229 cell lines; Pasi Kallio, Faculty of Medicine and Health Technology, Tampere, Finland, for providing the mouse embryonic fibroblast cell line; and QIMR Berghofer, Medical Research Institute, Australia, for providing the patient-derived GBM cell lines, MMK1, RN1, and JK2.

Conflicts of Interest: The authors declare no conflict of interest.

Abbreviations

GBM	Glioblastoma multiforme
GPCR	G protein-coupled receptor
GA-T0	GPR17 agonist T0510-3657
pDMG	Pediatric diffuse midline glioma
CysLT	Cysteinyl-leukotriene
TMZ	Temozolomide
ROS	Reactive Oxygen Species
RNA-seq	RNA-sequencing
DMEM	Dulbecco's Modified Eagle's Medium
DNA	Deoxyribonucleic acid
FBS	Fetal Bovine Serum
DEG	Differentially expressed gene

References

- Bocangel, D.B.; Finkelstein, S.; Schold, S.C.; Bhakat, K.K.; Mitra, S.; Kokkinakis, D.M. Multifaceted resistance of gliomas to temozolomide. *Clin. Cancer Res.* **2002**, *8*, 2725–2734.
- Stupp, R.; Mason, W.P.; Bent, M.V.D.; Weller, M.; Fisher, B.; Taphoorn, M.J.; Belanger, K.; Brandes, A.; Marosi, C.; Bogdahn, U.; et al. Radiotherapy plus Concomitant and Adjuvant Temozolomide for Glioblastoma. *N. Engl. J. Med.* **2005**, *352*, 987–996. [CrossRef]
- Silbergeld, D.L.; Chicoine, M.R. Isolation and characterization of human malignant glioma cells from histologically normal brain. *J. Neurosurg.* **1997**, *86*, 525–531. [CrossRef]
- Chen, J.; Li, Y.; Yu, T.-S.; McKay, R.M.; Burns, D.K.; Kernie, S.; Parada, L.F. A restricted cell population propagates glioblastoma growth after chemotherapy. *Nat. Cell Biol.* **2012**, *488*, 522–526. [CrossRef]
- Meacham, C.E.; Morrison, S.J. Tumour heterogeneity and cancer cell plasticity. *Nat. Cell Biol.* **2013**, *501*, 328–337. [CrossRef]
- Li, Z.; Bao, S.; Wu, Q.; Wang, H.; Eyler, C.; Sathornsumetee, S.; Shi, Q.; Cao, Y.; Lathia, J.; McLendon, R.E.; et al. Hypoxia-Inducible Factors Regulate Tumorigenic Capacity of Glioma Stem Cells. *Cancer Cell* **2009**, *15*, 501–513. [CrossRef]
- Parsons, D.W.; Jones, S.; Zhang, X.; Lin, J.C.-H.; Leary, R.J.; Angenendt, P.; Mankoo, P.; Carter, H.; Siu, I.-M.; Gallia, G.L.; et al. An Integrated Genomic Analysis of Human Glioblastoma Multiforme. *Science* **2008**, *321*, 1807–1812. [CrossRef]
- Bao, S.; Wu, Q.; McLendon, R.E.; Hao, Y.; Shi, Q.; Hjelmeland, A.B.; Dewhirst, M.W.; Bigner, D.D.; Rich, J.N. Glioma stem cells promote radioresistance by preferential activation of the DNA damage response. *Nature* **2006**, *444*, 756–760. [CrossRef]
- Verhaak, R.G.; Hoadley, K.; Purdom, E.; Wang, V.; Qi, Y.; Wilkerson, M.D.; Miller, C.; Ding, L.; Golub, T.; Mesirov, J.P.; et al. Integrated Genomic Analysis Identifies Clinically Relevant Subtypes of Glioblastoma Characterized by Abnormalities in PDGFRA, IDH1, EGFR, and NF1. *Cancer Cell* **2010**, *17*, 98–110. [CrossRef] [PubMed]
- Wang, Q.; Hu, B.; Hu, X.; Kim, H.; Squatrito, M.; Scarpace, L.; deCarvalho, A.C.; Lyu, S.; Li, P.; Li, Y.; et al. Tumor Evolution of Glioma-Intrinsic Gene Expression Subtypes Associates with Immunological Changes in the Microenvironment. *Cancer Cell* **2017**, *32*, 42–56.e6. [CrossRef]
- Neftel, C.; Laffy, J.; Filbin, M.G.; Hara, T.; Shore, M.E.; Rahme, G.J.; Richman, A.R.; Silverbush, D.; Shaw, M.L.; Hebert, C.M.; et al. An Integrative Model of Cellular States, Plasticity, and Genetics for Glioblastoma. *Cell* **2019**, *178*, 835–849.e21. [CrossRef]
- Furusawa, C.; Kaneko, K. Chaotic expression dynamics implies pluripotency: When theory and experiment meet. *Biol. Direct* **2009**, *4*, 17. [CrossRef]
- Patel, A.P.; Tirosh, I.; Trombetta, J.J.; Shalek, A.K.; Gillespie, S.; Wakimoto, H.; Cahill, D.; Nahed, B.; Curry, W.T.; Martuza, R.L.; et al. Single-cell RNA-seq highlights intratumoral heterogeneity in primary glioblastoma. *Science* **2014**, *344*, 1396–1401. [CrossRef]

14. Viswanathan, A.; Kute, D.; Musa, A.; Mani, S.K.; Sipilä, V.; Emmert-Streib, F.; Zubkov, F.; Gurbanov, A.V.; Yli-Harja, O.; Kandhavelu, M. 2-(2-(2,4-dioxopentan-3-ylidene)hydrazineyl)benzotrile as novel inhibitor of receptor tyrosine kinase and PI3K/AKT/mTOR signaling pathway in glioblastoma. *Eur. J. Med. Chem.* **2019**, *166*, 291–303. [CrossRef]
15. Doan, P.; Musa, A.; Murugesan, A.; Sipilä, V.; Candeias, N.R.; Emmert-Streib, F.; Ruusuvoori, P.; Granberg, K.; Yli-Harja, O.; Kandhavelu, M. Glioblastoma Multiforme Stem Cell Cycle Arrest by Alkylaminophenol through the Modulation of EGFR and CSC Signaling Pathways. *Cells* **2020**, *9*, 681. [CrossRef]
16. Barros, M.T.; Doan, P.; Kandhavelu, M.; Jennings, B.; Balasubramaniam, S. Engineering calcium signaling of astrocytes for neural–molecular computing logic gates. *Sci. Rep.* **2021**, *11*, 595. [CrossRef]
17. Drews, J. Drug Discovery: A Historical Perspective. *Science* **2000**, *287*, 1960–1964. [CrossRef]
18. Oprea, T.I.; Bologna, C.; Brunak, S.; Campbell, A.; Gan, G.N.; Gaulton, A.; Gomez, S.M.; Guha, R.; Hersey, A.; Holmes, J.; et al. Unexplored therapeutic opportunities in the human genome. *Nat. Rev. Drug Discov.* **2018**, *17*, 317–332. [CrossRef]
19. Hauser, A.S.; Attwood, M.M.; Rask-Andersen, M.; Schiöth, H.B.; Gloriam, D.E. Trends in GPCR drug discovery: New agents, targets and indications. *Nat. Rev. Drug Discov.* **2017**, *16*, 829–842. [CrossRef]
20. Ciana, P.; Fumagalli, M.; Trincavelli, M.L.; Verderio, C.; Rosa, P.; Lecca, D.; Ferrario, S.; Parravicini, C.; Capra, V.; Gelosa, P.; et al. The orphan receptor GPR17 identified as a new dual uracil nucleotides/cysteinyl-leukotrienes receptor. *EMBO J.* **2006**, *25*, 4615–4627. [CrossRef]
21. Fratangeli, A.; Parmigiani, E.; Fumagalli, M.; Lecca, D.; Benfante, R.; Passafaro, M.; Buffo, A.; Abbracchio, M.P.; Rosa, P. The Regulated Expression, Intracellular Trafficking, and Membrane Recycling of the P2Y-like Receptor GPR17 in Oli-neu Oligodendroglial Cells. *J. Biol. Chem.* **2013**, *288*, 5241–5256. [CrossRef]
22. Hennen, S.; Wang, H.; Peters, L.; Merten, N.; Simon, K.; Spinrath, A.; Blättermann, S.; Akkari, R.; Schrage, R.; Schröder, R.; et al. Decoding Signaling and Function of the Orphan G Protein-Coupled Receptor GPR17 with a Small-Molecule Agonist. *Sci. Signal.* **2013**, *6*, ra93. [CrossRef]
23. Lecca, D.; Trincavelli, M.L.; Gelosa, P.; Sironi, L.; Ciana, P.; Fumagalli, M.; Villa, G.; Verderio, C.; Grumelli, C.; Guerrini, U.; et al. The Recently Identified P2Y-Like Receptor GPR17 Is a Sensor of Brain Damage and a New Target for Brain Repair. *PLoS ONE* **2008**, *3*, e3579. [CrossRef]
24. Dziedzic, A.; Miller, E.; Saluk-Bijak, J.; Bijak, M. The GPR17 Receptor—A Promising Goal for Therapy and a Potential Marker of the Neurodegenerative Process in Multiple Sclerosis. *Int. J. Mol. Sci.* **2020**, *21*, 1852. [CrossRef] [PubMed]
25. Marucci, G.; Lammi, C.; Buccioni, M.; Ben, D.D.; Lambertucci, C.; Amantini, C.; Santoni, G.; Kandhavelu, M.; Abbracchio, M.P.; Lecca, D.; et al. Comparison and optimization of transient transfection methods at human astrocytoma cell line 1321N1. *Anal. Biochem.* **2011**, *414*, 300–302. [CrossRef]
26. Loveson, K.; Lepinay, E.; Robson, S.; Fillmore, H. DIPG-15. The Role of the G-Protein-Coupled Receptor, GPR17 in Paediatric Diffuse Midline Glioma. *Neuro. Oncol.* **2018**, *20*, i51. [CrossRef]
27. Dougherty, J.; Fomchenko, E.I.; Akuffo, A.A.; Schmidt, E.; Helmy, K.Y.; Bazzoli, E.; Brennan, C.; Holland, E.C.; Milosevic, A. Candidate Pathways for Promoting Differentiation or Quiescence of Oligodendrocyte Progenitor-like Cells in Glioma. *Cancer Res.* **2012**, *72*, 4856–4868. [CrossRef]
28. Mutharasu, G.; Murugesan, A.; Mani, S.K.; Yli-Harja, O.; Kandhavelu, M. Transcriptomic analysis of glioblastoma multiforme providing new insights into GPR17 signaling communication. *J. Biomol. Struct. Dyn.* **2020**, *3*, 1–14. [CrossRef]
29. Gnanavel, M.; Yli-Harja, O.; Kandhavelu, M. Protein-Protein Interaction and Coarse Grained Simulation Study of Glioblastoma Multiforme Reveals Novel Pathways of GPR17. *TASK Q.* **2015**, *18*, 321–325.
30. Saravanan, K.M.; Palanivel, S.; Yli-Harja, O.; Kandhavelu, M. Identification of novel GPR17-agonists by structural bioinformatics and signaling activation. *Int. J. Biol. Macromol.* **2017**, *106*, 901–907. [CrossRef]
31. Mantilla, J.G.; Ricciotti, R.W.; Chen, E.Y.; Liu, Y.J.; Hoch, B.L. Amplification of DNA damage-inducible transcript 3 (DDIT3) is associated with myxoid liposarcoma-like morphology and homologous lipoblastic differentiation in dedifferentiated liposarcoma. *Mod. Pathol.* **2018**, *32*, 585–592. [CrossRef]
32. Shoshani, T.; Faerman, A.; Mett, I.; Zelin, E.; Tenne, T.; Gorodin, S.; Moshel, Y.; Elbaz, S.; Budanov, A.; Chajut, A.; et al. Identification of a Novel Hypoxia-Inducible Factor 1-Responsive Gene, *RTP801*, Involved in Apoptosis. *Mol. Cell. Biol.* **2002**, *22*, 2283–2293. [CrossRef]
33. Wang, Z.; Malone, M.H.; Thomenius, M.J.; Zhong, F.; Xu, F.; Distelhorst, C.W. Dexamethasone-induced Gene 2 (dig2) Is a Novel Pro-survival Stress Gene Induced Rapidly by Diverse Apoptotic Signals. *J. Biol. Chem.* **2003**, *278*, 27053–27058. [CrossRef]
34. Hewitt, G.; Carroll, B.; Sarallah, R.; Correia-Melo, C.; Ogrodnik, M.; Nelson, G.; Otten, E.; Manni, D.; Antrobus, R.; Morgan, B.A.; et al. SQSTM1/p62 mediates crosstalk between autophagy and the UPS in DNA repair. *Autophagy* **2016**, *12*, 1917–1930. [CrossRef]
35. Garg, H.; Suri, P.; Gupta, J.C.; Talwar, G.P.; Dubey, S. Survivin: A unique target for tumor therapy. *Cancer Cell Int.* **2016**, *16*, 1–14. [CrossRef]
36. Krejci, P.; Koci, L.; Chlebova, K.; Hýžd'álová, M.; Hofmanova, J.; Jira, M.; Kysela, P.; Kozubik, A.; Kala, Z. Apoptosis inhibitor 5 (API-5; AAC-11; FIF) is upregulated in human carcinomas in vivo. *Oncol. Lett.* **2012**, *3*, 913–916. [CrossRef]
37. Han, J.W.; Flemington, C.; Houghton, A.B.; Gu, Z.; Zambetti, G.P.; Lutz, R.J.; Zhu, L.; Chittenden, T. Expression of *bbc3*, a pro-apoptotic BH3-only gene, is regulated by diverse cell death and survival signals. *Proc. Natl. Acad. Sci. USA* **2001**, *98*, 11318–11323. [CrossRef]

38. Kasof, G.M.; Goyal, L.; White, E. Btf, a Novel Death-Promoting Transcriptional Repressor That Interacts with Bcl-2-Related Proteins. *Mol. Cell. Biol.* **1999**, *19*, 4390–4404. [CrossRef]
39. McPherson, J.P.; Sarras, H.; Lemmers, B.; Tamblyn, L.; Migon, E.; Matysiak-Zablocki, E.; Hakem, A.; Azami, S.A.; Cardoso, R.; Fish, J.; et al. Essential role for Bclaf1 in lung development and immune system function. *Cell Death Differ.* **2009**, *16*, 331–339. [CrossRef]
40. Lopez-Cruzan, M.; Sharma, R.; Tiwari, M.; Karbach, S.; Holstein, D.; Martin, C.R.; Lechleiter, J.D.; Herman, B. Caspase-2 resides in the mitochondria and mediates apoptosis directly from the mitochondrial compartment. *Cell Death Discov.* **2016**, *2*, 16005. [CrossRef]
41. Zhivotovsky, B.; Samali, A.; Gahm, A.; Orrenius, S. Caspases: Their intracellular localization and translocation during apoptosis. *Cell Death Differ.* **1999**, *6*, 644–651. [CrossRef] [PubMed]
42. Chandra, D.; Tang, D. Mitochondrially Localized Active Caspase-9 and Caspase-3 Result Mostly from Translocation from the Cytosol and Partly from Caspase-Mediated Activation in the Organelle. Lack of Evidence for Apaf-1-Mediated Procaspase-9 Activation in the Mitochondria. *J. Biol. Chem.* **2003**, *278*, 17408–17420. [CrossRef] [PubMed]
43. Tadesse, S.; Anshabo, A.T.; Portman, N.; Lim, E.; Tilley, W.; Caldon, C.E.; Wang, S. Targeting CDK2 in cancer: Challenges and opportunities for therapy. *Drug Discov. Today* **2020**, *25*, 406–413. [CrossRef]
44. Reyes, J.; Chen, J.Y.; Stewart-Ornstein, J.; Karhohs, K.W.; Mock, C.S.; Lahav, G. Fluctuations in p53 Signaling Allow Escape from Cell-Cycle Arrest. *Mol. Cell* **2018**, *71*, 581–591e5. [CrossRef]
45. Li, R.-Y.; Chen, L.-C.; Zhang, H.-Y.; Du, W.-Z.; Feng, Y.; Wang, H.-B.; Wen, J.-Q.; Liu, X.; Li, X.-F.; Sun, Y.; et al. MiR-139 Inhibits Mcl-1 Expression and Potentiates TMZ-Induced Apoptosis in Glioma. *CNS Neurosci. Ther.* **2013**, *19*, 477–483. [CrossRef]
46. Du, W.; Pang, C.; Xue, Y.; Zhang, Q.; Wei, X. Dihydroartemisinin inhibits the Raf/ERK/MEK and PI3K/AKT pathways in glioma cells. *Oncol. Lett.* **2015**, *21*, 3266–3270. [CrossRef]
47. Wang, L.-M.; Chao, J.-R.; Chen, W.; Kuo, M.-L.; Yen, J.J.-Y.; Yang-Yen, H.-F. The Antiapoptotic Gene mcl-1 Is Up-Regulated by the Phosphatidylinositol 3-Kinase/Akt Signaling Pathway through a Transcription Factor Complex Containing CREB. *Mol. Cell. Biol.* **1999**, *19*, 6195–6206. [CrossRef]
48. Xu, Q.; Wu, N.; Li, X.; Guo, C.; Li, C.; Jiang, B.; Wang, H.; Shi, D. Inhibition of PTP1B blocks pancreatic cancer progression by targeting the PKM2/AMPK/mTOC1 pathway. *Cell Death Dis.* **2019**, *10*, 874. [CrossRef]
49. Herrmann, A.; Kortylewski, M.; Kujawski, M.; Zhang, C.; Reckamp, K.; Armstrong, B.; Wang, L.; Kowolik, C.; Deng, J.; Figlin, R.; et al. Targeting Stat3 in the Myeloid Compartment Drastically Improves the In vivo Antitumor Functions of Adoptively Transferred T Cells. *Cancer Res.* **2010**, *70*, 7455–7464. [CrossRef]
50. Kujawski, M.; Kortylewski, M.; Lee, H.; Herrmann, A.; Kay, H.; Yu, H. Stat3 mediates myeloid cell-dependent tumor angiogenesis in mice. *J. Clin. Investig.* **2008**, *118*, 3367–3377. [CrossRef]
51. Akgul, C.; Turner, P.C.; White, M.R.H.; Edwards, S.W. Functional analysis of the human MCL-1 gene. *Cell. Mol. Life Sci.* **2000**, *57*, 684–691. [CrossRef]
52. Nijhawan, D.; Fang, M.; Traer, E.; Zhong, Q.; Gao, W.; Du, F.; Wang, X. Elimination of Mcl-1 is required for the initiation of apoptosis following ultraviolet irradiation. *Genes Dev.* **2003**, *17*, 1475–1486. [CrossRef]
53. Tang, P.; Steck, P.A.; Yung, W.K.A. The autocrine loop of TGF- α /EGFR and brain tumors. *J. Neuro. Oncol.* **1997**, *35*, 303–314. [CrossRef] [PubMed]
54. Cheney, M.D.; McKenzie, P.P.; Volk, E.L.; Fan, L.; Harris, L.C. MDM2 displays differential activities dependent upon the activation status of NF κ B. *Cancer Biol. Ther.* **2008**, *7*, 38–44. [CrossRef] [PubMed]
55. Kashatus, D.; Cogswell, P.; Baldwin, A.S. Expression of the Bcl-3 proto-oncogene suppresses p53 activation. *Genes Dev.* **2006**, *20*, 225–235. [CrossRef]
56. Bredel, M.; Scholtens, D.M.; Yadav, A.K.; Alvarez, A. NFKBIA deletion in glioblastomas. *N. Engl. J. Med.* **2011**, *364*, 627–637. [CrossRef]
57. Spink, C.F.; Gray, L.C.; Davies, F.E.; Morgan, G.J.; Bidwell, J.L. Haplotypic structure across the I κ B α gene (NFKBIA) and association with multiple myeloma. *Cancer Lett.* **2007**, *246*, 92–99. [CrossRef] [PubMed]
58. Wang, K.; Wang, X.; Zou, J.; Zhang, A.; Wan, Y.; Pu, P.; Song, Z.; Qian, C.; Chen, Y.; Yang, S.; et al. miR-92b controls glioma proliferation and invasion through regulating Wnt/beta-catenin signaling via Nemo-like kinase. *Neuro. Oncol.* **2013**, *15*, 578–588. [CrossRef] [PubMed]
59. Iwai, S.; Yonekawa, A.; Harada, C.; Hamada, M.; Katagiri, W.; Nakazawa, M.; Yura, Y. Involvement of the Wnt- β -catenin pathway in invasion and migration of oral squamous carcinoma cells. *Int. J. Oncol.* **2010**, *37*, 1095–1103. [CrossRef]
60. Celik-Selvi, B.E.; Stütz, A.; Mayer, C.E.; Salhi, J.; Siegwart, G.; Sutterlüty, H. Sprouty3 and Sprouty4, Two Members of a Family Known to Inhibit FGF-Mediated Signaling, Exert Opposing Roles on Proliferation and Migration of Glioblastoma-Derived Cells. *Cells* **2019**, *8*, 808. [CrossRef]
61. Belletti, B.; Baldassarre, G. Stathmin: A protein with many tasks. New biomarker and potential target in cancer. *Expert Opin. Ther. Targets* **2011**, *15*, 1249–1266. [CrossRef]
62. Liu, X.; Dong, B.; Mu, L.; Qin, X.; Qiao, W.; Liu, X.; Yang, L.; Xue, L.; Rainov, N.G. Stathmin expression in glioma-derived microvascular endothelial cells: A novel therapeutic target. *Oncol. Rep.* **2011**, *27*, 714–718. [CrossRef]

63. Weingand, K.; Brown, G.; Hall, R.; Davies, D.; Gossett, K.; Neptun, D.; Waner, T.; Matsuzawa, T.; Salemink, P.; Froelke, W.; et al. Harmonization of animal clinical pathology testing in toxicity and safety studies. *Fundam. Appl. Toxicol.* **1996**, *29*, 198–201. [CrossRef]
64. Stringer, B.W.; Day, B.W.; D'Souza, R.C.J.; Jamieson, P.R.; Ensbey, K.S.; Bruce, Z.C.; Lim, Y.C.; Goasdoué, K.; Offenhäuser, C.; Akgül, S.; et al. A reference collection of patient-derived cell line and xenograft models of proneural, classical and mesenchymal glioblastoma. *Sci. Rep.* **2019**, *9*, 4902. [CrossRef]
65. Berrocal, A.; Segura, P.P.; Gil, M.; Balaña, C.; Lopez, J.G.; Yaya-Tur, R.; Rodríguez, J.; Reynés, G.; Gallego, O.; Iglesias, I.; et al. Extended-schedule dose-dense temozolomide in refractory gliomas. *J. Neuro. Oncol.* **2010**, *96*, 417–422. [CrossRef] [PubMed]
66. Huang, G.; Zhang, N.; Bi, X.; Dou, M. Solid lipid nanoparticles of temozolomide: Potential reduction of cardiac and nephric toxicity. *Int. J. Pharm.* **2008**, *355*, 314–320. [CrossRef] [PubMed]
67. Kim, S.-S.; Rait, A.; Kim, E.; DeMarco, J.; Pirolo, K.F.; Chang, E.H. Encapsulation of temozolomide in a tumor-targeting nanocomplex enhances anti-cancer efficacy and reduces toxicity in a mouse model of glioblastoma. *Cancer Lett.* **2015**, *369*, 250–258. [CrossRef]
68. Tentori, L.; Graziani, G. Recent approaches to improve the antitumor efficacy of temozolomide. *Curr. Med. Chem.* **2009**, *16*, 245–257. [CrossRef] [PubMed]
69. Li, Y.; Zhang, S.; Huang, S. FoxM1: A potential drug target for glioma. *Future Oncol.* **2012**, *8*, 223–226. [CrossRef]
70. Parravicini, C.; Lecca, D.; Marangon, D.; Coppolino, G.T.; Daniele, S.; Bonfanti, E.; Fumagalli, M.; Raveglia, L.; Martini, C.; Gianazza, E.; et al. Development of the first in vivo GPR17 ligand through an iterative drug discovery pipeline: A novel disease-modifying strategy for multiple sclerosis. *PLoS ONE* **2020**, *15*, e0231483. [CrossRef]
71. Mascelli, S.; Barla, A.; Raso, A.; Mosci, S.; Nozza, P.; Biassoni, R.; Morana, G.; Huber, M.; Mircean, C.; Fasulo, D.; et al. Molecular fingerprinting reflects different histotypes and brain region in low grade gliomas. *BMC Cancer* **2013**, *13*, 387. [CrossRef] [PubMed]
72. Carmeliet, P.; Jain, R.K. Molecular mechanisms and clinical applications of angiogenesis. *Nature* **2011**, *473*, 298–307. [CrossRef] [PubMed]
73. Durand, B.; Fero, M.; Roberts, J.M.; Raff, M.C. p27^{Kip1} alters the response of cells to mitogen and is part of a cell-intrinsic timer that arrests the cell cycle and initiates differentiation. *Curr. Biol.* **1998**, *8*, 431–440. [CrossRef]
74. Hindley, C.; Philpott, A. Co-ordination of cell cycle and differentiation in the developing nervous system. *Biochem. J.* **2012**, *444*, 375–382. [CrossRef]
75. Dobashi, Y.; Kudoh, T.; Matsumine, A.; Toyoshima, K.; Akiyama, T. Constitutive Overexpression of CDK2 Inhibits Neuronal Differentiation of Rat Pheochromocytoma PC12 Cells. *J. Biol. Chem.* **1995**, *270*, 23031–23037. [CrossRef] [PubMed]
76. Lange, C.; Calegari, F. Cdk5 and cyclins link G1 length and differentiation of embryonic, neural and hematopoietic stem cells. *Cell Cycle* **2010**, *9*, 1893–1900. [CrossRef]
77. Gilbert, M.R.; Dignam, J.J.; Armstrong, T.; Wefel, J.S.; Blumenthal, D.T.; Vogelbaum, M.A.; Colman, H.; Chakravarti, A.; Pugh, S.; Won, M.; et al. A Randomized Trial of Bevacizumab for Newly Diagnosed Glioblastoma. *N. Engl. J. Med.* **2014**, *370*, 699–708. [CrossRef]
78. Chinot, O.L.; Rouge, T.D.L.M.; Moore, N.; Zeaiter, A.; Das, A.; Phillips, H.; Modrusan, Z.; Cloughesy, T. AVAGlio: Phase 3 trial of bevacizumab plus temozolomide and radiotherapy in newly diagnosed glioblastoma multiforme. *Adv. Ther.* **2011**, *28*, 334–340. [CrossRef]
79. Taal, W.; Oosterkamp, H.M.; Walenkamp, A.M.E.; Dubbink, H.J.; Beerepoot, L.V.; Hanse, M.C.J.; Buter, J.; Honkoop, A.H.; Boerman, D.; De Vos, F.; et al. Single-agent bevacizumab or lomustine versus a combination of bevacizumab plus lomustine in patients with recurrent glioblastoma (BELOB trial): A randomised controlled phase 2 trial. *Lancet Oncol.* **2014**, *15*, 943–953. [CrossRef]
80. Eberini, I.; Daniele, S.; Parravicini, C.; Sensi, C.; Trincavelli, M.L.; Martini, C.; Abbracchio, M.P. In silico identification of new ligands for GPR17: A promising therapeutic target for neurodegenerative diseases. *J. Comput. Mol. Des.* **2011**, *25*, 743–752. [CrossRef]
81. Köse, M.; Ritter, K.; Thiemke, K.; Gillard, M.; Kostenis, E.; Müller, C.E. Development of [(3)H]2-Carboxy-4,6-dichloro-1H-indole-3-propionic acid ([3)H]PSB-12150): A Useful Tool for Studying GPR17. *ACS Med. Chem. Lett.* **2014**, *5*, 326–330. [CrossRef]
82. Baqi, Y.; Alshaibani, S.; Ritter, K.; Abdelrahman, A.; Spinrath, A.; Kostenis, E.; Müller, C.E. Improved synthesis of 4-/6-substituted 2-carboxy-1H-indole-3-propionic acid derivatives and structure-activity relationships as GPR17 agonists. *MedChemComm* **2014**, *5*, 86–92. [CrossRef]
83. Kimple, R.J.; Kimple, M.E.; Betts, L.; Sondek, J.; Siderovski, D.P. Structural determinants for GoLoco-induced inhibition of nucleotide release by Gα subunits. *Nature* **2002**, *416*, 878–881. [CrossRef] [PubMed]
84. Comeau, S.R.; Gatchell, D.W.; Vajda, S.; Camacho, C.J. ClusPro: A fully automated algorithm for protein-protein docking. *Nucleic Acids Res.* **2004**, *32*, W96–W99. [CrossRef]
85. De Vries, S.J.; van Dijk, M.; Bonvin, A.M. The HADDOCK web server for data-driven biomolecular docking. *Nat. Protoc.* **2010**, *5*, 883–897. [CrossRef]
86. Ishak, I.H.; Kamgang, B.; Ibrahim, S.S.; Riveron, J.M.; Irving, H.; Wondji, C.S. Pyrethroid Resistance in Malaysian Populations of Dengue Vector *Aedes aegypti* Is Mediated by CYP9 Family of Cytochrome P450 Genes. *PLoS Negl. Trop. Dis.* **2017**, *11*, e0005302. [CrossRef]

87. Yu, Y.; Li, L.; Zheng, Z.; Chen, S.; Chen, E.; Hu, Y. Long non-coding RNA linc00261 suppresses gastric cancer progression via promoting Slug degradation. *J. Cell. Mol. Med.* **2017**, *21*, 955–967. [CrossRef] [PubMed]
88. Kumon, R.; Aehle, M.; Sabens, D.; Parikh, P.; Han, Y.; Kourennyi, D.; Deng, C. Spatiotemporal Effects of Sonoporation Measured by Real-Time Calcium Imaging. *Ultrasound Med. Biol.* **2009**, *35*, 494–506. [CrossRef] [PubMed]
89. Vaiyapuri, P.S.; Ali, A.A.; Mohammad, A.A.; Kandhavelu, J.; Kandhavelu, M. Time lapse microscopy observation of cellular structural changes and image analysis of drug treated cancer cells to characterize the cellular heterogeneity. *Environ. Toxicol.* **2015**, *30*, 724–734. [CrossRef] [PubMed]
90. Day, B.W.; Stringer, B.; Al-Ejeh, F.; Ting, M.J.; Wilson, J.; Ensbey, K.S.; Jamieson, P.R.; Bruce, Z.C.; Lim, Y.C.; Offenhäuser, C.; et al. EphA3 Maintains Tumorigenicity and Is a Therapeutic Target in Glioblastoma Multiforme. *Cancer Cell* **2013**, *23*, 238–248. [CrossRef]
91. Pollard, S.M.; Yoshikawa, K.; Clarke, I.D.; Danovi, D.; Stricker, S.; Russell, R.; Bayani, J.; Head, R.; Lee, M.; Bernstein, M.; et al. Glioma Stem Cell Lines Expanded in Adherent Culture Have Tumor-Specific Phenotypes and Are Suitable for Chemical and Genetic Screens. *Cell Stem Cell* **2009**, *4*, 568–580. [CrossRef] [PubMed]

IV

Article

Alkylaminophenol and GPR17 Agonist for Glioblastoma Therapy: A Combinational Approach for Enhanced Cell Death Activity

Phuong Doan ^{1,2,3}, Phung Nguyen ^{1,2,3}, Akshaya Murugesan ^{1,2,4}, Nuno R. Candeias ⁵ , Olli Yli-Harja ^{2,3,6,7} and Meenakshisundaram Kandhavelu ^{1,2,3,*}

- ¹ Molecular Signaling Group, Faculty of Medicine and Health Technology, Tampere University, P.O. Box 553, 33101 Tampere, Finland; phuong.doan@tuni.fi (P.D.); phunghtien.nguyen@tuni.fi (P.N.); akshaya.murugesan@tuni.fi (A.M.)
 - ² BioMediTech Institute and Faculty of Medicine and Health Technology, Tampere University, Arvo Ylpön katu 34, 33520 Tampere, Finland; olli.yli-harja@tuni.fi
 - ³ Science Center, Tampere University Hospital, Arvo Ylpön katu 34, 33520 Tampere, Finland
 - ⁴ Department of Biotechnology, Lady Doak College, Thallakulam, Madurai 625002, India
 - ⁵ Faculty of Engineering and Natural Sciences, Tampere University, P.O. Box 553, 33101 Tampere, Finland; ncandeias@ua.pt
 - ⁶ Computational Systems Biology Group, Faculty of Medicine and Health Technology, Tampere University, P.O. Box 553, 33101 Tampere, Finland
 - ⁷ Institute for Systems Biology, 1441N 34th Street, Seattle, WA 98103, USA
- * Correspondence: meenakshisundaram.kandhavelu@tuni.fi; Tel.: +358-504-721-724



Citation: Doan, P.; Nguyen, P.; Murugesan, A.; Candeias, N.R.; Yli-Harja, O.; Kandhavelu, M. Alkylaminophenol and GPR17 Agonist for Glioblastoma Therapy: A Combinational Approach for Enhanced Cell Death Activity. *Cells* **2021**, *10*, 1975. <https://doi.org/10.3390/cells10081975>

Academic Editor: Markus Siegelin

Received: 3 July 2021

Accepted: 28 July 2021

Published: 3 August 2021

Publisher's Note: MDPI stays neutral with regard to jurisdictional claims in published maps and institutional affiliations.



Copyright: © 2021 by the authors. Licensee MDPI, Basel, Switzerland. This article is an open access article distributed under the terms and conditions of the Creative Commons Attribution (CC BY) license (<https://creativecommons.org/licenses/by/4.0/>).

Abstract: Drug resistance and tumor heterogeneity limits the therapeutic efficacy in treating glioblastoma, an aggressive infiltrative type of brain tumor. GBM cells develops resistance against chemotherapeutic agent, temozolomide (TMZ), which leads to the failure in treatment strategies. This enduring challenge of GBM drug resistance could be rational by combinatorial targeted therapy. Here, we evaluated the combinatorial effect of phenolic compound (2-(3,4-dihydroquinolin-1(2H)-yl)(p-tolyl)methyl)phenol (THTMP), GPR17 agonist 2-([5-[3-(Morpholine-4-sulfonyl)phenyl]-4-[4-(trifluoromethoxy)phenyl]-4H-1,2,4-triazol-3-yl]sulfanyl)-N-[4-(propan-2-yl)phenyl]acetamide (T0510.3657 or T0) with the frontline drug, TMZ, on the inhibition of GBM cells. Mesenchymal cell lines derived from patients' tumors, MMK1 and JK2 were treated with the combination of THTMP + T0, THTMP + TMZ and T0 + TMZ. Cellular migration, invasion and clonogenicity assays were performed to check the migratory behavior and the ability to form colony of GBM cells. Mitochondrial membrane permeability (MMP) assay and intracellular calcium, $[Ca^{2+}]_i$, assay was done to comprehend the mechanism of apoptosis. Role of apoptosis-related signaling molecules was analyzed in the induction of programmed cell death. In vivo validation in the xenograft models further validates the preclinical efficacy of the combinatorial drug. GBM cells exert better synergistic effect when exposed to the cytotoxic concentration of THTMP + T0, than other combinations. It also inhibited tumor cell proliferation, migration, invasion, colony-forming ability and cell cycle progression in S phase, better than the other combinations. Moreover, the combination of THTMP + T0 profoundly increased the $[Ca^{2+}]_i$, reactive oxygen species in a time-dependent manner, thus affecting MMP and leading to apoptosis. The activation of intrinsic apoptotic pathway was regulated by the expression of Bcl-2, cleaved caspases-3, cytochrome c, HSP27, cIAP-1, cIAP-2, p53, and XIAP. The combinatorial drug showed promising anti-tumor efficacy in GBM xenograft model by reducing the tumor volume, suggesting it as an alternative drug to TMZ. Our findings indicate the coordinated administration of THTMP + T0 as an efficient therapy for inhibiting GBM cell proliferation.

Keywords: glioblastoma; mesenchymal GBM; alkylaminophenol; GPR17 agonist; synergy; cell cycle arrest; intrinsic apoptotic pathway

1. Introduction

Glioblastoma multiforme (GBM), a grade IV astrocytoma, is the most common malignant adult brain cancer [1]. Although combination therapy post-surgery has become the cornerstone for the anti-glioma treatment, patients have a dismal median survival of less than 15 months [2,3]. Treatment challenges exist for GBM, primarily due to the tumor heterogeneity, resistance to drug, blood–brain barrier, glioma stem cells, drug efflux pumps and DNA damage repair mechanisms [4].

Despite using TMZ as a first line drug in GBM therapy, its therapeutic effects are far reduced due to the enhanced activity of O⁶-methylguanine-DNA methyltransferase (MGMT). This DNA repair enzyme counteracts the TMZ induced DNA alkylation leading to the chemo-resistance against GBM treatment [5]. Although the classification of GBM into four distinct molecular subgroups such as proneural, neural, classical and mesenchymal subtypes [6] address the heterogeneity in GBM, intra-tumoral heterogeneity is the key determinant in therapy resistance leading to treatment failure [7]. These challenges lead us to understand how a conceivable therapeutic treatment could be best developed against GBM treatment.

Phenolic compounds are proven to be involved in various biological functions such as antioxidant, anti-inflammatory, chemo-preventive, and anticancer activity [8–10]. Several phenolic compounds such as vincristine [11], paclitaxel [12], omacetaxine [13] are successfully used as a chemotherapeutic agent against many forms of cancer. Earlier studies reported the role of phenolic compounds as an apoptotic inducer of GBM cells, with THTMP as the top potential compound exhibiting anticancer property [14]. Recently, we also identified that interaction of GPR17 with its ligand T0510-3657 (T0) could potentially regulate the GBM signaling communication and proliferation [15]. T0, a potential activator of GPR17 was found to exhibit better binding efficiency with stronger inhibitory activity than the known GPR17 agonist, MDL29951 [16]. RNA seq data of several GBM patient's sample revealed the role of GPR17 in about 30 different crucial pathway interactions in the GBM signaling networks [15]. In addition, computational data analysis on the RNA-seq also have reported on the expression of GPR17 in 511 low-grade glioma (LGG) and 156 glioblastoma samples. Hence, we consider and evaluate the therapeutic effect of combination of THTMP and T0 with the TMZ, in GBM cells.

Several pre-clinical experiments have shown that the cytotoxic drugs against most of the cancers are effective to give synergism when given in combination. It is believed that a synergistic combination of different therapeutic agents against GBM cells could relapse the disease progression. Such combination therapies could be more efficient than monotherapy and chemotherapy against GBM. PTX combined with TMZ or cisplatin [17,18] showed an increased inhibitory effect against malignant GBM cells in-vitro. Notably, dual targeting of autophagic regulatory circuitry in gliomas using tricyclic antidepressants (TCAs) and P2Y12 inhibitors elicits the safe combination in treating glioma [19].

The rationale behind the combination therapy for treating GBM requires the identification of the best possible combination of the drug at effective doses that targets specific molecular mechanisms. Thus, the present study investigates the combinatorial administrations of a GPR17-ligand, phenolic compound with the chemotherapeutic agent. We evaluated the mechanistic effect and therapeutic potential of apoptosis induction in the mesenchymal GBM subtype using a combination of phenolic derivatives with GPR17 agonist and with a known anticancer agent, TMZ. We also identified the effect of combinatorial drug, THTMP + T0, in inducing cell death with higher cytotoxicity against GBM cell lines than TMZ through the activation of intrinsic apoptotic signaling pathways. We also assessed the anti-metastatic property of the combinatorial drug that inhibits the migration and invasion of the GBM cells. In-vivo preclinical validation also proves the potential of the drug in reducing the tumor volume in xenograft models, thereby suggesting its usability as a therapeutic agent against GBM treatment.

2. Materials and Methods

Chemistry: Preparation and spectral characterization of compound, THTMP was done as previously reported [20]. GPR17 agonist (T0510.3657 or T0) was purchased from AKos GmbH (Stuttgart, Germany).

Cell culture: Low-passage primary patients GBM cell lines, RN1, PB1, MMK1 and JK2 were procured from QIMR Berghofer, Medical Research Institute, Australia (gifted by Brett Stringer) and were approved by the human ethics committee of the Queensland Institute of Medical Research and Royal Brisbane and Women's Hospital [21]. The cells were cultured in the serum-free RHB-A medium (Takara Clontech Cellartis, USA, Inc.) supplemented with growth factors like EGF and FGFb (Gibco, Grand Island, NY, USA), 0.1 mg/mL Streptomycin, 100 U/mL Penicillin (Sigma-Aldrich, St. Louis, MO, USA) in 1% Matrigel-coated flasks (Corning Life Science, St. Louis, MO, USA). The cells were maintained and cultured in the incubator at 37 °C in humidified air with 5% CO₂ [22].

Cytotoxicity assay: RN1, PB1, MMK1 and JK2 cell lines were seeded in Matrigel-coated 12-well plates at a density of 1×10^5 cells per well. Dose dependent analysis of THTMP and/or T0 and/or TMZ was performed with varying concentrations, such as 10 µM, 25 µM, 50 µM, 75 µM and 100 µM. The cells were incubated for 48 h at 37 °C and the cell viability was analyzed using trypan blue solution and Countess II FL Automated Cell Counter (ThermoFisher Scientific, Waltham, MA, USA). The percentage of growth inhibition was calculated relative to the DMSO-treated control wells. Dose responsive curve was calculated to identify the IC₅₀. All the experiments were performed with three biological repeats and two technical repeats.

Synergy screening assay: Synergy screening assay was performed in MMK1 and JK2 cells with an initial density of 1×10^5 cells per well. The cells ($n = 6$) were treated with combination of three-point dose series of THTMP (10 µM, 30 µM, 50 µM) and/or T0510.3657 (10 µM, 40 µM, 70 µM) with TMZ (10 µM, 50 µM, 100 µM). Cells were incubated in nine-point combination doses of either THTMP + TMZ, THTMP + T0 and/or T0 + TMZ for 48 h and cell viability was determined as described previously. The coefficient of drug interaction (CDI) was calculated from each combination using COMPUSYN method [23].

Migration and invasion assay: Migration and invasion assay were performed to assess the chemotactic capability and invasion of cells through the extracellular matrix. The assay was done in 6-transwell plates ($n = 6$) with the pore size of 8 µM (Corning Life Science, St. Louis, MO, USA). MMK1 and JK2 cells with the initial density of 1×10^5 cells per well were seeded in 500 µL of fresh medium with THTMP (40 µM), T0 (40 µM) and THTMP + T0 (30 µM + 10 µM) and/or without compounds in the upper compartment. The lower compartment was filled with 1 mL of medium containing growth factors, such as EGF (20 ng/mL) and FGFb (10 ng/mL). The plates were then incubated at 37 °C with 5% CO₂ for 18 h. For invasion assay, the upper compartment was coated with 100 µL of Matrigel (0.5 mg/mL) and the cells were seeded after 2 h. After 18 h of incubation, the membrane was fixed in ethanol and acetic acid (3:1) and further stained with 0.5% crystal violet. The cells which are not migrated/invaded were removed using a cotton swab. The well area was divided into 3 sections and multiple random fields of each section were chosen for counting the cells. The total number of the cells were counted at 40× magnification.

Clonogenic assay: Clonogenic assay was performed as described previously [24]. Briefly, the cells ($n = 6$) were incubated with THTMP (40 µM), T0 (40 µM) and THTMP + T0 (30 µM + 10 µM) for 48 h, 72 h, and 96 h. The cells were then harvested and plated in 6-well plate with the density of 5×10^5 cells per well without Matrigel coating and incubated at 37 °C with 5% CO₂ for 14 days. Later, the cells were fixed in ice-cold ethanol and acetic acid (3:1) for 10 min. The colonies were stained with 0.5% crystal violet prior to counting. Six fields of the well were taken randomly and used for counting. The colonies smaller than 30 µM were not accounted.

Cell cycle assay: The cells ($n = 6$) were treated with THTMP (40 µM), T0 (40 µM) and THTMP + T0 (30 µM + 10 µM) for 48 h and fixed in 70% ice-cold ethanol at 4 °C for 1 h. The cells were then washed in PBS and resuspended in 500 µL of PBS containing 2 µg/mL

Propidium Iodide (Sigma-Aldrich, St. Louis, MO, USA), 0.2 mg/mL RNase and 0.1% triton X-100 and incubated at 37 °C for 30 min. The cells were maintained on ice before the image analysis using EVOS imaging system (ThermoFisher Scientific, Waltham, MA, USA). Images were analyzed using CellProfiler ver. 3.1.9 and Matlab ver. R2018b.

Apoptosis assay: MMK1 and JK2 cells at the initial density of 5×10^5 were seeded per well in 6-well plates and treated with the THTMP and T0 single dosage and combination of THTMP + T0. Dead Cell Apoptosis Kit with Annexin-V/FITC and PI (ThermoFisher Scientific, Waltham, MA, USA) was used to analyze the apoptosis induction following the manufacturer's protocol. The treated cells were incubated at RT for 15 min prior to the fluorescence measurements. The image acquisition was done using EVOS imaging system (ThermoFisher Scientific, Waltham, MA, USA) with 20× objective magnification.

ROS assay: MMK1 and JK2 cells were seeded in 12-well plates with the initial density of 1×10^5 cells per well. Cells were allowed to grow overnight at appropriate cell culture condition. The cells were treated with THTMP, T0 and combination of THTMP + T0 for 5 h. Cells were harvested and incubated with 2 μ M 2',7'-dichlorodihydrofluorescein diacetate (H2DCFDA, Sigma-Aldrich), for 30 min at 37 °C with 5% CO₂. Cultures were washed with PBS and recovered in pre-warmed medium for 20 min. Plate reader (Fluoroskan Ascent FL, Thermo LabSystems, Männedorf, Switzerland) was used to measure the fluorescence with the excitation at 485 nm and emission at 538 nm. Hydrogen peroxide (200 μ M) (Sigma-Aldrich, St. Louis, MO, USA) was used as the positive control. The fold increase in ROS production was calculated based on the fluorescence intensity of treated, untreated, and blank samples.

Calcium assay: Cells were seeded in 96-well plates with the initial density of 1×10^4 cells per well. At 60–70% confluency, the cells were incubated with 5 μ M Fura-2 AM (Sigma-Aldrich, St. Louis, MO, USA) for 30 min at 37 °C and washed with PBS twice before the addition of 50 μ L of medium. Fluorescent signal was measured every 5 min using a microplate reader (Spark[®], Tecan, Thermo LabSystems, Männedorf, Switzerland) at two dual excitation/emission wavelengths 340/510 nm and 380/310 nm. After 10 min of measurement, 50 μ L of PBS containing IC₅₀ concentration of the tested compounds (THTMP, T0 and THTMP + T0) were added to the wells. Fluorescence measurement was carried out further for 1 h 30 min. The ratio of the fluorescence at the dual wavelengths (340 nm/380 nm) was used to calculate the changes in [Ca²⁺]_i as previously described [25].

Mitochondrial membrane potential assay: The mitochondrial-specific cationic dye JC-1 (Thermo Fisher Scientific, Waltham, MA, USA) was used to measure the mitochondrial membrane potential [26]. The assay was performed with the same experimental protocol as described above for calcium assay except, the addition of 10 μ g/mL of JC-1 instead of Fura-2 AM. Fluorescence intensity was measured using microplate reader (Spark[®], Tecan, Thermo LabSystems, Männedorf, Switzerland) at an excitation and emission wavelength of 485 nm/530 nm and 535 nm/590 nm. The change in mitochondrial membrane potential was calculated based on the ratio at 590 nm to 530 nm.

Expression profiling of apoptosis array: A proteome profile of human apoptosis array was done (R&D systems, Minneapolis, MN, USA) following the manufacturer's instruction. The array can capture 35 different apoptosis antibodies in duplicate on nitrocellulose membrane. MMK1 and JK2 cells at a density of 1×10^7 cells/mL were treated with THTMP (30 μ M) and T0510.3657 (10 μ M) and DMSO as the control for 48 h. The procedure was performed according to the manufacturer's protocol. Briefly, the cell lysates along with the cocktail of biotinylated detection antibodies were incubated with Proteome Profiler Human apoptosis array. Streptavidin-HRP and chemiluminescent detection reagents are added which produce the signals at each spot that correspond to the amount of phosphorylated protein. Images were captured using XENOGEN (Vivo Vision IVIS Lumina, Männedorf, Switzerland). The data were analyzed using ImageJ software.

In-vivo anticancer studies: In vivo anti-cancer activity was evaluated against glioblastoma U373-MG Uppsala in human tumor xenograft mice model. This was originally established at the University of Uppsala (https://web.expasy.org/cellosaurus/CVCL_2818,

accessed on 24 June 2021) [27]. The protocols were approved by Institutional Animal Ethics Committee, ACTREC, Tata Memorial Centre, Navi Mumbai (Ethical number: 01/2015), adhering to CPCSEA guidelines (Registration Number: 65/GO/ReBiBt/S/99/CPCSEA). In-house bred six- to eight-week-old female mice were used in the experiments. Animals were maintained with utmost human care to minimize animal suffering before and during the experiments.

Toxicity studies: Intraperitoneal injection of THTMP + T0 was done in the immunocompetent Nod/Scid mice. Toxicity criteria was considered with the mortality and weight loss of ≥ 4 g/mouse. The dosage of the drug used was 20 mg/kg body weight of the animal and injected at every 7 days of interval for 36 days. The animals were continuously monitored for any mortality after post-dosing of drugs.

Experimental design: Human Tumor Xenograft-U-373MG Uppsala was developed in Nod/Scid female mice. Desired experimental groups of $n = 6$ /group was maintained. The experimental group consist of control (Group A), vehicle control–DMSO (Group B), Positive control–TMZ (Group C) and THTMP + T0 (Group D). Tumor growth and tumor volume was measured using digital Vernier caliper (Pro-Max, Electronic Digital Caliper, Fowler-NSK, USA). Body weight, tumor volume and mortality of the mice was continuously monitored throughout the experimentation period of 36 days. After the experimentation period, the animals were sacrificed following the Institutional Animal Ethics Committee by injecting Pentobarbital 45 mg/kg, intra peritoneally.

Statistical analysis: Relative tumor volume (RTV in cc), T/C (ratio of test versus control) and survival was calculated using the following formula. Tumor volume = $[(w1 \times w1 \times w2) \times (\pi/6)]$, where $w1$ and $w2$ were the smallest and the largest tumor diameter (cm), respectively. RTV was measured as tumor volume on the day of measurement/tumor volume on day 1. Antitumor effectiveness was indicated as T/C ratio.

The percentage treatment/control (T/C%) values and percent tumor regression values were calculated as follows:

$$\text{Relative Tumor Volume (RTV)} \frac{T}{C} (\%) = \frac{RTV_{\text{Test}}}{RTV_{\text{Control}}} \quad (1)$$

$$\text{Tumor Regression (\%)} = 100 - \left(\frac{T}{C} \times 100\right) \quad (2)$$

RTV = mean tumor volume of the drug-treated group on the study day of interest–mean tumor volume of the drug-treated group on the initial day of dosing; C = mean tumor volume of the control group. Biological activity was considered significant when T/C values were ≤ 0.42 , as per the NCI, USA guidelines.

3. Results

3.1. Synergic Effect of THTMP + T0 against Patient Derived GBM Cells

Considering the inter-tumor heterogeneity of the GBM that classifies them into molecular subtypes, patient-derived cell lines such as MMK1, JK2, RN1 and PB1 [28] were used for the analysis of cell growth inhibition. The cells were treated with varying concentrations of TMZ, THTMP and T0 as described in the method section. We observed two distinct responses including TMZ-resistant, THTMP-sensitive, T0-sensitive cells (Figure 1A) and TMZ-resistant, THTMP-sensitive, T0-resistant cells (Figure 1B).

At 48 h post-treatment, TMZ single treatment was not effective in reducing the cell viability in all the cell lines. It showed only 12% growth inhibition even at 100 μM and hence was denoted as TMZ resistant. Upon THTMP treatment, the cells which showed higher growth inhibition of about 90% at 75 μM were denoted as THTMP-sensitive. Likewise, PB1 and RN1 were classified as T0 resistant cell, since they showed only 12.5% and 37.5% of growth inhibition at 75 μM , whereas MMK1 and JK2 were considered as T0 sensitive cells due to their ability to moderately reduce the cell viability up to 73.4% at 75 μM (Figure 1A,B). The half maximal inhibitory concentration (IC_{50}) deduced from the dose-responsive curve was presented in Figure 1C. From the above observation, it was

noted that MMK1 and JK2 cells were sensitive to THTMP and T0 and hence selected for further analysis.

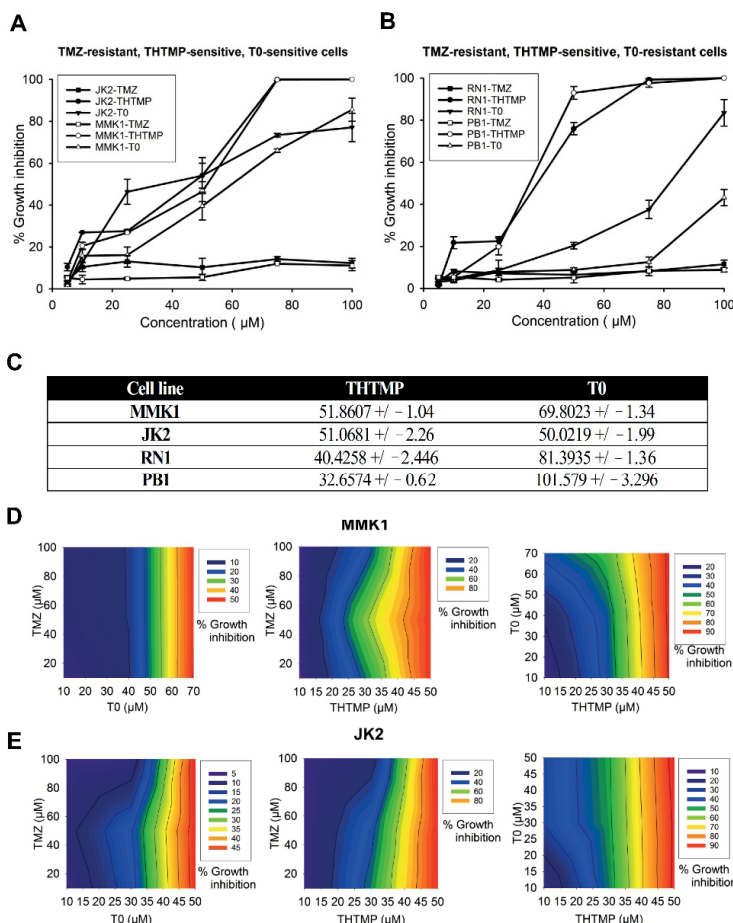


Figure 1. Effect of single and combination treatment of alkylaminophenol (THTMP) and GPR17 agonist (T0) on cell growth inhibition in multiple GBM patient tumor tissue-derived cells. The characteristics of TMZ-resistant, THTMP-sensitive, T0 sensitive cells (A), TMZ-resistant, THTMP-sensitive, T0-resistant cells (B) were observed at 48 h post-treatment. The IC₅₀ values of THTMP, T0 for multiple GBM patient tumor tissue-derived cells (C). Cells treated with different combinatorial conditions, TMZ + T0, TMZ + THTMP, and THTMP + T0 with a series of concentrations (10 μM, 25 μM, 50 μM, 75 μM and 100 μM) on MMK1 (D) and JK2 (E). The data were shown as means ± SD, with n = 5.

Synergistic effects of THTMP, T0 and TMZ were investigated upon combinatorial assessment of TMZ + THTMP, TMZ + T0 and THTMP + T0 using their respective IC₅₀ for the selected cell lines. It is discernible that the combination of TMZ + T0 at 70 μM and 100 μM concentration does not show more than 50% inhibitory effect in both MMK1 and JK2 cells. On treatment with TMZ + THTMP, we observed an increased cell death to about 80% with significant percentage of growth inhibition of about 90% on treatment with THTMP + T0 at 50 μM/10 μM concentration. The gradient color in the graph (blue to

red) shows the difference of the drug when given in combination. The color change was found to be possible only when there is an effect of combining drugs in a single effect. In addition, it is possible to observe from the graph that the % of growth inhibition at minimal concentration was lower for either drug, while we observed a promising effect at higher concentration (Figure 1D,E).

3.2. Evaluation of Drug Synergy by Combination Therapy

Drug combination effect of THTMP and T0 with TMZ was assessed by median effect analysis through the quantification of coefficient of drug interaction (CDI) using COMPUSYN method [23]. The (CDI) method has been used for the evaluation of the interaction combination effects in different ratios and concentrations [29–31]. To better understand and correlate the effect of combination of drugs on the growth inhibition, synergistic effect was calculated based on CDI value. The CDI was calculated based on the conservation assumption of drug interaction, and if $CDI = 1$ it was denoted as additivity, $CDI < 1$ as synergism and $CDI > 1$ as antagonism. The synergistic effect was best observed in THTMP + T0 combination, exhibiting lower CDI value than the THTMP + TMZ drug combination in both MMK1 and JK2 cells (Figure 2A,B). There was a negligible level of synergism in the TMZ + T0 combination. The increasing concentration of THTMP was found to be directly proportional to the increased synergistic effect, whereas T0 does not show significant differences in the CDI even at higher concentration. Although the ratio of THTMP:T0 corresponding to 50 μ M:10 μ M had significant synergistic effect with 90% growth inhibition, this particular concentration causes the cells to float and makes further analysis difficult. Hence, 30 μ M: 10 μ M (CDI value 0.9186 for JK2 and 0.97967 for MMK1) concentration was chosen for further studies, as it also exhibited synergism with approximately 50% cell growth inhibition.

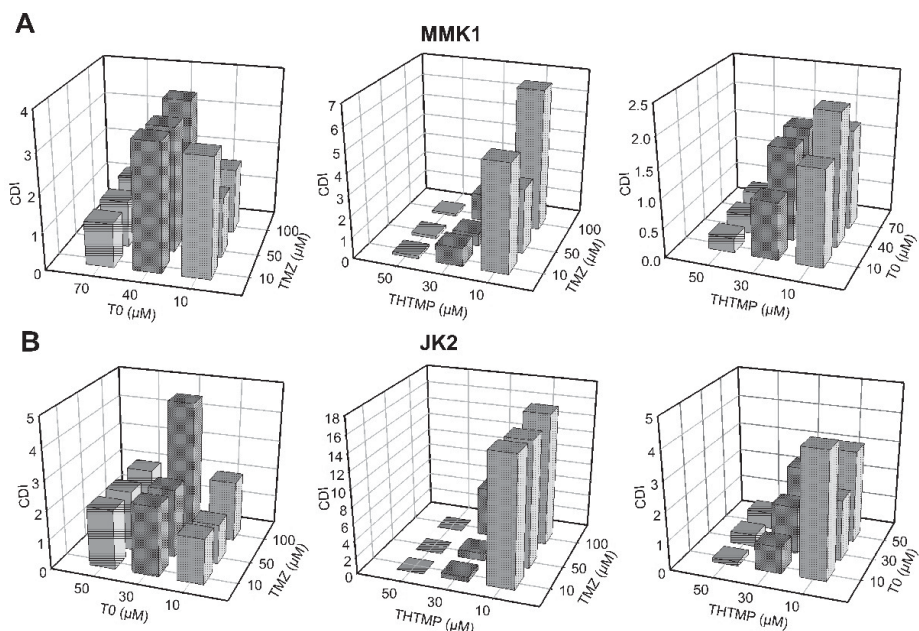


Figure 2. The coefficient of drug interaction (CDI) values for combinatorial drugs (T0 + TMZ), (THTMP + TMZ) and (THTMP + T0) of (A) MMK1 and (B) JK2 cells.

3.3. Combinatorial Drug THTMP + T0 Attenuates Migration and Invasion of GBM Cells

The decisive feature of metastasis is the migration and invasion of the cancer cells causing the disease progression. We investigated the anti-metastatic properties for the combinatorial drug, THTMP + T0 by assessing its ability to inhibit migration and invasion of GBM cells using transwell method. THTMP and T0 single treatment significantly inhibited the migration ability of MMK1 (22.5% and 12.9%) and JK2 (46.3% and 12.4%), with further decrease in the migration of less than 10% for the THTMP + T0 combination. It was also noted that THTMP has a better effect on MMK1 cell migration, whereas T0 affects the migration of JK2 cells more significantly than MMK1 cells (Figure 3A). A similar pattern was also observed in the invasion assay. THTMP and T0 single treatment reduced the invasion of cells to 44.3% and 57.5% in MMK1 and 61.1% and 48.7% of invaded cells in JK2, respectively. The combined effect of THTMP + T0 decreased the invasion of cells significantly to 27.2% and 20.7% in MMK1 and JK2 cells, respectively (Figure 3B). As a note, TMZ does not inhibit the migration and invasion of MMK1 and JK2 cells. Thus, the synergistic effect of THTMP + T0 facilitates the inhibition of migration and invasion activity in both the GBM cells.

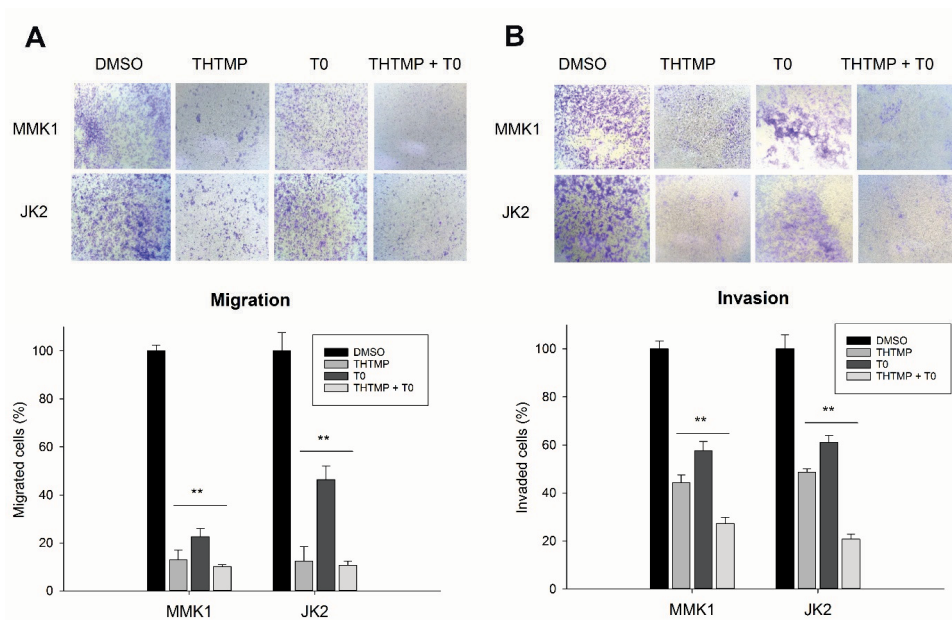


Figure 3. Analysis of cell migration and invasion assay. Effect of DMSO (control), THTMP, T0 and combination of THTMP + T0 on cell migration (A), invasion (B) on MMK1 and JK2 using transwell method. Microscopic images are the representation of the % of migration and invaded cells captured in 40× magnification. The data were shown as mean ± SD, $n = 3$, ** $p < 0.01$.

3.4. Clonogenicity of THTMP + T0 in Primary GBM Tumor Cells

We further performed the time-series clonogenic assay to analyze the efficacy of combinatorial drug THTMP + T0 in inducing the cell reproductive death by DNA damage. MMK1 and JK2 cells presented 47.9% and 55.5% reduction in the colony forming efficiency after the combinatorial treatment at 48 h, when compared with the control, DMSO. As the time increases, the effect of THTMP + T0 significantly reduced the number of cells to about 90% at 96 h of treatment. Although THTMP and T0 single treatment reduced the number of colony-forming cells, THTMP showed higher effect with 32.3% reduction on MMK1 cells when compared with T0 which showed only 24% reduction at 48 h post-treatment

(Figure 4A). An analogous result was also observed for JK2 cells with 52.0% and 44.1% of colony reduction upon THTMP and T0 treatment, respectively (Figure 4B). These data strongly suggest that the combination of THTMP + T0 significantly inhibits the clonogenic potential of patients' derived GBM cells.

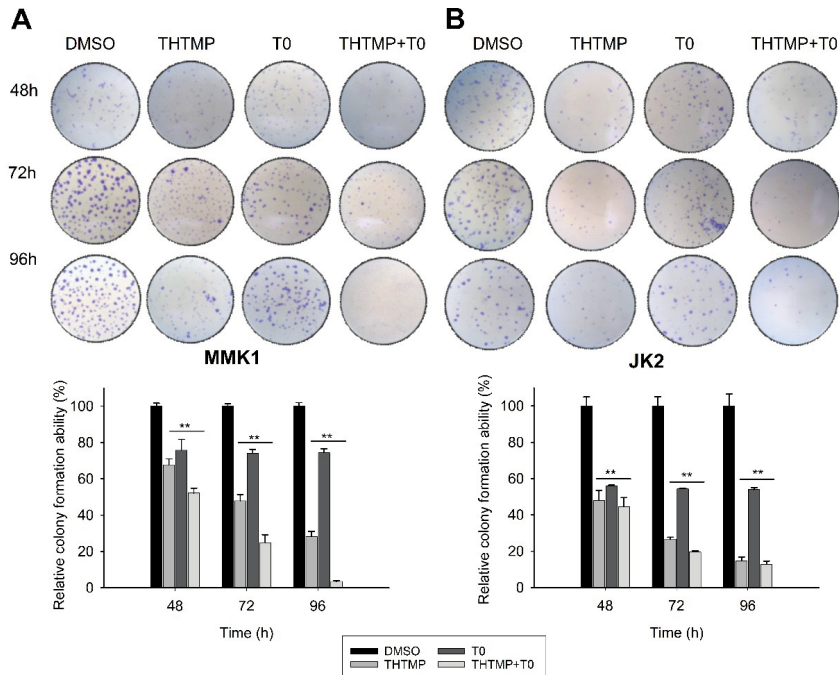


Figure 4. Effect of THTMP, T0 and combination of THTMP + T0 on colony formation ability on (A) MMK1 and (B) JK2. Time-lapse microscopic images of GBM cells upon treatment at 48 h, 72 h, and 96 h. The data were shown as mean \pm SD, $n = 3$, ** $p < 0.01$.

3.5. THTMP + T0 Unveils the Cell Cycle Checkpoints in GBM

Dysregulation of cell cycle leading to uncontrolled cell division is one of the major characteristic features of tumor cells and thus arresting the cell cycle is considered an important mechanism for anti-glioma drugs. It was evident from the earlier experiments that THTMP + T0 induces cell death significantly, which prompted us to determine its effect on the cell cycle. Cell cycle analysis was performed using PI staining and the analysis of the fluorescence images was done using CellProfiler ver 3.1.9 (Figure 5A).

Upon THTMP + T0 treatment, the percentage of cells entering from G₂ to M phase did not show significant differences in both cell lines. The shifting of MMK1 cells from G₂ to M phase was 3.5% to 6.5%, whereas JK2 cells shifted from 14.0% to 19.3% (Figure 5B), with the corresponding increase in the percentage of cells in S phase than the control. It was also observed that approximately 10% of cells were seen in the S phase of DMSO-treated MMK1 cells with 23.7%, 13.5% and 22.10% of cells in THTMP, T0 and THTMP + T0 treated cells, respectively. Similarly, 40.8% of JK2 cells were seen at S phase in the DMSO treated cells, while 66.4%, 50.7% and 69.6% were noted in THTMP, T0 and THTMP + T0 treatment, respectively. Image analysis on the DNA content in both the cells treated with THTMP and/or T0 revealed the cell cycle arrest in S phase. This complements the data observed in

the cell death analysis where a higher percentage of cells was observed in the S phase upon THTMP and THTMP + T0 treated cells when compared to T0 treated cells.

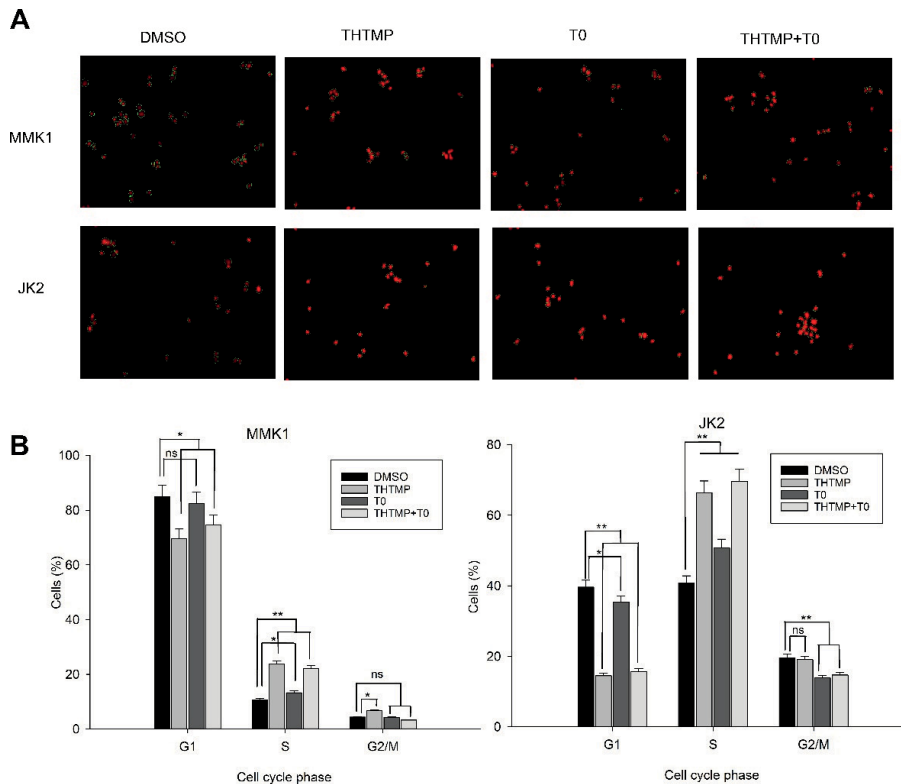


Figure 5. Effect of combinatorial drug on cell cycle analysis. THTMP and/or T0 compounds induced cell cycle arrest at S phase. Representative images of cell cycle analysis in which red color indicates DNA content of cells and green color indicates the area of cell segmentation (A). Percentage of cells in different cell cycle phases upon the treatment in MMK1 and JK2 cell lines (B). The data were shown as mean \pm SD, $n = 3$, * $p < 0.05$, ** $p < 0.01$, ns = non-significance.

3.6. THTMP + T0 Activates Intrinsic Pathways of Apoptosis Induction

More detailed analysis on the effect of combinatorial drug, THTMP + T0 on cell death was evaluated by assessing the rate of apoptosis, intracellular calcium level, change in mitochondrial membrane potential and ROS production. The GBM cells were treated with the combinatorial drug, and the percentage of apoptotic and necrotic cells were determined using Annexin V and propidium iodide staining. Consistent with the cytotoxicity assay, the highest percentage of apoptosis was achieved in response to THTMP + T0 treatment, followed by THTMP and T0. The rate of apoptosis was found to be 34.2%, 18.9% and 15.2% in MMK1 cells, whereas JK2 showed 37.6%, 29.3% and 21.3%, respectively. The very least percentage of necrotic cells was observed in response to T0 treatment with 6.1% and 7.9% in MMK1 and JK2 cells, respectively (Figure 6A).

Ca^{2+} signaling is known to be critically involved in effectuation of the cell death. The key events in the apoptosis are triggered by the intracellular Ca^{2+} signals and hence the estimation of $[Ca^{2+}]_i$ was performed upon induction by THTMP, T0, THTMP + T0 using Fura-2 assay. We observed a sustained increase in the $[Ca^{2+}]_i$ in a time-dependent manner in both cell lines (Figure 6B). In MMK1 cells, $[Ca^{2+}]_i$ signaling was increased till 100 min

on treatment with either THTMP and THTMP + T0 than T0 treatment. JK2 cells showed higher $[Ca^{2+}]_i$ signaling upon THTMP treatment than T0 and THTMP + T0 treatment, which might be varied due to the cell line specificity. All these data revealed the induction of calcium influx by THTMP, T0 and THTMP + T0 contributed the calcium mediated cell death of GBM cells.

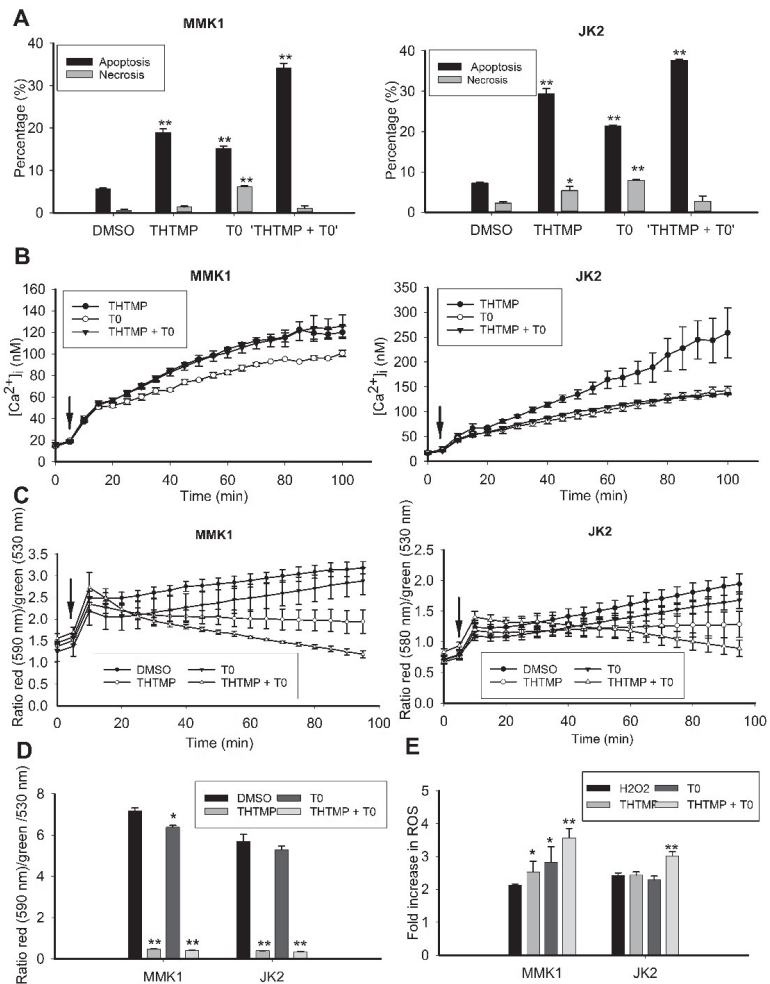


Figure 6. Cell death induction by THTMP, T0 and combination of THTMP + T0 on MMK1 and JK2 cells. Analysis of apoptosis induction in MMK1 and JK2 cells upon THTMP, T0 and THTMP + T0 (A). Time course measurement of $[Ca^{2+}]_i$ using fluorescence spectrophotometry from Fura-2 loaded cells. Arrows indicate the time of the addition of the compounds (B). Change in mitochondrial membrane potential in MMK1 and JK2 cells within 100 min (C) and 24 h of treatment (D). Arrows indicate the time of the addition of the compounds. Fold change in ROS production (E). The data were shown as mean \pm SD, $n = 3$, * $p < 0.05$, ** $p < 0.01$.

The dissipation of mitochondrial membrane potential is an early indicator of apoptosis. It is also well known that mitochondria plays a key role in calcium homeostasis, and the

rapid $[Ca^{2+}]_i$ elevation leads to calcium overloading, and thus damages the mitochondrial membrane. Subsequently, apoptogenic factors released due to this damage also triggers the intrinsic apoptotic pathway [32–34]. Thus, to examine the effect of the compounds on the mitochondrial integrity, JC-1 assay was performed to evaluate the change in mitochondrial membrane potential (MMP). As the time increases, there was a significant loss in the MMP upon treatment with THTMP + T0 and THTMP than T0 and DMSO treated GBM cells. The intensity of the green fluorescence represents the cells losing its MMP which was directly correlated with the cell death or unhealthy cells, whereas the red fluorescence represents the healthy cells (Figure 6C). It was also evident that T0 treatment increased MMP over 24 h of treatment than the THTMP and THTMP + T0, which was correlated with the observation as less calcium influx on T0 treated GBM cells (Figure 6D). These experiments prove that the combinatorial drug was effective in inducing mitochondria-dependent pathway of apoptosis through calcium signaling.

To further explore the impact of combinatorial treatment induced apoptosis, we examined the fold change of ROS. As illustrated in Figure 6E, the compounds significantly induced ROS production in both GBM cells than the DMSO control. The combinatorial treatment increased the production of ROS with 3.5-fold change in MMK1 and approximately 3.0-fold in JK2 cells. This result agreed with the previous data, that the overexpression of GPR17 stimulates apoptosis by inducing ROS production and thereby inhibits glioma cell proliferation [35]. This data also suggested that THTMP + T0 was more efficient in inducing ROS-mediated apoptosis.

3.7. Combination of THTMP/T0 Induces Intrinsic Apoptotic Pathway Rather Than Extrinsic Apoptotic Pathway in GBM Cells

Proteomic analysis was performed in both GBM cells to identify the potentially altered proteins associated with the intrinsic and extrinsic pathways of apoptosis. Human apoptosis proteome array was used, which includes 35 apoptosis-related proteins (Figure 7A). ImageJ was used to analyze apoptotic proteomic array to extrapolate the weak and strong signals from the images. The relative expression was quantified using the ratiometric analysis of the signals received from the sample and control. Various intrinsic proteins such as Bcl-2, cleaved caspases-3, cytochrome c, HSP27, cIAP-1, cIAP-2, p53, and XIAP were regulated upon combinatorial drug treatment in both GBM cells. The expression of Bcl-2, an anti-apoptotic protein family that regulates the mitochondria mediated apoptosis, was significantly reduced in both cell lines. In addition, the protein expression of cleaved caspase-3 and cytochrome c was found to be increased which deregulated the HSP27 (cytochrome c inhibitor) and Survivin (caspases 9 inhibitor) in both cell lines. We also noticed an increase in the expression of phospho-p53 (S15 and S46) in both the cells, which plays a key role in modulating its expression to induce apoptosis. We could observe a specific downregulation of cellular inhibitor of apoptosis proteins, cIAP-1 and cIAP-2 only in MMK1 cells, which remained unchangeable in JK2 cells. In addition, the level of XIAP (X-linked Inhibitor of Apoptosis Protein), which was highly correlated with a poor prognosis, significantly decreased upon combinatorial treatment than the control. Phospho p53 protein expression was found to be significantly increased in the treated cells, which plays a key role in both intrinsic and extrinsic apoptotic pathway. Other extrinsic proteins like the upregulation of death receptors, TNFR, TRAIL R1, TRAIL R2, FADD and Fas was observed, of which TNFR and TRAIL 1 function as proinflammatory receptors, while the remaining principally activate cell death pathways (Figure 7B,C).

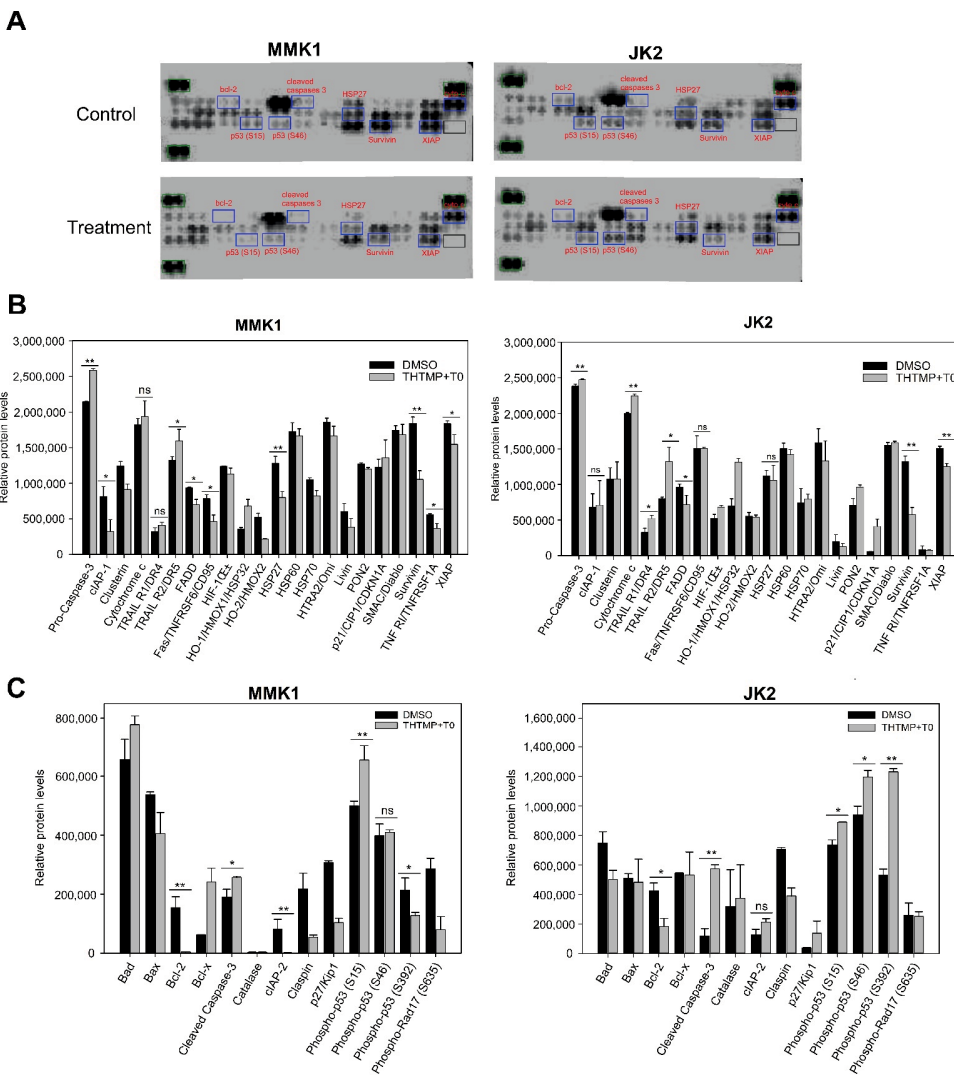


Figure 7. Proteome profiling of apoptosis-associated proteins. (A) Array images showing the expression of total 35 apoptosis-associated proteins upon combinatorial treatment with DMSO as control. (B) Relative level of expression of total 22 apoptotic proteins in the cell lysate of control and combinatorial treatment of MMK1 and JK2 cells (C) Integrated pixel intensity of 13 apoptotic proteins. The data were shown as mean ± SD; ns: not significant * indicates $p < 0.05$, ** $p < 0.01$.

3.8. In Vivo Anti-Tumor Efficacy of Combinatorial Drug, THTMP + T0

In-vivo anti-tumor efficacy of combinatorial drug, THTMP + T0 was evaluated in a xenograft animal model (Figure 8A). In-vivo anti-cancer activity was evaluated against glioblastoma U373-MG Uppsala human tumor xenograft mice model. We used U373-MG Uppsala cell line, since it was challenging to develop a PDX model with RN1, PB1, MMK1, JK2 cell lines. The U373-MG Uppsala cell line was considered as the suitable cell line for developing tumor xenograft mice model, since it carries the same characteristics

features of cell lines tested in vitro for high-grade human glioblastoma and confirmed the clinical correlation for testing drug. In addition, U373-MG Uppsala cell line derived animal model is the most frequently used model for testing the drug TMZ, an anti-GBM drug. Figure 8B,C revealed the relative tumor volume (RTV) and the relative activity criteria (T/C) of the combinatorial drug which was notably decreased when compared to the untreated and the DMSO control. Of note, less toxicity for the combinatorial drug was observed than the TMZ after the 8th day of treatment with similar trend effect throughout the experimental period of 36 days. Figure 8C revealed that the relative toxicity value decreased from 0.80 for combinatorial drug to 0.48 for TMZ treatment. This suggests that the TMZ has higher toxicity than the combinatorial treatment. The combinatorial drug has shown a time-sensitive reaction that was able to reduce the tumor volume with least toxicity compared to TMZ, thus it can prevent the GBM disease progression free survival through the targeted therapy. We also noticed the animal body weight was maintained in all conditions indicating non-systemic toxicity of the compounds (Supplementary Material).

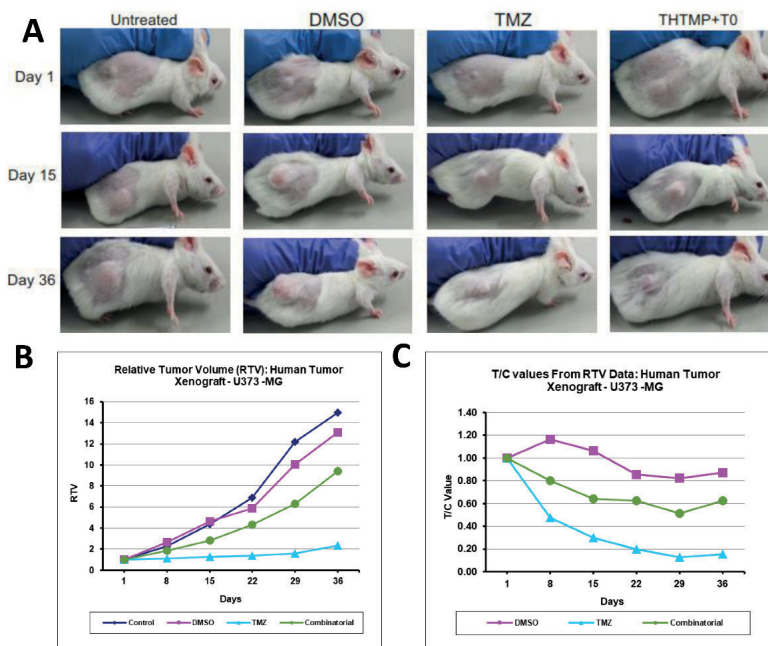


Figure 8. The anti-tumor efficacy of combinatorial treatment on glioblastoma xenograft model images of xenograft mice up to 36 days of treatment (A). Tumor growth curves of combinatorial treatment with TMZ as the positive control (B). The percentage treatment/control (T/C%) values or percent tumor regression values of combinatorial treatment and TMZ (C). No significant body weight change was observed after the drug treatment. RTV changes after the combinatorial treatment with p -value < 0.05 representing significant differences compared to vehicle control (DMSO) and positive control (TMZ).

4. Discussion

Currently TMZ is considered as a promising chemotherapeutic agent that significantly prolongs the survival of GBM patients. However, its clinical applicability was greatly reduced due to the resistance developed by MGMT expression and heterogeneity of GBM leading to treatment failure [36]. Previously, we characterized the phenolic compound, THTMP as an apoptosis inducer that significantly inhibited the GBM proliferation [14,37].

In addition, it was evident from the in-silico and in-vitro analysis, T0, a GPR17 agonist, strongly binds with GPR17 receptor and acts as a potent anticancer agent [16]. Thus, the approach of combining these two drugs along with TMZ could possibly favor the therapeutic effect against GBM treatment.

In the present study, we evaluated the cytotoxicity effect of THTMP, T0 and TMZ either as an individual drug and/or as combinatorial drug, against the GBM cells. The cells were found to be sensitive to THTMP and developed resistance to TMZ, which might be due to the unmethylation of the MGMT promoter of the GBM cells leading to the resistance to the alkylating chemotherapy agent, TMZ [28]. Despite the unmethylation of the cells, the combinatorial drug THTMP + TMZ has shown improved synergistic effect against GBM cells, with an additive effect for THTMP + T0 combination.

Our study not only demonstrated the anticancer property of the combinatorial treatment but also shed light on its possible molecular signaling pathway against GBM cells. The proliferation of cancerous cells occurs due to the absence of activated apoptotic signaling pathway [38]. The combinatorial treatment leads to the programmed cell death against GBM cells by activating various apoptotic factors, and increased cAMP level, an inhibitor of cell cycle progression and apoptosis inducer in cancer cells [39].

Moreover, various key parameters, like increased calcium, decreased MMP and increased ROS activate the intrinsic apoptotic signaling pathway upon combinatorial treatment. Intrinsic stimuli such as the accumulation of apoptotic mediators within the cell, in turn promotes Bax-induced cytochrome c release leading to the downstream activation of caspase 3 and 7 [40,41]. Survivin, a member of the apoptosis protein inhibitor, inhibits the activation of caspase 3 and 7 and thus blocks the cell death in most of the cancers [42]. The protein array data revealed that the upregulation of cleaved caspase-3 and cytochrome c with the downregulation of survivin [43] activates the intrinsic apoptotic pathway in GBM cells. Phosphor-p53, a tumor suppressor protein found to be upregulated, could control a wide number of genes involved in cellular processes including cell cycle arrest, cell senescence, DNA repair, metabolic adaptation and cell death. Induction of apoptotic death in nascent neoplastic cells was viewed as the primary mechanism by which p53 prevents tumor development [44]. Thus, p53 being both intrinsic and extrinsic apoptotic protein induces cell death and prevents the advancing of the disease.

The preclinical validation of the combinatorial drug in the in-vivo animal model also confirmed its promising anti-tumor role against GBM. THTMP + T0 was able to inhibit the GBM progression in-vivo that attributes for the prolonged survival. However, the inhibitory effect on GBM progression was not as robust as TMZ with the standard glioma cell lines, U373 Uppsala, which was used for xenograft animal model. TMZ exerts resistance to the prolonged therapy with hematological toxicity [45], oral ulceration, hepatotoxicity [46] and pneumocystis pneumonia [47] leading to discontinued therapy. Overall, the THTMP + T0 exerts less cytotoxicity at reduced concentration and could help in preventing the progression of the GBM disease through targeted therapy. The investigation on the combination of THTMP and T0 as GBM-selective anticancer agent in subcutaneous xenograft model explored the therapeutic potential of the drug. However, the ability of the combinatorial drug in crossing the blood-brain barrier needs further validation in GBM animal models. In addition, analyzing the in vitro and in vivo pharmacokinetics profiling might reveal the toxicity risk of the drug and thereby render its potentiality for the development of anti-GBM drug.

5. Conclusions

Our findings demonstrate that THTMP + T0 have a strong inhibitory effect on multiple GBM cells derived from GBM patient samples. THTMP also has a synergism effect with TMZ and T0, against GBM cell lines. Our study indicates that the combination of THTMP + T0 possesses better cytotoxicity effect in comparison to single THTMP or T0 or TMZ treatment on mesenchymal GBM cells. Moreover, the combinatorial treatment explores its ability to reduce migration, invasion, and colony formation of GBM cells and

arrest the cell cycle at S phase. The mechanism of action of combinatorial drug against GBM cells occurs through the activation of mitochondrial-mediated apoptosis. In addition, the combinatorial treatment has a promising anti-tumor efficacy in GBM xenograft model, thereby possibly reducing the disease progression. Thus, we conclude that combination treatment of THTMP + T0 might be a promising candidate for the GBM drug development.

Supplementary Materials: The following are available online at <https://www.mdpi.com/article/10.3390/cells10081975/s1>, Figure S1: (A) Survival data: Human tumor xenograft-U373-MG, (B) Animal body weight (grams) data: human tumor xenograft-U373-MG.

Author Contributions: Conceptualization, O.Y.-H. and M.K.; methodology, P.D., P.N., A.M. and M.K.; validation, P.D., P.N., A.M.; formal analysis, P.D., P.N. and A.M.; investigation, P.D., P.N., A.M., N.R.C. and M.K.; resources, A.M., O.Y.-H. and M.K.; data curation, P.D., P.N., A.M.; writing—original draft, P.D., P.N., A.M., N.R.C., O.Y.-H. and M.K. (with feedback from all authors); writing—review and editing, P.D., A.M. and M.K.; visualization, P.D., P.N. and M.K.; supervision, O.Y.-H. and M.K.; funding acquisition, O.Y.-H. and M.K. All authors have read and agreed to the published version of the manuscript.

Funding: TUT presidents grant for the salary support of P.D. and P.N.; Research materials support by Academy of Finland project grant support (decision no. 29720; P.D., P.N., A.M., O.Y.-H. and M.K.).

Institutional Review Board Statement: The study was conducted according to the guidelines of the Declaration of Institutional Animal Ethics Committee, ACTREC, Tata Memorial Centre, Navi Mumbai (Ethical number: 01/2015, Registration Number: 65/GO/ReBiBt/S/99/CPCSEA).

Informed Consent Statement: All protocols involving xenograft mouse model were approved by the Institutional Animal Ethics Committee, ACTREC, Tata Memorial Centre, Navi Mumbai (Ethical number: 01/2015) and adhered to CPCSEA guidelines (Registration Number: 65/GO/ReBiBt/S/99/CPCSEA).

Data Availability Statement: The data are available from the corresponding authors upon request.

Acknowledgments: We would like to thank Kirsi Granberg (Faculty of Medicine and Health Technology, Tampere, Finland) for providing SNB19 and LN229 cell lines; and QIMR Berghofer, Medical Research Institute, Australia for providing patient-derived GBM cell lines, MMK1, RN1 and JK2; TUT presidents grant for the salary support of P.D. and P.N.; Research materials support by Academy of Finland project grant support (decision no. 29720; P.D., P.N., A.M., O.Y.H and M.K). We would like to thank Ville Santala and Rahul Mangayil for providing the luminescence reader for protein study.

Conflicts of Interest: The authors declare no conflict of interest.

References

- Ostrom, Q.T.; Cote, D.J.; Ascha, M.; Kruchko, C.; Barnholtz-Sloan, J.S. Adult Glioma Incidence and Survival by Race or Ethnicity in the United States from 2000 to 2014. *JAMA Oncol.* **2018**, *4*, 1254–1262. [CrossRef]
- Stupp, R.; Mason, W.; van den Bent, M.J.; Weller, M.; Fisher, B.M.; Taphoorn, M.J.B.; Belanger, K.; Brandes, A.A.; Marosi, C.; Bogdahn, U.; et al. Radiotherapy plus Concomitant and Adjuvant Temozolomide for Glioblastoma. *N. Engl. J. Med.* **2005**, *352*, 987–996. [CrossRef]
- Koshy, M.; Villano, J.L.; Dolecek, T.A.; Howard, A.; Mahmood, U.; Chmura, S.J.; Weichselbaum, R.R.; McCarthy, B.J. Improved survival time trends for glioblastoma using the SEER 17 population-based registries. *J. Neurooncol.* **2012**, *107*, 207–212. [CrossRef]
- Zhao, M.; van Straten, D.; Broekman, M.L.D.; Pr at, V.; Schiffelers, R.M. Nanocarrier-based drug combination therapy for glioblastoma. *Theranostics* **2020**, *10*, 1355. [CrossRef]
- Hegi, M.E.; Diserens, A.-C.; Gorlia, T.; Hamou, M.-F.; de Tribolet, N.; Weller, M.; Kros, J.M.; Hainfellner, J.A.; Mason, W.; Mariani, L.; et al. MGMT Gene Silencing and Benefit from Temozolomide in Glioblastoma. *N. Engl. J. Med.* **2005**, *352*, 997–1003. [CrossRef]
- McLendon, R.; Friedman, A.; Bigner, D.; Van Meir, E.G.; Brat, D.J.; Mastrogiannis, G.M.; Olson, J.J.; Mikkelsen, T.; Lehman, N.; Aldape, K.; et al. Comprehensive genomic characterization defines human glioblastoma genes and core pathways. *Nature* **2008**, *455*, 1061.
- Qazi, M.A.; Vora, P.; Venugopal, C.; Sidhu, S.S.; Moffat, J.; Swanton, C.; Singh, S.K. Intratumoral heterogeneity: Pathways to treatment resistance and relapse in human glioblastoma. *Ann. Oncol.* **2017**, *28*, 1448–1456. [CrossRef]
- Karjalainen, A.; Yli-Harja, O.; Kandhavelu, M.; Doan, P.; Candeias, N.R.; Sandberg, O.; Chandraseelan, J.G. Synthesis of Phenol-derivatives and Biological Screening for Anticancer Activity. *Anticancer. Agents Med. Chem.* **2017**, *17*, 1710–1720. [CrossRef] [PubMed]
- Tanaka, T.; Shnimizu, M.; Moriwaki, H. Cancer chemoprevention by carotenoids. *Molecules* **2012**, *17*, 3202–3242. [CrossRef] [PubMed]

10. Doan, P.; Karjalainen, A.; Chandraseelan, J.G.; Sandberg, O.; Yli-Harja, O.; Rosholm, T.; Franzen, R.; Candeias, N.R.; Kandhavelu, M. Synthesis and biological screening for cytotoxic activity of N-substituted indolines and morpholines. *Eur. J. Med. Chem.* **2016**, *120*, 296–303. [CrossRef] [PubMed]
11. Von Pawel, J.; Schiller, J.H.; Shepherd, F.A.; Fields, S.Z.; Kleisbauer, J.P.; Chrysson, N.G.; Stewart, D.J.; Clark, P.I.; Palmer, M.C.; Depierre, A.; et al. Topotecan versus cyclophosphamide, doxorubicin, and vincristine for the treatment of recurrent small-cell lung cancer. *J. Clin. Oncol.* **1999**, *17*, 658. [CrossRef] [PubMed]
12. Miller, K.; Wang, M.; Gralow, J.; Dickler, M.; Cobleigh, M.; Perez, E.A.; Shenkier, T.; Cella, D.; Davidson, N.E. Paclitaxel plus Bevacizumab versus Paclitaxel Alone for Metastatic Breast Cancer. *N. Engl. J. Med.* **2007**, *357*, 2666–2676. [CrossRef]
13. Alvandi, F.; Kwitkowski, V.E.; Ko, C.-W.; Rothmann, M.D.; Ricci, S.; Saber, H.; Ghosh, D.; Brown, J.; Pfeiler, E.; Chikhale, E.; et al. U.S. Food and Drug Administration Approval Summary: Omacetaxine Mepesuccinate as Treatment for Chronic Myeloid Leukemia. *Oncologist* **2013**, *19*, 94. [CrossRef]
14. Doan, P.; Musa, A.; Candeias, N.R.; Emmert-Streib, F.; Yli-Harja, O.; Kandhavelu, M. Alkylaminophenol induces G1/S phase cell cycle arrest in glioblastoma cells through p53 and cyclin-dependent kinase signaling pathway. *Front. Pharmacol.* **2019**, *10*, 330. [CrossRef] [PubMed]
15. Mutharasu, G.; Murugesan, A.; Mani, S.K.; Yli-Harja, O.; Kandhavelu, M. Transcriptomic analysis of glioblastoma multiforme providing new insights into GPR17 signaling communication. *J. Biomol. Struct. Dyn.* **2020**, 1–14. [CrossRef]
16. Saravanan, K.M.; Palanivel, S.; Yli-Harja, O.; Kandhavelu, M. Identification of novel GPR17-agonists by structural bioinformatics and signaling activation. *Int. J. Biol. Macromol.* **2018**, *106*, 901–907. [CrossRef]
17. Azzabi, A.; Hughes, A.N.; Calvert, P.M.; Plummer, E.R.; Todd, R.; Griffin, M.J.; Lind, M.J.; Maraveyas, A.; Kelly, C.; Fishwick, K.; et al. Phase I study of temozolomide plus paclitaxel in patients with advanced malignant melanoma and associated in vitro investigations. *Br. J. Cancer* **2005**, *92*, 1006–1012. [CrossRef] [PubMed]
18. Ni, S.; Fan, X.; Wang, J.; Qi, H.; Li, X. Biodegradable implants efficiently deliver combination of paclitaxel and temozolomide to glioma C6 cancer cells in vitro. *Ann. Biomed. Eng.* **2014**, *42*, 214–221. [CrossRef]
19. Shchors, K.; Massaras, A.; Hanahan, D. Dual Targeting of the Autophagic Regulatory Circuitry in Gliomas with Repurposed Drugs Elicits Cell-Lethal Autophagy and Therapeutic Benefit. *Cancer Cell* **2015**, *28*, 456–471. [CrossRef]
20. Doan, P.; Nguyen, T.; Yli-Harja, O.; Kandhavelu, M.; Yli-Harja, O.; Doan, P.; Nguyen, T.; Yli-Harja, O.; Candeias, N.R. Effect of alkylaminophenols on growth inhibition and apoptosis of bone cancer cells. *Eur. J. Pharm. Sci.* **2017**, *107*, 208–216. [CrossRef]
21. Day, B.W.; Stringer, B.W.; Al-Ejeh, F.; Ting, M.J.; Wilson, J.; Ensbeys, K.S.; Jamieson, P.R.; Bruce, Z.C.; Lim, Y.C.; Offenhäuser, C.; et al. EphA3 Maintains Tumorigenicity and Is a Therapeutic Target in Glioblastoma Multiforme. *Cancer Cell* **2013**, *23*, 238–248. [CrossRef]
22. Pollard, S.M.; Yoshikawa, K.; Clarke, I.D.; Danovi, D.; Stricker, S.; Russell, R.; Bayani, J.; Head, R.; Lee, M.; Bernstein, M.; et al. Glioma Stem Cell Lines Expanded in Adherent Culture Have Tumor-Specific Phenotypes and Are Suitable for Chemical and Genetic Screens. *Cell Stem Cell* **2009**, *4*, 568–580. [CrossRef]
23. Chou, T.C. Drug combination studies and their synergy quantification using the chou-talalay method. *Cancer Res.* **2010**, *70*, 440–446. [CrossRef] [PubMed]
24. Franken, N.A.P.; Rodermond, H.M.; Stap, J.; Haveman, J.; van Bree, C. Clonogenic assay of cells in vitro. *Nat. Protoc.* **2006**, *1*, 2315–2319. [CrossRef]
25. Gryniewicz, G.; Poenie, M.; Tsieng, R.Y. A new generation of Ca²⁺ indicators with greatly improved fluorescence properties. *J. Biol. Chem.* **1985**, *260*, 3440–3450. [CrossRef]
26. Vaiyapuri, P.S.; Ali, A.A.; Mohammad, A.A.; Kandhavelu, J.; Kandhavelu, M. Time lapse microscopy observation of cellular structural changes and image analysis of drug treated cancer cells to characterize the cellular heterogeneity. *Environ. Toxicol.* **2015**, *30*, 724–734. [CrossRef]
27. Westermark, B. The deficient density-dependent growth control of human malignant glioma cells and virus-transformed glia-like cells in culture. *Int. J. Cancer* **1973**, *12*, 438–451. [CrossRef]
28. Stringer, B.W.; Day, B.W.; D'Souza, R.C.J.; Jamieson, P.R.; Ensbeys, K.S.; Bruce, Z.C.; Lim, Y.C.; Goasdoué, K.; Offenhäuser, C.; Akgül, S.; et al. A reference collection of patient-derived cell line and xenograft models of proneural, classical and mesenchymal glioblastoma. *Sci. Rep.* **2019**, *9*, 1–14. [CrossRef] [PubMed]
29. Xu, S.; Sun, G.; Shen, Y.; Peng, W.; Wang, H.; Wei, W. Synergistic effect of combining paeonol and cisplatin on apoptotic induction of human hepatoma cell lines. *Acta Pharmacol. Sin.* **2007**, *28*, 869–878. [CrossRef]
30. Chen, L.; Ye, H.-L.; Zhang, G.; Yao, W.-M.; Chen, X.-Z.; Zhang, F.-C.; Liang, G. Autophagy Inhibition Contributes to the Synergistic Interaction between EGCG and Doxorubicin to Kill the Hepatoma Hep3B Cells. *PLoS ONE* **2014**, *9*, 1–12. [CrossRef] [PubMed]
31. Xu, Y.; Shen, M.; Li, Y.; Sun, Y.; Teng, Y.; Wang, Y.; Duan, Y. The synergistic antitumor effects of paclitaxel and temozolomide co-loaded in mPEG-PLGA nanoparticles on glioblastoma cells. *Oncotarget* **2016**, *7*, 20890–20901. [CrossRef]
32. Hajnóczky, G.; Csordás, G.; Das, S.; Garcia-Perez, C.; Saotome, M.; Sinha Roy, S.; Yi, M. Mitochondrial calcium signalling and cell death: Approaches for assessing the role of mitochondrial Ca²⁺ uptake in apoptosis. *Cell Calcium* **2006**, *40*, 553–560. [CrossRef]
33. Kruman, I.; Guo, Q.; Mattson, M.P. Calcium and reactive oxygen species mediate staurosporine-induced mitochondrial dysfunction and apoptosis in PC12 cells. *J. Neurosci. Res.* **1998**, *51*, 293–308. [CrossRef]
34. Orrenius, S.; Zhivotovsky, B.; Nicotera, P. Calcium: Regulation of cell death: The calcium-apoptosis link. *Nat. Rev. Mol. Cell Biol.* **2003**, *4*, 552–565. [CrossRef] [PubMed]

35. Liu, H.; Xing, R.; Ou, Z.; Zhao, J.; Hong, G.; Zhao, T.J.; Han, Y.; Chen, Y. G-protein-coupled receptor GPR17 inhibits glioma development by increasing polycomb repressive complex 1-mediated ROS production. *Cell Death Dis.* **2021**, *12*, 1–14. [CrossRef]
36. Quinn, J.A.; Desjardins, A.; Weingart, J.; Brem, H.; Dolan, M.E.; Delaney, S.M.; Vredenburgh, J.; Rich, J.; Friedman, A.H.; Reardon, D.A.; et al. Phase I trial of temozolomide plus O6-benzylguanine for patients with recurrent or progressive malignant glioma. *J. Clin. Oncol.* **2005**, *23*, 7178–7187. [CrossRef]
37. Doan, P.; Musa, A.; Murugesan, A.; Sipilä, V.; Candeias, N.R.; Emmert-Streib, F.; Ruusuvoori, P.; Granberg, K.; Yli-Harja, O.; Kandhavelu, M. Glioblastoma Multiforme Stem Cell Cycle Arrest by Alkylaminophenol through the Modulation of EGFR and CSC Signaling Pathways. *Cells* **2020**, *9*, 681. [CrossRef] [PubMed]
38. Ouyang, L.; Shi, Z.; Zhao, S.; Wang, F.T.; Zhou, T.T.; Liu, B.; Bao, J.K. Programmed cell death pathways in cancer: A review of apoptosis, autophagy and programmed necrosis. *Cell Prolif.* **2012**, *45*, 487–498. [CrossRef] [PubMed]
39. Boucher, M.J.; Duchesne, C.; Rivard, N.; Lainé, J.; Morisset, J. cAMP protection of pancreatic cancer cells against apoptosis induced by ERK inhibition. *Biochem. Biophys. Res. Commun.* **2001**, *285*, 207–216. [CrossRef] [PubMed]
40. Douglas, R.G.; John, C.R. Mitochondria and Apoptosis. *Science* **1998**, *281*, 1309–1312.
41. Tait, S.W.G.; Green, D.R. Mitochondria and cell death: Outer membrane permeabilization and beyond. *Nat. Rev. Mol. Cell Biol.* **2010**, *11*, 621–632. [CrossRef] [PubMed]
42. Mita, A.C.; Mita, M.M.; Nawrocki, S.T.; Giles, F.J. Survivin: Key regulator of mitosis and apoptosis and novel target for cancer therapeutics. *Clin. Cancer Res.* **2008**, *14*, 5000–5005. [CrossRef]
43. Elmore, S. Apoptosis: A review of programmed cell death. *Toxicol. Pathol.* **2007**, *35*, 495–516. [CrossRef] [PubMed]
44. Aubrey, B.J.; Kelly, G.L.; Janic, A.; Herold, M.J.; Strasser, A. How does p53 induce apoptosis and how does this relate to p53-mediated tumour suppression? *Cell Death Differ.* **2018**, *25*, 104–113. [CrossRef]
45. Berrocal, A.; Perez Segura, P.; Gil, M.; Balaña, C.; Garcia Lopez, J.; Yaya, R.; Rodríguez, J.; Reynes, G.; Gallego, O.; Iglesias, L. Extended-schedule dose-dense temozolomide in refractory gliomas. *J. Neurooncol.* **2010**, *96*, 417–422. [CrossRef]
46. Kim, S.S.; Rait, A.; Kim, E.; DeMarco, J.; Pirolo, K.F.; Chang, E.H. Encapsulation of temozolomide in a tumor-targeting nanocomplex enhances anti-cancer efficacy and reduces toxicity in a mouse model of glioblastoma. *Cancer Lett.* **2015**, *369*, 250–258. [CrossRef] [PubMed]
47. Tentori, L.; Graziani, G. Recent Approaches to Improve the Antitumor Efficacy of Temozolomide. *Curr. Med. Chem.* **2008**, *16*, 245–257. [CrossRef]

